Effect of Pressure and Temperature on Electrical Conductivity of CNT-PEEK Composites

Mohammad Mohiuddin

A Thesis

In the Department

of

Mechanical and Industrial Engineering

Presented in Partial Fulfillment of the Requirements

For the Degree of

Doctor of Philosophy (Mechanical Engineering) at

Concordia University

Montréal, Québec, Canada

February, 2012

CONCORDIA UNIVERSITY

SCHOOL OF GRADUATE STUDIES

This is to certify that the thesis prepared

By: **Mohammad Mohiuddin**

Entitled: **Effect of Pressure and Temperature on Electrical Conductivity of CNT-PEEK Composites**

and submitted in partial fulfillment of the requirements for the degree of

DOCTOR OF PHILOSOPHY (Mechanical Engineering)

complies with the regulations of the University and meets the accepted standards with respect to originality and quality.

Signed by the final examining committee:

_____ Chair
Dr. P. Fazio

_____ External Examiner
Dr. J. Denault

_____ External to Program
Dr. M. Nokken

_____ Examiner
Dr. M. Pugh

_____ Examiner
Dr. P. Wood-Adams

_____ Thesis Supervisor
Dr. S.V. Hoa

Approved by _____
Dr. W-F. Xie, Graduate Program Director

February 6, 2012

_____
Dr. Robin A.L. Drew, Dean
Faculty of Engineering & Computer Science

ABSTRACT

Effect of Pressure and Temperature on Electrical Conductivity of CNT-PEEK Composites

Mohammad Mohiuddin, Ph.D.
Concordia University, 2012

This thesis investigates the effect of pressure and temperature on electrical conductivity of CNT-PEEK composites. The nanocomposites were manufactured using a co-rotating intermeshing twin screw extruder and the samples of required size and shape were fabricated by compression molding. Electrical properties of the nanocomposite samples were measured by Dielectric Analyzer (DEA) and a detailed analysis is presented in the framework of percolation theory. It was identified that nanotube contact resistance due to the formation of a thin insulating polymer layer around carbon nanotubes plays an important role in determining the overall conductivity of the samples. Detailed analysis of this contact resistance is presented based on experimental results in combination with theoretical models.

To investigate the effect of temperature and pressure on electrical conductivity, highly conductive samples with three different nanotube weight concentrations (8%, 9% and 10%) were selected. Metallic coatings (gold/silver epoxy) are conventionally used as electrodes to measure electrical conductivity at ordinary temperature and pressure. To measure electrical conductivity of these samples at elevated pressure and temperature, a new technique was developed to measure DC electrical conductivity by introducing a conductive copper mesh. Change of electrical conductivity of the samples was

investigated under application of high compression, high temperature and a combination of both. Conduction mechanisms for both pressure and temperature were discussed on the basis of experimental findings. It was found that electrical conductivity increases up to a certain level due to application of both pressure and temperature. The effect was more significant at lower pressure and temperature. In the case of repeated loading-unloading and heating-cooling cycles, hysteresis and electrical set were observed. The pressure always acts favorably in increasing electrical conductivity while the effect of temperature was found to be complex, controlled by parameters that counteract each other, especially when it was heated above the glass transition temperature and the nanotube content was high. Two possible mechanisms, namely, 'conduction by electron transport (nanotube contact)' and 'conduction by electron tunneling' were identified to explain such contradicting behavior. Sensitivity of the samples was also checked for possible application as sensor.

Acknowledgment

I express my sincere gratitude to Prof. Dr. Suong V. Hoa for his supervision, continuous guidance, constant encouragement and untiring support throughout this work. His constructive comments, motivational ability and open door policy to meet and discuss throughout the course of this doctoral research made my journey easy. As professor and my thesis supervisor, I will always admire Dr. Hoa for his broad intellect and aptitude for composites science and technology.

Sincere gratitude and thanks go to the members of my doctoral thesis examination committee for their insightful comments and suggestions.

I am especially grateful to Professor Dr. A. K. Waizuddin Ahmed who first introduced me with Dr. Hoa in 2004. His guidelines, inspiration and many kinds of help during my stay at Concordia made me indebted to him. I am also grateful to Professors Dr. Nabil Esmail, Dr. Ion Stiharu and Dr. G. H. Vatistas with whom I had opportunity to work as a part time faculty in the department. They always enquired of my research progress and inspired me to produce a good piece of work.

I would like to thank Dr. Ming Xie and Mr. Heng Wang for their valuable time and unconditional help in experimental works and laboratory procedures. Special thanks are due to Dr. Iosif Rosca for helping me in taking SEM images, Mr. Robert Oliver and Mr. Gilles Huard for their technical assistance in setting up the electrical instruments.

Thanks to all members of CONCOM group, especially to my fellow lab members: Ali, Asgar, Ahmed Kabir, Farjad, Hasna, Mohammed Elgeuchy, Pooya, Roham, Sayyad for their friendly assistance, support and laughter. Thank you all for maintaining a congenial dynamic environment in CONCOM for learning in all possible ways. Many other friends and colleagues including Ahmad Mostafa, Dr. Abu Hana, Imran, Musaddeque and Dr. Shah Asaduzzaman deserve my thanks for their kind advice, suggestions and help during the period of my doctoral study.

The administrative staff at the department of Mechanical and Industrial Engineering are very supportive, helpful and warm. I thank all of them wholeheartedly.

My heartfelt thanks and supreme gratitude to my parents and other family members for their love and support, constant care, relentless prayer and limitless patience although being far away from me. Last but not least, I owe a lot to my newly married wife Dilruba for her inspiration and understanding during the period of thesis preparation.

To

My two little angels 'Rumaysa' and 'Arsheya'

whose separation always makes me cry.

Table of Contents

Table of Contents ..... **viii**

List of Figures ..... **xiv**

List of Tables ..... **xix**

List of Abbreviations ..... **xx**

List of Symbols ..... **xxii**

Chapter 1: Introduction **1**

1.1 General 1

1.2 Background and relevant literature 2

1.2.1 Electrical properties of CNTs 2

1.2.2 Polymer nanocomposites 3

1.2.3 Processing of thermoplastic polymer nanocomposites 3

1.2.4 Challenges in processing nanocomposites 4

1.2.4.1 Alignment of CNTs 5

1.2.4.2 Uniform dispersion 5

1.2.4.3 Methods of uniform dispersion 6

1.3 Percolation theory and percolation threshold 8

1.3.1 Regimes of percolation threshold 10

1.4 Electrical properties of polymer nanocomposites 11

1.4.1 Effect of type of nanotubes 12

1.4.2 Effect of nanotube quality and dispersion 14
1.4.3 Effect of nanotube alignment 15
1.4.4 Effect of processing conditions 16
1.4.5 Effect of physical properties of filler 17
1.4.6 Nature and properties of polymer 17
1.4.6.1 Polarity of polymer 18
1.4.6.2 Viscosity of polymer 18
1.4.6.3 Degree of polymer crystallization 19
1.5 Theoretical studies on electrical conductivity of polymer composites 19
1.5.1 Effect of nanotube alignment 20
1.5.2 Effect of contact resistance and tunneling resistance 20
1.5.3 Effect of nanotube waviness 21
1.6 Application of CNT composites 23
1.7 Rationale and objectives of the thesis 25
1.8 Organization of the thesis 27
Chapter 2: Materials and Experiments 29
2.1 Introduction 29
2.2 Materials 30
2.3 Choice of manufacturing technique 31
2.4 Determination of optimum processing parameters 32
2.4.1 Mixing temperature 33

2.4.2 Rotor speed 34

2.4.3 Mixing time 35

2.5 Preparation of nanocomposite samples 36

2.6 Scanning Electron Microscopy (SEM) 37

2.7 Variability in electrical conductivity as a function of CNT concentration 39

Chapter 3: Electrical Properties of CNT-PEEK Composites 41

3.1 Introduction 41

3.1.2 Background 44

3.2 Experimental 45

3.2.1 Measurement of electrical properties 45

3.3 Results and discussion 46

3.3.1 Scaling law of electrical conductivity 55

3.3.1.1 Discussion on percolation and percolation threshold 57

3.3.1.2 Discussion on critical exponent 't' 60

3.3.1.3 Discussion on 'σ_f' 61

3.3.2 Scaling law of dielectric constant 62

3.3.3 Scaling law of critical frequency 63

3.4 Summary 65

Chapter 4: Estimation of Contact Resistance and its Effect on Electrical Conductivity of CNT-PEEK Composites 67

4.1 Introduction 67

4.2 Tunneling contact model 69

4.3 Calculation of contact resistance 73

4.3.1 Holm-Kirschstein model 73

4.3.2 Simmons' model 73

4.3.3 Discussion on results by Holm-Kirschstein and Simmons' models 76

4.3.4 Kovacs' model 80

4.3.5 Discussion on contact resistance 81

4.4 Summary 83

Chapter 5: Effect of Pressure on Electrical Conductivity of CNT-PEEK Composites 84

5.1 Introduction 84

5.1.1 Rubber composites 85

5.1.2 Polymer composites 86

5.1.3 Application of conductive composites as pressure sensors 89

5.2 Experimental 93

5.2.1 Sample preparation 93

5.2.2 DC measurement of electrical conductivity 94

5.2.3 Mechanical properties of CNT-PEEK composites 99

5.2.4 Testing of samples 100

5.2.5 Dynamic Mechanical Analysis (DMA) 101

5.3 Results and discussion 101

5.3.1 Effect of pressure 101

5.3.2 Loading-unloading cycle 102

5.4 Theoretical considerations 107

5.4.1 Derivation of piezoresistance model 110

5.4.2 Mechanism of change in electrical resistance 117

5.4.3 Parameters affecting the electrical conductivity of CNT composites 118

5.4.3.1 Change of volume of the sample 119

5.4.3.2 Change of angle of an individual CNT 122

5.4.3.3 Change of electrical property of an individual CNT 129

5.4.3.4 Change of tunneling distance between CNTs 129

5.5 Development of pressure model 133

5.6 Summary 136

Chapter 6: Effect of Temperature on Electrical Conductivity of CNT-PEEK Composites 137

6.1 Introduction 137

6.2 Experimental 141

6.2.1 Testing of samples 141

6.2.2 Investigation of the effect of Joule heating 142

6.2.3 Thermo Mechanical Analysis (TMA) 143

6.2.4 Thermal Analysis (DSC) 143

6.3 Results and discussion 144

6.3.1 Thermo-mechanical Properties 144

6.3.2 Thermal properties 145

6.3.3 Effect of temperature 147

6.3.3.1 Heating-cooling curves 149

6.4 Charge transport mechanism 153

6.4.1 Fluctuation Induced Tunneling (FIT) 155

6.4.2 General conduction mechanism 159

6.5 Combined effect of temperature and pressure on electrical conductivity 163

6.5.1 Explanation of the effect of temperature and pressure on electrical conductivity of CNT-polymer composites 166

6.6 Application to sensor 174

6.7 Summary 176

Chapter 7: Summary, Conclusions, Contributions and Recommendations for Future Work 178

7.1 Summary 178

7.2 Conclusions 179

7.3 Contributions and list of publications 182

7.4 Recommendations for future work 186

***References* 187**

List of Figures

Figure 1.1: Maximum conductivities versus respective CNT concentration in different polymer composites 13

Figure 1.2: Effect of thickness of insulating layer on tunneling resistance 21

Figure 1.3: Effect of nanotube waviness on electrical conductivity of composites 22

Figure 2.1: Electrical conductivity as a function of mixing temperature 33

Figure 2.2: Electrical conductivity as a function of rotor speed 34

Figure 2.3: Electrical conductivity as a function of mixing time 36

Figure 2.4: SEM Micrographs of fracture surface of PEEK containing different concentrations of CNTs 38

Figure 2.5: Variation of Electrical Conductivity of CNT-PEEK composites for different wt% of CNTs 39

Figure 3.1: AC conductivity of CNT-PEEK composites as a function of frequency for the samples indicated in the legend 47

Figure 3.2: Dielectric constant of CNT-PEEK composites as a function of frequency ... 49

Figure 3.3: Best fit of frequency dependent conductivity for (a) 3.5 wt% CNT-PEEK and (b) 3.6 wt% CNT-PEEK according to equation (3.6) 52

Figure 3.4 : Best fit of frequency dependent dielectric constant for (a) 3.5 wt% CNT-PEEK and (b) 3.6 wt% CNT-PEEK according to equation (3.7) 52

Figure 3.5: Electrical conductivity (σ_{dc}) as a function of reduced volume concentration ($\phi - \phi_c$). Inset shows the best linear fit at $\phi_c = 2.05$ vol% and t = 2.517. 56

Figure 3.6: Electrical conductivity (σ_{dc}) as a function of volume concentration (ϕ). Inset shows the best linear fit at for $\phi < \phi_c$ and q' = 1.305. 56

Figure 3.7: Dielectric constant as a function of CNT volume concentration. Inset shows the best fit of ε_{dc} vs. ($\phi_c - \phi$). 63

Figure 3.8: Best fit of critical frequency f_c vs. CNT volume concentration ($\phi - \phi_c$). Inset shows the relationship between f_c and σ_{dc} 64

Figure 4.1: Schematic of the model of resistor network to calculate composite resistance 71

Figure 4.2: Electrical conductivity as a function of CNT volume concentration. The solid and dotted lines are fit to equation (4.6) 76

Figure 4.3: Thickness of the insulating film as a function of nanotube volume concentration..... 77

Figure 4.4: Expt. Electrical Conductivity as a function of insulating PEEK film thickness 79

Figure 4.5: Tunneling resistance as a function of insulating PEEK film thickness..... 79

Figure 4.6: log-log plot of electrical conductivity vs. weight concentration 80

Figure 4.7: Contact resistance as a function of CNT volume concentration 81

Figure 4.8: Effect of contact resistance on the electrical conductivity of nanotube composites..... 82

Figure 5.1: CNT-PEEK samples (a) with copper mesh, (b) with silver-epoxy paste..... 95

Figure 5.2: V_i-I characteristics of the composite samples 98

Figure 5.3: Schematic diagram of the experimental set up..... 100

Figure 5.4: Electrical conductivity vs. applied pressure at room temperature (20°C).... 101

Figure 5.5: Comparison of loading-unloading curves of 8 wt% – 10 wt% CNT-PEEK composites at room temperature 103

Figure 5.6: Repeated loading-unloading of 8 wt% CNT-PEEK composites at room temperature (20°C) 104

Figure 5.7: Repeated loading-unloading of 9 wt% CNT-PEEK composites at room temperature (20°C) 105

Figure 5.8: Repeated loading-unloading of 10 wt% CNT-PEEK composites at room temperature (20°C) 106

Figure 5.9: Formation of three dimensional conductive paths in CNT-PEEK composites without any externally applied pressure 108

Figure 5.10: Formation of conductive paths in CNT-PEEK composites under externally applied pressure 109

Figure 5.11: Schematic diagram for the inner structure of CNT-PEEK composites..... 109

Figure 5.12: Schematic of the formation of conducting paths under applied pressure .. 111

Figure 5.13: Experimental data of 9 wt% CNT-PEEK samples compared to equation (5.13) (tunneling, $N = N_0$) and equation (5.18) (tunneling & redistribution) .. 115

Figure 5.14: SEM micrograph of 9 wt% CNT-PEEK sample after compression 116

Figure 5.15: Unit volume of CNT-PEEK composite under compression 119

Figure 5.16: Volume change of 9 wt% CNT-PEEK composite under uniaxial compression strain 121

Figure 5.17: Different angles of a CNT in 3-D co-ordinate axes. 122

Figure 5.18: Change of Angle of a CNT in PEEK induced by compression..... 125

Figure 5.19: Schematic of RVE and boundary conditions for finite element analysis... 126

Figure 5.20: Finite element analysis showing the effect of modulus of polymer matrix on CNT's rotation 127

Figure 5.21: Relative contact resistance against applied pressure for 8 wt% – 10 wt% CNT-PEEK composites. 132

Figure 5.22: Schematic of a composite sample under applied pressure 133

Figure 5.23: Dynamic Mechanical Analysis (DMA) of 9 wt% CNT-PEEK Composites 134

Figure 5.24: Comparison of electrical resistance of 9 wt% CNT-PEEK composites at room temperature obtained by experiment and the proposed model. 135

Figure 6.1: Schematic of the Experimental Set-up 141

Figure 6.2: Plot of thermocouple temperature versus oven temperature 142

Figure 6.3: Relative change of composite sample thickness with temperature. Inset shows TMA of a representative 9 wt% CNT-PEEK sample. 144

Figure 6.4: DSC thermograms of PEEK and the CNT-PEEK composites 145

Figure 6.5: Electrical conductivity of samples of 8 wt% – 10 wt% of CNTs at different temperatures 148

Figure 6.6: Electrical Conductivity vs. temperature during 1st heating-cooling cycle of 8 wt% – 10 wt% CNT-PEEK composites 150

Figure 6.7: Repeated heating-cooling curves for 8 wt% CNT-PEEK composites 152

Figure 6.8: Repeated heating-cooling curves for 9 wt% CNT-PEEK composites 152

Figure 6.9: Repeated heating-cooling curves for 10 wt% CNT-PEEK composites 153

Figure 6.10: Fitting of Electrical conductivity to FIT model for 8 wt% – 10 wt% CNT-PEEK samples 156

Figure 6.11: linear relationship of ln σ vs. $p^{-1/3}$ 158

Figure 6.12: Plot of the logarithm of conductivity versus the reciprocal of temperature (1/T) for 8 wt% – 10 wt% CNT-PEEK composite samples 159

Figure 6.13: Plot of the logarithm of conductivity versus the reciprocal of temperature (1/T) for 10 wt% CNT-PEEK composite sample showing two slopes..... 160

Figure 6.14: Temperature dependence of electrical conductivity of samples with $\phi > \phi_c$ in which effect of thermal expansion has been taken into account..... 162

Figure 6.15: Electrical conductivity of 8 wt% CNT-PEEK composites as a function temperature for different applied pressures [2, 4, 6, 8,….40 MPa] 164

Figure 6.16: Electrical conductivity of 9 wt% CNT-PEEK composites as a function temperature for different applied pressures [2, 4, 6, 8,….40 MPa]. 164

Figure 6.17: Electrical conductivity of 10 wt% CNT-PEEK composites as a function temperature for different applied pressures [2, 4, 6, 8,….40 MPa]. 165

Figure 6.18: Electrical conductivity vs. Pressure at room temperature (20°C) and 140°C 166

Figure 6.19: Electrical conductivity of 8 wt%, 9 wt% and 10 wt% CNT-PEEK composites from room temperature to 200°C (T_g of PEEK = 144°C)..... 171

Figure 6.20: Electrical conductivity of 3 wt%, 4 wt% and 5 wt% CNT-PEEK composites from room temp to 200°C (T_g of PEEK = 144°C)..... 172

Figure 6.21: Temperature sensitivity of CNT-PEEK samples at different pressures 175

Figure 6.22: Pressure sensitivity of CNT-PEEK samples at different temperatures 175

List of Tables

Table 1.1 Percolation Thresholds in two and three-dimensional lattices 9

Table 2.1: Physical properties of PEEK (Supplier's data)..... 31

Table 2.2: Physical properties of MWCNTs (Supplier's data unless otherwise stated)... 31

Table 3.1: Parameters indicating the frequency dependence of electrical and dielectric properties of CNT-PEEK Composites 54

Table 3.2: Percolation thresholds of melt processed thermoplastic nanocomposites..... 58

Table 5.1: Comparison of electrical conductivity obtained by AC measurement and DC measurement 97

Table 5.2: Comparison of electrical conductivity measured at room temperature using fluke digital multimeter and Precision current source/voltmeter (V_i-I measurement) 98

Table 5.3: Comparison of electrical conductivity measured at room temperature using copper mesh and silver epoxy paste as electrodes 99

Table 5.4: Mechanical properties of CNT-PEEK composites 99

Table 5.5: Comparison of change of angle (γ) without matrix and with matrix..... 128

Table 6.1: Thermal properties of PEEK and CNT-PEEK composites obtained by DSC146

Table 6.2: Coefficients of determination in FIT model 156

Table 6.3: Constants obtained from curve fitted to equation (6.6) 161

Table 6.4: Summary of the effect of parameters on electrical conductivity of nanocomposites..... 174

List of Abbreviations

ACVD	Aerosol Chemical Vapor Deposition
BRW	Biased Random Walk
BT	Barium Titanate
CB	Carbon Black
CCVD	Catalytic Chemical Vapor Deposition
CMC	Carbon Microcoils
CNF	Carbon Nanofibers
CNT	Carbon Nanotube
DEA	Dielectric Analysis/Analyzer
DMA	Dynamic Mechanical Analysis
EMI	Electromagnetic Interference
EPDM	Ethylene-Propylene-Diene-Monomer
EVA	Ethylene Vinyl Acetate
FEF	Fast Extrusion Furnace
FG	Foliated Graphite
FIT	Fluctuation Induced Tunneling
HDPE	High density Poly Ethylene
LDPE	Low Density Poly Ethylene
MWCNT	Multi Walled Carbon Nanotube
MWS	Maxwell-Wagner-Sillars
NBR	Acrylonitrile Butadiene Rubber
NR	Natural Rubber
NPC	Negative Pressure Coefficient (of resistivity)
NTC	Negative Temperature Coefficient (of resistivity)
OTC	Zero Temperature Coefficient (of resistivity)
PA	Polyamide
Pa	Pascal
PAT	Poly(3-alkylthiophene)

PC	Poly Carbonate
PE	Poly Ethylene
PEEK	Poly Ether Ether Ketone
PEO	Poly Ethylene Oxide
PEKK	Poly Ether Ketone Ketone
PET	Poly Ethylene Terephthalate
PmPV	poly(*m*-phenylenevinylene)
PMMA	Poly Methyl Methacrylate
PMVS	Poly Methyl Vinyl Siloxane
PP	Poly Propylene
PPC	Positive Pressure Coefficient (of resistivity)
PPE	Poly (phenyleneethynylene)
PPM	Parts Per Million
PS	Polystyrene
PTC	Positive Temperature Coefficient (of resistivity)
PVA	Polyvinyl Alcohol
PVDF	Polyvinylidene Fluoride
RFI	Radio Frequency Interference
RVE	Representative Volume Element
SBS	Styrene Butadiene Styrene
SCF	Short Carbon Fiber
SEM	Scanning Electron Microscopy
SWCNT	Single walled Carbon nanotube
TMA	Thermo Mechanical Analysis
UDR	Universal Dynamic Response
UHMWPE	Ultra High Molecular Weight Poly Ethylene
UPR	Unsaturated Polyester
VGCF	Vapor Grown Carbon Fiber
VGNF	Vapor Grown Carbon nanofiber

List of Symbols

A	Cross-sectional area
A_c	Area of capacitance
B	Temperature dependent parameter in Jonscher equation
E	Modulus of Elasticity
J	Current density (Amp/cm^2)
K	Fitting parameter
M, N	Number of contacts in series and in parallel in tunneling contact model / piezoresistive model
P	Uniaxial Pressure/compression/stress
Q_c	crystallization enthalpy of matrix
Q_m	Melting enthalpy of matrix
Q_X	Melting enthalpy of 100% crystallized matrix
$S_{contact}$	Surface area of CNTs in contact
R	Electrical Resistance in Ohm (Ω)
$R_{contact}$	Contact Resistance in Ohm (Ω)
R_c	Constriction (direct contact between CNTs) resistance of CNTs in Ohm (Ω)
R_t	Tunnel Resistance in Ohm (Ω)
T_g	Glass Transition Temperature
T_m	Melting Temperature
T_t	Transition temperature
V	Volume of composite sample
V_i	Voltage
X_c	Degree of crystallinity in percent (%)

a	Radius of the contact area
d	Diameter of a Carbon Nanotube
e	Charge of an electron
f	Frequency in Hz
h	Planck's constant = 6.62×10^{-34} J.s
k_B	Boltzman Constant = 8.617×10^{-5} eV/K
l	Length of a Carbon Nanotube
m	Mass of an electron = 9.11×10^{-31} Kg
n	number of contacts per unit volume
p	Mass fraction (Mass concentration) of Carbon Nanotubes in composites
p_c	Critical mass concentration of Carbon Nanotubes in composites
q, q'	Exponents in scaling laws of percolation below percolation threshold
r	Radius of a Carbon Nanotube
s	Insulating polymer film thickness/gap between two CNTs/ inter-nanotube spacing/tunneling distance (Å)
t, t'	Exponents in scaling laws of percolation above percolation threshold
u, v	critical exponents in AC conductivity and dielectric constant
w_m	Weight fraction of matrix in composites
z	Thickness of a composite sample
α, β, γ	Angles made by a CNT with X, Y and Z axis in three dimensional coordinates
δ	Thickness of one layer in tunneling contact model
ε	Strain of the polymer matrix
$\varepsilon_x, \varepsilon_y, \varepsilon_z$	strain along X, Y and Z direction

ε_r	Relative permittivity
ε_0	Permittivity of vacuum = 8.85×10^{-12} F/m
ϕ	Volume fraction (Volume concentration) of Carbon Nanotubes in composites
ϕ_c	Critical Volume concentration of Carbon Nanotubes in composites
η	Fitting parameter
λ	Mass density
λ_f	Mass density of filler (CNTs) in g/cm^3
λ_m	Mass density of matrix (PEEK) in g/cm^3
μ	Aspect ratio
ν	Poisson's ratio
θ	Phase angle shift between current and voltage
ρ	Volume resistivity of composites in Ohm-cm (Ω-cm)
ρ_c	Constriction (direct contact between CNTs) resistivity of CNTs in Ohm-cm
ρ_t	Tunnel Resistivity in Ohm-cm^2 (Ω-cm^2)
σ, σ_0, σ_{dc}	DC Electrical conductivity (S/cm)
σ_0'	Pre-exponential factor used in temperature models
σ' , σ_{ac}	AC Electrical conductivity (S/cm)
σ_f	Electrical conductivity of filler (S/cm)
σ_{cnt}	Intrinsic Electrical conductivity of carbon nanotubes (S/cm)
ω	Angular frequency (rad/sec)
ψ	Height of potential barrier/Work function
ψ_0	Work function of CNTs
ζ, ξ	Exponents used in scaling law of percolation

Chapter 1

Introduction

1.1 General

After Ijima's identification of multi walled carbon nanotubes (MWCNTs) in 1991 [1], a huge interest in CNTs has been sparked by their extraordinary intrinsic properties. Because of their nanoscale dimensions, exceptionally high electrical and thermal conductivities, low density, high tensile strength and Young's modulus, MWCNTs have attracted considerable attention from both academic and technological areas to be an ideal filler material for polymeric composites [2]. Since polymeric composites are multi-phase systems, their properties can be tailored by modification of the polymer and amount of fillers. Research in exploiting their unique physical properties such as high electrical conductivity has been intensive for multifunctional applications in the last few decades. A number of factors, such as uniform dispersion of CNTs, their purity and alignment in the expected directions are the biggest hurdles in preparing such conductive composites. For large scale applications, despite all challenges in processing highly conductive composites, their potential as the best filler material continues to be a dominant motivation for further research in this field. Manufacture of conductive nanocomposites having capability in sensing and actuating under varying conditions of environment such as pressure and temperature is, therefore, an emerging need in many industrial applications.

1.2 Background and relevant literature

1.2.1 Electrical properties of CNTs

Three different kinds of CNTs are produced: single walled CNTs (SWCNTs), double walled CNTs (DWCNTs) and multi walled CNTs (MWCNTs). MWCNTs are the coaxial assembly of SWCNT cylinders rolled up with one another. Based on chirality and diameters, they are classified as chiral, armchair and zigzag. Chirality or twist of CNTs is the main characteristic that strongly determines electrical and other properties. According to the chirality, CNTs can be either metallic or semiconducting in nature. The exceptional electrical properties of CNTs are due to their one-dimensional character and uncommon electronic structure [3]. They possess extremely low electrical resistance. Electrical resistance is due to the collisions with defects in the crystal structure of a material when an electron flows. This defect can be a defect in the crystal structure, or vibration or impurity of an atom; electrons get deflected from their path because of such collisions and this scattering produces electrical resistance. But peculiarly, electrons in CNTs are not easily scattered due to their small diameter and very high length to diameter (aspect) ratio. Another peculiarity is that electrons in CNTs can move only forward and backward (1-D character). Only backscattering (moving forward and backward) can generate electrical resistance in CNTs. Backscattering occurs under the circumstances of strong collisions and it is very less likely to happen in case of CNTs. Thus due to very small possibilities of scattering, electrons in CNTs have extremely low electrical resistance. CNTs can be produced by many techniques of which (i) Chemical Vapor Deposition (CVD), (ii) Arc discharge and (iii) Laser Ablation methods are very common.

1.2.2 Polymer nanocomposites

A composite material is a combination of two or more physically or chemically dissimilar materials separated by an interface in order to obtain specific characteristics or properties that were not there before. Two major constituents of composite materials are filler (reinforcement) and matrix. Based on the type of matrix, they are categorized into polymer matrix, ceramic matrix and metal matrix composites. A polymer nanocomposite is a class of polymer composites when at least one of the dimensions of the filler material is in the order of nanometer. Most commonly used nanomaterials are nanoclays, carbon nanofibers (CNFs) and carbon nanotubes (CNTs). Combination of nanomaterials' excellent characteristics such as high electrical and thermal properties, low concentration necessary to produce a high synergistic effect in composite properties etc. together with advanced processing technique has made them the most sought after materials for a wide range of applications [4]. Since the focus of this thesis is using carbon nanotubes as the reinforcing agent, the following sections present a brief review of polymer nanocomposite processing and their electrical properties.

1.2.3 Processing of thermoplastic polymer nanocomposites

Properties of polymer nanocomposites depend on the type of nanotubes, their aspect ratios, dispersion and orientation into the matrix [5]. Ajayan et al. [6] first mixed CNTs in epoxy in 1994 to prepare nanocomposites. After that, a number of fabrication methods using CNTs were developed and most of them focused on improving the nanotube dispersion to obtain composites with improved properties. Three general methods to process the thermoplastic composites are solution blending, melt blending and in-situ polymerization technique. Melt blending in the liquid state is commercially much more

attractive than the other two, as it is environmentally sound since no solvents are required, and gives freedom to end use manufacturers, and minimizes capital costs due to its compatibility with existing processes. In fact, nanocomposites can be made by using a number of shear devices, e.g. extruders, mixers, ultrasonicators. Of these melt-processing techniques, twin-screw extruder is the most appropriate one for high performance thermoplastic resins like PEEK. A co-rotating intermeshing twin screw configuration is usually accepted as an effective tool to achieve a high degree of dispersion and distribution of nanoparticles in molten polymers [7].

Literature reveals that common methods of solution mixing/casting [8-10] and in-situ polymerization [9-11] are widely reported while coagulation [12], electrospinning [13], latex technology [14] , melt-mixing [15-18] are reported in a limited number. Shear intensive melt mixing is a simple, large scale processing technique that is probably the most straightforward route to manufacture thermoplastic nanocomposites [19]. Melt mixing of CNTs into thermoplastic polymers using conventional processing techniques, particularly twin screw extrusion, has been used to prepare a wide range of nanotube polymer blends, including matrices such as polyethylene [16], polypropylene [18], poly (ethylene terephthalate) [20], poly carbonate [17], poly amide [21].

1.2.4 Challenges in processing nanocomposites

The effective utilization of carbon nanotubes in advanced composite applications is strongly dependent on two main factors: (a) alignment of CNTs in the expected direction and (b) homogeneous/uniform dispersion of CNTs throughout the matrix without reducing their intrinsic aspect ratio.

1.2.4.1 Alignment of CNTs

Since CNTs conduct along their length, alignment is a factor that needs to be considered in improving directional anisotropic electrical properties. Due to their small sizes, it is extremely difficult to align nanotubes in polymer materials in a manner accomplished in traditional short carbon fiber (SCF) composites. Lack of control of their orientation reduces the effectiveness of nanotube reinforcement in composites whether for structural or functional performance [22]. During processing, application of magnetic field, AC and DC electric field, spinning the melt in expected direction are some possible ways to improve the nanotube alignment.

1.2.4.2 Uniform dispersion

Uniform dispersion of nanotubes in a polymer matrix is an issue that must be considered. Because of their high aspect ratio, physical entanglements of the tubes, substantial van der Waals attractive interactions arising at nanoscale (0.5 eV/nm) [23], lower surface energy of the nanotube clusters than that of corresponding collection of individual nanotubes, CNTs tend to agglomerate and form aggregates of different sizes which makes their uniform dispersion difficult. The challenge specially comes when the nanotube loading is high. During mixing with a polymer matrix, nanotubes usually experience high shear forces which cause a substantial drop of aspect ratio. Thus, there should be a tradeoff between high aspect ratio and homogenous dispersion. Quantitative characterization of dispersion of CNTs is also a difficult task. Direct microscopic observation and indirect estimative methods are the two main approaches. Dynamic rheological measurements and measurement of electrical conductivity are two indirect estimative methods to characterize the degree of nanotube dispersion in polymer

matrices. The later one is based on the fact that higher electrical conductivity is obtained with better CNT dispersion as more conducting paths are formed. Uniform dispersion depends on the types of polymer, polymer properties especially viscosity and the interaction between polymer and nanotubes.

1.2.4.3 Methods of uniform dispersion

Dispersion of CNTs in a polymer matrix is primarily dependent on the processing methods used. Solution blending, functionalization, ultrasonication and surfactant wrapping, high shear mixing are some of the methods that help in achieving uniform dispersion of nanotubes, but only with small nanotube loadings (less than 5 wt%) [24].

Solution-blending can result in a comparatively fine dispersion of CNTs [25]. Carbon nanotubes are firstly suspended in water or an organic solvent with the help of a surfactant or copolymer, and then a matrix is mixed with the suspended solution to prepare the composites. This is not a suitable technique for many thermoplastic matrices because of poor compatibility of copolymers with the host polymer. Moreover, involvement of too many organic solvents is not desirable in large scale production.

Chemical modification on the carbon nanotube surface, i.e., functionalization at defect sites is an alternative way to improve dispersion of CNTs. An active group such as carboxylic acid or a polymer is introduced onto the surface of CNTs [16] which improves the solubility of CNTs into the polymer and thus processability of composites. But when the electrical conductivity of the composites is under consideration, such chemical functionalization may result in a poor electrical conductivity because of structural change of CNTs arising from chemical reaction.

The dispersion of carbon nanotubes in solvents or polymers with the help of a surfactant or a copolymer is another important method that does not contain any chemical reaction. In a single-step solubilization scheme, nanotubes are mixed with surfactants in low-power, high-frequency sonicators, and the scheme enhances the disaggregation of bundles with dramatically reduced nanotube breakage [16]. However, to prepare nanotube–polymer composites with a homogeneous dispersion of nanotubes, the polymers are required to be water-soluble. In other words, even though CNTs can be dispersed in water with the help of surfactants or copolymers, it is still difficult to uniformly disperse CNTs into a thermoplastic polymer matrix.

Direct mixing using mechanical, shear or ultrasonic techniques is usually used to mix carbon nanotubes into low viscosity thermosetting resins (like epoxy). Therefore, for high viscosity PEEK matrix (viscosity of PEEK at zero shear and 370°C is 687 Pa.sec [26] while viscosity of honey at zero shear and 25°C is about 10 Pa.sec), ultrasonication is not a suitable technique for its mixing.

High shear melt mixing is usually carried out when the nanoparticles are in solid and the polymer matrix is in liquid or powder form [27]. Under these conditions, high shear mixing breaks the initial (primary) aggregates and disperses the nanotubes into the polymer matrix. However, when mixed with a high temperature polymer matrix (like PEEK, PEKK etc.), the achievement of fully homogeneous dispersion of CNTs by melt-mixing is still an unresolved challenge. Depending on the processing equipment and the nature of the polymer matrix, such melt-mixing operation often leads to the formation of undesirable (secondary) agglomerates within the final blends. In order to remove these agglomerates, further high shear stresses are required. In addition, the magnitude of

shearing action is intensified if the polymer to which CNTs are added has high viscosity. PEEK, the polymer used in this study, is one of the highest viscosity thermoplastic polymers. Therefore, PEEK exerts high shear stress on CNTs during mixing which can cause extensive breakage of CNTs. Consequently, nanotubes undergo severe damage which reduces their aspect ratio [18] and electrical performance of the final composites is thus compromised.

1.3 Percolation theory and percolation threshold

Electrical conductivity of polymer composites filled with conductive fillers is strongly dependent on filler concentration, ϕ. At low concentrations, the distance between conductive fillers is larger than their size. Electrical conductivity in such composite systems shows a non-linear increase with increase in filler concentrations up to certain limit, called the 'percolation threshold (ϕ_c)'. Below this critical concentration ($\phi < \phi_c$), there is no obvious conductive path throughout the matrix due to sufficient gaps between the fillers; the fillers are just randomly dispersed in the matrix as isolated individuals. Thus, electrical properties of the whole composites are governed by the properties of insulating matrix. In this region, with increasing filler concentration, local clusters are formed which do not show any significant effect on electrical conductivity. At the percolation threshold, a continuous three-dimensional conductive network of connected fillers is formed through the matrix and a small increase in filler content results in a rapid increase in conductivity of the composite. Above this percolation threshold ($\phi > \phi_c$), electrical conductivity of the composite depends on the conductive networks formed by the fillers. Since the conductive networks are already present in the system, further increase in filler concentration is just similar to an increase in the diameter of a

conductive wire, thus the conductivity will increase marginally against the increase in filler concentration.

Broadbent and Hammersley [28] first introduced the term "percolation theory" in 1957 to show how random properties of a ‘medium’ influence the spread of a ‘fluid’ through it. Using a geometrical and statistical approach, initially they solved fluid flow problems on the determination of the percolation thresholds in simple two and three-dimensional geometries. They considered two types of percolations: site percolation and bond percolation. In site percolation, all the sites in a lattice are either occupied or empty; and in bond percolation, all the sites in a lattice are occupied, but are either connected or not. Stauffer and Aharony [29, 30] calculated the values of percolation threshold for different lattices presented in Table 1.1.

Table 1.1 Percolation Thresholds in two and three-dimensional lattices [30]

Dimension	Lattice	Site percolation threshold	Bond percolation threshold
2	Honeycomb (6)	0.696	0.653
	Triangular (3)	0.500	0.347
	Square (4)	0.593	0.500
	Diamond (4)	0.428	0.388
3	Simple Cubic (6)	0.312	0.249
	Body Centered Cubic (8)	0.245	0.179
	Face Centered Cubic (12)	0.198	0.119

Percolation theory has been applied to many diverse applications, including spread of disease in a population, flow through a porous medium, quarks in nuclear matter, and variable range hopping in amorphous semiconductors [31]. Over the last few decades,

percolation theory has been successfully applied to interpret the electrical conductivity of random mixtures of conductors and insulators [32]. The change in electrical conductivity (σ) above the percolation threshold follows a power law of the form developed by Kirkpatrick [32] and Stauffer [29]:

$$\sigma = \sigma_f \left(\phi - \phi_c\right)^t \quad for \;\; \phi > \phi_c \tag{1.1}$$

where σ_f is the intrinsic electrical conductivity of the filler, ϕ is the concentration of conductive filler, ϕ_c is the percolation threshold and t is an exponent reflecting the dimensionality of the composite. This equation is valid at concentrations above the percolation threshold, i.e., when $\phi > \phi_c$. Application of this equation and further discussion is presented in chapter 3.

1.3.1 Regimes of percolation threshold

Percolation behavior of conductive CNT networks can be categorized into two regimes: a kinetic/rheological percolation threshold at lower CNT concentration and a statistical/ electrical percolation threshold at higher CNT concentration. The difference between them can be explained with the help of following two different viewpoints: (i) inter-nanotube distances required for electrical or rheological percolation (ii) formation of an insulating polymer layer around CNTs.

(i) Assuming that electron hopping applies to the electrical conductivity of nanotube–polymer composites, then required inter-nanotube distance has to be less than 5 nm for the composites to be electrically conductive (electrical percolation) [33]. However, when the inter-nanotube distance becomes smaller than the radius of gyration of the polymer chains i.e. inter-nanotube distance is comparable to the diameter of random coils of the

polymer chains, which is approximately more than 10 nm, the regions of restricted polymer chain motion begin to interact (rheological percolation) [12]. An infinite network of conducting connected paths is then established which causes a rapid increase in electrical conductivity of the composites.

(ii) On the other hand, there exists a possibility of formation of an adsorbed polymer layer around individual carbon nanotubes, which reduces the number of electrical contacts between the nanotubes, whereas the adsorbed polymer layer may have a slight influence on the rheological properties [34]. Therefore, electrical percolation threshold for a given nanotube–polymer system needs high loading level of nanotubes than rheological percolation threshold.

1.4 Electrical properties of polymer nanocomposites

The investigation of electrical properties of CNT reinforced polymer composites has been a challenging and interesting topic for researchers. Because of conductive fillers in an insulating matrix, the existence of a percolated network is an unambiguous criterion. Therefore, electrical properties of the conducting polymer nanocomposites are often analyzed in terms of percolation theory. Due to their exceptional electronic properties in combination with high aspect ratio (l/d = length to diameter ratio >1000), the addition of small amounts of CNTs in an insulating polymer matrix increases the overall electrical conductivity of the composites by several orders of magnitude when a three-dimensional conductive network above the percolation threshold is formed. This threshold amount of CNTs should be as small as possible in the composites while fulfilling its electrical requirements, otherwise the mixing process becomes difficult and the final cost of the

composites becomes high. Sandler et al. [35] first noticed the ultra-low threshold of approximately 0.005 wt% in epoxy-based nanocomposites. Moisala et al. [36] also found the same (0.005 wt%) percolation threshold using MWCNTs in epoxy, but a much higher threshold (0.05 wt% – 0.23 wt%) using SWCNTs in the same matrix. On the other hand, Yoshino et al. [37] reported a high value of the percolation threshold of 12 wt% for MWCNT-PAT composites. Thus, a wide range in the percolation threshold and hence electrical conductivity of nanocomposites can be observed from the results published by many authors, which can be due to some factors, including fabrication route of CNTs, their purification, functionalization, degree and level of dispersion, nature and properties of the host polymer, manufacturing techniques of composites etc. The electrical conductivity of polymer nanocomposites is also affected by CNTs' waviness [38], contact resistance at junctions between CNT–CNT and CNT–polymer due to the formation of thin insulating polymer layers around CNTs [39-44]. Evaluation and optimization of each these parameters are essential in understanding the electrical properties of nanocomposites. The effects of various parameters on electrical properties of different polymer systems are discussed in the following sections.

1.4.1 Effect of type of nanotubes

The percolation threshold of polymer nanocomposites depends on the type of nanotubes (SWCNTs, DWCNTs and MWCNTs) and the surface treatment (purification, oxidation). Threshold values from around 0.06 wt% for arc discharge MWCNTs in PVA [45] to around 5 wt% for oxidized catalytic MWCNTs in PVA [34] have been reported. An extensive experimental study on the electrical conductivity of CNT-epoxy composites was made by Gojny et al. [46] to investigate the effect of types of nanotubes, surface

functionalization, nanotube concentration, their aspect ratio, dispersibility and specific surface area.

In a review, Bauhofer and Kovacs [47] listed 100 publications which report 147 experimental results on electrical percolation threshold of CNTs and the resulting conductivity in different polymer systems. They summarized the published data based on many parameters like CNT type, synthesis method, treatment, dimensionality, polymer type, dispersion methods, composite processing methods, entanglement and non-entanglement of the nanotubes.

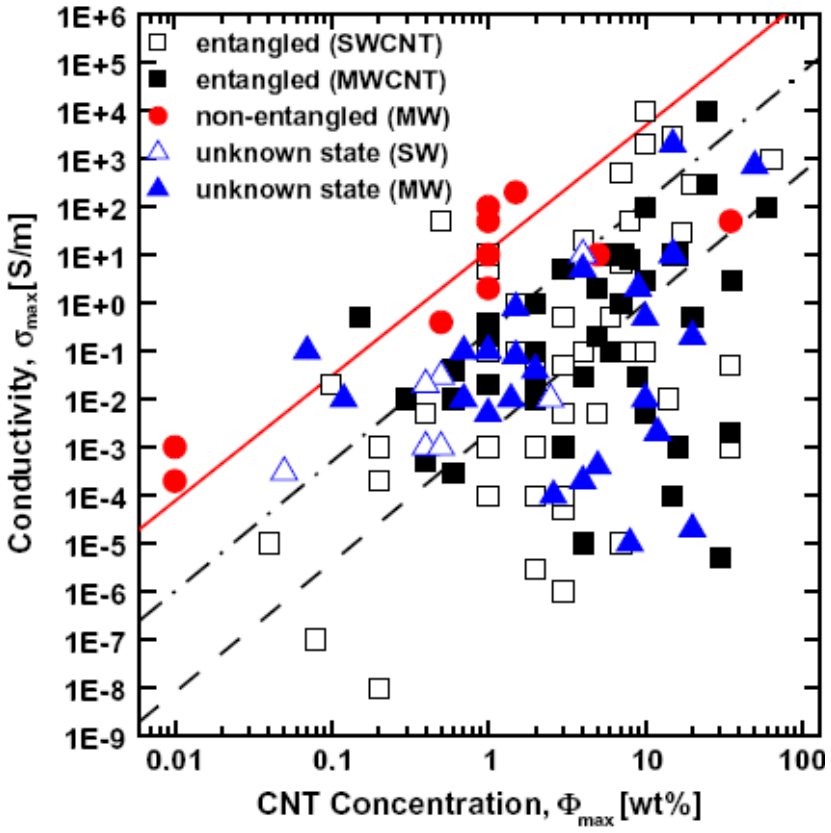

Figure 1.1: Maximum conductivities versus respective CNT concentration in different polymer composites [47].

Figure 1.1 shows the maximum conductivity obtained for different polymers using different types of nanotubes (entangled SWCNT, entangled and non entangled MWCNT, unknown state of SWCNTs and MWCNTs). Different nanotubes impart different amount of conduction to the composites because of their different inherent natures. Non-entangled CNTs gave much higher (50 times) composite conductivities than entangled ones. Two possible explanations for this difference were mentioned: either entangled CNTs could not be dispersed homogeneously or the intrinsic conductivities of entangled and non-entangled CNTs differed by a factor of 50. They also found an indirect proportional relation between maximum conductivity reached for a given CNT concentration and the percolation threshold.

1.4.2 Effect of nanotube quality and dispersion

A detailed study on the electrical conductivity of polystyrene (PS) nanocomposites using industrially produced MWCNT powders (denoted as IPCNTs) and vertically aligned MWCNT films grown in-house by thermal CVD was presented by Grossiord et al. [48]. They found two times higher electrical conductivity and five times lower percolation threshold in the same PS nanocomposites using MWCNT films compared to MWCNT powders, although both sets of the composites showed uniform and stable dispersion in the polymer. The higher performance of MWCNT film based composites was attributed to their aspect ratios which were about 3 times higher than those of MWCNT powders. This was owing to the better structural quality of CNTs from vertically aligned films. Thus, aspect ratios of the CNTs and their intrinsic quality play a role in determining the electrical conductivity of the final composites.

Ramasubramanium et al. [49] investigated the effect of dispersion of CNTs using poly (phenyleneethynylene) (PPE) functionalized SWCNTs on the electrical properties of PS and Polycarbonate (PC) composites. At 7 wt% of SWCNT concentration, they found electrical conductivity of 7 S/m for PS composites and 4.81×10^2 S/m for PC composites. Their study reveals that polymer matrix plays an important role in dispersion of nanotubes and in electrical conductivity of the composites.

1.4.3 Effect of nanotube alignment

Choi et al. [50] reported the contribution of nanotube alignment to the improvement of electrical conductivity of CNT-polymer composites. They explained that a more efficient percolation path in the parallel direction and/or decrease of disorder by alignment of nanotubes was responsible for this improvement. But the opposite result was presented by Du et al. [51] where they claimed to obtain significantly lower electrical conductivity with aligned CNTs than that with unaligned CNTs with the same nanotube concentration in the same polymer matrix. This contradiction was later explained by Behnam et al. [52] who theoretically investigated the effects of CNT alignment on percolation resistivity using a Monte Carlo Simulation. Their conclusion was "*Minimum resistivity occurred for a partially aligned rather than a perfectly aligned nanotube film*". Li et al. [53] also drew a similar conclusion based on their simulation result that, the highest electrical conductivity can be obtained when the alignment angle (with respect to the direction of conductivity measurement) is about 70°~80°. Further alignment tends to reduce the conductivity, because at such alignment, CNTs do not touch each other and there is no network for electron conduction. This explanation supports the experimental results obtained by Du et al. [54] in another analysis. Therefore, the best result in terms of

electrical conductivity can be obtained when the nanotubes are slightly aligned. Concentration of CNTs and viscosity of the polymer also plays a role in determining nanotube alignment. Nanotube alignment, especially when the nanotube concentration is small, affects the anisotropy of conductivity, but the effect of nanotube alignment becomes weaker at large nanotube concentrations [55].

1.4.4 Effect of processing conditions

Using CNT based epoxy composites; Kovacs et al. [56] studied the effect of production method, dimensionality and entanglement state of CNTs and preparation of nanocomposite samples on their electrical conductivity. They used aligned and non-entangled MWCNTs processed by Aerosol Chemical Vapor Deposition (ACVD) and Catalytic Chemical Vapor Deposition (CCVD) and varied each parameter while keeping others constant to assess its effect. Their studies showed that initial conductivity of the nanotubes did not play any role in improving the electrical conductivity of the composites. Formation of a thin insulating polymer layer between CNTs that blocks their conduction path was attributed to this effect. They also found that at higher concentrations, entanglement of nanotubes improved the electrical conductivity of composites. Grossiord et al. [57] also studied the effect of processing parameters on electrical conductivity using CNT-PS composites. They found higher electrical conductivity and lower percolation threshold by changing the processing conditions, such as increasing the time and temperature of compression.

1.4.5 Effect of physical properties of filler

Based on an excluded volume analysis made by Celzard et al. [58], the percolation threshold of a composite should decrease with increasing filler aspect ratio. For MWCNT-epoxy composites, Bai et al. [59] found decreasing percolation threshold with increasing CNT length, but Martin et al. [60] found an opposite result. The explanation given by Bauhofer et al. [47] for this inconsistency is that Bai et al. obtained electrical/statistical threshold while Martin et al. obtained rheological/kinetic threshold. Available theoretical analysis cannot take into account the movement of filler particles and hence predict only the dependence of the statistical threshold on the filler aspect ratio. Narkis and Vaxman [61] also showed that the conductivity of a polymer composite is highly dependent on filler aspect ratio. Using carbon fiber, they found that higher conductivity can be achieved at higher aspect ratio. Therefore, filler attrition should be minimized during processing of the composites. After investigation of SCF-NBR composites, Pramanik et al. [62] suggested that inter-particle contact is more likely when surface to volume ratio of the carbon fiber is high, which gives rise to higher electrical conductivity and hence lower percolation threshold.

1.4.6 Nature and properties of polymer

The percolation threshold can be minimized and electrical conductivity of the composites can be optimized by a right choice of host polymer, because it affects the behavior of fillers in the composite during the processing stage. Polarity, viscosity and degree of crystallization of the polymer etc. are some criteria of the choice of polymer.

1.4.6.1 Polarity of polymer

Miyasaka et al. [63] investigated electrical conductivity of composites with respect to percolation threshold of fillers using different types of polymer matrices. They found higher percolation threshold for polymers with higher polarity. A similar correlation has also been demonstrated in [64] between electrical conductivity of composites and polarity of the polymer. However, a contradictory relationship of polymer polarity and percolation threshold was shown by Sau et al. [65] in their study using ethylene-propylenediene monomer rubber (EPDM)/acrylonitrile butadiene rubber (NBR)/their blends and acetylene black systems. Usually, EPDM and NBR are considered as non-polar and highly polar polymers respectively. But EPDM- acetylene black systems exhibited higher critical concentration than NBR-acetylene black systems.

1.4.6.2 Viscosity of polymer

Percolation threshold and hence electrical conductivity are also affected by viscosity of the polymer [66]. Diffusivity of CNTs in the polymer depends on the polymer viscosity as it determines the extent of reorganization of CNTs within a given amount of time. High percolation threshold is obtained with a high viscosity polymer matrix. Earlier it was mentioned for CNT composites that the structure of CNTs degrades due to the high shearing action experienced during the mixing process. The higher is the viscosity of the polymer, the higher is the shearing force experienced by the CNT aggregates and thus the greater is the degree of CNT-structure breakdown. Consequently, the formation of a conductive three dimensional network throughout the matrix is more difficult and occurs at a higher concentration. A similar trend was also found true for carbon fiber filled systems [65].

1.4.6.3 Degree of polymer crystallization

Generally in semicrystalline polymers, CNT aggregates tend to concentrate in amorphous regions due to short-distance order of molecular structure in contrast to the crystals having long-distance order. As a result, the percolation concentration in semicrystalline systems should be lower than that in amorphous polymers. Narkis and Vaxman [61] studied electrical resistivity of high density polyethylene (HDPE) mixed with conductive carbon blacks and reported that polymer crystallization plays an important role in obtaining electrical conductivity.

1.5 Theoretical studies on electrical conductivity of polymer composites

In addition to the experimental works, a significant number of theoretical investigations were also made on the electrical conductivity of polymer composites. Using a continuum theory, Kyrylyuk and Schoot [67] predicted the effect of polydispersity, bending flexibility and attractive interactions between CNTs on the electrical conductivity of nanotube polymer systems. They discussed that formation of a CNT network is dependent on electron tunneling distance between the CNTs which in turn depends on the properties of the polymer and CNTs. Li et al. [38, 39] as well as Li and Chou [39, 53, 68, 69] have examined the contributing factors to electrical conductivity of nanocomposites and performed Monte Carlo simulation of the percolation threshold. In their modeling, some of the key issues were to identify filler contact status, establish a wavy nanotube network, determine the percolation threshold and modeling the contact resistance.

1.5.1 Effect of nanotube alignment

As mentioned earlier, Behnam et al. [52] and Li et al. [53] investigated the effect of nanotube alignment on electrical conductivity above the percolation threshold using three-dimensional Monte Carlo simulation and explained the experimental results reported by Choi et al. [50] and Du et al. [51]. White et al. [70] also found similar results in terms of filler alignment in their study of the effect of alignment and concentration of fillers on the electrical conductivity of composites. Using a random resistor model and filler aspect ratio of 10, 20 and 80, they showed that fillers with higher aspect ratio gave wider range of concentration and filler orientation compared to those of the fillers with lower aspect ratio to achieve same level of electrical conductivity.

1.5.2 Effect of contact resistance and tunneling resistance

Contact resistance and intrinsic electrical conductivity of CNTs are the most important factors in developing highly conductive composites. The contact resistance between metallic–metallic and semiconducting–semiconducting CNTs can be close to 100–400 kΩ and two orders higher for metallic–semiconducting CNTs [71]. Contact resistance between CNTs can vary from 100 kΩ to 3.4 MΩ [40] and an insulating polymer layer between CNTs further increases this contact resistance ($\approx 10^{13}$ Ω) [44] by making electron tunneling difficult when the polymer thickness is considerably high [72].

Li et al. [39] theoretically investigated the effect of nanotube–nanotube contact resistance and tunneling resistance on electrical conductivity of CNT-epoxy and CNT-alumina composites. Their results showed (Figure 1.2) that with the increase of insulating thickness layer, tunneling resistance increases rapidly. An increase in diameter resulted in a moderate effect of decrease in tunneling resistance.

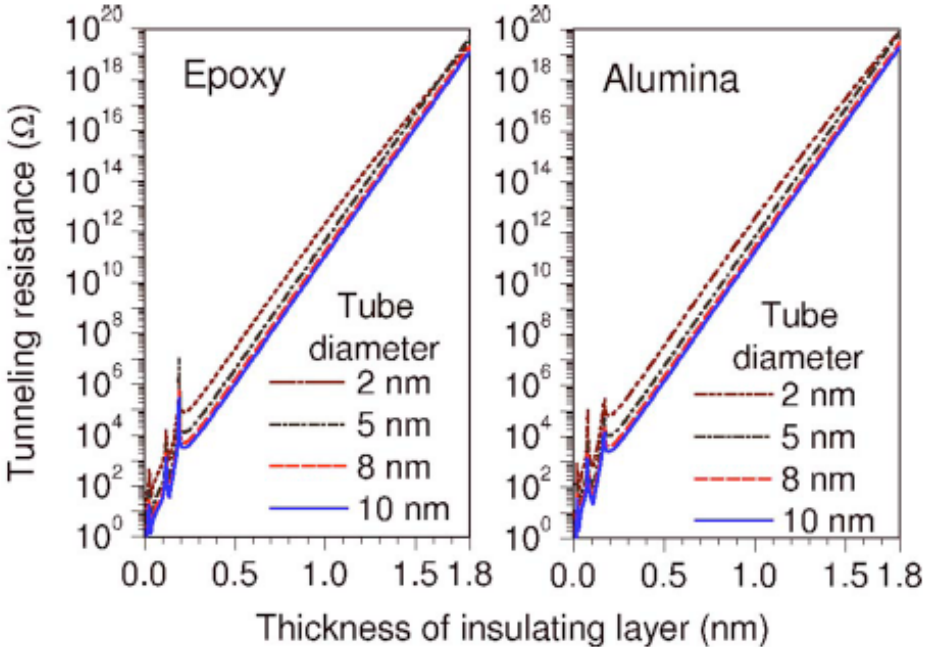

Figure 1.2: Effect of thickness of insulating layer on tunneling resistance [39].

Electrical conductivity of the composites was also strongly affected by tunneling resistance. Their simulation results showed that highest allowable thickness of the insulating layer can be 1.8 nm for tunneling and proved that tunneling resistance plays a dominant role in determining the properties of nanocomposites as compared to the intrinsic resistance of CNTs in CNT mats.

1.5.3 Effect of nanotube waviness

Waviness of CNTs affects percolation threshold and hence electrical conductivity because of dominant role of contact resistance. Assuming a constant contact resistance for all contacts and a uniform thickness of insulating film for a homogeneous and ideal dispersion of nanotubes in the matrix, Li et al. [38] investigated the effect of nanotube waviness on electrical conductivity. Their results shown in Figure 1.3 (a) indicates that the conductivity of composites increases with nanotube concentration for different curl

ratios of nanotubes and electrical conductivity of composites with wavy nanotubes is much lower than that of composites with straight nanotubes. Two neighboring wavy nanotubes dispersed in a polymer matrix tend to have a higher chance of contacting each other at more contact points than straight nanotubes. As a result, the contact resistance in the case of wavy nanotubes is higher than that of straight nanotubes which affects the overall conductivity of the composites. Shown in Figure 1.3 (b), electrical conductivity gradually decreases with increasing nanotube curl ratio for a given nanotube concentration. This decrease of conductivity is due to the increase of nanotube waviness which was also confirmed by the numerical simulation results of Dalmas et al.[73].

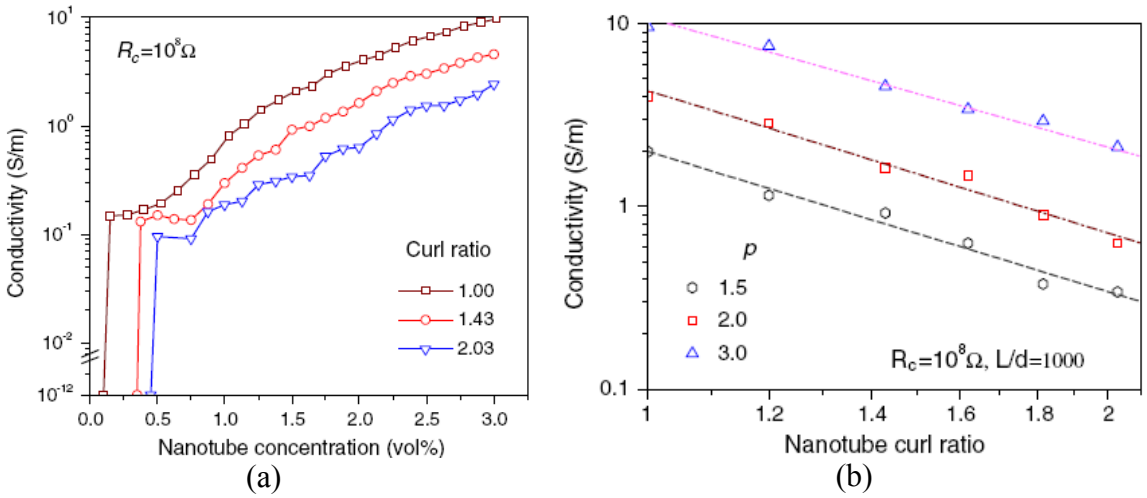

Figure 1.3: Effect of nanotube waviness on electrical conductivity of composites [38]. (Here R_c denotes contact resistance)

However, from percolation point of view, wavy nanotubes having contact points more than straight nanotubes should help to reduce dependence on tunneling and as such, it should provide increased conductivity for the composites.

1.6 Application of CNT composites

CNTs when mixed with a polymer matrix produce a low percolation threshold and a high electrical conductivity while retaining other mechanical properties – that cannot be obtained with any other filler. A number of research work using SWCNTs and MWCNTs as reinforcing fillers with thermoplastic polymers (e.g. PP, PS, PMMA, nylon 12) have been conducted in the last few years. CNTs find their applications as conductive filler in thermoplastics across the field of automotive, aerospace, electronics, sensors, hydrogen storage, space research, pharmaceuticals and so on. In multifunctional polymeric composites, they can be used as pressure and temperature dependent resistors, over temperature protection devices etc. They can be used as sensing and actuating element where the ambient pressure and temperature are not constant. Their dependence of electrical conductivity for conductive thermoplastic composites is an omnipresent but complicated phenomenon. It has been the topic of research for many authors. According to the rate of decrease or increase in resistivity with pressure and temperature, different behaviours are observed. Depending on the type of polymer, concentration of fillers and their properties, the temperature coefficient (TC) of resistance can be positive (PTC), negative (NTC) or zero (OTC). Similarly, pressure coefficient of resistance may be positive (PPC), negative (NPC) or zero. The combined result of several processes that the composites undergo at high pressure and temperature determines this coefficient. The number of filler particle contact, thermal expansion of polymer matrix and filler particle, the modulus of polymer matrix etc. are the important factors contributing to those processes. Several other phenomena are also simultaneously operative in the system which can cause a decrease in electrical resistance (increase in conductivity):

(i) Flocculation: rearrangement of filler particle leading to the formation of further conductive networks (of woolly cloudlike aggregations) during heating, and

(ii) Thermal emission: High temperature electron emission between two filler aggregates separated by a small distance (but distance of separation is not equivalent to their physical contact)

Usually the polymer matrix expands more than the conductive filler and their differential thermal expansion results in an increase of distance between conductive fillers, thus making the electron tunneling more difficult. The modulus of the polymer matrix plays an opposite role in this case, i.e. a polymer with lower modulus expands more and vice versa against temperature.

Several authors investigated the effect of pressure and temperature on the electrical conductivity of rubber composites, polymer composites and some of their works were specially focused on the application of composites as pressure sensors and temperature sensors. For example, Sau et al. [65] in their investigation found that the volume resistivity of all fiber-rubber composites increases with increase in temperature and the change in volume resistivity during heating and cooling cycle leads to the phenomena of electrical hysteresis and electrical set. They also measured the change in electrical conductivity of CB-rubber composites subjected to different modes of pre-strain [74]. Das et al. [75] studied the effect of processing parameters like mixing time, rotor speed, mixing temperature, vulcanization time and pressure and service conditions like applied pressure and temperature on the electrical resistivity of rubber based composites. They used carbon black and short carbon fiber (SCF) as the filler material in their study.

According to their result, the temperature dependence of volume resistivity of conductive CB-filled composites showed a negative temperature co-efficient (NTC) and SCF-filled composites showed a positive temperature co-efficient (PTC). Electrical resistivity decreased with increasing applied pressure up to a certain level for all CB-filled composites except EPDM based CB composites whereas electrical resistivity of SCF-filled composites increased with increasing applied pressure.

Carmona and Amarti [76] experimentally showed that electrical anisotropy of unidirectional composites varies with temperature and pressure. Their main observation was that as the fiber volume concentration increases, the change of relative anisotropy undergoes opposite variations when temperature or pressure is increased. The effect of polymer molecular weight on the percolation threshold of PEO-Carbon composite and incremental sensor temperature effects on PEO-Carbon sensor response were investigated by Holmer et al. [77]. They showed a correlation between polymer molecular weight and percolation threshold and also observed sensor properties as a function of temperature at different carbon loadings. Further literature reviews are categorically provided in chapters 5 and 6.

1.7 Rationale and objectives of the thesis

Surveying of the literature shows that most of the research in the field of nanocomposites reports the use of CNTs in composites containing thermosetting resins (especially epoxy), elastomers (e.g. natural rubber, SBS) and thermoplastics (e.g. poly ethylene, polypropylene, polycarbonate) and these are mostly concerned with mechanical or thermo-mechanical properties. Electrical properties of these systems, specifically with

high performance thermoplastics have scarcely been investigated and their potential has not yet been fully harnessed. A fundamental understanding of electrical conductivity of composites with embedded carbon nanotubes is necessary. Therefore, the objectives of this thesis are:

(i) an investigation on how systematic incorporation of CNTs in thermoplastics (specifically PEEK) and the resulting electrical conductivity response to an applied electric field,

(ii) identification and evaluation of the parameters influencing this response, and

(iii) the fundamental understanding of the mechanisms determining this response and their verification.

Despite the availability of mechanisms to explain the behaviour of such conductive polymer composites filled with nanotubes, there are some areas that lack sufficient explanation and examination. True understanding of the phenomena involved in the effect of pressure and temperature on electrical conductivity is one of them. A convincing explanation of PTC and NTC effect especially with a varying concentration of nanotube and different polymer systems at temperatures above the glass transition temperature is not available.

This thesis addresses the above by developing electrically conductive polymer composites made of MWCNTs and thermoplastic polymer PEEK and by analyzing both experimentally and theoretically the change in their electrical conductivity under application of high pressure and temperature. Special emphasis is given to understand the basic parameters and their effect towards this change in conductivity.

1.8 Organization of the thesis

Chapter 1 describes the scope and objectives of this dissertation with some highlights of nanocomposites' background and their applications. Processing techniques, challenges in manufacturing nanocomposites and factors affecting their electrical properties are also presented with relevant references.

Materials used in this study, experimental aspects and preparation of nanocomposite samples, optimum processing parameters and characterization of the samples by scanning electron microscopy are addressed in chapter 2.

Chapter 3 presents an elaborate study and analysis of electrical and dielectric properties of nanocomposites obtained by Impedance spectroscopy measurement in the light of percolation theory.

Chapter 4 presents an estimation of contact resistance in combination with tunneling resistance by different models. It shows a detailed analysis how nanotube film thickness affects the tunneling resistance and hence electrical conductivity of the nanocomposite samples.

Chapter 5 is based on the experimental results of the electrical conductivity under application of compression. Contribution of nanotube film thickness in increasing electrical conductivity is highlighted.

Chapter 6 elaborates the effect of temperature on electrical conductivity of these conductive composites. Analysis of conduction mechanism and effect of parameters

involved in conduction are also presented. Effect of temperature when it is combined with pressure is also investigated.

Finally, the findings of this thesis are summarized in chapter 7 with conclusion, contribution and recommendations for possible future work.

Chapter 2

Materials and Experiments

2.1 Introduction

In many applications the need for materials with high temperature resistance and high strength is gradually increasing. Thermoplastics are attractive for their high strain to break, ability to thermoform, indefinite shelf life and light weight, but they are not strong and tough like metals and other conventional engineering materials. Reinforcement of thermoplastics with nanoparticles can improve the strength and rigidity of the resulting composites.

Poly ether ether ketone (PEEK) is a high performance engineering thermoplastic with a high glass transition and melting temperatures, excellent mechanical properties, and good solvent and abrasion resistance. Due to molecular rigidity of its repeat unit, its semi crystalline nature admits it to the orientation processes to provide high strength over a wide range of temperatures. It shows a unique combination of thermal stability, chemical inertness, high wear resistance and friction coefficient. It can be compression molded, extruded or injection molded using conventional equipment at sufficiently high processing temperatures (≈ 350°C ~ 400°C). It has been used in wide range of applications such as medicine, electronics, telecommunication and transport industries (automobiles and aerospace) [78]. PEEK is sometimes used in space applications to replace aluminum because of its excellent performance at high temperatures. However, adverse processing conditions and comparatively higher cost limit the use of this resin to some extent in commercial applications. On the other hand, because of their intrinsically

superior properties, improvements in both rheological and composite properties might be obtained at lower concentrations of carbon nanotubes (CNTs) among other nanoparticles, while retaining their large aspect ratio. Since PEEK is a high cost, high performance polymer, improvements obtained by adding CNTs are relatively cost-effective.

Since the electrical properties of CNTs are dependent on the nanotube diameter, number of concentric shell and chirality, electrical properties of the nanocomposites can conveniently be adjusted by selecting proper parameters [79]. The intrinsic conductivity of carbon nanotubes in this regard plays an important role and is the upper limit for electrical conductivity of the composites. Diez-Pascual et al. [80, 81] demonstrated that properties of PEEK can significantly be improved by the addition of SWCNTs. Gojny et al. [46] showed that MWCNTs offer the highest potential for enhancement of electrical conductivity. In this study, MWCNTs were chosen to mix in PEEK, because they are generally conducting, comparatively easier to disperse in PEEK due to much lower absorption energy than that of single walled carbon nanotubes (SWCNTs).

2.2 Materials

Poly ether ether ketone (PEEK) powder purchased from Good Fellow, England was used as polymer matrix and multi walled carbon nanotubes (MWCNTs) Bay tubes C150P (C-purity $\geq$ 95 wt%, synthesized by chemical vapor deposition) purchased from Bayer Material Science, Germany was used as the filler to fabricate the samples. Both MWCNTs and PEEK were used 'as received' without any further treatment in this study.

Their properties are given in the following Table 2.1 and Table 2.2.

Table 2.1: Physical properties of PEEK (Supplier's data)

Mass Density	1.263 g/cm^3
Average Powder size	80 micron (μm)
Young's Modulus, E	3.7 ~ 4.0 GPa
Poisson's ratio,ν	0.4
Co-efficient of thermal expansion (CTE)	25 μm/m°C
Glass Transition Temperature (T_g)	143~146°C
Melting Temperature (T_m)	350~390°C
Electrical resistivity (ρ)	10^{15} ~ 4.9 × 10^{16} Ω-cm
Relative permittivity (ε_r)	2.8~3.3 @ 10^3 Hz

Table 2.2: Physical properties of MWCNTs (Supplier's data unless otherwise stated)

Mass Density	2.2 g/cm^3
Young's Modulus	1.0 ~ 1.2 TPa
Poisson's ratio,ν	≈ 0.07 From reference [82]
Electrical conductivity	10^2 ~ 10^5 S/cm
Length	1 ~ >10 μm
Outer diameter	13 ~ 16 nm
Inner diameter	4 nm

2.3 Choice of manufacturing technique

Considering the relative advantages and disadvantages of the all methods mentioned in 1.2.4.3 for improving CNT dispersion, high shear melt mixing was simply adopted to manufacture nanocomposite samples for this study without any further mechanical/chemical treatment of the nanotube and PEEK. This is because, melt-mixing is a practical and industrially-relevant process as it allows the manufacture of either semi-finished (extrusion) or finished (injection-molded) parts, independently of volume and complexity [33]. It is particularly desirable because the process is fast, simple, inexpensive, free of solvents and contaminants and available in the plastic industries [83].

2.4 Determination of optimum processing parameters

In high shear melt mixing, three parameters are considered to be important in manufacturing composite samples possessing high electrical conductivity, namely mixing temperature, rotor speed and mixing time. To determine the optimum magnitude of one single processing parameter, mixing was done while keeping other parameters constant. Three different concentrations (2 wt%, 3 wt% and 3.4 wt% were arbitrarily selected) of CNTs are mixed with PEEK to determine the optimum point of those processing parameters. Based on material properties, equipment specification and literature data, several values for each of the parameters were selected. For mixing temperature: 360°C, 370°C, 380°C and 390°C, for rotor speed: 80 rpm, 100 rpm and 120 rpm, for mixing time: 10 min, 15 min, 20 min and 25 min were selected. The melting and high temperature shear mixing was carried out in a laboratory scale Torque Rheometry system Brabender Intelli-Torque Plasti-Corder (type IT 7150). To achieve uniform dispersion of nanotubes, helical shaped twin screw extruders were used in the mixing machine.

The irregular shaped extrudates of CNT-PEEK melt were cooled very quickly and milled at room temperature and then dried in an oven at 100°C for 3 hours to remove the moisture. Then it was processed in a Wabash compression molding machine at 380°C with compaction load of 10 tons and a holding time of 15 minutes using a rectangular stainless steel plate of 152.4 mm × 152.4 mm × 1.4 mm with six holes of 25.4 mm diameter. This produces six samples having 25.4 mm diameter and 1.4 mm thickness at a time. Cooling of the samples were progressively done first by air (slow cooling rate, from 380°C to 175°C), then by air and water (medium cooling rate, 175°C to 90°C) and finally by water (fast cooling rate, from 90°C to room temperature). After cooling and

solidification, the samples were removed from the mold, polished and checked for electrical conductivity using an Agilent High Resistance meter (Model 4339B). This model is designed for measuring very high resistance and related parameters of insulating materials. All measurements were made at 1.0 Volt. The instrument was calibrated according to the manufacturer's recommendations before use.

2.4.1 Mixing temperature

2 wt%, 3 wt% and 3.4 wt% of CNTs were mixed with PEEK and melted in the Brabender at 360°C, 370°C, 380°C and 390°C at constant rotor speed of 80 rpm and mixing time of 15 min. Then following the procedure mentioned above, the samples' electrical conductivity was checked.

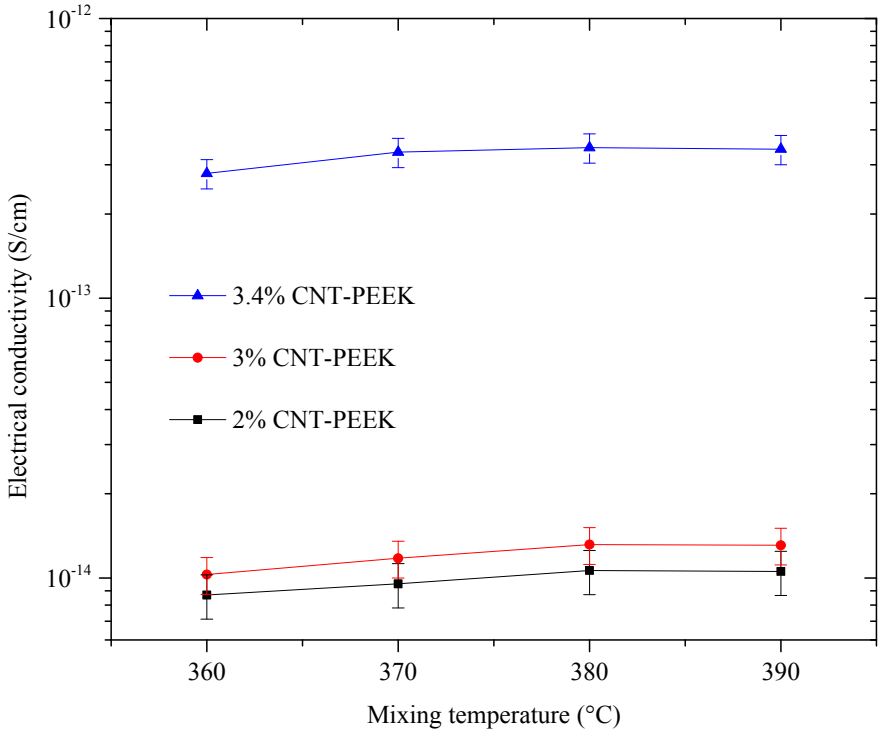

Figure 2.1: Electrical conductivity as a function of mixing temperature.

Figure 2.1 shows the mixing temperature vs. Electrical conductivity. Electrical conductivity gradually increases with increasing mixing temperature from 360°C to 380°C and then it becomes almost constant. With the increase in mixing temperature, the viscosity of PEEK decreases which results in less shear of CNTs during mixing. Therefore, increase in mixing temperature favours the formation of the conductive network. At 380°C and above, the saturation point of electrical conductivity has been reached. Further increase in temperature may cause thermal degradation of the polymer and substantial decrease of electrical conductivity.

2.4.2 Rotor speed

The same concentrations of CNTs were again mixed with PEEK and melted in the Brabender at 80 rpm, 100 rpm and 120 rpm at a constant mixing temperature of 380°C and a mixing time of 15 min.

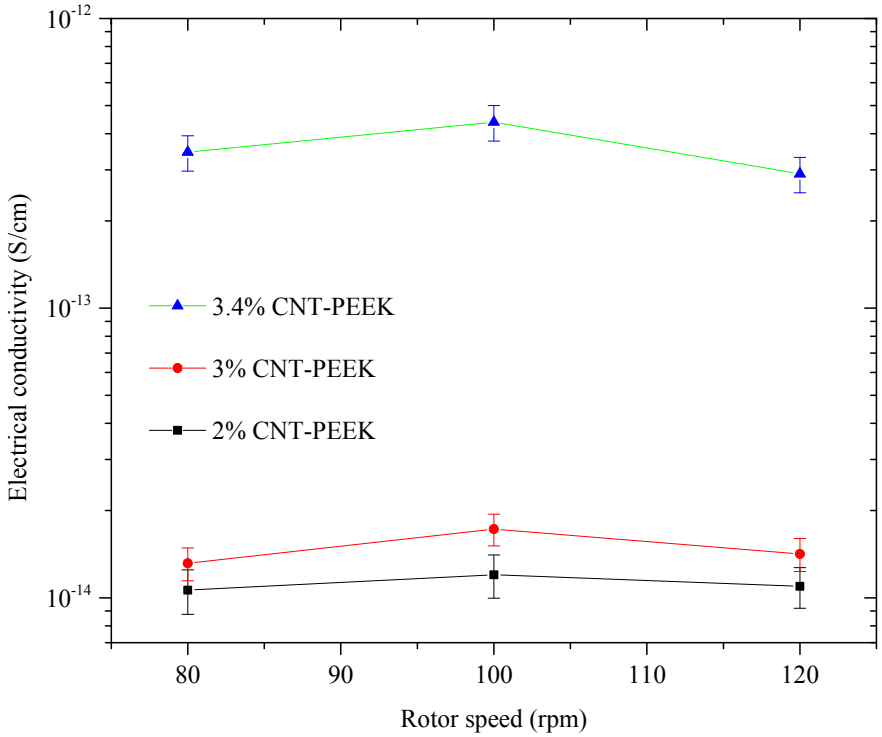

Figure 2.2: Electrical conductivity as a function of rotor speed.

The samples thus obtained are presented in Figure 2.2 in terms of their electrical conductivity vs. rotor speed. It has been observed that for all the samples, electrical conductivity moderately increases when rotor speed increases from 80 to 100 rpm at constant mixing time and temperature, but beyond 100 rpm, conductivity decreases. It can be argued that with the initial increase of rotor speed, CNT aggregates undergo breakage sufficient to form the conductive network, but further increase of rotor speed beyond 100 rpm leads to appreciable breakdown of CNT-structure due to high shearing action. As a result, nanotube aspect ratio decreases causing a drop in electrical conductivity.

2.4.3 Mixing time

The same concentrations of CNTs were mixed with PEEK and melted in the Brabender for 10 min, 15 min, 20 min and 25 min at a constant rotor speed of 100 rpm and a mixing temperature of 380°C. The effect of mixing time on electrical conductivity is similar to that of rotor speed as shown in Figure 2.3. Initially electrical conductivity increases with increasing mixing time from 10 to 20 minutes. Initially mixing facilitates better distribution and dispersion of CNTs into PEEK and causes breakdown of primary agglomerates, the eventual result of which is the increase in electrical conductivity. But further increase in mixing time causes (i) reduction of nanotube aspect ratio along with gradual increase in inter-nanotube distance due to the breakdown of continuous conducting network that was initially formed and (ii) formation of secondary agglomerates. As a result, electrical conductivity of the system decreases.

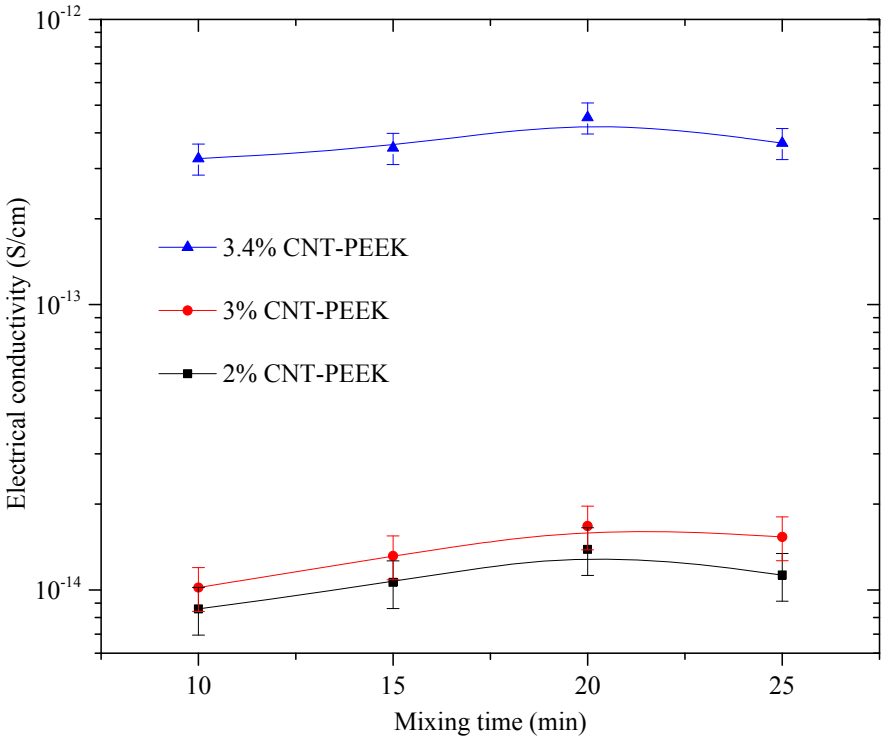

Figure 2.3: Electrical conductivity as a function of mixing time.

In the above discussion, electrical conductivity of the composites was found to be nonlinearly dependent on the processing parameters. It was observed that processing conditions affect the formation of conductive network favourably or adversely and thus have a positive or negative effect on the conductivity. The highest electrical conductivity was obtained for the processing conditions of mixing temperature 380°C, rotor speed 100 rpm and mixing time 20 minutes, thus they are considered to be optimum processing parameters for the rest of the analysis.

2.5 Preparation of nanocomposite samples

After determination of the optimum processing parameters, different weight concentrations of CNTs (p) ranging from 1% to 10% were mechanically mixed with

PEEK to prepare nanocomposite samples for the next investigation. Volume concentrations of CNTs (ϕ) were calculated using the equation

$$\phi = \frac{p}{p + (1-p)\frac{\lambda_f}{\lambda_m}} \tag{2.1}$$

where λ_f = density of CNTs and λ_m = density of PEEK extracted from Table 2.1 & Table 2.2 respectively. It was melted in the Brabender at 380°C at rotor speed of 100 rpm for 20 minutes and then processed according to the procedure described in the previous section 2.4. The measurement of electrical conductivity of the samples was made according to the procedure described later in section 5.2.2.

2.6 Scanning Electron Microscopy (SEM)

The SEM observations of fractured surfaces of composites containing different concentrations of CNTs were made using a Hitachi S-4700 scanning electron microscope in order to correlate the morphology of the samples with electrical conductivity. The samples were subjected to brittle fracture in liquid nitrogen and the fractured surfaces were sputter-coated with a thin layer of gold before observation. Figure 2.4 shows the morphology and dispersion of pure PEEK and PEEK composites containing 3.5, 3.6, 8, 9 and 10 wt% of CNTs for same magnification and scale (1 μm).

In semicrystalline materials, amorphous state is in general more disorderly than crystalline state. There is more empty space in the amorphous region as compared to the crystalline region. As such, it is easier for foreign particles to enter the amorphous region.

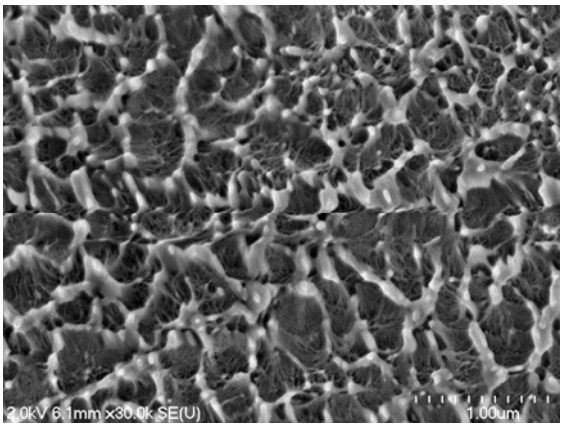

(a) Pure PEEK

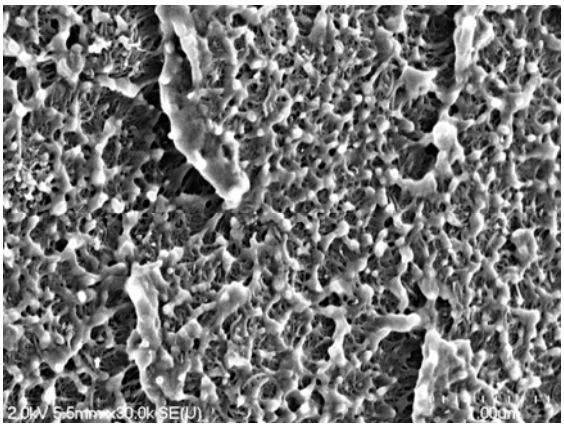

(b) 3.5 wt% CNT-PEEK

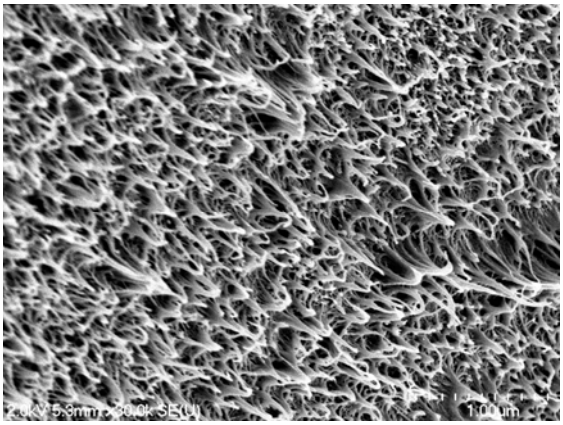

(c) 3.6 wt% CNT-PEEK

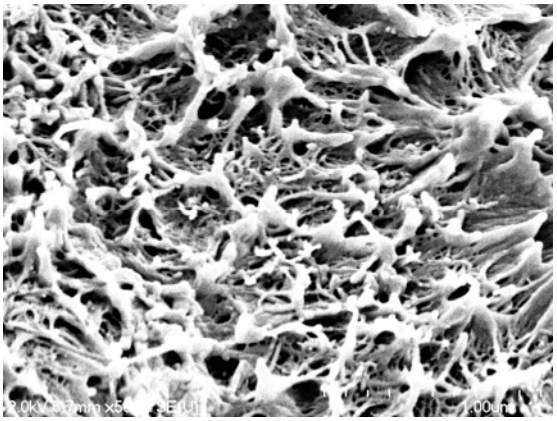

(d) 8 wt% CNT-PEEK

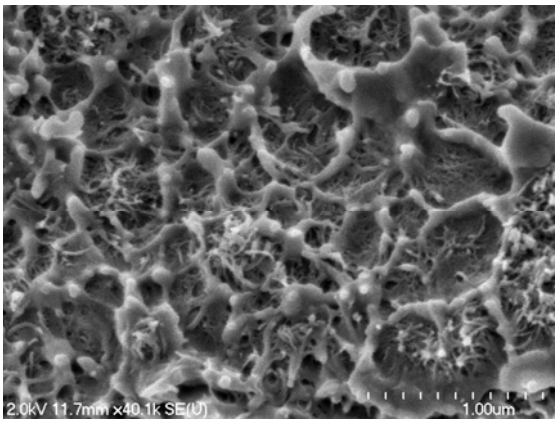

(e) 9 wt% CNT-PEEK

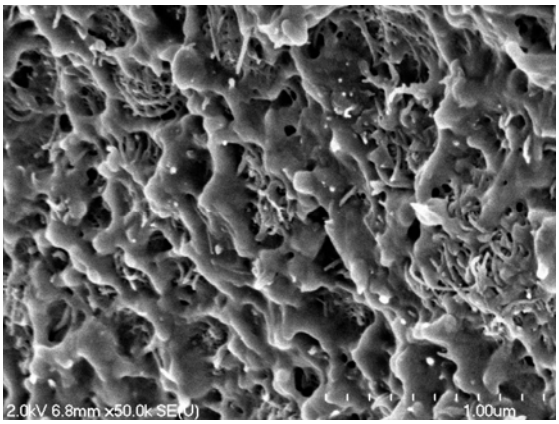

(f) 10 wt% CNT-PEEK

Figure 2.4: SEM Micrographs of fracture surface of PEEK containing different concentrations of CNTs.

For pure PEEK shown in Figure 2.4(a), there appear to be grains surrounded by the boundaries. Similar observation is made in Figure 2.4(d), (e) and (f). However, the granular structure does not appear in Figures 2.4 (b) and (c). These two figures correspond to the amount of CNTs at percolation. One possible explanation for this is that at percolation, there is a good dispersion of CNTs such that the grain structure disappears. At higher loading of CNTs, the excess amount of CNTs concentrates more in the grain boundaries. This makes the grain boundaries thicker (compare between Figure 2.4 (a) and Figures 2.4 (d), (e) and (f)).

2.7 Variability in electrical conductivity as a function of CNT concentration

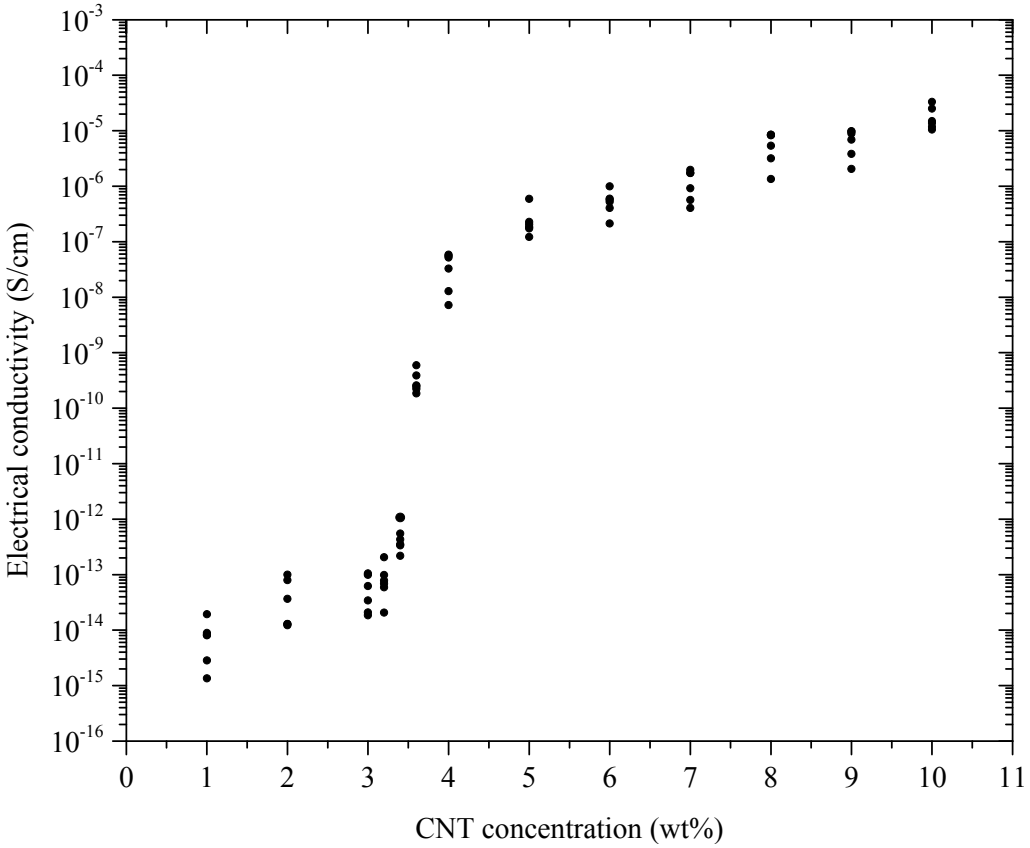

Figure 2.5: Variation of Electrical Conductivity of CNT-PEEK composites for different wt% of CNTs.

During the fabrication of samples by compression molding, six samples were manufactured at a time in one batch. Several batches for each concentration of CNTs were made to check the variability of electrical conductivity of the samples.

Figure 2.5 shows the variation of electrical conductivity for one representative batch with different weight concentrations (from 1% to 10%) of CNTs mixed in PEEK. At the same mixing condition, as the amount of CNTs was increased, average deviation of magnitude of electrical conductivity from the mean value was found to be decreasing. For example, typical values of standard deviation of electrical conductivity were 90% for 2 wt% CNTs, 68% for 3 wt% CNTs, 61.5% for 4 wt% CNTs, 47% for 6 wt% CNTs, 45% for 7 wt% CNTs, 40% for 8 wt% CNTs, 37% for 9 wt% CNTs and 35% for 10 wt% CNTs. From the samples of all batches together, at least three samples having minimum difference in magnitude in their electrical conductivity were chosen for the next study of electrical characterization and the effect of pressure and temperature on electrical conductivity.

Chapter 3

Electrical Properties of CNT-PEEK Composites

3.1 Introduction

Conductive filler particles are incorporated into an insulating polymer matrix mainly to produce conductive composites. The fillers play an important role in improving mechanical, electrical and thermal properties of polymer composites. Electrical properties of the composites may vary from those of the insulating matrix to those of conducting filler depending on filler concentration, property of the fillers and dispersion of the fillers into the polymer matrix. The conductive fillers increase the overall electrical conductivity and dielectric properties by several orders of magnitude when a continuous conductive network develops throughout the matrix above a critical concentration of fillers (percolation threshold). Below this percolation threshold, conducting fillers are dispersed as isolated clusters, whereas above the percolation threshold, filler clusters begin to connect to each other to form a three-dimensional conductive network [84]. Transition from isolated clusters to connected network of conducting filler is called the percolation transition [85].

Many studies on the electrical properties of thermoplastic polymer matrix composites filled with CNTs and other nanofillers have been reported in the literature. For example, Liang and Tjong [84] presented the results of electrical properties of melt compounded MWCNT-low density polyethylene (LDPE) as a function of CNT volume concentration, frequency and temperature. Logakis et al. extensively analyzed the frequency dependent electrical and dielectric properties of melt processed CNT reinforced Poly Methyl

Methacrylate (PMMA) [83] and polyamide [86] composites. Yu et al. [87] manufactured polypropylene based MWCNT and bariam titanate (BT) nanocomposites by melt compounding and showed that electrical conductivity increases by 6 orders of magnitude at 10^2 Hz when MWCNT loading increases from 3 wt% to 5 wt%. Surface modification of CNT by titanate coupling agent greatly improves the electrical conductivity and reduces the percolation threshold of PP nanocomposites. They also observed a significant improvement in dielectric properties of PP/BT nanocomposites with incorporation of MWCNT. Ounaies et al. [88] discussed percolation issues for SWCNT-Polyimide composites (prepared by in-situ polymerization with sonication) through a combination of experimental and computational methods. Dai et al. [89] used very well aligned SWCNT in PMMA matrix to investigate mechanical, thermal and electrical properties. Peng and Sun [90] synthesized highly aligned CNT composites using high quality CNT arrays in PMMA, polystyrene (PS) and PEEK matrices and obtained much improved electrical conductivities (10 S/cm, 13.3 S/cm and 22 S/cm respectively) at room temperature. Khattari et al. [91] recently published their work on dielectric properties of MWCNT-PMMA composites using impedance spectroscopy technique in the frequency range of 10 to 10^5 Hz and in the temperature range of 30°C-110°C at different CNT concentrations. They obtained percolation threshold to be between 8.5 wt% and 10 wt% and explained the results by space charge polarization effect. Zheng et al. [92] presented a comparative results of electrical and dielectric properties of PMMA nanocomposites using CB, graphite and expanded graphite (EG) particles as filler materials. They found percolation threshold of 1.0 wt% with EG and 3.5 wt% with graphite while CB-PMMA composites required about 8 wt%. Using EG, Li et al. [93] investigated the frequency and

temperature dependences of electrical and dielectric properties of PVDF composites in a wide range of frequencies (10^2 to 10^8 Hz). They described the charge transport of percolating EG-PVDF system in terms of percolation and biased random walk (BRW) approach. More investigations on electrical and dielectric behaviours of PVDF composites were recently made by El Shafee et al. [94] using MWCNTs and Xu et al. [95] using CB and metal powders (Ni, Zn and W). George et al. [96] developed different nanocomposites with Ethylene Vinyl Acetate (EVA) as base matrix and EG, MWCNT and CNF as conducting fillers and studied the pressure dependence of their electrical and dielectric properties. In a similar investigation, Zhang and his colleagues [97] measured electrical conductivity and dielectric properties of three-dimensional polyvinyl alcohol (PVA)-MWCNT composites. They explained the dielectric behavior near the percolation threshold using intercluster polarization and anomalous diffusion. The influences of DC conductivity and interfacial polarization on dielectric relaxation process and the correlation between the dielectric behaviours and the molecular motions were also investigated.

A survey of literature reveals that only a limited number of studies on CNT-PEEK composites prepared by melt mixing has so far been done even though this method has widely been used in other thermoplastic matrices. Bangarusampath and his group [19, 33] recently published their work on rheology and properties of CNT-PEEK composites. They examined strain dependence, frequency dependence and temperature dependence of viscoelastic behaviour of the composites by dynamic shear rheological measurements. In addition, they measured melt strength and elongational viscosity to investigate elongational response of the composites. A brief discussion on electrical conductivity and

thermal/mechanical properties with some experimental results was also presented. To the best of knowledge, this is the only work so far available in the literature referring to the electrical properties of melt-processed CNT-PEEK composites; however a detailed analysis of electrical and dielectric properties is missing in their study. In this chapter, electrical and dielectric properties of CNT-PEEK composites at room temperature were extensively examined. Their percolation behavior is discussed in light of experimental observations and theoretical predictions for better understanding of the parameters affecting both AC and DC responses. Some fundamental aspects regarding critical volume fraction and percolation parameters are discussed to improve the ability to design better composites with incorporation of CNTs.

3.1.2 Background

Macroscopic conductivity and permittivity of a percolating system are given by $\sigma^* = \sigma' + i\,\sigma''$ and $\varepsilon^* = \varepsilon' + i\,\varepsilon''$ respectively. The frequency dependence of AC conductivity at constant temperature follows power law behaviour and the real part of the complex conductivity can be expressed by the Jonscher's equation known as the Universal Dynamic Response (UDR) [98]:

$$\sigma'(\omega) = \sigma_{dc} + \sigma_{ac}(\omega) = \sigma_0 + B\omega^u = \sigma_0\left[1 + \left(\frac{\omega}{\omega_c}\right)^u\right] \tag{3.1}$$

where $\omega = 2\pi f$ is the angular frequency, $\sigma_0 = \sigma_{dc} = \sigma$ (at $\omega \rightarrow 0$) corresponds to the dc conductivity of the system, B is a temperature dependent constant and u is an exponent dependent on both frequency and temperature. The value of u varies between 0.5 and 1.0 [99] and its value increases with decreasing temperature and increasing frequency [100].

Both theoretical and experimental works show that near the critical concentration ϕ_c, the DC conductivity and static permittivity follow the power laws as [32]:

$$\sigma_{dc} = \sigma'(\phi, f = 0) = \sigma_f (\phi_c - \phi)^{q'} \quad for \ \ \phi < \phi_c \tag{3.2}$$

$$\sigma_{dc} = \sigma'(\phi, f = 0) = \sigma_f (\phi - \phi_c)^{t} \quad for \ \ \phi > \phi_c \tag{3.3}$$

$$\varepsilon_s = \varepsilon'(\phi, f = 0) = \varepsilon_{dc} = \varepsilon_m (\phi_c - \phi)^{-q} \ for \ \ \phi < \phi_c \tag{3.4}$$

where f is the measurement frequency, σ_f is the conductivity of filler, ϕ is the volume concentration of filler, ϕ_c is the percolation threshold, ε_m is the dielectric constant of matrix, ε_s is the static permittivity of composites. The critical exponents t, q, q' are assumed to be universal constants [29, 32, 101, 102].

3.2 Experimental

3.2.1 Measurement of electrical properties

The electrical properties were investigated by means of impedance spectroscopy using a dielectric analyzer (TA Instrument DEA 2970) in ceramic parallel plate mode. The experiments were performed at room temperature and at testing frequencies ranging from 1 to 10^5 Hz. Nitrogen gas at a flowing rate of 500 ml/min was used to provide an inert atmosphere. The samples were placed between two gold electrodes. A low amplitude sinusoidal voltage ($V_{applied}$) was applied, creating an alternating electric field. This produces polarization in the sample, which oscillates at the same frequency as the electric field, but has a phase angle shift (θ). The current ($I_{measured}$) through the sample was measured to get the AC conductivity given by

$$\sigma_{ac} = \frac{I_{measured}}{V_{applied}} (\cos\theta) \frac{z}{A} \tag{3.5}$$

where z is the thickness and A is the surface area of the sample.

3.3 Results and discussion

To investigate the percolation of CNTs in PEEK, electrical conductivity, σ_{ac} was measured as a function of frequency for the composites at different CNT concentrations. For each concentration, at least three samples were examined and the result was reproducible with minimum standard deviation less than 10%. Figure 3.1 shows the real part of the complex electrical conductivity, σ' (AC conductivity) as a function of frequency for pure PEEK and nanocomposites with different CNT concentrations measured at room temperature.

Depending on the concentration of CNTs, three distinct regions are observed:

(i) Insulating region: Pure PEEK and composites containing up to 3.5 wt% of CNTs showed a typical insulating behavior where AC conductivity is frequency dependent in the frequency range studied with an almost identical slope on a log-log scale. The composite with 3.5 wt% has a shift of its conductivity more than two orders of magnitude compared to the pure PEEK.

A transition from insulating to conducting phase known as 'percolation threshold' (p_c) was observed between 3.5 wt% and 3.6 wt% of CNTs where a sharp increase in conductivity of about three orders of magnitude was noticed. At this transition region, the jump observed in electrical conductivity is due to the space charge polarization which can

be attributed to accumulation and release of charge carriers (electrons) at the interfaces between regions with significantly different conductivities and permittivities (Maxwell-Wagner-Sillars (MWS) relaxation), such as CNT and PEEK.

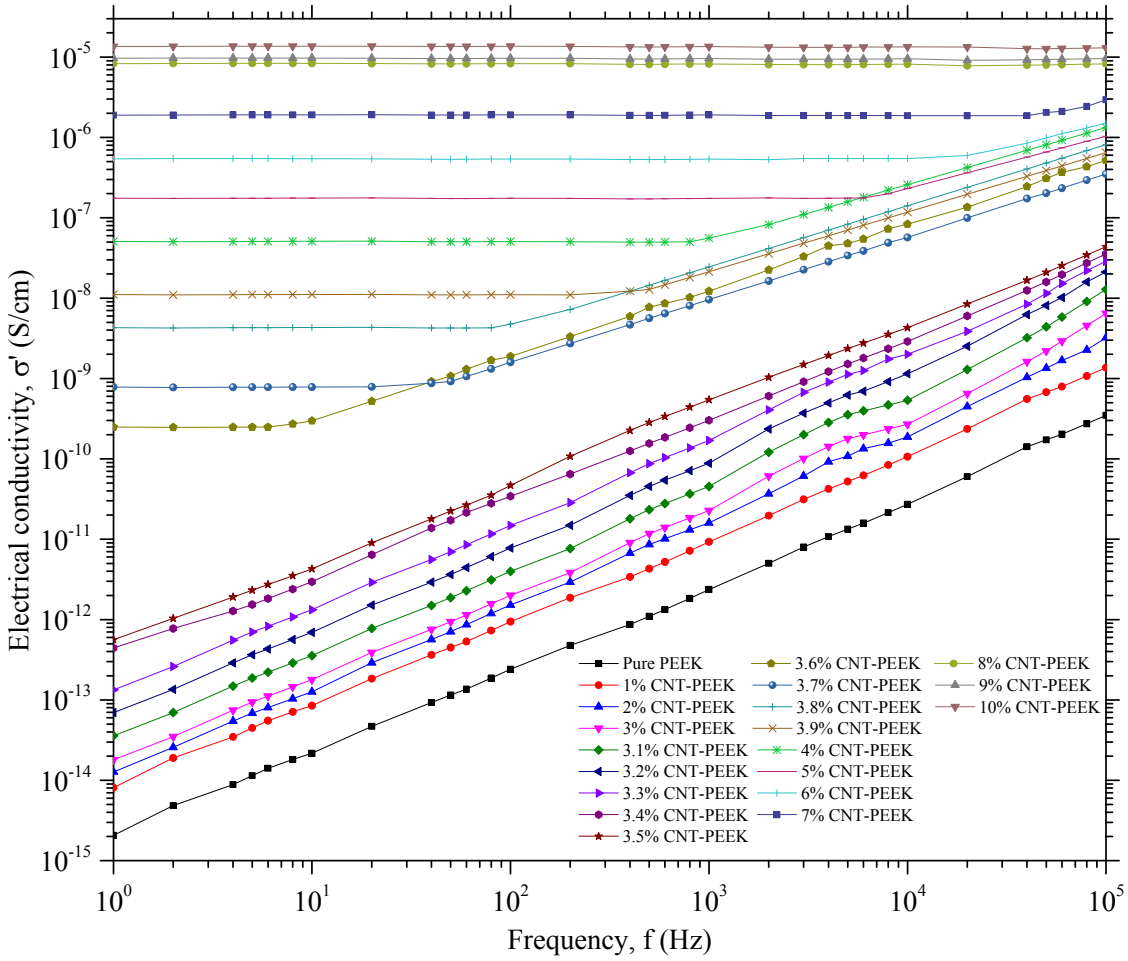

Figure 3.1: AC conductivity of CNT-PEEK composites as a function of frequency for the samples indicated in the legend.

(ii) Semi-conducting region: Composites with 3.6 wt% CNTs exhibit semi-conducting behavior with a DC plateau, corresponding to DC conductivity (σ_{dc}), where σ' is independent of frequency. This DC plateau bends off at some crossover frequency (f_c or ω_c), also known as critical frequency or onset frequency, above which i.e. for $f > f_c$ ($\omega > \omega_c$) conductivity increases according to power law. The critical frequency was measured

at which AC conductivity reaches 110% of σ_{dc} [45]. The independence of frequency, which is a characteristic of conductive materials, is extended in the whole frequency range as the amount of CNTs further increases. From 3.6 wt% to 7 wt% of CNTs, the same behavior was observed with a shift of crossover frequency f_c to higher frequencies with increasing CNT concentration.

(iii) Conducting region: A transition from semiconducting to fully conducting phase has been observed at 7 wt% of CNTs which can be termed as 'conduction threshold'. For higher CNT concentrations ($\geq$ 7 wt%), the crossover frequency disappeared, conductivity became saturated of frequency and the composite showed fully conducting behavior over the entire range of frequency studied.

In equation (3.1) the first component (σ_{dc}) refers to ionic/electronic conductivity while the second part comes out of polarization (restricted movement) of permanent dipoles/induced dipoles and accumulation and release of interfacial charges [103]. With the increase of frequency, total conductivity increases because of this polarization. However, the effect of actual mobility of dipole and induced dipole mainly depends on relaxation phenomenon. MWS relaxation becomes more significant at lower frequency of applied electric field, but when σ_{dc} becomes predominant, the polarization part becomes insignificant. Above the percolation threshold (above 3.5 wt% in the present case), a continuous conductive network starts to form with many conducting CNTs coming close to each other giving appreciable rise in electrical conductivity. The free flow of charged particles through the continuous conductive network just formed in the system governs the electrical conductivity. In these composites (3.6 wt% – 7.0 wt% CNT-PEEK), frequency independent conductivity at low frequencies is due to the resistive conduction

through the bulk composites, while frequency dependent conductivity at high frequencies is due to the capacitance of the host polymer PEEK between CNTs [103]. At high frequencies, electrons get excited so that they can hop from one CNT to the next thereby increasing conductivity. As the CNT concentration increases, the gap between two neighboring CNTs decreases and thus formation of conducting paths minimizes the hopping effect which is observed from the cross-over frequencies. At relatively high frequencies, this hopping prevails until 7 wt% of CNTs.

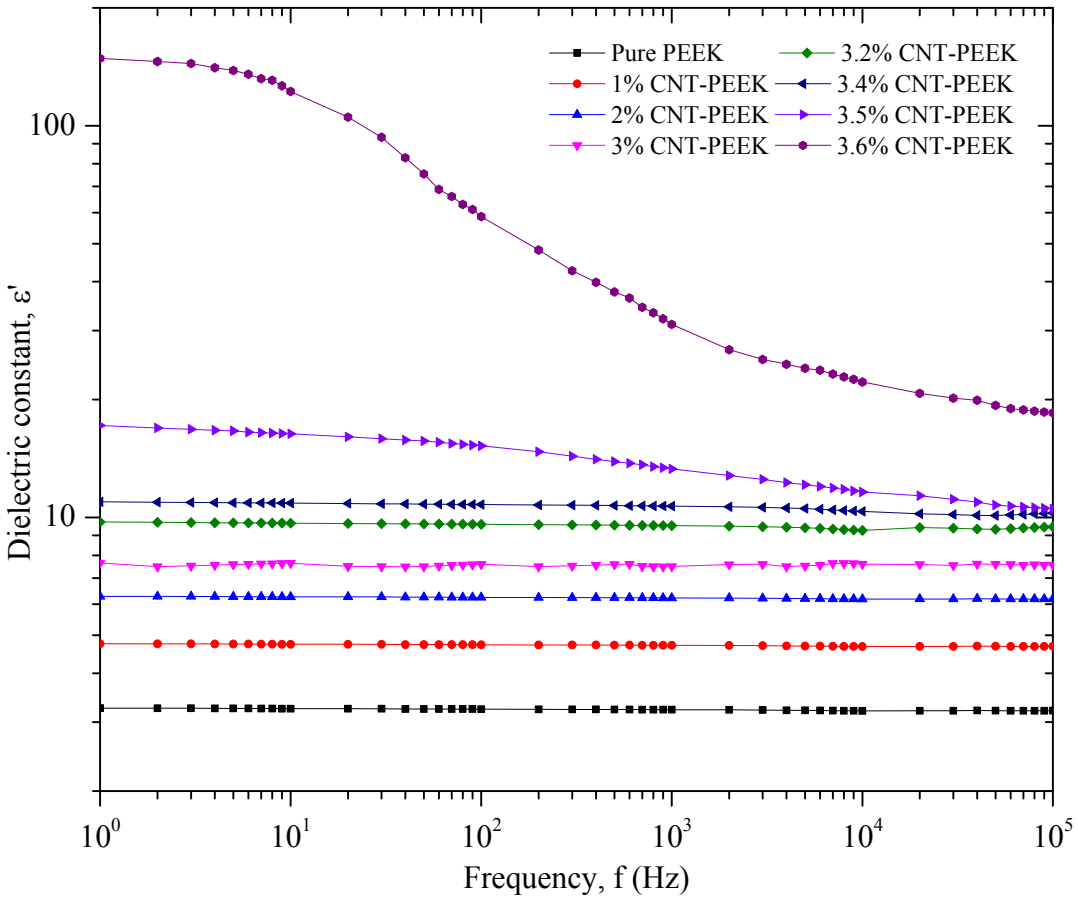

Figure 3.2: Dielectric constant of CNT-PEEK composites as a function of frequency

Figure 3.2 shows the variations of ε' (the real part of the complex dielectric constant or permittivity: $\varepsilon* = \varepsilon' - i\varepsilon''$) of CNT-PEEK composites as a function of frequencies at room temperature. As expected, the variational tendency of dielectric constant with frequency

is the opposite of electrical conductivity. The bulk conductivity of pure PEEK is very low, less than 10^{-14} S/cm and hence it shows a dielectric response with increasing frequency as expected for insulating materials. The addition of up to 3.5 wt% CNTs has no significant effect on the electrical response. For concentrations of CNTs up to 3.5 wt%, the dielectric constant of the composites is independent of frequency at room temperature and mainly determined by PEEK. The dielectric constant increases dramatically when CNT concentration approaches to the percolation threshold. The value of dielectric constant reaches from 17.17 to 148.6 at 1 Hz when the CNT concentration increases from 3.5 wt% to 3.6 wt%. It is nearly 46 times higher than that of virgin PEEK. This enhancement of dielectric constant near the percolation threshold can be explained in terms of minicapacitor effect consisting of conducting clusters of CNTs separated by thin insulating polymer layers [104]. In addition, polarization effects among the clusters further improves their electric charge storage. This high dielectric behavior can be used in manufacturing high charge storage devices [105]. The dielectric constant increases with increasing concentration of CNTs and reaches higher value at lower frequencies. For higher values of dielectric constant above the percolation limit, since total conductivity is governed by DC conductivity due to the free flow of large number of electrons through the continuous network available in the system and the mobility of electrons increases with an increase of the frequency of applied electric field, dielectric relaxation becomes evident at elevated frequencies, resulting in a decrease of the dielectric constant. Again for conductive systems at higher frequencies, polarization effect becomes insignificant because of the dominance of electronic conduction and hence a phase mis-match of interfacial polarization of composites to the external electric field occurs which causes a

decrease in dielectric constant [106]. One of the advantages of this kind of composites is weak dependence of dielectric constant in the low frequency range [107].

The conductivity spectra shown in Figure 3.1 and the permittivity spectra shown in Figure 3.2 can be quantitatively analyzed in terms of percolation theory. According to this theory [85], the frequency dependence of electrical conductivity, $\sigma'(f)$ and dielectric constant, $\varepsilon'(f)$ near the percolation threshold can be expressed as:

$$\sigma'(f, p_c) \infty \omega^u \tag{3.6}$$

$$\varepsilon'(f, p_c) \infty \omega^{-v} \tag{3.7}$$

where $\omega = 2\pi f$ is the angular frequency, u, v are critical exponents and theoretically, u + v = 1 [108]. Since AC conductivity as shown in equation (3.1) can be regarded as combination of DC conductivity ($f \rightarrow 0$ Hz) caused by migrating charge carriers and frequency induced dielectric dispersion, a large DC conductivity caused by formation of conducting path-way significantly dominates the transport behavior in a wide frequency range as seen in the plateau region in Figure 3.1. Below the percolation threshold, σ_{dc} is very small and can often be neglected.

Two different mechanisms namely, intercluster polarization (u = 0.72, v = 0.28) and anomalous charge carrier diffusion (u = 0.58, v = 0.42) have been proposed to explain the behavior of effective conductivity and permittivity of such a three dimensional random mixture [29, 100-102, 104]. To examine the suitability of those models, u and v were calculated for representative samples of 3.5 wt% and 3.6 wt% of CNT-PEEK composites in the vicinity of the percolation threshold. Figures 3.3(a) and 3.3 (b) show the best fit of frequency dependent conductivity of 3.5 wt% and 3.6 wt% samples fitted to equations

(3.6) and (3.1) respectively, while Figures 3.4 (a) and 3.4 (b) show the best fit of corresponding dielectric constants for these nanocomposites fitted to equation (3.7).

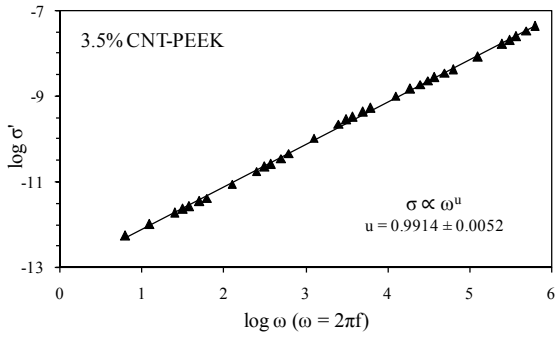

(a)

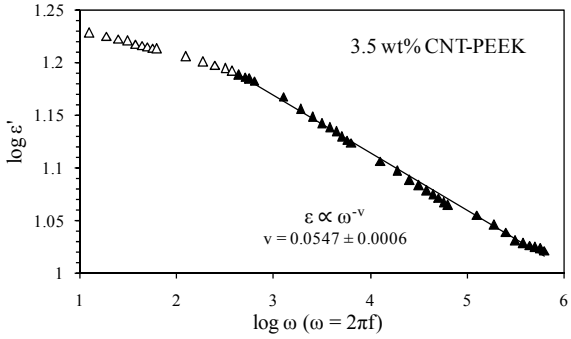

(a)

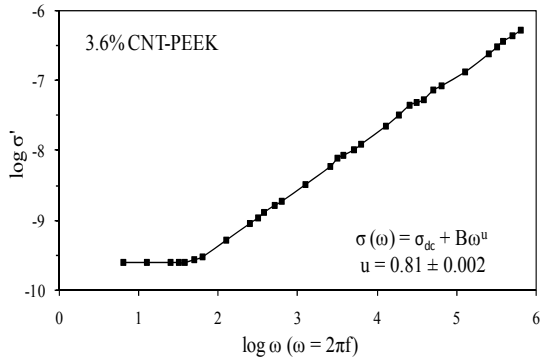

(b)

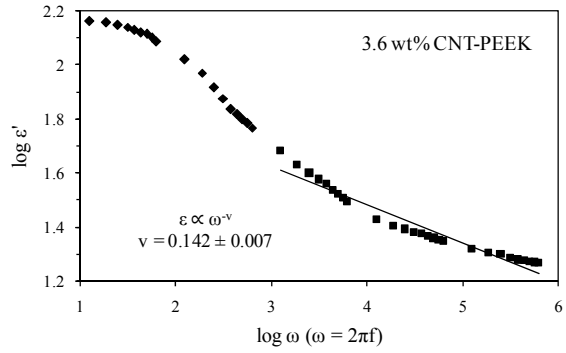

(b)

Figure 3.3 : Best fit of frequency dependent conductivity for (a) 3.5 wt% CNT-PEEK and (b) 3.6 wt% CNT-PEEK according to equation (3.6).

Figure 3.4 : Best fit of frequency dependent dielectric constant for (a) 3.5 wt% CNT-PEEK and (b) 3.6 wt% CNT-PEEK according to equation (3.7).

As seen in Figures 3.3(a) and 3.4(a) for 3.5 wt% CNT-PEEK composite, the electrical conductivity in the tested frequency region gives a critical exponent (u) of 0.9914 ± 0.0052 and the dielectric constant (curve fitted only in high frequency region) of this composite gives a critical exponent (v) of 0.0547 ± 0.0006 . It is because the influence of frequency prevails or the dipolar polarizations of composites lose the response to electric fields in the high frequency region and the analyzed value in this region according to

equation (3.7) is therefore much more precise to predict the frequency dependence of dielectric constant [93]. In Figure 3.3 (b) in the case of 3.6 wt% CNT-PEEK composite, the combined effect of σ_{dc} and f is clearly seen. Above f_c, the influence of frequency on conductivity becomes significant. The critical value u derived by using equation (3.1) is 0.81. A decrease of u from 0.9914 to 0.81 can be attributed to the effect of large DC conductivity which results in the plateau region of the curve. Accordingly, the dielectric constant for 3.6 wt% CNT-PEEK composite shows much more frequency dependence and hence the derived critical value v = 0.142 is little larger than that of 3.5 wt% CNT-PEEK composite. The values of u + v for 3.5 wt% and 3.6 wt% CNT composites are 1.0461 and 0.952, respectively and for higher wt% of CNTs, this sum value gradually decreases. Deviance of this (u + v) value from the theoretical value of 1 indicates the inappropriateness of the use of percolation theory to interpret the real composites with filler concentration far away from the percolation threshold (p_c). Therefore, it can be said that the investigated real CNT-PEEK composites (from 8 wt% to 10 wt% CNTs) do not closely correspond to the proposed mechanisms (incluster polarization or anomalous diffusion inside cluster).

To determine the values of σ_{dc}, f_c and u, a nonlinear curve fitting [109] was applied to the experimental curves of Figure 3.1 according to the modified form of equation (3.1) as

$$\sigma'(f) = \begin{cases} \sigma_{dc} & f < f_c \\ \sigma_{dc}\left(f / f_c\right)^{u} & f \geq f_c \end{cases} \tag{3.8}$$

The first part of above equation implies that, for composites below p_c (and hence f_c), σ_{dc} can be determined from σ_{ac} versus f response by simply extrapolating the values to $f \rightarrow 0$ Hz. In the same way, ε_{dc} can be obtained from ε' versus f curves. Correspondingly, the

temperature dependent parameter B can be obtained by applying the AC universal law (equation (3.1)). The values of σ_{dc}, ε_{dc}, u, v, B and f_c of nanocomposites investigated are listed in Table 3.1.

Table 3.1: Parameters indicating the frequency dependence of electrical and dielectric properties of CNT-PEEK Composites

p (wt%)	ϕ (vol%)	σ_{dc} (S/cm)	f_c (Hz)	u	B	ε_{dc}	v
0	0	2.07×10^{-15}	--	1.039 ± 0.031	2.97×10^{-16}	3.259	--
1	0.58	8.09×10^{-15}	--	1.038 ± 0.026	2.98×10^{-16}	4.759	--
2	1.16	1.27×10^{-14}	--	1.075 ± 0.022	1.55×10^{-15}	6.288	--
3	1.75	1.80×10^{-14}	--	1.099 ± 0.017	1.88×10^{-15}	7.648	--
3.2	1.86	6.97×10^{-14}	--	1.119 ± 0.023	5.68×10^{-15}	9.7325	--
3.4	1.98	4.43×10^{-13}	--	0.99 ± 0.021	5.52×10^{-14}	10.963	--
3.5	2.04	5.62×10^{-13}	--	0.991 ± 0.005	8.07×10^{-14}	17.17	0.055±0.001
3.6	2.1	2.49×10^{-10}	8	0.81 ± 0.002	1.03×10^{-11}	148.62	0.142±0.07
3.7	2.16	7.82×10^{-10}	40	0.78 ± 0.015	1.03×10^{-11}	Not determined	Not determined
3.8	2.22	4.3×10^{-9}	100	0.76 ± 0.001	3.19×10^{-11}	,,	,,
3.9	2.28	1.11×10^{-8}	400	0.74 ± 0.001	3.31×10^{-11}	,,	,,
4	2.34	5.08×10^{-8}	1,000	0.71 ± 0.002	1.01×10^{-10}	,,	,,
5	2.93	1.76×10^{-7}	8,000	0.652 ± 0.005	1.71×10^{-10}	,,	,,
6	3.54	5.41×10^{-7}	20,000	0.583 ± 0.03	6.21×10^{-10}	,,	,,
7	4.14	1.89×10^{-6}	50,000	0.53 ± 0.05	2.42×10^{-9}	,,	,,
8	4.76	8.29×10^{-6}	--	--	--	,,	,,
9	5.37	9.66×10^{-6}	--	--	--	,,	,,
10	6.0	1.36×10^{-5}	--	--	--	,,	,,

3.3.1 Scaling law of electrical conductivity

Extrapolated values of σ_{dc} (Table 3.1, Figure 3.1) obtained from the fitting procedure described above are plotted in Figures 3.5 and 3.6 . It shows a sharp increase in electrical conductivity when the CNT concentration reaches 2.1 vol% (3.6 wt%). An obvious abrupt increase in electrical conductivity values was observed between 3.5 wt% and 3.6 wt% where the conductivity changed from 5.62×10^{-13} S/cm to 2.49×10^{-10} S/cm. At this concentration of CNTs, a very high percentage of electrons are permitted to flow through the sample at the applied electric field due to interconnected physical paths formed by the nanotubes. This electrical conductivity is about five orders of magnitude higher than that of pure PEEK (2.07×10^{-15} S/cm).

In order to get the exact value of ϕ_c, the experimental σ_{dc} data of Table 3.1 were fitted for $(\phi - \phi_c)$ to the well known scaling law given by equation (3.3). The best linear fit for σ_{dc} vs. $(\phi - \phi_c)$ data on a log-log scale was obtained for $\phi_c = 2.05 \pm 0.01$ vol% (3.53 wt%) and $t = 2.517 \pm 0.119$ (Figure 3.5). The data points of the solid curve on Figure 3.5 were calculated from equation (3.3) using the above fit values of ϕ_c and t.

As seen in Figure 3.5, the power law dependence of the conductivity with CNT concentration is obeyed about two orders of magnitude above the threshold for the calculated fit values. It proves that conductivity of the composites at room temperature is controlled by percolating network of CNTs [110]. A similar linear fit of the conductivity data fitted to the log log plot (inset in Figure 3.6) of power law given by equation (3.2) yields the exponent $q' \approx 1.305 \pm 0.144$.

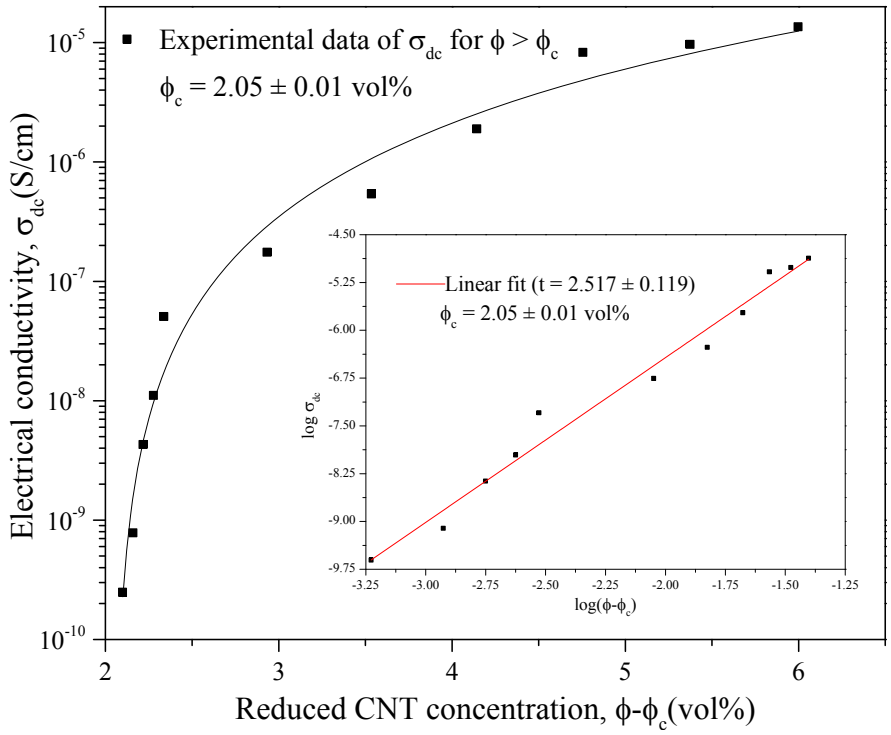

Figure 3.5: Electrical conductivity (σ_{dc}) as a function of reduced volume concentration ($\phi - \phi_c$). Inset shows the best linear fit at $\phi_c = 2.05$ vol% and t = 2.517.

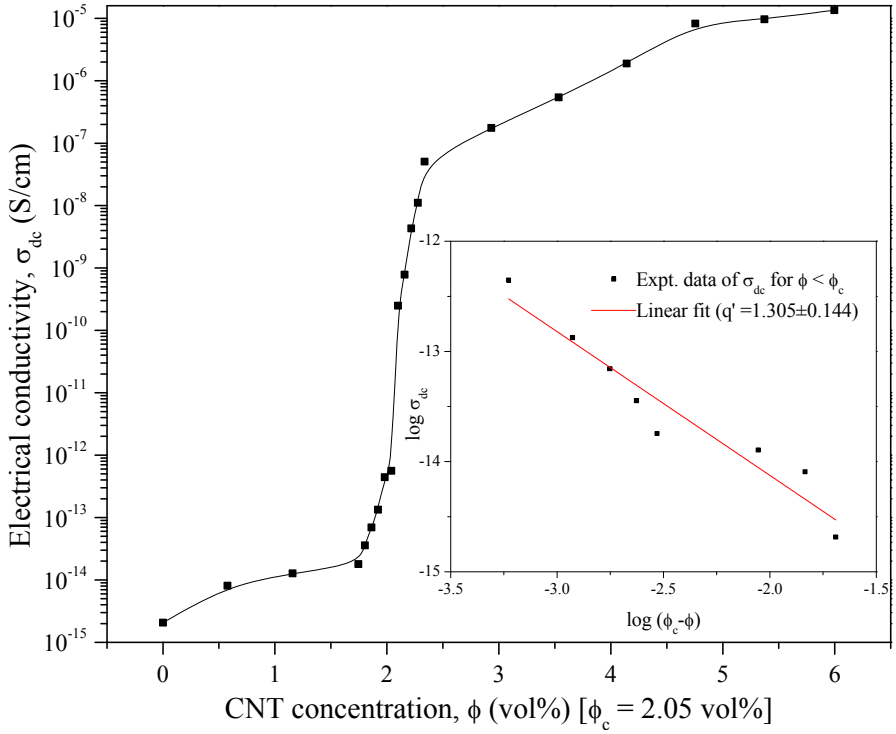

Figure 3.6: Electrical conductivity (σ_{dc}) as a function of volume concentration (ϕ). Inset shows the best linear fit at for $\phi < \phi_c$ and q' = 1.305.

3.3.1.1 Discussion on percolation and percolation threshold

It is well known that the formation of continuous CNT networks is responsible for percolation in insulating polymer matrices. In general, statistical percolation refers to a situation where randomly distributed filler particles form conducting paths by their direct physical contact and it does not directly describe the conductivity increase due to the percolation behavior of conducting particles, but merely the amount of particles of a given size needed to form infinite clusters of particles which are in contact with each other. The magnitude of conductivity improvement through percolation is determined by whether the particles include an insulating layer or not and its possible thickness. On the other hand, in kinetic percolation, filler particles can move freely, interact with each other via polymer chains and thus form a conducting network at much lower filler concentration than that of statistical percolation. Such filler movement can easily be produced by diffusion, convection, shearing etc. in most of the thermoset matrices because of its lower viscosity than thermoplastic matrices. Consequently, statistical (or higher) percolation is more typically observed in thermoplastic systems in line with excluded volume expectations [47, 111]. Especially for non spherical fillers, the percolation threshold is discussed in terms of excluded volume theory. Assuming the CNTs as randomly oriented cylinders with volume $V = d^2 l \pi/4$ and aspect ratio $\mu = l/d$, total excluded volume $\langle V_{ex} \rangle \approx d l^2 \pi/2$ can be correlated to the theoretical percolation threshold, ϕ_c through the following equation [112, 113]:

$$\phi_c \approx \frac{V}{\langle V_{ex} \rangle} = \frac{C \times d}{l} = \frac{C}{\mu} \tag{3.9}$$

where C is a constant. Taking C equal to 1.0 [114], 0.7 [58], 0.6 [44] and 0.5 [112] and using aspect ratio $\mu \approx 1000$, the theoretically expected ϕ_c is found to be 0.1 vol%, 0.07

vol%, 0.06 vol% and 0.05 vol% respectively. Percolation thresholds lower than $\phi_c \approx 0.1$ vol% are mainly due to the kinetic percolation which allows movement and reaggregation of filler particles as mentioned above and such lower percolation is typically observed in thermoset systems [35, 115, 116]. This value is significantly lower compared to the value of 2.05 vol% (3.53 wt%) obtained from scaling law of percolation for this thermoplastic PEEK system. This theoretically lower value of ϕ_c can be regarded as a rough estimation only and not as the absolute lower limit of ϕ_c as the percolation theory is a statistic model and it does not take into account the dynamics of network formation or any polymer–filler and filler–filler interactions [83, 117].

For melt processed composite systems, both lower and higher percolation thresholds than what was obtained in this research were reported by many researchers. Some of their results are given below in Table 3.2.

Table 3.2: Percolation thresholds of melt processed thermoplastic nanocomposites

Filler	Matrix	Percolation threshold	Reference	Comments
MWCNT	PA6	1.7 vol%	Logakis et al. [86]	Less than percolation threshold of this study (2.05 vol% or 3.5 wt% of MWCNT)
MWCNT	PMMA	0.5 vol%	Logakis et al. [83]	
MWCNT	PEEK	1.3 wt%	Bangarusampath et al. [33]	
MWCNT	PVDF	2.5 wt%	Hong & Hwang [118]	
MWCNT	PVDF	3.8 vol%	Li et al. [119]	More than percolation threshold of this study (2.05 vol% or 3.5 wt% of MWCNT)
SWCNT	PVDF	4 wt%	Zhang et al. [16]	
Expanded Graphite	PVDF	> 6 wt%	Li et al. [93]	
MWCNT	Polyimide	>7 wt%	Zhu et al. [8]	
MWCNT	PMMA	8.5 ~ 10 wt%	Khattari et al.[91]	

In the literature it has been reported that the percolation threshold lies in a wide range of weight concentrations of CNTs, depending on the type of polymer of both thermoset [35] and thermoplastics [45], processing technique and the type of CNTs used. Bauhofer et al. [47] in their recent review reported a wide range of percolation threshold from 0.0021 wt% to 12 wt% of CNTs. Based on their observations, electrical percolation for thermoplastic systems usually occurs at around 1.0 wt% ~ 5.0 wt% [19]. Thus the percolation threshold obtained for CNT-PEEK system is ($p_c \approx 3.5$ wt%) within the range reported by other researchers for similar material system and processing technique.

Electrical percolation of nanotube filled composites critically depends on geometry of nanotubes (aspect ratio), nanotube concentrations, properties of host polymer and processing methods, and eventually on the dispersion of nanotubes in the matrix. Lower percolation thresholds are obtained because of kinetically stabilized networks formed by nanotube aggregates [47] and higher percolation thresholds are obtained when CNTs are coated or grafted with polymer, limiting the inter-nanotube contacts or when CNTs are highly aligned [34]. When CNTs are used as conducting fillers, a lower percolation threshold is theoretically expected because of their strong anisotropy, high aspect ratio and thin diameter. However processing route for fabricating nanocomposites, specifically harsh melt processing has a detrimental effect on percolation threshold and hence electrical performance of the eventual composites. In the present study, 'as-produced' CNTs were used which are usually in an agglomerated state. When dry powder of CNTs were directly mixed with PEEK powder and mechanically stirred, aggregates of CNT were not properly disentangled. In order to remove these agglomerates, high shear forces were applied in the twin screw extruder to overcome both the van der Waals interactions

of individual nanotubes and the mechanical entanglements. Such high shear force can break the nanotubes and reduce their aspect ratio [18] resulting in a higher percolation threshold.

3.3.1.2 Discussion on critical exponent 't'

According to theoretical predictions [29, 102] of the scaling law of percolation given by equation (3.3), the critical exponent t is independent of material and has a theoretical value $t_0 \approx 1.6 \sim 2.0$ for three dimensional, and $1.0 \sim 1.3$ for two dimensional systems. Several experimental investigations were in good agreement with equation (3.3), but the critical exponent t is not universal in many practical systems. The exponent t (≈ 2.517) obtained in the present study is higher than the theoretically expected value ($t \approx 2$) for a statistical percolation network in three dimensions. In the literature, even higher values of t have been reported before for thermoplastic systems, such as 8.4 for melt processed CNT-PEEK composites [86], 8.0 for polyethylene/polyoxymethylene blends filled with iron particles [120], 6.27 for graphite-polyethylene composites [121], 3.8 for melt mixed CNT-polycarbonate composites [17] etc. Kovacs et al. [111] carried out the experiment for CNT-epoxy system and observed two percolation thresholds, suggesting a change in t from low values (≈1.7) in the case of lower (kinetic) percolation threshold to high values (≈2.3) for higher (statistical) percolation threshold. Weber et al. [30] reported experimental values of t between 1.3 and 3.1 for different matrix and reinforcement systems. These high values of t are responsible for a gradual rather than the expected steep increase of σ_{dc} with filler concentration [86]. Since nanotubes are possibly coated with a thin polymer layer which acts as a potential barrier to inter-nanotube hopping, electrical conductivity is achieved by tunneling between nanotubes, giving rise to the

non-conventional percolation model, called the tunneling percolation system and in that case, as proposed by Balberg [122], a wide inter-particle distance distribution or specific distributions of both conducting and non-conducting phases [123] can lead to non-universal and material dependent high t values. In addition, statistical percolation theory holds good only for ideal systems satisfying some prerequisite conditions: the particles must be spherical, monodisperse (means same size and shape) and have an isotropic conductivity. If any of these conditions is not satisfied, the value of t obtained from experimental results will deviate from the theoretical one, but in some cases, it is not clear which condition is not satisfied. Due to the variation in CNT properties, i.e. length, diameter, waviness, entanglement etc., CNT-polymer systems are far away from being ideal systems. Again, lower percolation thresholds are produced kinetically which makes the application of statistical percolation theory questionable [47].

Thus, it can be concluded that the critical exponent 't' of the present composite system is in reasonable agreement with both experimental results reported in the literature and theoretical predictions.

3.3.1.3 Discussion on 'σ_f'

The value of constant σ_f in the scaling law (equation (3.3)) refers to the intrinsic electrical conductivity of CNTs ($\approx 10^4$ S/cm). By extrapolation to $\phi \approx 100\%$ (Figure 3.5), a significantly lower value (4.3×10^{-2} S/cm) was achieved which is six orders of magnitude lower than expected. As mentioned above, around the individual carbon nanotube walls in polymer composites, a thin polymer layer forms in solution phase. This layer is responsible for the solubility of nanotubes in composite solutions. The formation of such polymer layers prevents the direct physical contact between adjacent carbon

nanotubes, resulting in lower effective conductivity. Logakis et al. [124] and McCarthy et al. [125] showed the formation of such insulating polymer layers in the case of melt processed CNT-polyamide and CNT-PmPV composites respectively. Such insulating layers give rise to the phenomenon of tunneling. According to percolation theory, conductive paths are formed by CNTs in direct contact, but in the case of tunneling, a contact resistance due to a thin insulating polymer layer exists within the conductive path between two CNTs and conduction of electrons can occur only by hopping from one nanotube to a neighboring one when the inter-particle distance between CNTs is only few nanometers. A critical distance of less than 5 nm (≈1.8 nm reported by Li et al.[39]) is required for this electron hopping or tunneling at which electrons can easily jump across the gap separating individual nanotubes. The value of σ_f in this analysis is low because CNTs do not form this conductive network by physical contact. It is reasonable to believe that at a higher CNT loading, a second threshold would be obtained when the CNTs can make the network by direct physical contact, eliminating the contact resistance [88]. Such second threshold was not prominent in the present case of CNT-PEEK system.

3.3.2 Scaling law of dielectric constant

The variation of dielectric constant in the neighborhood of ϕ_c follows the scaling law given by equation (3.4). Figure 3.7 shows the extrapolated values of dielectric constant, ε_{dc} with CNT volume concentration for CNT-PEEK composites.

The best linear fit of dielectric constant data to the power law using equation (3.4) gives q = 0.428 ± 0.057. Universality of the percolation theory suggests that the dielectric constant should exhibit the same power law dependence on volume fraction below ϕ_c which requires that q ≈ q'.

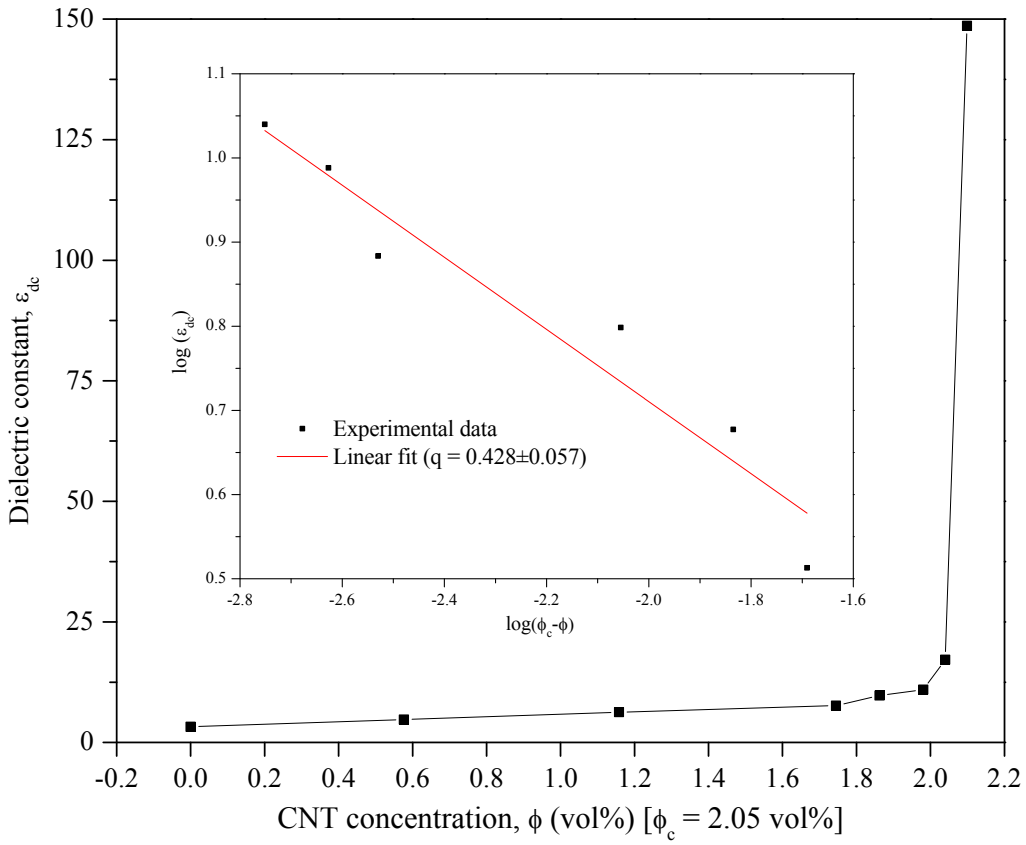

Figure 3.7: Dielectric constant as a function of CNT volume concentration. Inset shows the best fit of ε_{dc} vs. ($\phi_c - \phi$).

However, this is not always observed in practical continuum system. In the present case, q obtained by equation (3.4) is different than q' obtained by equation (3.2). Such different values of q and q' were previously reported by Wang and Dang [105] for CNT-PVDF composites, Wu and McLachlan [114] for graphite-boron nitride system.

3.3.3 Scaling law of critical frequency

The critical frequency f_c observed in the AC investigation of conductivity provides an advantage of checking percolation threshold. It follows the same scaling law of percolation theory with volume concentration of filler [126] showing the similar dependence like σ_{dc} given in equation (3.3):

$$f_c \propto (\phi - \phi_c)^{\zeta} \quad for \quad \phi > \phi_c \tag{3.10}$$

where ζ is a scaling exponent. The f_c values listed in Table 3.1 are plotted in Figure 3.8 against the CNT volume concentrations. The best linear fit of f_c vs. $(\phi - \phi_c)$ data according to equation (3.10) (straight line in the inset of Figure 3.8) gives $\phi_c = 2.059 \pm 0.02$ vol% and $\zeta = 2.446 \pm 0.118$. These values are very similar, obtained from equation (3.3). It has also been reported that f_c has the relationship with σ_{dc} above ϕ_c by a scaling power law [99, 127]:

$$f_c \propto \sigma_{dc}^{\xi} \quad for \quad \phi > \phi_c \tag{3.11}$$

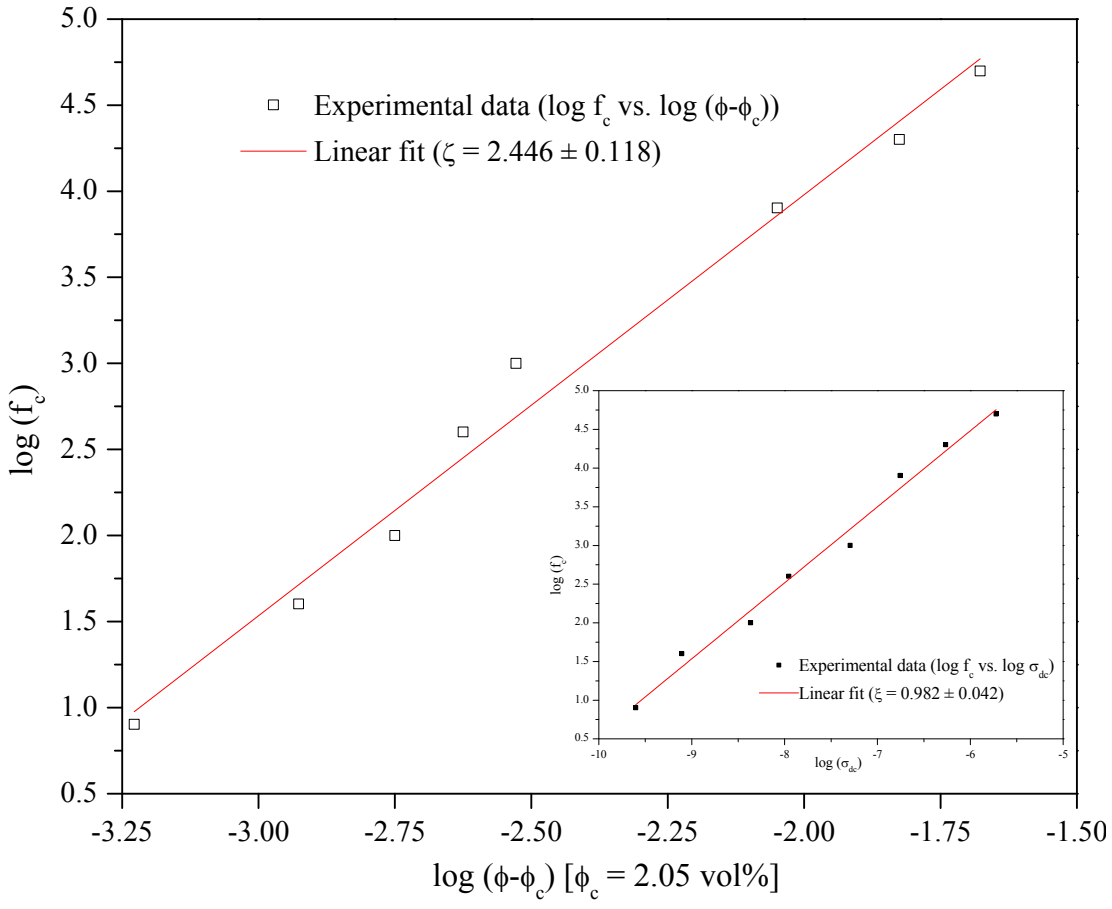

Figure 3.8: Best fit of critical frequency f_c vs. CNT volume concentration $(\phi - \phi_c)$. Inset shows the relationship between f_c and σ_{dc}

The inset in Figure 3.8 shows that the experimental data well obeys the above equation for an exponent ξ = 0.982 ± 0.042. From equations (3.10) and (3.11), a relationship of $\sigma_{dc} \propto (\phi - \phi_c)^{\frac{\zeta}{\xi}}$ can be established which corresponds to the classical percolation given by equation (3.3). Accordingly, t = ζ/ξ = 2.446/0.982 = 2.49. This value is close to 2.51 obtained directly from classical percolation equation (3.3).

3.4 Summary

Electrically conductive MWCNT reinforced PEEK composites were manufactured by melt processing technique and their electrical and dielectric properties were investigated in a wide range of frequencies (1 to 10^5) at room temperature. The conductivity in these composites results from the formation of a continuous conductive path in the polymer matrix by the CNTs. A jump of electrical conductivity was observed at lower frequency when the concentration of CNTs increased from 3.5 wt% to 3.6 wt%. The results shows that conductivity is frequency dependent below the percolation threshold, frequency independent above percolation threshold, equal to dc conductivity below a critical frequency f_c, whereas it follows a power law above f_c. The dielectric constant of the composites has been significantly increased in the neighborhood of percolation threshold. The dielectric constant showed the opposite behavior as expected with frequency, it was frequency independent below the percolation threshold and dependent above percolation threshold with obvious dielectric relaxation at higher frequencies. Following the well known scaling law of percolation theory, the electrical percolation threshold was determined to be ϕ_c = 2.05 vol% CNTs with a critical exponent t = 2.517 and q = 0.428 from σ_{dc} and dielectric constant respectively, extrapolated from AC results. A similar

value of ϕ_c and t were independently determined from f_c using a similar scaling law. In general, the electrical and dielectric properties of PEEK can be improved by addition of CNTs and these kinds of composites can be used for practical applications in many electrical devices.

Chapter 4

Estimation of Contact Resistance and its Effect on Electrical Conductivity of CNT-PEEK Composites

4.1 Introduction

CNTs dispersed in insulating polymer matrix can dramatically increase the electrical conductivity of the composites. Electrical conductivity of a composite strongly depends on CNT concentration, morphology of nanotube network and the number of nanotube contact points. Some other factors like size, geometric shape and hardness of the conductive fillers, filler distribution, properties of host matrix and processing methods can also influence the conductivity and percolation [128-133]. Experimental electrical conductivities typically range from 10^{-7} S/cm to 10^{-4} S/cm for nanotube concentrations above percolation threshold [45, 134] while intrinsic electrical conductivity of individual CNTs are essentially in the order of 10^{2} to 10^{5} S/cm [25, 135-137] in the longitudinal direction and 10^{0} S/cm in the transverse direction [138]. A large spread of electrical conductivity reflects the complex nature of CNT-based conductive composites that cannot be explained only by increased nanotube content. Measured electrical conductivity above the percolation threshold should theoretically tend to the intrinsic conductivity of CNTs. The large discrepancy on average in the order of 10^{10} S/cm is, therefore, the motivation in this chapter to calculate the contact resistance between individual CNTs embedded within polymer matrix.

Calculation of contact resistance is complicated, because contact resistance in an actual composite material may be affected by a number of factors, such as the type of

nanotubes, nanotube diameter, contact area, tunnelling gap (thickness of insulating film) at contact points and matrix material filling that tunnelling gap. For a specific contact, it is often difficult to know the thickness of an insulating film and to determine the exact value of the contact resistance.

Several attempts have been made to calculate contact resistance of CNT-based polymer composites. Theoretical calculations [40] demonstrated that contact resistance between nanotubes can vary from 100 kΩ to 3.4 MΩ and is strongly dependent on atomic structures in the contact region and the structural relaxation of the nanotubes. By fitting their simulation results to the experimental data of other researchers, Foygel et al. [44] estimated the contact resistance between carbon nanotubes in composites to be in the order of 10^{13} Ω and suggested that the high resistance was caused by tunnelling-type contacts between the CNTs belonging to the percolation cluster. Kovacs et al.[111], based on their experimental observations, developed a simple relation between sample conductivity (that can be measured) and the filler concentration for the region above statistical percolation threshold to estimate the inter-particle contact resistance inside a polymer matrix (that cannot be measured, but affects the effective conductivity). They applied their calculations to the conductivity measurements published by other groups.

Phenomenon of contact resistance becomes more complex when a thin insulating layer forms between the contact points of junction nanotubes. Formation of such insulating polymer layers were previously reported in the case of melt processed CNT-polyamide [124] and CNT-PmPV [125] composites. Kilbride et al. [45] also found significantly lower electrical conductivity than expected in the study of their CNT-PmPV and CNT-

PVA thin films. They suggested that conduction in composite films was dominated by electric tunneling and a thick coating of polymer around nanotubes results in poor electrical conductivity.

This chapter reports studies on calculation of contact resistance for CNT-PEEK composites by the Holm-Kirschstein and Simmons' model and comparing the results with those obtained using Kovacs' model. The same experimental data presented in chapter 3 were used for the present calculation and analysis. The equation for electrical conductivity of composites was obtained using the model described by Allaoui et al. [115].

4.2 Tunneling contact model

Previously the formation of insulating polymer layers which limits the physical contact between carbon nanotubes and thus lowers the electrical conductivity was discussed. In the presence of such an insulating film, electrons must enter the conduction band of the insulator, i.e. they must possess sufficient energy to cross the insulating barrier, a process known as thermoionic emission. According to classical physics, electrons cannot penetrate through the barrier unless the electron energy is equal to or more than the height of the interfacial barrier. But according to quantum mechanics, there exists a finite (nonzero) probability to find an electron on the other side of the film and the electrons can cross this insulating barrier by a ‘‘tunnel effect’’ depending on the size and shape of the barrier encountered by electrons, usually if the insulating film is sufficiently small (< 5 nm). To explain conductive behavior of such composites using the tunnel effect, Allaoui [115] evaluated the thickness of this thin film by modeling the composite as a

stacking of layers, each layer consisting of a number of contacts. They derived the equation of electrical conductivity of the composite from the view point of resistor network and assumed that (i) in each layer, the network is perfectly three dimensionally random and all contacts participate in the conduction (they did not take into account aggregation and dead-end branches of carbon nanotubes, the latter may have a limited effect). (ii) All resistors have the same resistance, that is, they did not take into account the distribution of CNT diameter or variation of insulating film thickness.

A schematic of the model is shown in Figure 4.1. The resistance of one layer is that of a network of parallel resistors. Each resistor has the same resistance, noted as $R_{contact}$ and represents the contact resistance between the CNTs with a matrix film in their vicinity along with the segment of CNTs between contacts. The thickness of one layer is assumed to be equal to the distance between two contacts, noted as δ, which is equal to twice the nanotube diameter plus inter-nanotube spacing. The inter-nanotube spacing, i.e. gap between two adjacent CNTs can be in the range between 0 to the largest possible thickness of insulating film that allows the tunneling percolation of electrons. A composite sample of thickness z is therefore a stacking of M (= z/δ) layers (in series). The electrical resistance of the composite is obtained by

$$R = \frac{z}{\delta}\frac{R_{contact}}{N} \tag{4.1}$$

where N is the number of contacts (in parallel) in one layer. Considering a composite sample of surface area A, the electrical conductivity is thus

$$\sigma = \frac{1}{R}\frac{z}{A} = \frac{\delta}{z}\frac{n\delta A}{R_{contact}}\frac{z}{A} = \frac{n\delta^2}{R_{contact}} \tag{4.2}$$

where n is the number of contacts per unit volume in a three-dimensional random fiber network given by van Wyk [139] as $n = \frac{4\phi^2}{\pi d^3}$ with ϕ the volume fraction of fibers and d their diameter.

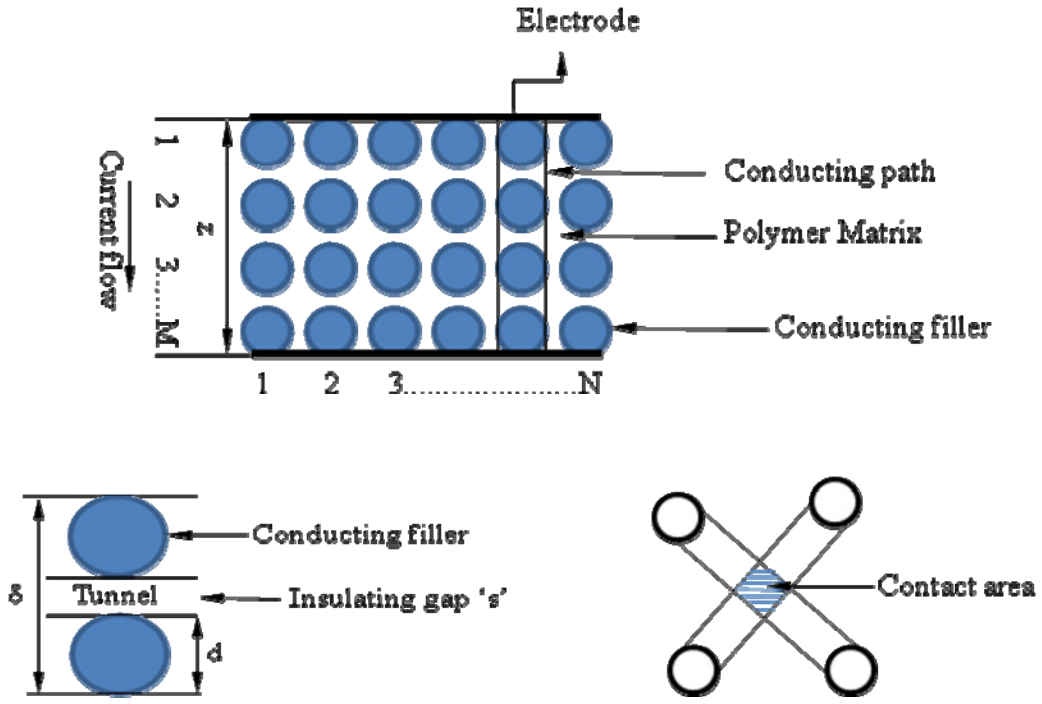

Figure 4.1: Schematic of the model of resistor network to calculate composite resistance [39, 140].

The average contact distance δ in the network is given [139, 141] as $\delta = \frac{\pi d}{8\phi}$

Finally, the electrical conductivity of the composite is simply

$$\sigma = \frac{\pi}{16d}\frac{1}{R_{contact}} \tag{4.3}$$

In a percolating network of carbon nanotubes, two sources of resistance can be recognized, one is the intrinsic ohmic resistance along the carbon nanotube itself, and the other is the tunnelling resistance determined by the thickness of the insulating matrix layer around CNTs. Thus, total contact resistance is considered to be the sum of nanotube contact resistance without an insulating thin film (i.e. constriction resistance/resistance of the CNT portion between two contacts) noted as R_c and the resistance from the electric tunneling effect due to the matrix film, i.e. $R_{contact} = R_c + R_t$

The electrical resistance of the CNT portion between two contacts in the network is calculated by

$$R_c = \frac{1}{\sigma_{cnt}} \frac{\delta}{\frac{\pi d^2}{4}} = \frac{1}{\sigma_{cnt}} \frac{1}{2d\phi} \tag{4.4}$$

where σ_{cnt} is the electrical conductivity of CNTs given in Table 2.2.

Tunneling resistance depends on material, thickness and surface area of the insulating layer. CNTs are assumed to be straight and randomly dispersed in the matrix. For simplicity of the analysis, CNTs at a contact point in the network can be assumed to be overlapping/crossing at right angles and not penetrating with each other i.e. there is no thickness variation along the section. Accordingly, contact surface area $S_{contact}$ of insulating film is equal to that of a CNT–CNT contact obtained by square of a side equal to the diameter of a CNT, i.e. $S_{contact} = d^2$. Therefore,

$$R_t = \frac{\rho_t}{d^2} \tag{4.5}$$

where ρ_t is the tunneling resistivity of the matrix film in Ω-cm^2 (not to be confused with volume resistivity in Ω-cm).

Combining equations (4.3), (4.4) and (4.5), final expression of electrical conductivity of the composite can be written as

$$\sigma = \frac{\frac{\pi}{16d}}{R_{contact}} = \frac{\frac{\pi}{16d}}{R_t + R_c} = \frac{\frac{\pi}{16d}}{\frac{\rho_t}{d^2} + \frac{1}{2d\phi\sigma_{cnt}}} \tag{4.6}$$

Volume concentrations of CNTs (ϕ) were calculated using the equation (2.1).

4.3 Calculation of contact resistance

4.3.1 Holm-Kirschstein model

Based on quantum considerations, Holm-Kirschstein [72, 142] derived the following equation for low voltages to calculate the tunnel resistivity in Ω-cm^2:

$$\rho_t = \frac{10^{-22}}{2}\frac{X^2}{1+XY}e^{XY} \tag{4.7}$$

$$\text{with X} = 7.32\times10^5\left(s - \frac{7.2}{\psi_0}\right) \text{ and Y} = 1.265\times10^{-6}\sqrt{\psi_0 - \frac{10}{s\,\varepsilon_r}} \tag{4.8}$$

4.3.2 Simmons' model

Simmons [143] derived a formula for tunneling current density through a potential barrier of a rectangular shape between two similar electrodes separated by a thin insulating film of uniform thickness. The analysis presented in [143] was for low temperatures, where the thermal current was neglected and thus electron transport between the electrodes was restricted to the tunnel effect. Neglecting the variation of barrier height along the thickness of the film, the current density (J) for a voltage drop V_i across the contact area of crossing CNTs can be expressed as:

$$J = \frac{6.2\times10^{10}}{(\Delta s)^2}\left\{\psi \exp\left(-1.025\,\Delta s\,\psi^{1/2}\right) - (\psi + V_i)\exp\left(-1.025\,\Delta s\,(\psi + V_i)^{1/2}\right)\right\} \tag{4.9}$$

$$\text{where } \psi = \psi_0 - \frac{V_i}{2s}(s_1 + s_2) - \frac{5.75}{\varepsilon\,\Delta s}\ln\frac{s_2(s - s_1)}{s_1(s - s_2)}, \quad \Delta s = s_2 - s_1 \tag{4.10}$$

$$\text{and } s_1 = \frac{6}{\varepsilon_r \psi_0}, \tag{4.11}$$

$$s_2 = s\left(1 - \frac{46}{3\psi_0\varepsilon_r s + 20 - 2V_i\,\varepsilon_r s}\right) + \frac{6}{\varepsilon_r \psi_0} \text{ for } V_i < \psi_0 \tag{4.12}$$

The voltage drop V_i across the film of thickness s, surface area $S_{contact}$ and capacitance C is given by

$$V_i = \frac{e}{C} = \frac{e}{\varepsilon_r\varepsilon_0 S_{contact}/s} \tag{4.13}$$

In the above expressions, ψ stands for the height of the rectangular barrier, e denotes unit electric charge passing through the film, ε_r is the relative permittivity of matrix and $\varepsilon_0 \approx 8.85\times10^{-12}$ F/m denotes the absolute permittivity of vacuum. Units of J is in Ampere/cm^2, ψ and V_i are in Volt, s, s_1 and s_2 are in Å. Tunneling resistivity is then obtained as

$$\rho_t = \frac{V_i}{J} \tag{4.14}$$

Using above two models given by equations (4.7) and (4.14), the tunnel resistivity was calculated. In the calculation, ψ_0 was taken approximately equal to the work function of CNTs (≈ 4.80~4.95 eV) [144], relative permittivity (dielectric constant) of insulating PEEK, $\varepsilon_r \approx 3.3$ and an average CNT diameter d = 10 nm. Substituting equation (4.7) or (4.14) in equation (4.6), the composite conductivity, σ was obtained as a function of film

thickness (s) and volume concentration of CNTs (ϕ). As can be seen from equation (4.9) the relation between current and voltage is non linear. Therefore, it is not possible to derive an explicit relation for the tunnel resistance. Moreover, since ϕ and Δs are functions of voltage drop, the tunnel resistance is non-ohmic and decreases with increasing voltage. It is understood that the gap between adjacent nanotubes is most likely to decrease when the nanotube volume concentration is increased and thus the corresponding tunnel resistance and contact resistance also decrease. But in practice, it is difficult to predict the relationship between the insulating film thickness and nanotube volume concentration. In conventional particle composites, the average spacing between particles may be estimated from the matrix volume fraction assuming a pattern of particle packing. However, in nanotube-based composites, especially conductive composites, the pattern of particle packing does not apply because of the very small nanotube content. To address this issue, Li et al. [53] proposed the assumption that the film thickness follows a normal distribution and they found it to be reasonable in their analysis. Considering all those facts, the film thickness is assumed to vary with the CNT volume concentration following a power law dependence [115]; $s = K\phi^{\eta}$ with K and η are two free parameters. The experimental data were fitted to equation (4.6) and K and η were evaluated using the two different models for tunnel resistivity; Holm-Kirschstein model and Simmons' model.

4.3.3 Discussion on results by Holm-Kirschstein and Simmons' models

The experimental data and the fitting curves for the best fit of K and η are shown in Figure 4.2. The values of fitting parameters indicated on the graph are quite similar. Although the two fitting curves are superimposed, Simmons took into account the true shape of the potential while Holm-Kirschstein assumed an approximate parabolic form. A kink or bend is observed in the plot which arises due to the nonlinear relationship between current and voltage.

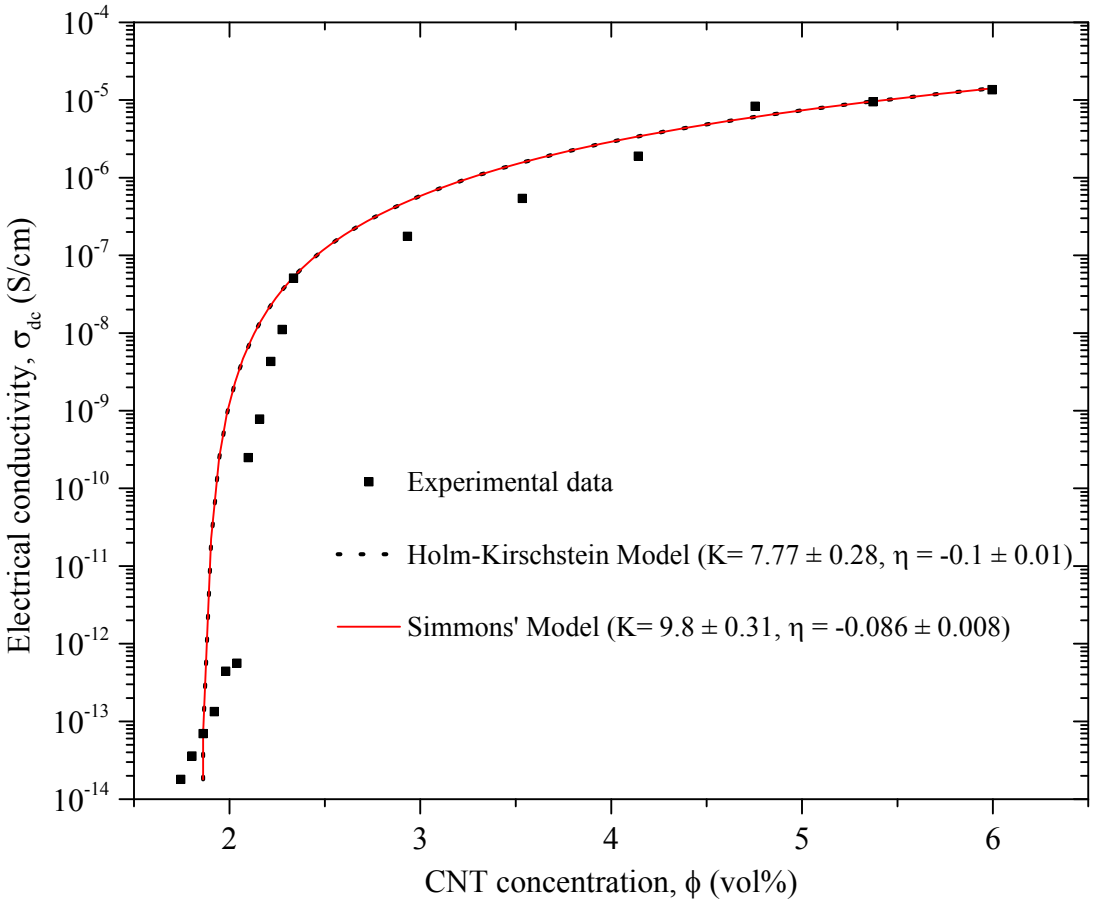

Figure 4.2: Electrical conductivity as a function of CNT volume concentration. The solid and dotted lines are fit to equation (4.6).

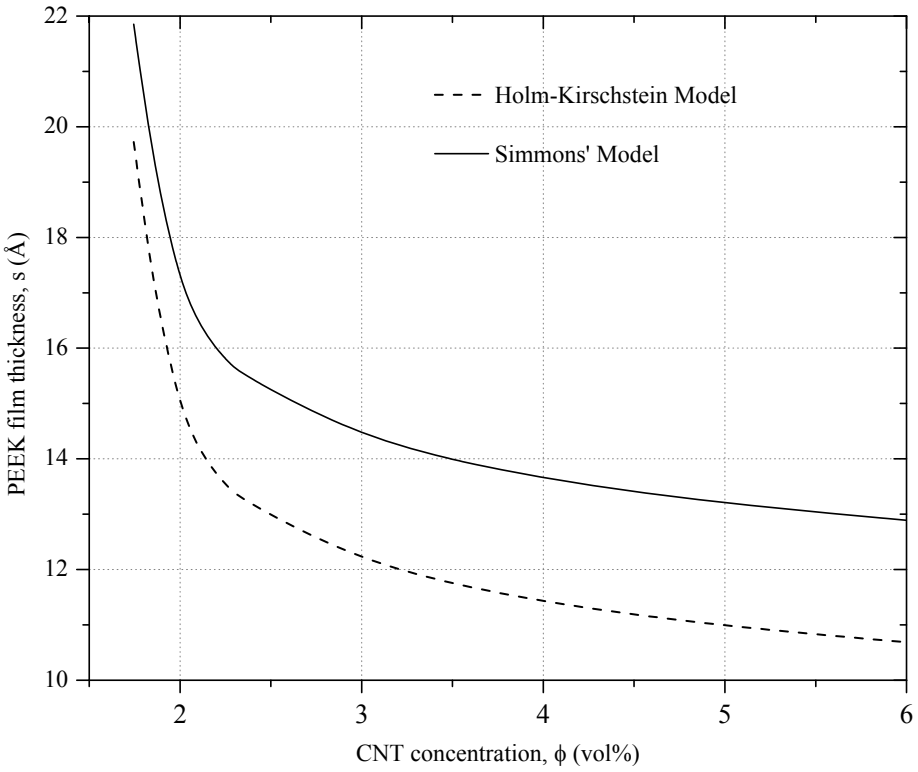

Figure 4.3: Thickness of the insulating film as a function of nanotube volume concentration.

Figure 4.3 represents the insulating PEEK film thickness obtained by using the values of the fitting parameters of both Holm-Kirschstein model and Simmons' model as a function of nanotube volume concentration. It has been observed that film thickness decreases with increase in CNT volume concentration. The Holm-Kirschstein model predicts a comparatively lower film thickness than the Simmons' model at certain volume concentration. The difference in film thickness predicted by the two models gradually increases up to the percolation threshold (ϕ_c = 2.05 vol%) where the maximum difference is about 2.266 Å and then gradually decreases (2.2 Å at 6 vol%) but the trend is quite similar.

Almost similar observations were also noticed in Figures 4.4 and 4.5 where electrical conductivity and tunneling resistance respectively are plotted against the film thickness. For the same film thickness, Simmons' model predicts higher electrical conductivity and lower tunneling resistance than those predicted by Holm-Kirschstein model. Differences in the values of electrical conductivity between the two models increase with decreasing film thickness up to a certain limit and then decreases (Figure 4.4), but their difference in tunneling resistance remains almost same for all nanotube concentration (Figure 4.5). It is seen that insulating film thickness between crossing CNTs plays a significant role in the tunneling resistance, which increases rapidly with increasing layer thickness. When the thickness is about 11 Å (1.1 nm) tunneling resistance is in the order of 10^{10} Ω (Holm's model in Figure 4.5) which is several orders of magnitude larger than the contact resistance between carbon nanotubes without any insulating film. Another important observation is that a sudden rise in electrical conductivity was obvious near the percolation threshold where the film thickness is predicted to be about 17 Å by Simmons' model and 14.5 Å by Holm-Kirschstein model (indicated by dashed line and solid line respectively in Figure 4.4). Since Simmons' model is more refined than the Holm's model, 17 Å can be considered to be the threshold value (maximum possible insulating film thickness) of inter-nanotube gap for the occurrence of electron tunneling. This value is very close to 1.8 nm (≈18Å) previously reported by Li et al. [39] for CNT-epoxy and CNT-alumina composites.

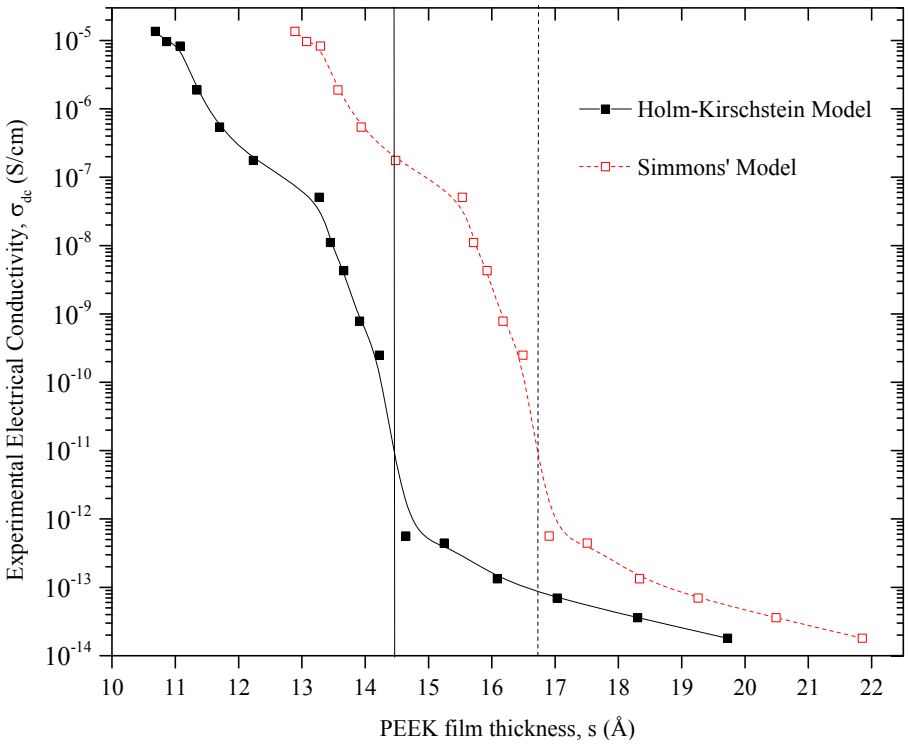

Figure 4.4: Expt. Electrical Conductivity as a function of insulating PEEK film thickness.

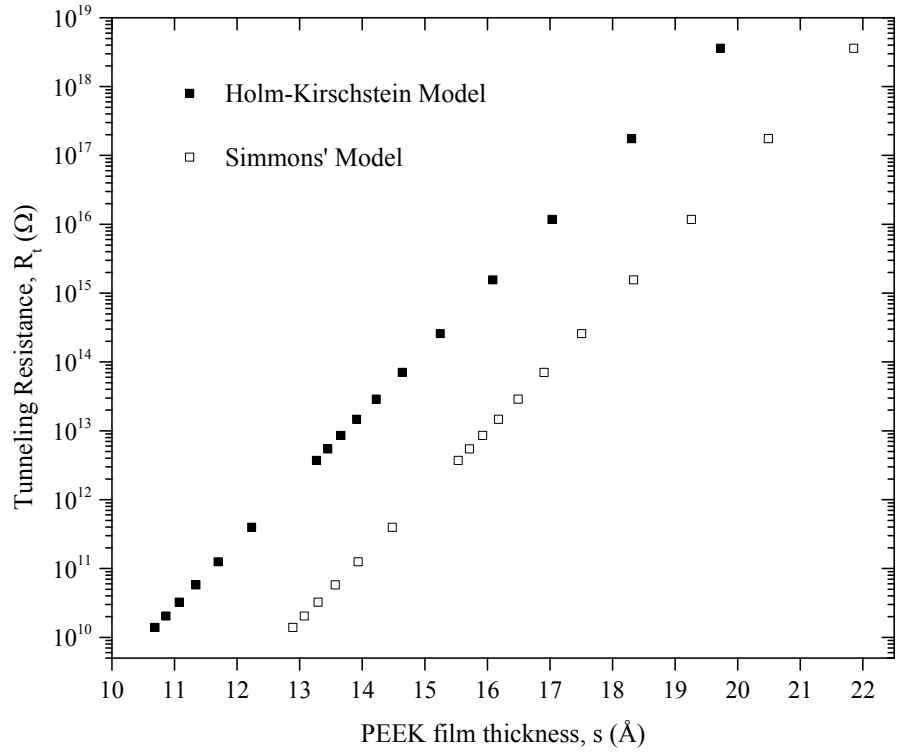

Figure 4.5: Tunneling resistance as a function of insulating PEEK film thickness.

4.3.4 Kovacs' model

For homogeneously dispersed, rigid and immobile particles of cylindrical shape, the following equation was derived [111]:

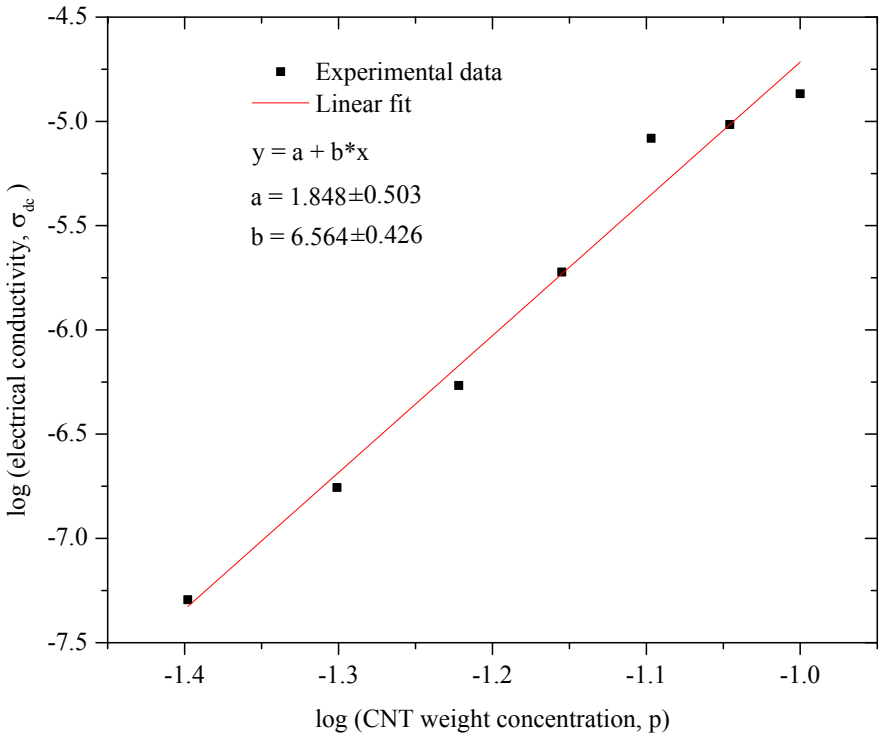

Figure 4.6: log-log plot of electrical conductivity vs. weight concentration.

$$\sigma_{sample} \approx \frac{l}{2\pi . r^2} \cdot \frac{p^{2x+1}}{R_c + R_t} \tag{4.15}$$

where σ_{sample} is the measured conductivity of the sample, p is the filler weight concentration, l is the length of the particle, r and R_c are the radius and resistance of a single particle, R_t is the tunnel resistance of its contact to the next particle and x is an exponent. Equating $2x+1$ to the slope of log σ_{sample} vs log p plot (Figure 4.6) above the percolation threshold and then solving equation (4.15) with the help of known parameters: length and radius of filler particle and resistance as well as conductivity and

concentration values at a single data point, R_c and R_t can be calculated for all concentration values. In the present calculation, values of d = 2r = 10 nm, l = 1000 nm and $\sigma_{cnt} = 10^4$ S/cm were used for an individual CNT.

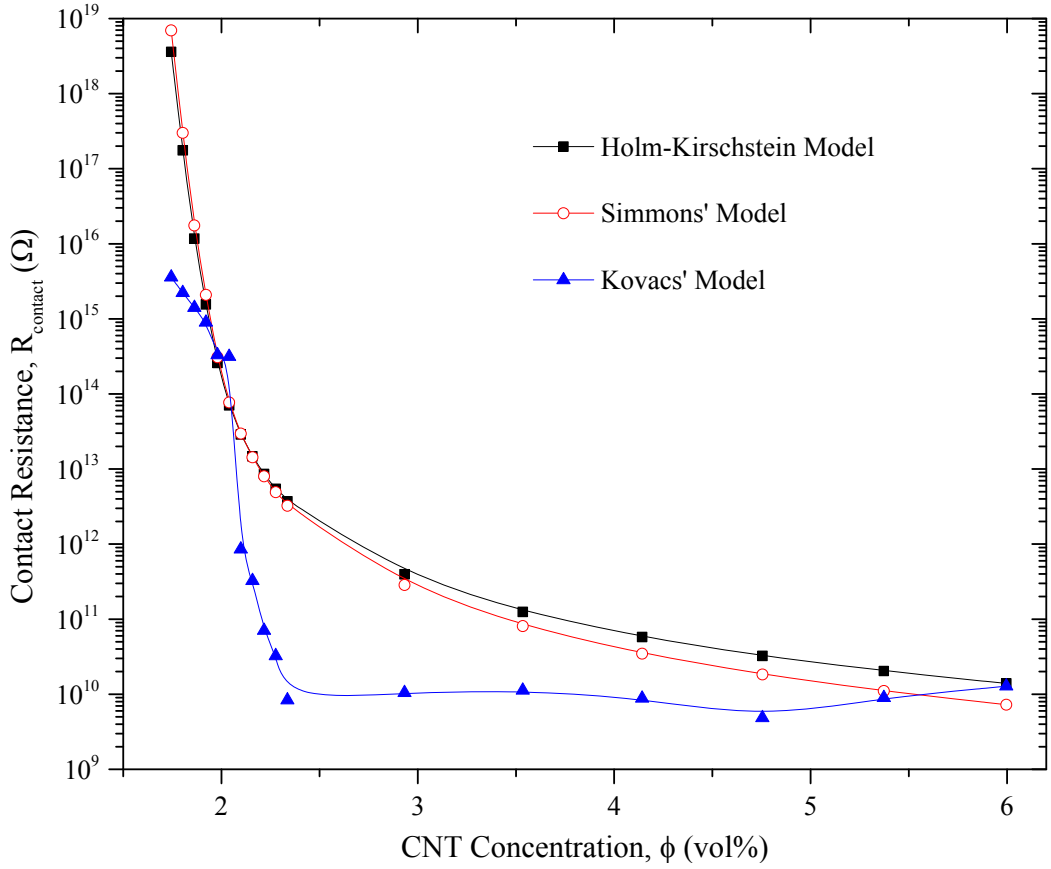

Figure 4.7: Contact resistance as a function of CNT volume concentration.

4.3.5 Discussion on contact resistance

Figure 4.7 shows a comparative picture of contact resistances obtained by the above discussed three models as a function of CNT volume concentration. As expected, contact resistance decreases with increase of CNT volume concentration. Similar to the tunneling resistance, Holm Kirschstein model predicts higher contact resistance than Simmons' model and with the increase of nanotube concentration, their difference gradually

increases. Among the three models, Kovacs' model gives the lowest estimate of contact resistance. In the case of Kovacs' model, contact resistance is almost constant (in the order of 10^{10} Ω) above the percolation limit with a trend of increase for higher CNT volume concentrations. The observed high values of $R_{contact}$ indicate the existence of an insulating polymer layer which prevents the direct physical contact between nanotubes. Because of such a layer, the conductivity phenomenon becomes complex.

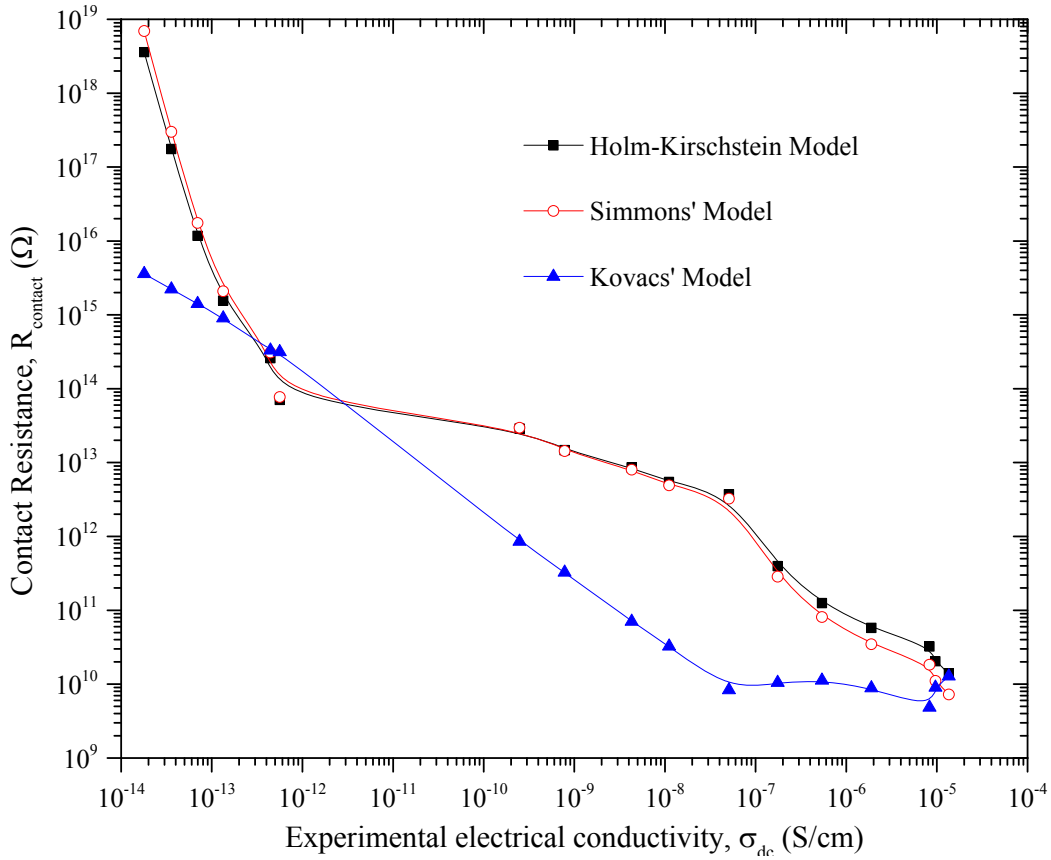

Figure 4.8: Effect of contact resistance on the electrical conductivity of nanotube composites.

As seen in Figure 4.8, there is a sharp jump of electrical conductivity at the vicinity of the percolation threshold and then gradually increases with increasing CNT concentrations. A sharp linear decrease of contact resistance was observed in the neighborhood of

percolation threshold in Kovacs' model which is more than two orders of magnitude compared with Holm-Kirschstein or Simmons' model. While graphs obtained by Holm-Kirschstein model and Simmons' model follow the same pattern, graph by Kovacs' model behaves differently from them. This different behaviour results from the fact that Kovacs' model does not accurately account for electron tunneling across the thin film formed between CNTs. However, at region of higher CNT concentrations, both contact resistance and electrical conductivity anticipated by three different models are almost comparable.

4.4 Summary

(1) By employing Holm-Kirschstein equation, Simmons' equation and Kovacs' equation, contact resistances of crossing CNTs with an insulating layer in between were calculated.

(2) Holm-Kirschstein model predicts lower film thickness, lower electrical conductivity, higher tunneling resistance and higher contact resistance than Simmons' model.

(3) Maximum tunneling distance in this composite system was predicted to be 14.5 Å by Holm-Kirschstein model and 17Å by Simmons' model. This value (17Å) is very close to the previously reported one of 18 Å [39].

(4) Kovacs' model estimates significantly lower contact resistance than Holm's or Simmons' model, because it does not take into account the effect of electron tunneling accurately.

Chapter 5

Effect of Pressure on Electrical Conductivity of CNT-PEEK Composites

5.1 Introduction

Extensive research has been carried out to take advantage of the outstanding properties of CNTs, especially in the field of aerospace, electrical, biomedical and computer science, the efforts for the application of CNTs have been very active. Enhancement of the electrical conductivity of polymers by mixing them with multi walled carbon nanotubes (MWCNTs) has found significant applications in newer areas such as electronic equipment, pressure sensitive switches, important strategic materials such as Electromagnetic Interference (EMI)/Radio Frequency Interference (RFI) shielding in computer and cellular phone housing. Future air vehicles are likely to adopt sensor/actuator embedded composites for structural health monitoring to reduce their maintenance cost. Such materials known as 'smart materials' can identify a change in the environment and respond to it by performing both sensing and actuation. The usual stimuli are pressure, temperature, electricity, vibration etc. whereas the useful responses are changes of conductivity, heating, mechanical/acoustic damping etc.[145].

CNT-filled conductive polymeric composites can be used as sensing elements in many engineering applications such as biomedical industry, automotive industry, food industry, environmental monitoring, agriculture and fishing industry, manufacturing industry, security and others [146]. Their electrical conductivity changes with application of external pressure. Many authors published their works on the changes of electrical

resistance or conductivity under the effect of external pressure. A brief review of the previous works is summarized below:

5.1.1 Rubber composites

Pedroni and his co-workers [147] prepared samples of conducting elastomeric composites based on MWCNTs and SBS block copolymers by using a solution casting technique and evaluated their electrical conductivity and mechanical properties. They claim that by the addition of MWCNTs, they have produced conductive elastomers with the lowest percolation threshold reported so far which imply that these materials could be used as charge dissipaters in electronic equipment and EMI shielding. Their results also show that MWCNTs act as a reinforcing agent which overcomes the plasticizer effect observed for polymeric dispersant agent, leading to an overall improvement in the mechanical properties.

Taya et al. [148] analyzed the piezoresistive behavior of a conductive short fiber–elastomer matrix composite by applying a percolation model. They applied fiber reorientation model to the composite system to predict the relation between the applied finite strain and the reorientation of conductive short fibers. Their results show that threshold fiber volume fraction increases as the applied strain increases and initially conductive composite becomes non-conductive around the critical strain, exhibiting a switching behavior.

Pramanik et al. [149] studied the resistivity and mechanical properties of nitrile-rubber based conductive composites filled with short carbon fibers (SCFs) and mixed filler system (SCF and CB). They found an appreciable effect of static extensional strain on the

tensile modulus and electrical resistivity of the composites where electrical resistivity decreases with increasing fiber concentration in the matrix and also with increased proportions of particulate CB in the filler-blend composition.

Yoshimura et al. [150] developed spring-shaped carbon microcoils (CMCs) embedded in silicone rubber and claimed that CMC–silicone rubber composites stand a good chance in making tactile sensors because of their high sensitivity. They also investigated mechanical and electrical properties of composites involving CMCs.

5.1.2 Polymer composites

Influence of unidirectional pressure on the electrical conductivity of carbon black filled polyethylene was examined by Wang and his team members [151]. In their analysis, they used High Density Polyethylene (HDPE) and applied various pressures along the thickness direction of the samples at constant ambient temperature. Using three different weight concentrations (10%, 12.5% and 15%) of CB, they found that at a low pressure the conductivity of CB–HDPE compounds decreases with the increase of pressures, reached a minimum value, then increased with the further increase of pressure. The conductivity was not very sensitive to the pressure in the high concentration CB-containing composite.

Yongliang and his group [152] also conducted similar experiments to investigate the piezoresistive behavior of carbon black filled poly (methyl vinyl siloxane) (PMVS) vulcanites under uniaxial compression. At CB weight fractions (p) slightly above the percolation threshold (p_c), they found that electrical resistance first increased with pressure and then turned to decrease at a critical compressive stress, thus exhibiting a

positive pressure coefficient of resistance (PPCR) and a negative pressure coefficient of resistance (NPCR) respectively. They also noticed that effect of NPCR was strong and the effect PPCR was weak when $p >> p_c$. They related the PPCR-NPCR transition process to true stress believing that change in microstructure in the percolating network, i.e. breakdown and reformation of infinite conducting clusters under pressure were responsible for the uniaxial piezoresistance and plastic deformation of the filled vulcanites.

Chen et al. [153] investigated time-dependence of piezoresistance, reproducibility and stability of the piezoresistive behavior for high density polyethylene (HDPE)–foliated graphite (FG) nanocomposites. Their experimental results show that relative resistance decreases with time under a lower fixed pressure, whereas the composite resistance increases with time under a higher fixed pressure. They also observed that electrical response with time under compression is sharper at higher fixed pressures and lower FG concentrations.

Qu and Wong [154] also experimentally investigated time dependent piezoresistive properties of conductive polymer composites. Using a melt compounding method, they prepared samples from expanded graphite reinforced polypropylene modified by maleic anhydride and found that resistivity decreased rapidly with compressive stress of less than 10 MPa, reached a plateau value at a higher compressive stress from 10 MPa to 30 MPa and then slightly increased with the increase in the stress beyond 30 MPa. Their results also showed that electrical resistivity decreased significantly with time under high mechanical stress while it increased slightly at a compressive stress of 31 MPa.

In an interesting study by Kchit and Bossis [155], piezoresistivity of magnetorheological elastomers (*are smart materials made by aligning magnetic microparticles inside a liquid polymer before the curing process has started. Once cured, the composite presents new properties such as a large change of elasticity when applying a magnetic field*) are analyzed. They observed power law decrease of the resistivity versus pressure when the particles inside the matrix are in contact and exponential decrease of the resistivity versus pressure when the particles inside the matrix are not in contact. They explained both behaviours with the help of tunnel effect on the area of contact.

By means of an analytic solution of piezoresistive stress co-efficient based on percolation like power law of resistivity, Wang et al. [156] showed that for the composite materials where Young's modulus of the insulating matrix phase is much less than that of conducting phase, the piezoresistive stress co-efficient (given by $\Pi = \frac{d\rho/\rho}{dP} = \frac{d\ln\rho}{dP}$ where ρ is the resitivity) depends (decreases) on the applied stress (P) reversely (i.e. follows log Π vs. log P plot) at lower stresses and logarithmically (i.e. follows Π vs. log P plot) at higher stresses at the percolation threshold. They demonstrated that the prediction of the model agrees well with experimental results of carbon reinforced polymer (epoxy and polyurethane) composites and polymer derived ceramics (silicon carbonitride).

Pham and his group [157] recently worked on development of strain sensors using MWCNTs and thermoplastic matrix PMMA. They found a wide range of sensitivity which is comparable to the conventional resistance-type strain gauges. They claim that numerous potential military and industrial applications of their developed strain sensor

are available ranging from macroscopic to nano-scale devices. They also developed a semi-empirical model based on percolation theory to identify the relationship between applied strain and sensitivity factor.

Park and his team [158] developed MWCNT film using Polyethylene Oxide (PEO) as the polymer matrix. In their experiments, the unique characteristics in macro scale deformation-dependent electrical resistance change for different volume fractions imply that MWCNT-PEO composite films can be used as tunable strain sensors and for application into systems such as embedded sensors in composite structures.

Wang et al. [159] developed a novel route to fabricate a new flexible force sensor using carbon composites that consist of micro carbon particles as conductive matrix, silicone rubber as the insulating matrix and elastomer fillers as the elastic matrix. The force sensor not only shows a gradual change in electrical resistivity with applied quasi-static pressure, but also measures the changes of compression stress relaxation in soft substrates under it. Since their samples were flexible and thin (1.2 mm) enough to be adhered on the measured soft substrates, they estimated the result of relaxation to be obtained directly instead of presumption from sample testing.

5.1.3 Application of conductive composites as pressure sensors

Hussain and others [160] fabricated a new pressure sensitive composite by dispersing homogeneously conductive carbon particles in an insulating silicone rubber matrix which showed a gradual change in electrical resistivity with applied pressure within the percolation threshold region at a constant temperature. They observed a significant improvement in successive measuring of resistivity variation when composites were

fabricated in hexane solvent media. To control the resistivity variation and to improve mechanical properties of the composites, they dispersed nano sized Al_2O_3 and suggested that, this material can uniquely be used as pressure sensors for robot applications.

Flandin and his team [161] presented a 3D numerical simulation of electrical properties of polymer nanocomposites. They showed that a.c. electrical properties measurements under large strain, strongly contrasted in the view point of their electrical and mechanical properties, can be used as an effective tool to monitor in situ the damage of composites made of electrically conductive fillers dispersed in an insulating matrix.

Compounding natural rubber (NR) and carbon black (CB), Job and his group [162] prepared high electrical conductivity composites where the electrical conductivity changes from 10^{-11} S/cm to 10^{-2} S/cm depending on the concentrations of CB in the composite. According to their claim, the linear and reversible dependence of the conductivity on the pressure in the range from 0 to 1.6 MPa is a warranty that these composites can be used as pressure sensors in orthopedic areas.

Knite et al. [163] used polyisoprene and carbon black to fabricate conductive nanocomposites that could be used as tensile strain and pressure sensor materials. The maximum sensitivity of the nanocomposites they made was observed in the vicinity of the transition of electro-conductive percolation and it exhibited a very weak semi-conductor like temperature dependence of resistance as tenso-resistive and piezo-resistive effects were practically thermally stable in the region of 20°C –70°C.

Sinha et al. [146] in a review presented the distinct physical, electronic and mechanical properties of CNT to highlight the present and future research and development work in the area of carbon nanotube sensors for real-world applications.

Mahmoud et al. [164] experimentally investigated conductive acrylonitrile butadiene rubber (NBR) compound filled with different concentrations of fast extrusion furnace (FEF) black. They found the most sensitive to compressive strain samples in the region of percolation phase transition which is about 65 phr. The piezoresistive effects of all of their samples were practically thermally stable within the interval of 24°C –35°C.

Effects of instantaneous compression pressure on electrical resistance during compressive stress relaxation were experimentally studied by Wang and his co-workers [165]. They used carbon black powder as the conductive phase and room temperature vulcanized silicone rubber as the insulating matrix and found that a sudden increment of composite resistance increases with the increase of instantaneous compression pressure. They also made a very thin (1.25μm) flexible pressure sensor array [166] to calculate nonlinear error, hysteresis error, repeatability error, resolution, time drift, temperature drift and moisture drift. The area, the thickness, and the number of sensing elements of the pressure sensor proposed can be adjusted according to different requirements in other engineering applications, such as the artificial skin, the finger-tip haptics of the robot.

Recently Wang et al. [167] studied piezoresistance of a MWCNT filled silicone rubber composite under uniaxial pressure to estimate the effects of carboxyl radical group on their electrical resistance. They showed that active carboxyl radical on MWCNTs can effectively improve the homogeneous distribution and alignment of conductive paths in the composite thereby producing positive piezoresistance with improved sensitivity, sensing range and sensing linearity for pressure.

According to Dharap et al. [168] existing conventional sensors such as strain gauges are discrete point and fixed directional sensors, and are separate from the material or structure that is being monitored; hence, not embedded in the material level. To overcome this limitation, they developed a CNT film by using randomly oriented bundles of SWCNT for strain sensing on the macro scale. Their experimental results are very encouraging and indicate the potential for multidirectional and multiple location strain sensors on the macro scale due to the isotropic properties of SWCNT films.

Wu et al. [169] showed that hydrostatic pressure can induce radial deformation, and therefore electrical transition of SWCNTs which provides a basis for designing nanoscale tunable pressure sensors.

A significant number of papers have been published over the last 20 years on piezoelectric and pyro-electric polymers, especially on poly vinylidene fluoride (PVDF). Recent investigations in this field have been directed to understanding the nature of ferroelectricity exhibited by PVDF and its copolymers [170]. Li et al. [55] published a paper elaborating a thorough review of sensors and actuators based on carbon nanotubes and their composites.

To date, most of the studies on sensing material investigated electrical properties of composites made of SWCNT, CB, CMC as conducting element in elastomeric rubber materials, Polyvylidene fluoride (PVDF) as matrix [150, 151, 169]. However, there is limited application of most of the research outcomes and some pressure sensors based on those material still needs to be improved or adjusted to meet specific requirements of engineering application. Possibility of using advanced thermoplastic materials e.g. PEEK,

PMMA as matrix and MWCNTs as filler material to develop pressure sensing element has rarely been attempted.

The change of electrical resistance (or conductivity) of the composites with pressure depends on the polymer characteristics such as aggregate structure, on structures of CNT fillers and on the interaction between the polymer and the filler. In this chapter, the change of electrical conductivity of thermoplastic composites made of MWCNTs and PEEK for different CNT loadings with high compression pressure is investigated. The effect on insulating film thickness on the change of electrical conductivity is also presented. A simple model based on compression is developed to explain the change in electrical resistance with the application of pressure.

5.2 Experimental

5.2.1 Sample preparation

Nanocomposite samples were prepared according to the procedure described in chapter 2. At low weight concentrations of CNTs, even though the material is conductive, there is significant variation in conductivity. Measurement of AC conductivity by DEA (Figure 3.1) shows that for the samples with 8 wt% – 10 wt% of CNTs, electrical conductivity was frequency independent over the entire range of frequency studied. Therefore, further investigation of the effect of temperature and pressure on electrical conductivity was carried out only on samples of these three weight concentration: 8 wt%, 9 wt% and 10 wt% of CNTs.

5.2.2 DC measurement of electrical conductivity

The DC measurement of electrical conductivity was done in the following two different ways depending on the magnitude of the samples' volume resistivity:

(i) Electrical volume resistivity of the composites with resistivity ≥ 10^8 Ω-cm was measured using an Agilent high resistance meter (Model 4339B). From volume resistivity and geometry of the sample, electrical resistance R was calculated using the equation

$$R = \rho \frac{z}{A} \tag{5.1}$$

And electrical conductivity, σ (in S/cm) was calculated by

$$\sigma = \frac{1}{\rho} \tag{5.2}$$

where z is the thickness in cm, A is the cross sectional area in cm^2, ρ is the volume resistivity of the sample in Ω-cm.

(ii) When samples' volume resistivity was below the limit of Agilent high resistance meter (< 10^8 Ω-cm), electrical resistance across the thickness of the sample was measured by using a Fluke digital multimeter, which can measure resistances up to 100 MΩ. The sample electrical conductivity, σ (in S/cm) was then calculated according to the following equation

$$\sigma = \frac{z}{R\,A} \tag{5.3}$$

where z = sample thickness in cm, R = Sample Resistance in ohm and A = cross-sectional area of the sample in cm^2

The electrical resistance measured by the Fluke digital multimeter, R consists of following three components:

$R = R_{sample} + R_{contact} + R_{wires}$

A metallic hook was connected to a highly conductive copper wire of short length (about 300 mm) so that magnitudes of the component R_{wires} is much smaller than the other terms and can be ignored. Contact resistance ($R_{contact}$) plays a significant role relative to the overall specimen resistance. Contact resistance depends on contact area, contact gap, type of junction (metallic–metallic or metallic–semiconducting) etc. Conventionally metallic coats (like silver-epoxy, gold-epoxy etc.) are used as electrodes for better electrical connection and to minimize contact resistance. The present investigation is desired to be carried out at high temperatures (up to 140°C) and pressures (up to 40 MPa). Under such high pressure and temperature, the contact points might be expanded as metallic epoxy coats might become softened which affects the measurement of actual sample resistance. To overcome this situation and to get repeatable result, conductive copper mesh was selected as an alternative electrode for high temperature and pressure application. The mesh was impregnated on both surfaces of the samples (Figure 5.1a) by pressing them in the Wabash hot press at 340°C for one minute with a small compaction pressure of ½ ton.

(a) (b)

Figure 5.1: CNT-PEEK samples (a) with copper mesh, (b) with silver-epoxy paste.

To impregnate the copper mesh onto the round shaped CNT-PEEK sample, a very thin film of same wt% of CNTs and PEEK was used on top and bottom of the sample so that the copper mesh is impregnated permanently and does not move laterally during the compression experiment. With this arrangement, the contact resistance does not change under application of compression and temperature. As such, for comparison purposes, the effect of the contact resistance on different samples can be factored out. Electrical wires are connected to the copper meshes for electrical resistance measurement.

A comparison of dc electrical conductivity (σ_{dc}) data obtained by AC measurement (done by DEA) and DC measurement (done by either Agilent High Resistance meter or Fluke digital multimeter) is presented in Table 5.1. The differences in the values are quite acceptable for higher wt% of CNT samples under the investigation in this chapter and in the next chapter. Conductivity obtained by DEA is larger in most samples than that obtained by DC measurements. With the increase of CNT concentration, conductivity by DC measurement approaches to that of DEA. This is because the number of nanotube contacts increases with increasing nanotube concentration and many conductive paths become available. As a result, potential charge carriers travelling through the network follows the paths which avoid larger barriers [45].

Table 5.1: Comparison of electrical conductivity obtained by AC measurement and DC measurement

wt% of CNT	σ_{dc} (S/cm) obtained by AC measurement (DEA)	σ_{dc} (S/cm) obtained by DC measurement (Agilent meter/Fluke Digital multi meter)	% difference
1.0	8.09×10^{-15}	7.38×10^{-15}	8.80
2.0	1.27×10^{-14}	1.16×10^{-14}	8.93
3.0	1.80×10^{-14}	1.63×10^{-14}	9.14
3.1	3.58×10^{-14}	3.16×10^{-14}	11.70
3.2	6.97×10^{-14}	6.30×10^{-14}	9.50
3.3	1.34×10^{-13}	1.23×10^{-13}	7.85
3.4	4.43×10^{-13}	4.00×10^{-13}	9.74
3.5	5.62×10^{-13}	5.18×10^{-13}	7.72
3.6	2.49×10^{-10}	2.26×10^{-10}	9.09
3.7	7.82×10^{-10}	7.10×10^{-10}	9.12
3.8	4.30×10^{-9}	3.92×10^{-9}	8.86
3.9	1.11×10^{-8}	9.87×10^{-9}	10.97
4.0	5.08×10^{-8}	4.68×10^{-8}	7.97
5.0	1.76×10^{-7}	1.59×10^{-7}	9.31
6.0	5.41×10^{-7}	4.97×10^{-7}	8.06
7.0	1.89×10^{-6}	1.75×10^{-6}	7.67
8.0	8.29×10^{-6}	8.21×10^{-6}	1.00
9.0	9.66×10^{-6}	9.86×10^{-6}	2.01
10.0	1.36×10^{-5}	1.27×10^{-5}	6.64

To check the accuracy of the Fluke digital multimeter, measurements of voltage-current (V_i-I) relationship were made at room temperature using a Keithley 6220DC precision current source and a Keithley 2182A voltmeter and presented in Figure 5.2 for

conductive samples with CNT concentration 8 wt% to 10 wt%. From the slope of the linear fit and geometry of the sample, the electrical conductivity was calculated and presented in Table 5.2 to compare with those obtained from the measurement of Fluke digital multimeter. The results are in good agreement with accuracy more than 99%.

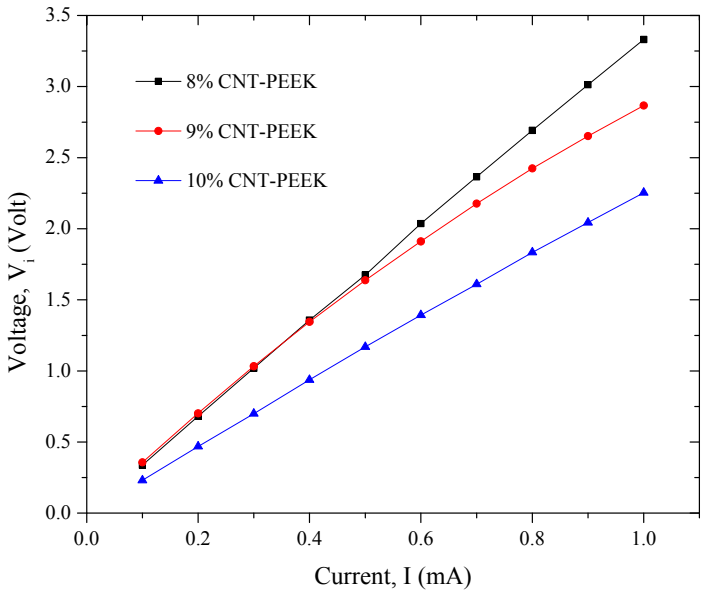

Figure 5.2: V_i-I characteristics of the composite samples.

Table 5.2: Comparison of electrical conductivity measured at room temperature using fluke digital multimeter and Precision current source/voltmeter (V_i-I measurement)

wt% of CNT	σ (by Fluke digital multimeter) S/cm	σ (by V_i-I measurement) S/cm
8	8.31×10^{-6}	8.29×10^{-6}
9	9.86×10^{-6}	9.92×10^{-6}
10	1.27×10^{-5}	1.23×10^{-5}

For comparison purpose, a few room temperature electrical conductivity measurements were performed using silver epoxy paste (Figure 5.1b) as electrodes to verify the results obtained with copper meshes. Table 5.3 shows the comparison of electrical conductivity

of samples obtained at room temperature using copper mesh and silver epoxy paste as electrodes. The difference between them is less than 6%. This can be due to variation of contact resistance from sample to sample.

Table 5.3: Comparison of electrical conductivity measured at room temperature using copper mesh and silver epoxy paste as electrodes

wt% of CNT	σ (by copper mesh) S/cm	σ (by silver epoxy paste) S/cm	% of difference
8	8.31×10^{-6}	8.65×10^{-6}	4.1
9	9.86×10^{-6}	1.03×10^{-5}	4.5
10	1.27×10^{-5}	1.34×10^{-5}	5.5

5.2.3 Mechanical properties of CNT-PEEK composites

In order to study the effect of pressure on electrical conductivity of CNT-PEEK composites by applying compression load, the mechanical properties of the composites should be known. Ogasawara et al. [171] recently published their experimental results on mechanical properties of CNT-PEEK composites. The relevant mechanical properties are presented in the following Table 5.4.

Table 5.4: Mechanical properties of CNT-PEEK composites [171]

Mechanical Properties	Pure PEEK	9 wt% CNT-PEEK
Young's modulus, E (GPa)	4.2	6.3
Yield stress (MPa)	68	69

The yield stress has been found almost same for pure PEEK and PEEK-CNT composites. To avoid the yielding of the CNT-PEEK composite samples under present investigation, a pressure (40 MPa) which is much less than the above yield stress has been selected as the highest level of pressure.

5.2.4 Testing of samples

A schematic of the test set up is shown in Figure 5.3. The samples were compressed by applying a pressure from zero to 40 MPa in increments of 2 MPa using an MTS testing machine. Using a program in the MTS machine, the pressure (2 MPa) was increased by ramping at intervals of 2 minutes and after each increment of load, the pressure level was kept constant for an additional 5 minutes so that fluctuation of the experimental data is minimized. The sample resistance was measured across the thickness of the sample using a Fluke digital multimeter, which can measure resistances up to 100 MΩ. Deformation of the sample in the thickness direction was recorded at each loading. After one cycle of loading up to 40 MPa, the unloading was done following the same procedure in the reverse direction and the corresponding data of electrical resistance and deformation were recorded. This loading-unloading was repeated several times to check the hysteresis of electrical resistance data. For each pressure level of both loading and unloading, deformation of the sample was taken into account to find sample thickness, z and to calculate the corresponding electrical conductivity.

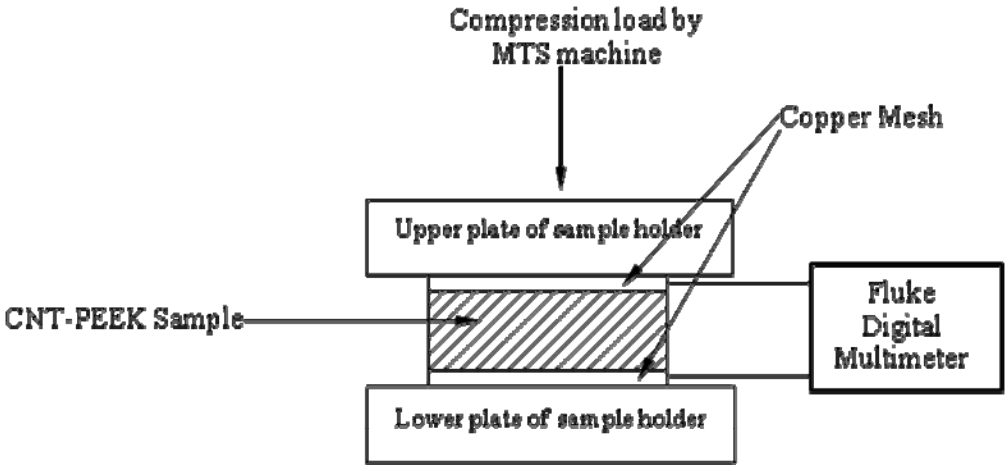

Figure 5.3: Schematic diagram of the experimental set up.

5.2.5 Dynamic Mechanical Analysis (DMA)

Dynamic Mechanical Analysis (DMA) of nanocomposite sample was performed with a TA instruments dynamic mechanical analyzer (DMA 983) at a fixed frequency of 1 Hz and at oscillation amplitude of 0.5 mm. The temperature range was 0 to 250°C with a heating rate of 5 °C/min.

5.3 Results and discussion

5.3.1 Effect of pressure

The electrical conductivity data reported here is the average of three samples of each nanotube concentration and is reproducible within 2% variation. The variation of electrical conductivity of samples containing three different weight concentrations of CNTs at different pressures are shown in Figure 5.4.

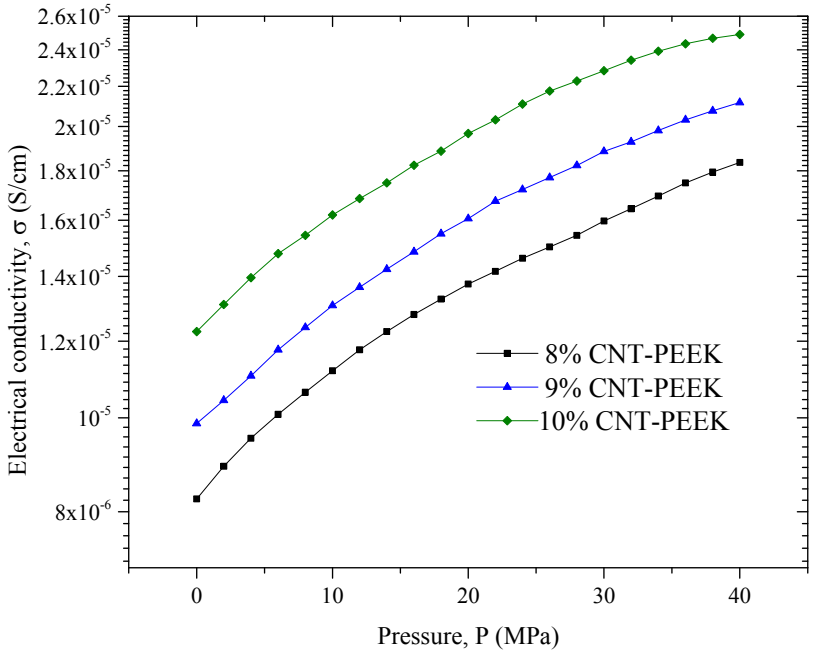

Figure 5.4: Electrical conductivity vs. applied pressure at room temperature (20°C).

Electrical conductivity increases sharply with increasing applied pressure up to a certain level and further increase in applied pressure has only a marginal effect on the change in conductivity. This variation in electrical conductivity with pressure follows a similar pattern at different CNT concentrations. At room temperature, the effect of pressure is more pronounced at lower pressure range than that at higher pressure range for all the samples. With the increase of pressure, rate of increase of electrical conductivity (slope of σ vs. P) decreases. Therefore, there exists a critical pressure below which an appreciable change in conductivity takes place and the samples act as pressure sensitive conductive composites. Beyond this critical value of pressure, the composite samples do not behave like an efficient sensor as the change in conductivity with increase in pressure is small. The range of this critical pressure is found to be almost same, but the range of conductivity variation is found to be different for the samples of different CNT concentrations studied here. For example, over the same range of pressure variation from 0 to 40 MPa, the magnitude of change in conductivity is highest for 8 wt% CNT samples (8.25×10^{-6} S/cm to 1.836×10^{-5} S/cm) while the magnitude is lowest for 10 wt% CNT samples (1.23×10^{-5} S/cm to 2.49×10^{-5} S/cm).

5.3.2 Loading-unloading cycle

The effect of loading-unloading cycle on the electrical conductivity of different samples at room temperature is shown in Figure 5.5. It is found that for all samples conductivity increases with the increase of number of cycles, but the loading and unloading cycles do not follow the same route. The change of electrical conductivity in the unloading cycle is very marginal at upper pressure region (above 20 MPa) while at lower pressure region,

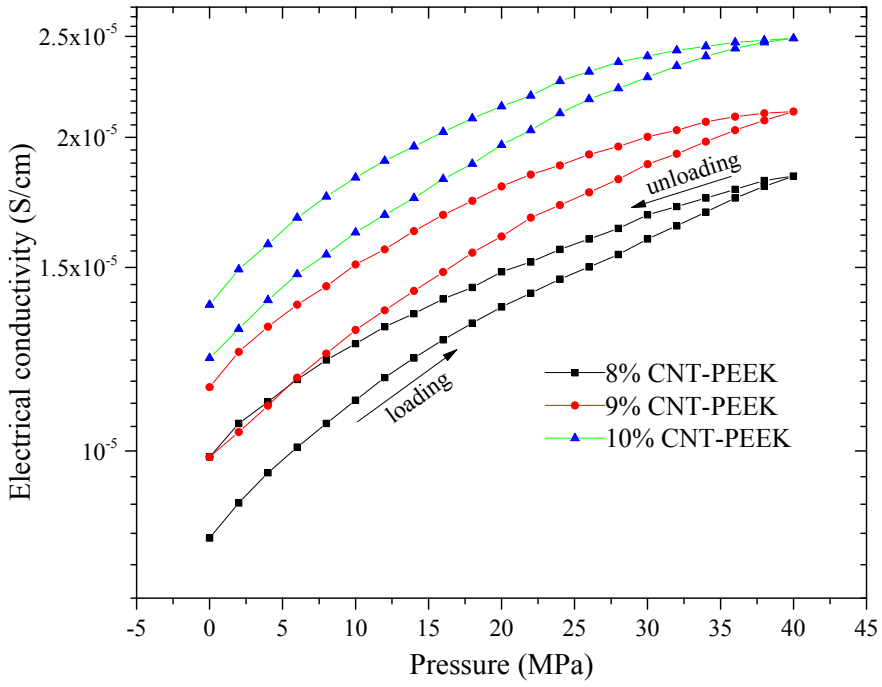

Figure 5.5: Comparison of loading-unloading curves of 8 wt% – 10 wt% CNT-PEEK composites at room temperature (20°C).

this change is appreciable. Thus, a difference between initial conductivity and final conductivity before the loading and after the unloading cycle is observed which can be termed as 'electrical set'. This electrical set gradually decreases with the increase of nanotube concentration, but the rate of decrease is very nominal. Relative to the initial conductivity, the magnitude of electrical set in first loading-unloading cycle in Figure 5.5 was calculated to be 19.64%, 16.67% and 12.5% for 8 wt%, 9 wt% and 10 wt% CNT-PEEK composites respectively. In the case of repeated loading-unloading cycle (Figures 5.6, 5.7 & 5.8) where results for only 1st and 2nd cycles are shown) of a particular sample, electrical set decreases rapidly and after second cycle, it becomes very marginal.

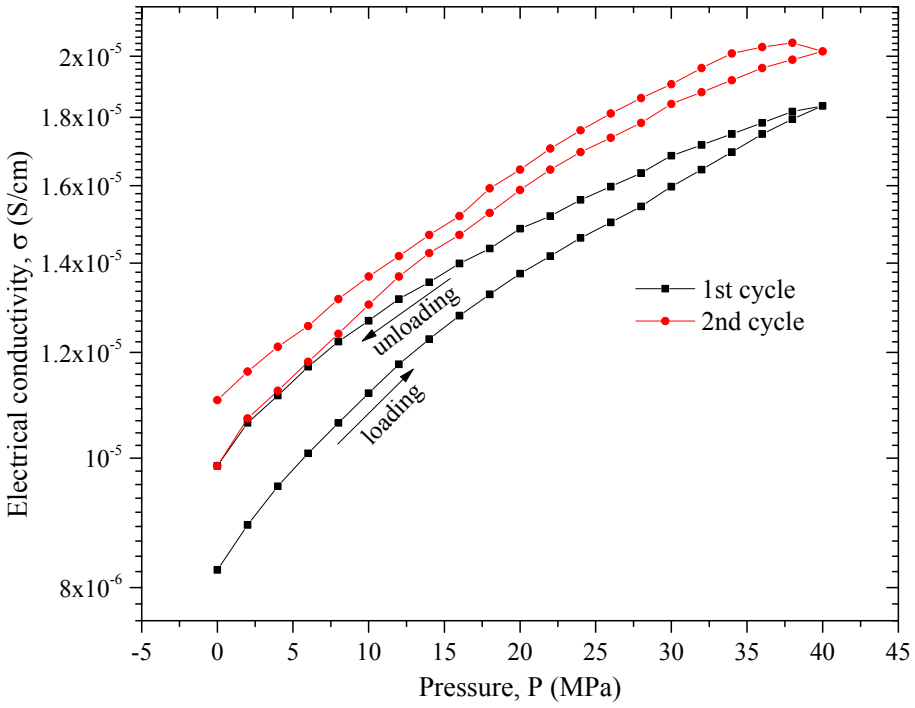

Figure 5.6: Repeated loading-unloading of 8 wt% CNT-PEEK composites at room temperature (20°C).

The electrical hysteresis (i.e. difference between areas under conductivity vs. pressure curves for loading and unloading) was also found to be higher in the first loading-unloading cycle for all samples than the second one, but this hysteresis was found to be of similar magnitude for all concentrations of nanotube in their identical loading-unloading cycle. For example, in first loading-unloading cycle, hysteresis (area enclosed by the 1st loading-unloading curves in conductivity vs. pressure graphs) for 8 wt%, 9 wt% and 10 wt% CNT samples are almost same by observation. Therefore, it indicates that for these highly conductive composites, nanotube content has very little effect on the change of electrical conductivity under subsequent compression loading-unloading cycle.

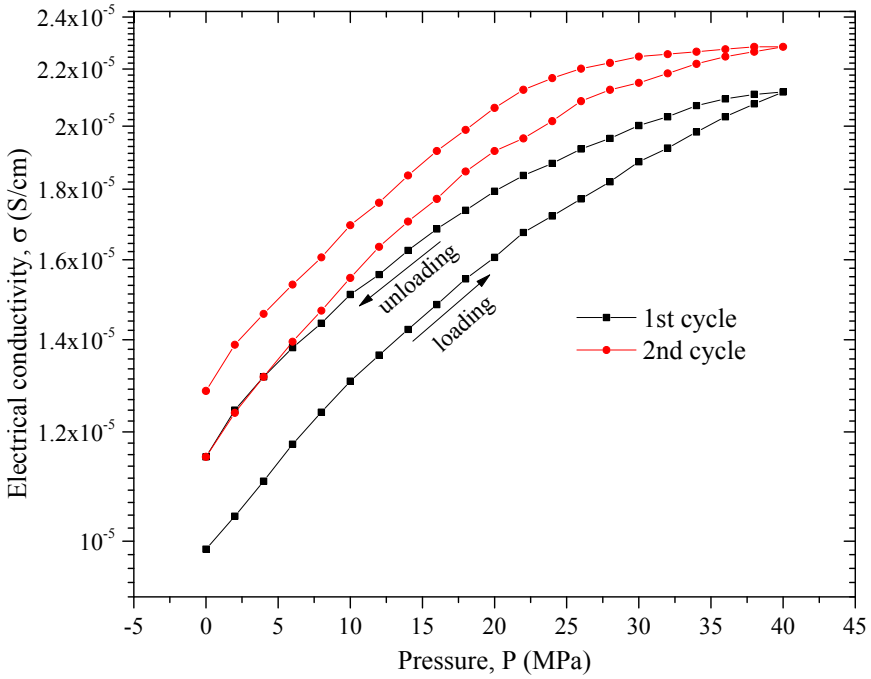

Figure 5.7: Repeated loading-unloading of 9 wt% CNT-PEEK composites at room temperature (20°C).

Again electrical conductivity also increases after each repeated loading-unloading cycles. At 40 MPa, for example for 8 wt% CNT samples (Figure 5.6), the conductivity after first cycle is 9.87×10^{-6} S/cm and after second cycle it is 1.11×10^{-5} S/cm. The difference between these two values gradually decreases for 9 wt% and 10 wt% CNT samples (Figures 5.7 & 5.8). It suggests that during first loading-unloading cycle, the system has attained a somewhat stabilized electrical network, which remains unaffected during further loading-unloading cycles. On successive loading-unloading, formation of new conducting paths and breakdown of existing conducting paths balance each other and thus composite conductivity becomes almost stable.

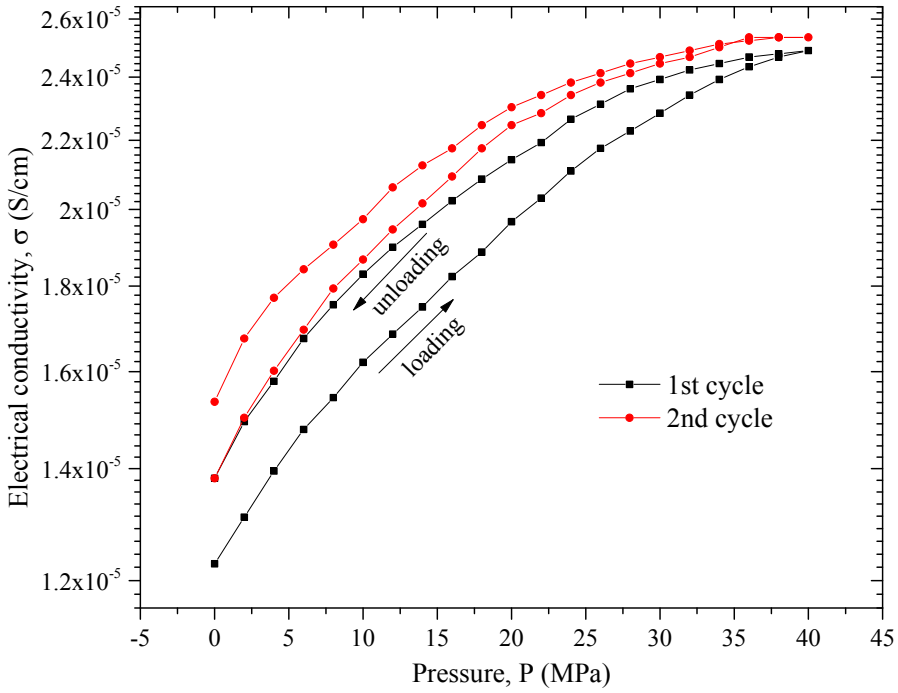

Figure 5.8: Repeated loading-unloading of 10 wt% CNT-PEEK composites at room temperature (20°C).

Explanation of such behavior mentioned above lies in the fact that the intrinsic structure of the material changes due to the bulk deformation of the sample caused by external compression. In other words, when a compression is exerted on polymer composites filled with conductive CNTs, it causes movement of the polymer chains which in turn affects the nanotube structure. The change in electrical conductivity of the samples during deformation comes partially from nanotube displacement which affects the conducting paths in the material. Since nanotube and polymer molecules are interlinked in these highly conductive composites, the change in their electrical conductivities with applied pressure is determined by three simultaneous processes operative in the system:

(i) Compression leads to the formation of new conducting paths or redistribution of existing conducting paths because of nanotube orientation in the direction perpendicular to the applied load.

(ii) Compression can cause a substantial decrease of inter-nanotube distance. When this distance is sufficiently small, electrons can hop easily because of inter-nanotube contact.

(iii) Sufficiently high compression can cause a decrease in CNT–CNT contact resistance by squeezing out the matrix from the inter-nanotube gap. As such, CNT–CNT contact resistance with the presence of thin matrix film (in the order of $10^{13}\Omega$ [44]) becomes direct CNT–CNT contact resistance (in the order of kΩ-MΩ [40]).

Since above the percolation threshold, the electrical conductivity of the composites are controlled by the conductivity of the CNTs and the quantity and quality of their physical contacts, the above mentioned three processes play the dominant role in determining the change of overall conductivity of the composites under compression. Furthermore, the structure of the CNT network created by van der Waals forces is unstable and compression can change the unstable structure to a stable one by making unrecoverable changes to the conductive network. Therefore with the increase of compression cycles, structure of CNT network becomes steady and the relation between composite conductivity and applied pressure becomes stable as shown in the graphs (Figures 5.6, 5.7 & 5.8).

5.4 Theoretical considerations

The electrical conductivity of conductive CNT based polymer composite materials depends on several factors including the amount of nanotube, type of polymer matrix,

prehistory of the sample, applied pressure and temperature. Under application of pressure or temperature, the mechanism of charge transport has a strong effect on the behavior of conductivity. The commonly used mechanisms are conductivity through direct contact between nanotubes and tunneling or hopping through the polymer film separating adjacent CNTs. At a certain volume fraction of CNTs, the inter-particle gap between CNTs become small enough to come close to or touch each other so that one to three dimensional continuous structures of conducting network be formed (Figure 5.9).

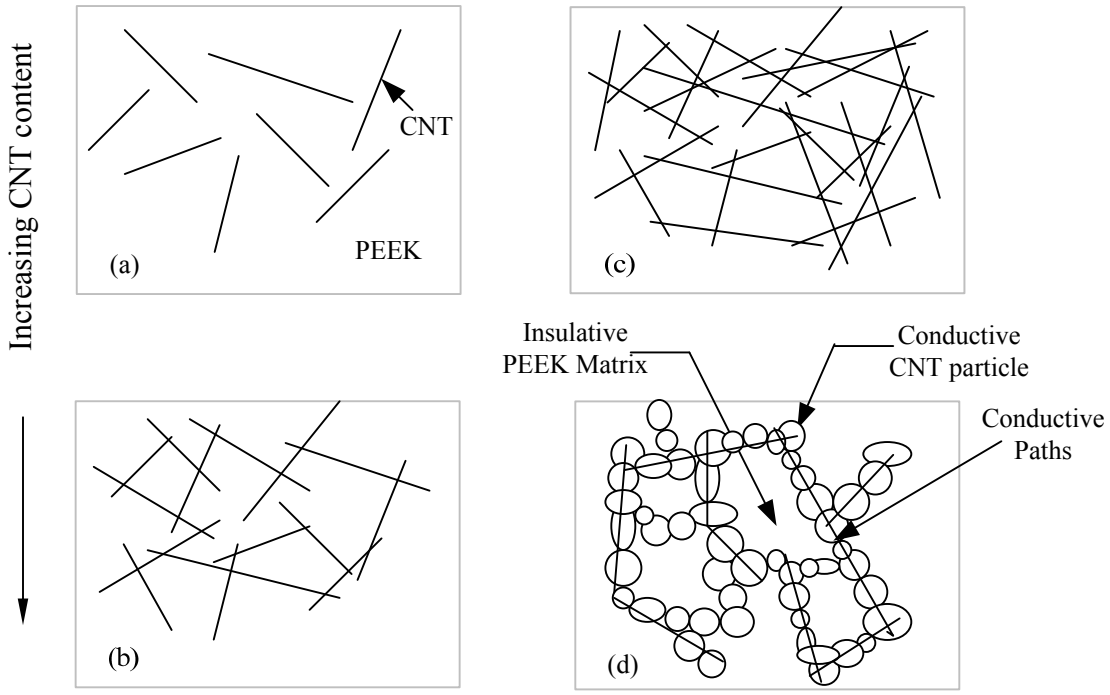

Figure 5.9: Formation of three dimensional conductive paths in CNT-PEEK composites without any externally applied pressure [160, 172].

As a result, contact effect or tunneling effect occurs and the local conductive path is formed in the insulating PEEK matrix. When external pressure is applied on the composites, the local conductive path can easily penetrate into the insulating matrix, thus forming effective conductive path. When the pressure is released, this conductive path is

discontinued. Figure 5.10 shows a schematic view of the formation of such conductive paths under the application of external pressure. With applied pressure, the conductive path is established at a lower volume fraction of CNTs than that of composites without applied pressure.

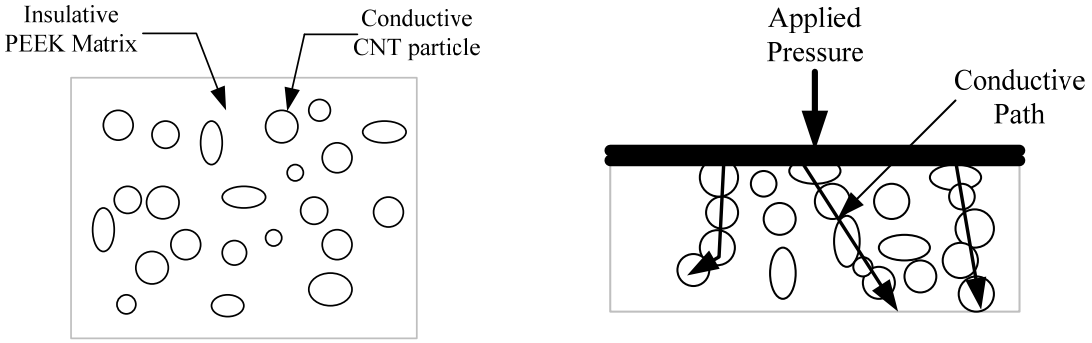

Figure 5.10: Formation of conductive paths in CNT-PEEK composites under externally applied pressure [160].

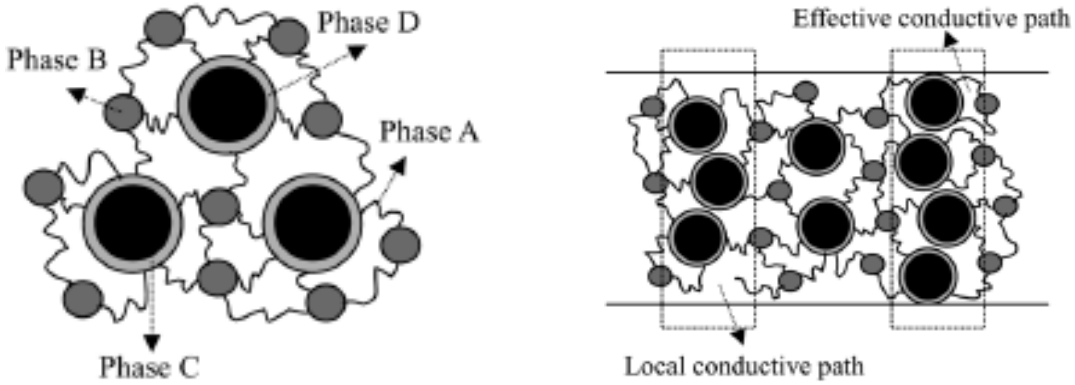

(a) Shell Structure (b) Local and effective conductive path

Figure 5.11: Schematic diagram for the inner structure of CNT-PEEK composites [173].

Wang et al. [173] described the above phenomenon by a shell structure model as shown in Figure 5.11. According to this model applied to CNT-PEEK composite, phase A is a PEEK molecule chain with active micro-Brownian motion, which is not absorbed by CNTs; Phase B is a PEEK molecule chain, the motion of which has been restricted by

phase A; Phase C is macro PEEK molecule chain and is absorbed on the surface of CNTs to form a thin insulating layer; Phase D is a CNT. Elastic phases A and B are attached to Phase C, which acts as a framework, forming a 3-D network composed of CNTs and PEEK molecules. The schematic view of the local conductive path and effective conductive path are shown in Figure 5.11(b).

5.4.1 Derivation of piezoresistance model

A phenomenon of changing electrical resistance of a material due to applied mechanical stress is called piezoresistance. The piezoresistive effect differs from the piezoelectric effect in the sense that the piezoresistive effect only causes a change in resistance; it does not produce any electric potential. In conducting composites the total resistance is a function of both the resistance through each conducting particle and the polymer matrix. Assuming that the resistance of the matrix is constant everywhere, the resistance of the paths perpendicular to the current flow may be neglected, and, thus, the number of conducting particles between electrodes becomes a factor in this relationship, as well as the number of conducting paths. Reproducing the Figure 4.1 here in Figure 5.12, the total resistance can then be described by [72, 131]

$$R = \frac{(M-1)R_t + MR_c}{N} \approx \frac{M(R_t + R_c)}{N} = \frac{M}{N}\left(\frac{\rho_t}{\pi a^2} + \frac{\rho_c}{2a}\right) \tag{5.4}$$

where R is the composite resistance, R_t and ρ_t are the tunnel resistance and tunnel resistivity between two adjacent particles, R_c and ρ_c are the constriction resistance and constriction resistivity across one particle, a is the radius of contact area, M is the number of particles forming one conducting path and N is the total number of conducting paths.

When the inter-particle separation is very large, no current flows through the inter-particle separation [174]. But if the separation is small, the tunneling current may flow through the separation. According to the analyses of Simmons [143, 175-177] the tunneling current J at low applied voltage is given by

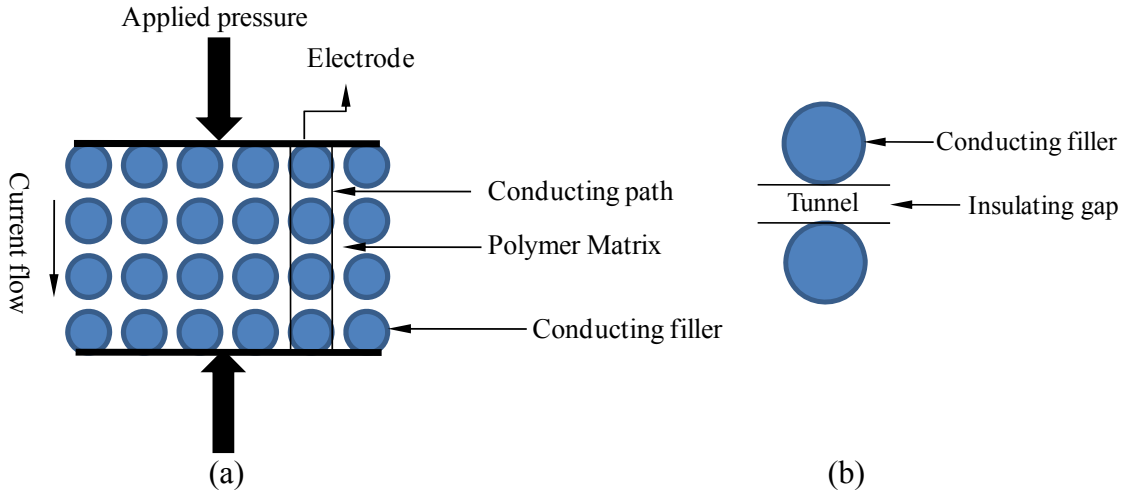

Figure 5.12: Schematic of the formation of conducting paths under applied pressure [140]

$$J(s,\psi) = \frac{3\sqrt{2m\psi}}{2s}\left(\frac{e}{h}\right)^2 V_i \exp\left(-\frac{4\pi s}{h}\sqrt{2m\psi}\right) \tag{5.5}$$

where m and e are the electron mass and charge respectively, h Plank's constant, V_i the applied voltage, s the thickness of the insulating film, and ψ the height of the potential barrier between the adjacent particles that can be obtained by the subtraction of polymer's work function from the conductor's. Because the electron tunneling probability depends on the insulating barrier thickness, it is considered that practically all the tunneling occurs within the small surface areas. Thus, as shown in Figure 5.12(b), s in equation (5.5) equals the separation between the surfaces of two adjacent particles, which is the least distance between the particles.

Using equations (5.4) and (5.5) tunneling resistance R_t can be obtained as

$$R_t(s,\psi) = \frac{\rho_t}{\pi a^2} = \frac{1}{\pi a^2}\frac{V_i}{J} = \frac{2h^2 s}{3\pi a^2 e^2\sqrt{2m\psi}}\exp\left(\frac{4\pi s}{h}\sqrt{2m\psi}\right) \tag{5.6}$$

The resistance of the composites depends on the nature of the contact between adjacent particles. The total resistance is the sum of the constriction resistance and tunnel resistance [142]. As the conductivity of the conducting particle is very large compared with that of the polymer matrix, the constriction resistance (resistance across the conducting particle) can be neglected ($R_c \approx 0$). Then substitution of equation (5.6) into equation (5.4) gives

$$R(s,\psi) = \frac{M}{N}\left[\frac{2h^2 s}{3\pi a^2 e^2\sqrt{2m\psi}}\exp\left(\frac{4\pi s}{h}\sqrt{2m\psi}\right)\right] \tag{5.7}$$

Using this equation, the composite resistance can be theoretically calculated.

When the conducting particles are not in contact and separated by a thin polymer film (Figure 5.12(b)), the resistance (only tunnel resistance in this case) given by above equation (5.7) is not constant, because the inter-particle distance s changes with pressure.

Let us assume that initially N_0 conducting paths are available and if all M particles in each of N_0 conducting paths are separated with the same initial thickness s_0, then the total initial resistance of the composite can be calculated as:

$$R_0(s_0,\psi) = \frac{M}{N_0}\left[\frac{2h^2 s_0}{3\pi a_0{}^2 e^2\sqrt{2m\psi}}\exp\left(\frac{4\pi s_0}{h}\sqrt{2m\psi}\right)\right] \tag{5.8}$$

Under compression, if the inter-particle separation decreases from s_0 to s and the resistance changes from R_0 to R:

$$\frac{R}{R_0} = \frac{s}{s_0}\frac{a_0^2}{a^2}\frac{N_0}{N}\exp\left[-\frac{4\pi}{h}\sqrt{2m\psi}(s_0 - s)\right] \approx \frac{N_0}{N}(1-\varepsilon_g)\exp(-\chi s_0 \varepsilon_g) \tag{5.9}$$

where $\frac{a_0^2}{a^2} \approx 1$, $\chi = \frac{4\pi}{h}\sqrt{2m\psi}$ and $\varepsilon_g = \frac{s_0 - s}{s_0}$ is the local strain between two adjacent particles. This local strain is supposed to be proportional to the macroscopic strain: $\varepsilon_g = \mu\varepsilon$ where μ ≫ 1 is a parameter to be determined by fitting experimental data. Assuming μ =1 and $\chi s_0 = A_0$ (a constant),

$$\frac{R}{R_0} = \frac{N_0}{N}(1-\varepsilon)\exp(-A_0\varepsilon) \tag{5.10}$$

If the applied pressure is uniaxial, the separation *s* can be expressed as follows:

$$s = s_0(1-\varepsilon) = s_0\left(1-\frac{P}{E}\right) \tag{5.11}$$

where ε is the strain of the polymer matrix, P is the applied pressure and E is the compressive modulus of the polymer matrix.

The separation s under high compression is calculated as

$$s = s_0(1-\varepsilon) = s_0\left[1-\left(\frac{\Delta z}{z_0}\right)\right] \tag{5.12}$$

where ε is the compressive strain of the matrix, Δz the deformation of composite sample, and z_0 the initial thickness of the sample. Substitution of equation (5.12) into equation (5.10) yields

$$\ln\frac{R}{R_0} = \ln\frac{N_0}{N} + \ln\left[1-\left(\frac{\Delta z}{z_0}\right)\right] - A_0\left(\frac{\Delta z}{z_0}\right) \tag{5.13}$$

Now let us consider two situations:

(a) During tunneling of conducting particles, the number of conducting paths remains unchanged, i.e. N = N_0.Then the first term on the right hand side of equation (5.13) becomes zero. As shown in Figure 5.13 (dotted line), the experimental data obtained on samples of 9 wt% CNT-PEEK composites at room temperature with R_0 = 2800 ohm is compared to equation (5.13) under this situation. It is seen that the model of the tunneling current does not describe the experimental data very well. The fitted curve shown was obtained with A_0 = 5.962379.

(b) Suppose that the high rate of the decrease of R/R_0 at larger deformations $\Delta z/z_0$ is related to redistribution of the conducting network, i.e. the number of initial conducting paths N_0 increases to N. To fit the curve, it can be assumed that

$$N = N_0 \exp\left[A\left(\frac{\Delta z}{z_0}\right) + B\left(\frac{\Delta z}{z_0}\right)^2 + C\left(\frac{\Delta z}{z_0}\right)^3 + D\left(\frac{\Delta z}{z_0}\right)^4 \right] \tag{5.14}$$

where A, B, C and D are constants.

By rearranging and taking logarithm,

$$\ln\frac{N_0}{N} = -A\left(\frac{\Delta z}{z_0}\right) - B\left(\frac{\Delta z}{z_0}\right)^2 - C\left(\frac{\Delta z}{z_0}\right)^3 - D\left(\frac{\Delta z}{z_0}\right)^4 \tag{5.15}$$

Substitution of equation (5.15) to equation (5.13) gives

$$\ln\frac{R}{R_0} = \ln\left[1 - \left(\frac{\Delta z}{z_0}\right)\right] - A_0\left(\frac{\Delta z}{z_0}\right) - A\left(\frac{\Delta z}{z_0}\right) - B\left(\frac{\Delta z}{z_0}\right)^2 - C\left(\frac{\Delta z}{z_0}\right)^3 - D\left(\frac{\Delta z}{z_0}\right)^4 \tag{5.16}$$

Using logarithmic expansion series

$$\ln\left[1-\left(\frac{\Delta z}{z_0}\right)\right]=-\left(\frac{\Delta z}{z_0}\right)-\frac{1}{2!}\left(\frac{\Delta z}{z_0}\right)^2-\frac{1}{3!}\left(\frac{\Delta z}{z_0}\right)^3-\frac{1}{4!}\left(\frac{\Delta z}{z_0}\right)^4-.....\infty \quad (5.17)$$

Equation (5.16) can be simplified as

$$\ln\left(\frac{R}{R_0}\right)=A'\left(\frac{\Delta z}{z_0}\right)+B'\left(\frac{\Delta z}{z_0}\right)^2+C'\left(\frac{\Delta z}{z_0}\right)^3+D'\left(\frac{\Delta z}{z_0}\right)^4 \quad (5.18)$$

Using curve fitting to obtain A', B', C' and D', the same experimental data with R_0 = 2800 ohm compared to equation (5.18) are shown in Figure 5.13 (solid line). A good agreement between the theoretical and experimental curves is achieved at

$A' = -35.815,\ B' = 2732.972,\ C' = -57638.503,\ D' = 344345.842$

Here, the first co-efficient (A') is an indicative of nanotube separation distance (A' ≈ f(χs)) and the other three terms signify the redistribution of conducting paths.

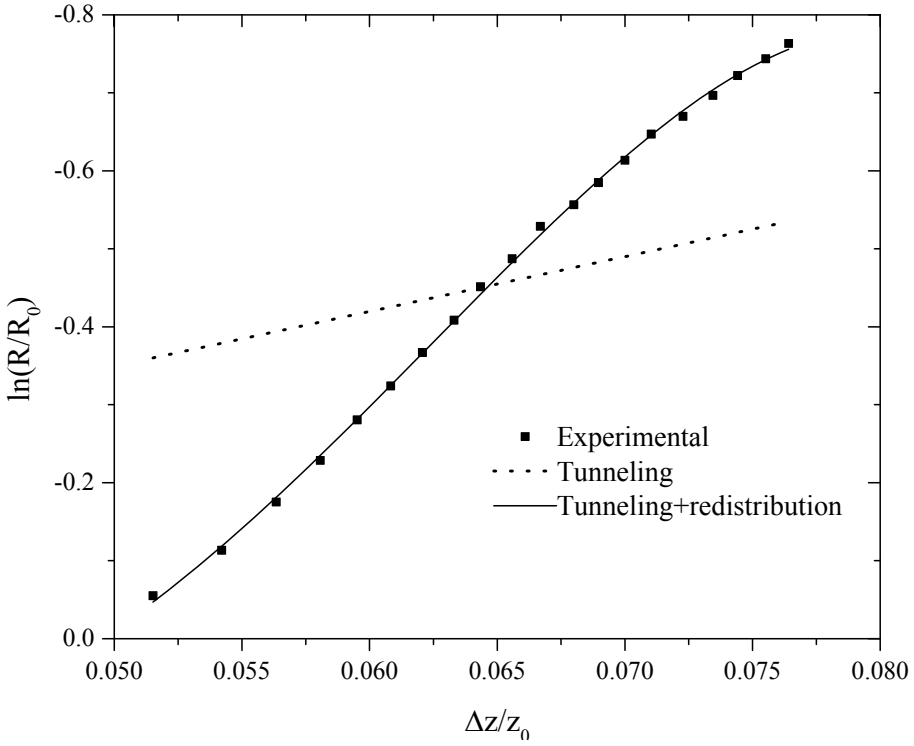

Figure 5.13: Experimental data of 9 wt% CNT-PEEK samples compared to equation (5.13) (tunneling, N = N_0) and equation (5.18) (tunneling & redistribution).

As described in Table 2.1 and Table 2.2, the Young's modulus of CNTs is about 300 times higher than that of pure PEEK, therefore CNTs can be regarded as almost incompressible compared with PEEK and the application of external compression may theoretically induce translation and rotation of CNTs that causes redistribution of conducting paths and a change of electrical conductivity of one single effective conductive path and the number of the effective conductive paths [173]. Scanning electron micrograph of 9 wt% CNT-PEEK sample after compression shown in Figure 5.14 confirms this redistribution of CNTs. With addition of CNTs, plastic deformation is increased, only the pull out of matrix is visible after compression on the fractured surface as compared with Figure 2.4 (e).

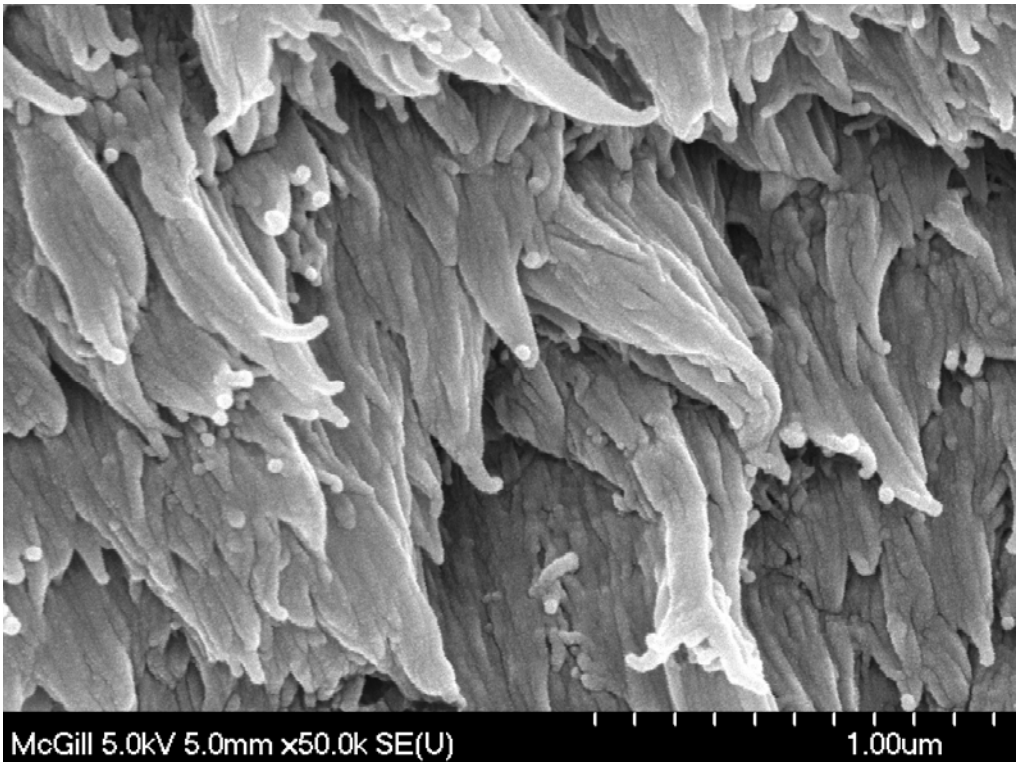

Figure 5.14: SEM micrograph of 9 wt% CNT-PEEK sample after compression.

5.4.2 Mechanism of change in electrical resistance

According to [173], changes in effective conductive path may occur as follows:

1. Change in One Effective Conductive Path: The uniaxial pressure makes the gaps between two adjacent CNTs smaller, decreasing the electrical resistance of one effective conductive path. The electrical resistance of one single effective conductive path is described by equation (5.7)

As shown in equation (5.7), the decrease of s, caused by uniaxial pressure causes a decrease in R, i.e. the gaps between CNTs becomes smaller and smaller during compression, leading to the increase of the tunneling current and consequently the resistance of one single effective conductive path decreases.

2. Formation of Effective Conductive Paths: As the compressive pressure goes on increasing, the inter-particle distance between adjacent CNTs goes on decreasing which leads to the formation of new effective conductive paths.

3. Redistribution of Effective Conductive paths: CNTs are incompressible compared with PEEK; therefore, compression can induce translation and rotation of a CNT. Because of transverse slippage, CNTs can be reoriented and redistributed within the matrix. This effect might have two opposite phenomena:

(a) The effective conductive paths can be destroyed or the number of conductive paths can be decreased,

(b) Because of the redistribution of CNTs, more effective conductive paths can be formed.

The changes (1), (2) and 3(b) contribute to the decreasing tendency of composite resistance as in the present case of CNT-PEEK composites, while the change 3(a) contributes to the increase in composite resistance as mostly observed in the cases of rubber matrix composite [74, 178]

In conducting composites the total electrical conductivity is a function of both the resistance of each conducting particle and of the polymer matrix. Since the conductivity of a conducting particle is very high compared to that of polymer matrix, the resistance across the conducting particle can be neglected. When the inter-particle separation is very large, no current flows through the inter-particle separation, but if the separation is small, the tunneling current may flow through the separation [173].

5.4.3 Parameters affecting the electrical conductivity of CNT composites

CNTs can be assumed to have a rod like geometry. For a better understanding of the change of electrical conductivity of CNT composites, four different parameters are taken into consideration and analyzed in this section: (a) change of volume of the sample, (b) change of angle of an individual CNT, (c) change of electrical property of an individual CNT and (d) change of tunneling distance between CNTs.

Let us consider a unit volume of CNT-PEEK composite sample having L_x, L_y and L_z as the initial length, width and thickness respectively. The unit volume contains a CNT of length *l* before the compression is applied.

5.4.3.1 Change of volume of the sample

When a thin composite sample is compressed, the geometry of the sample changes resulting in a corresponding change in its volume and hence affects the volume concentration of CNTs (ϕ). The initial volume of the composite sample is given by

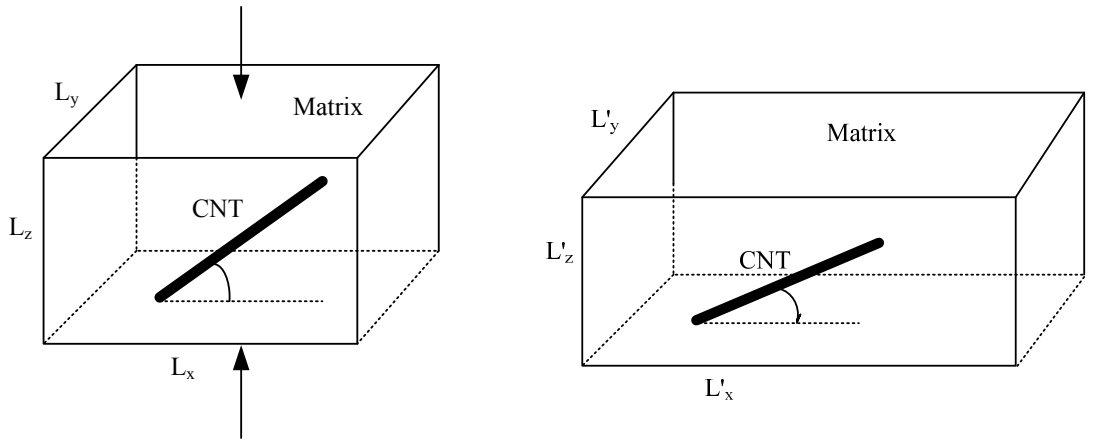

(a) before compression (b) after compression

Figure 5.15: Unit volume of CNT-PEEK composite under compression.

$$V = L_x L_y L_z \tag{5.19}$$

It is assumed that application of compressive force along Z direction causes a change in the dimension of the unit volume and shear force (along X and Y direction) causes a change in the shape of the unit volume. Under compression, the dimension along Z direction decreases while incremental uniaxial tension occurs along the X and Y direction and the corresponding changes in the orientation and location of the CNT are taken into consideration by following affine transformation as shown in the Figure 5.15 where (a) and (b) denote respectively the configuration before and after incremental compression strain ε_z. An affine transformation or affine map between two vector spaces consists of a linear transformation followed by a translation, i.e. under the external loading the length

components of the CNT change by the same ratio as the corresponding dimension of the matrix. This assumption can be justified from the fact that although the Young's modulus of an individual CNT is about 300 times higher than that of pure PEEK, the Young's modulus of 9% CNT-PEEK composites shown in Table 5.4 is only 1.5 times higher than that of pure PEEK.

Therefore, changes of length in each direction as a function of incremental strain can be expressed as

$$L_x' = L_x\left(1-\varepsilon_z \nu_{zx}\right) \tag{5.20}$$

$$L_y' = L_y\left(1-\varepsilon_z \nu_{zy}\right) \tag{5.21}$$

$$L_z' = L_z\left(1+\varepsilon_z\right) \tag{5.22}$$

Similarly the centre co-ordinates (X, Y, Z) of the CNT are changed to

$$x' = x\left(1-\varepsilon_z \nu_{zx}\right) \tag{5.23}$$

$$y' = y\left(1-\varepsilon_z \nu_{zy}\right) \tag{5.24}$$

$$z' = z\left(1+\varepsilon_z\right) \tag{5.25}$$

where the L_x', L_y', L_z' are the current dimensions of the CNT after compression by ε_z; ν_{zx} and ν_{zy} are the Poisson's ratio of the film in X direction and Y direction respectively. The changed volume can simply be expressed by combining the above three equations

$$\mathrm{V}' = L_x'L_y'L_z' = L_xL_yL_z\left(1-\varepsilon_z\nu_{zx}\right)\left(1-\varepsilon_z\nu_{zy}\right)\left(1+\varepsilon_z\right) \tag{5.26}$$

Dividing the equation (5.26) by equation (5.19), the normalized volume is obtained as

$$\frac{\mathrm{V}'}{\mathrm{V}} = \left(1-\varepsilon_z\nu_{zx}\right)\left(1-\varepsilon_z\nu_{zy}\right)\left(1+\varepsilon_z\right) \tag{5.27}$$

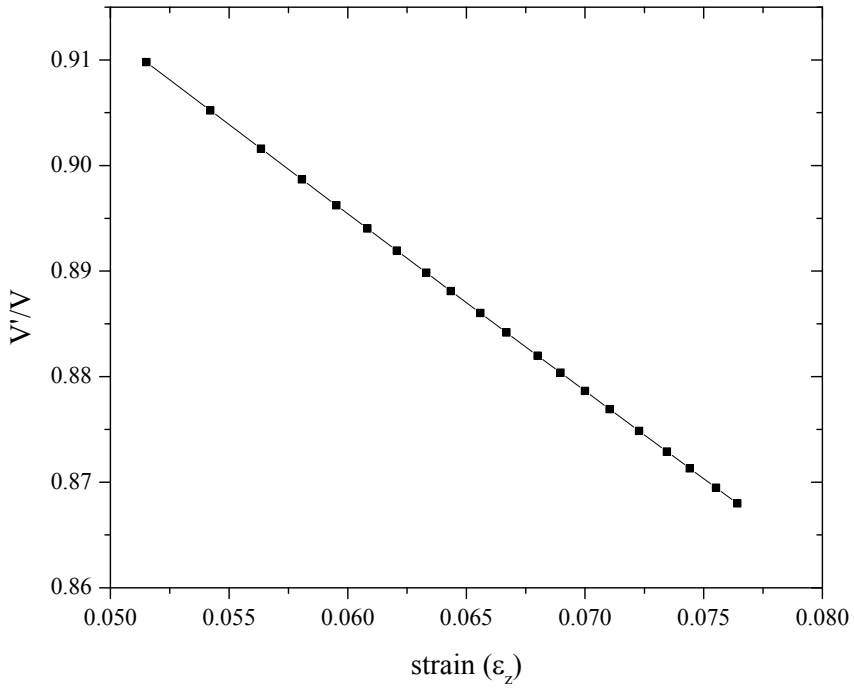

Figure 5.16: Volume change of 9 wt% CNT-PEEK composite under uniaxial compression strain.

Poisson's ratio of PEEK at room temperature is taken as 0.4 (Table 2.1). The normalized volume was calculated by using equation (5.27) and plotted in the Figure 5.16 as a function of strain ε_z along Z direction. From the graph shown in Figure 5.16, for 9 wt% CNT-PEEK sample, highest value of changed volume corresponding to lowest 0.0515 strain is 90.98% and lowest value of changed volume corresponding to highest 0.0764 strain is 86.8% of original volume.

It can be concluded that the total volume of the CNT-PEEK sample decreases under the application of compression which decreases the percolation threshold, ϕ_c and increases electrical conductivity, σ as predicted by the percolation-based scaling rule (equation (3.9) and equation (3.3) respectively in chapter 3). The analysis presented above provides an estimate whether this volume change under compression is strong enough or not to

change the overall electrical conductivity. For 9 wt% CNT-PEEK sample at 0.0764 strain corresponding to 40 MPa applied pressure and changed volume 86.8% of original volume, the changed percolation threshold ϕ'_c is calculated using equation 3.9. Then using the value of σ_f (4.3×10^{-2} S/cm) and t (2.517) in equation (3.3), σ is obtained to be 9.957×10^{-6} S/cm which is only 0.9% more than the unstressed sample. Thus, the contribution in the change of electrical conductivity made by volume change of the sample is negligible.

5.4.3.2 Change of angle of an individual CNT

The direction cosines of a vector are merely the cosines of the angles that the vector makes with the X, Y, and Z axes, respectively. These angles are labeled as α (angle with the X axis), β (angle with the Y axis) and γ (angle with the Z axis) as shown in Figure 5.17.

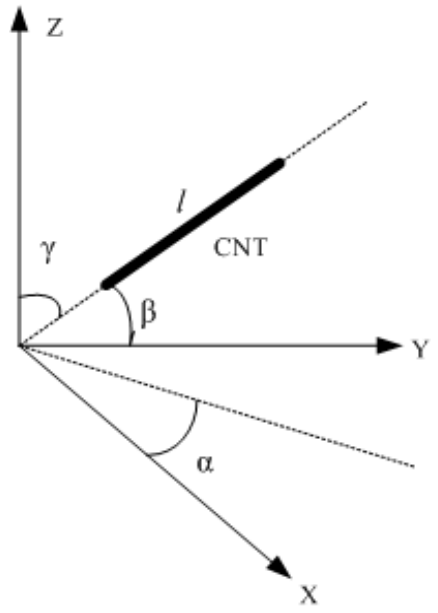

Figure 5.17: Different angles of a CNT in 3-D co-ordinate axes

The change of angle of a CNT inside the matrix under uniaxial compression can be studied with respect to the chosen co-ordinate system in three-dimensional consideration, where a CNT can have the abovementioned three different angles (α: azimuthal angle, β: angle between Y axis and the CNT and γ: angle between Z axis and the CNT).

The change of angle of a CNT can be calculated using the equations derived by Taya et al. [148]. Before compression, length components of a CNT in Cartesian co-ordinates can be expressed as

$$l_x = l \sin\gamma \cos\alpha \tag{5.28}$$

$$l_y = l \sin\gamma \sin\alpha \tag{5.29}$$

$$l_z = l \cos\gamma \tag{5.30}$$

where l_i (i = X, Y, Z) are the length of the CNT rod and γ and α are the angles before compression.

For compressive normal component of load along Z axis

The length components of the CNT rod due to compressive strain can be written as

$$l'_x = l' \sin\gamma' \cos\alpha' \tag{5.31}$$

$$l'_y = l' \sin\gamma' \sin\alpha' \tag{5.32}$$

$$l'_z = l' \cos\gamma' \tag{5.33}$$

where l'_i (i = X, Y, Z) are the length of the CNT rod and γ' and α' are the angles after compression.

For shear component of load along negative X axis

The length components of the CNT rod due to compressive strain can be written as

$$l_x'' = l'' \sin\gamma'' \cos\alpha'' \tag{5.34}$$

$$l_y'' = l'' \sin\gamma'' \sin\alpha'' \tag{5.35}$$

$$l_z'' = l'' \cos\gamma'' \tag{5.36}$$

where l_i'' (i = X, Y, Z) are the length of the CNT rod and γ'' and α'' are the angles after compression.

For shear component of load along negative Y axis

The length components of the CNT rod due to compressive strain can be written as

$$l_x''' = l''' \sin\gamma''' \cos\alpha''' \tag{5.37}$$

$$l_y''' = l''' \sin\gamma''' \sin\alpha''' \tag{5.38}$$

$$l_z''' = l''' \cos\gamma''' \tag{5.39}$$

where l_i''' (i = X, Y, Z) are the length of the CNT rod and γ''' and α''' are the angles after compression.

Applying affine transformation assuming proportional change in *L* and *l,*

$$\frac{L_i'}{L_i} = \frac{l_i'}{l_i}\left(i = x, y, z\right) \tag{5.40}$$

By applying this relationship of equation (5.40) to the equations (5.20) – (5.22), (5.28) – (5.30) and (5.31) – (5.39), the following relations are obtained

$$1 - \varepsilon_z \nu_{zx} = \frac{L_x'}{L_x} = \frac{l_x'}{l_x} = \frac{l' \sin\gamma' \cos\alpha'}{l \sin\gamma \cos\alpha} \tag{5.41}$$

$$1 - \varepsilon_z \nu_{zy} = \frac{L_y'}{L_y} = \frac{l_y'}{l_y} = \frac{l' \sin\gamma' \sin\alpha'}{l \sin\gamma \sin\alpha} \tag{5.42}$$

$$1 + \varepsilon_z = \frac{L_z'}{L_z} = \frac{l_z'}{l_z} = \frac{l' \cos\gamma'}{l \cos\gamma} \tag{5.43}$$

By using equations (5.41) – (5.43), the reorientation angles of a CNT after compression are derived as

$$\alpha' = \tan^{-1}\left(\frac{1-\varepsilon_z \nu_{zy}}{1-\varepsilon_z \nu_{zx}}\tan\alpha\right) \tag{5.44}$$

$$\gamma' = \tan^{-1}\left(\frac{\left(1-\varepsilon_z \nu_{zy}\right)\sin\alpha}{\left(1+\varepsilon_z\right)\sin\alpha'}\tan\gamma\right) \tag{5.45}$$

The relative angle changes for both angles are plotted in Figure 5.18 from 0 to π/2. Here, assuming CNT-PEEK composite as a homogeneous isotropic material, same value of 0.4 was used for both ν_{zx} and ν_{zy}. The strains of 0, 0.05151, 0.068 and 0.07641 indicated in the legend of the Figure 5.18 correspond to the applied experimental pressures of 0, 2 MPa, 24 MPa and 40 MPa respectively.

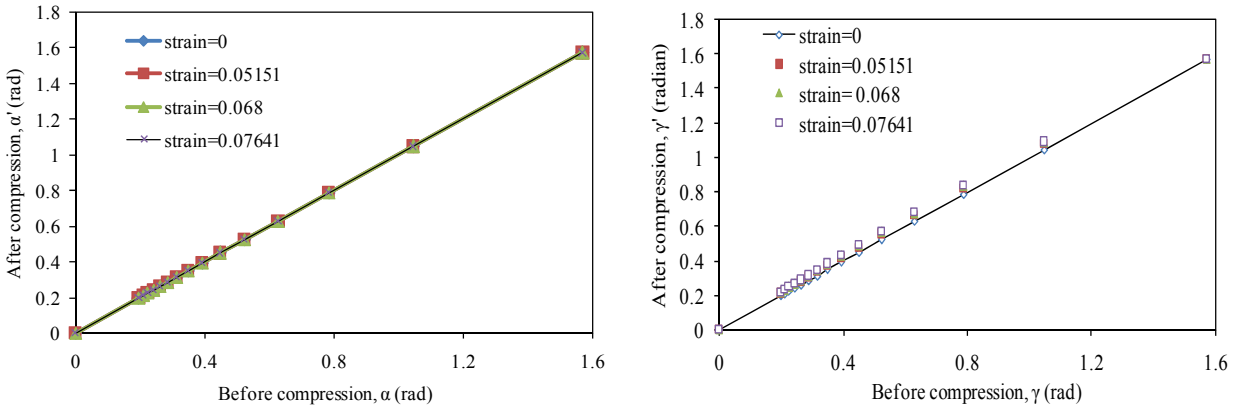

(a) Angle between X axis and CNT (α) (b) Angle between Z axis and CNT (γ)

Figure 5.18: Change of Angle of a CNT in PEEK induced by compression.

From the above graphs (Figure 5.18), it is seen that azimuthal angle, α does not change at all when the external compression load is applied along Z axis, while the angle between Z axis and the CNT changes slightly. This change of angle is related to the parameters of equation (3.3) affecting ϕ_c and contributes in the increase of electrical conductivity.

Qualitatively, it can be said that because of compression, randomness in angle distribution decreases which in turn can decrease ϕ_c and thus it can increase the value of σ in equation (3.3).

In the above analysis, the modulus of elasticity of polymer matrix was not considered. To investigate the effect of modulus of polymer, a Finite Element Analysis in ANSYS 12 has been carried out using the technique of representative volume element (RVE) modeling. Based on continuum mechanics, RVE modeling predicts the effective properties of randomly distributed heterogeneous materials by considering a given volume of microstructure. Using the concept of RVE and simulating a single CNT and its surrounding matrix, Liu and Chen [179] showed the accuracy and feasibility of evaluating material properties.

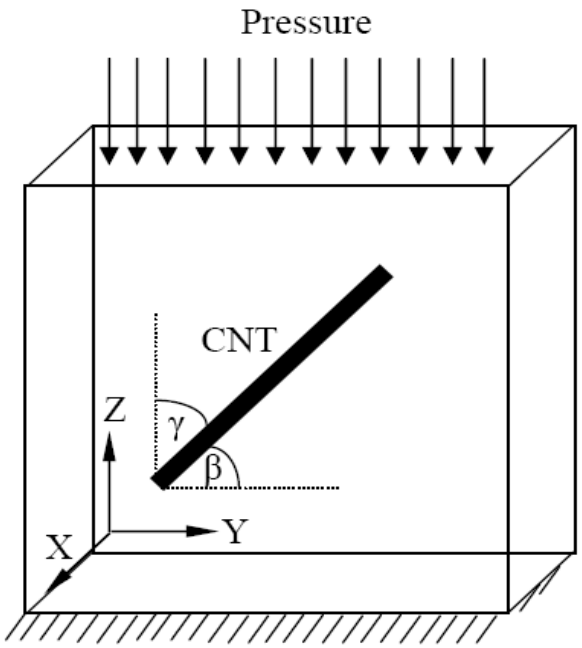

Figure 5.19: Schematic of RVE and boundary conditions for finite element analysis.

A RVE of 100 nm × 100 nm × 20 nm was considered where a single CNT of length 70.71 nm and diameter 10 nm surrounded by PEEK matrix was assumed to be inclined at an arbitrary initial angle of 45° with Z axis. The material constants are extracted from Table 2.1 and Table 2.2. The schematic of the RVE and the boundary conditions are shown in Figure 5.19.

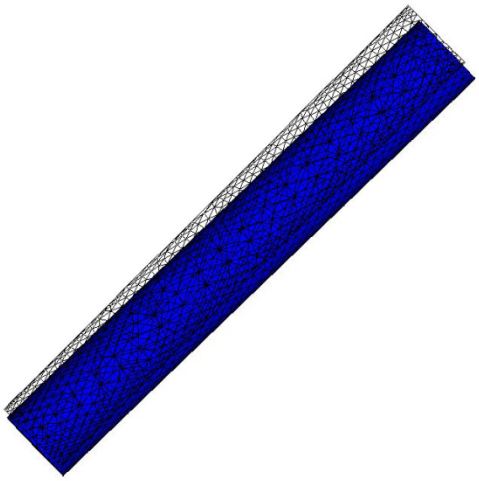

(a) Applied pressure 2 MPa (strain = 0.0515)

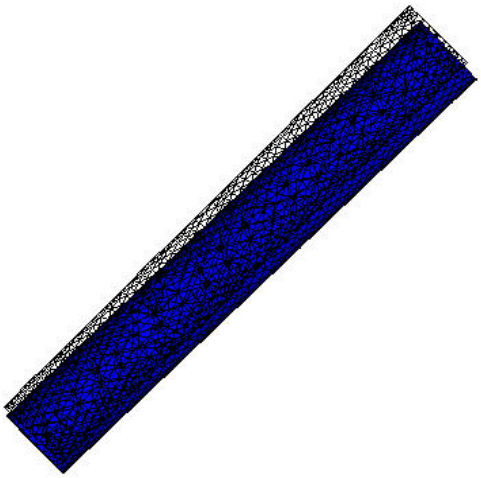

(b) Applied pressure 24 MPa (strain = 0.068)

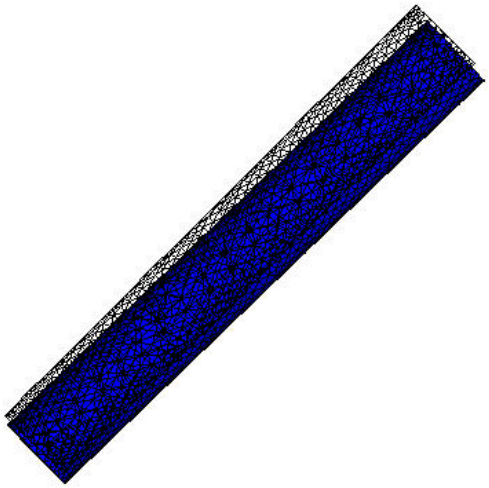

(c) Applied pressure 40 MPa (strain = 0.0764)

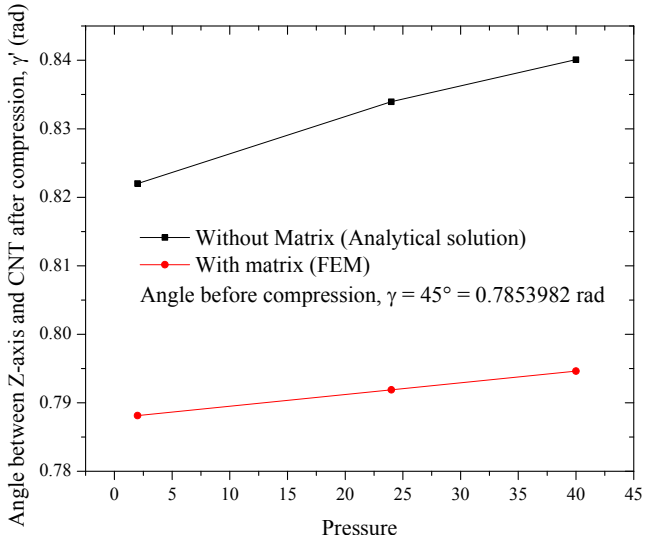

(d) Comparison of γ' (after compression)

Figure 5.20: Finite element analysis showing the effect of modulus of polymer matrix on CNT's rotation.

The analysis was done in static mode using element 'solid45' for both CNT and PEEK. Distributed pressures of 2 MPa, 24 MPa and 40 MPa corresponding to the compressive strains of 0.0515, 0.068 and 0.0764 respectively were applied on the RVE. The resulting deformations together with undeformed shape of the CNT are shown in Figure 5.20 (a) to (c).

To calculate the angular rotation with respect to Z axis, two central nodes on both ends of the nanotube were selected. Using the geometry of deformed and undeformed shape, the calculated values of angle (γ) between Z axis and the CNT are compared in Figure 5.20 (d) with those presented in Figure 5.18. The effect of the modulus of elasticity of PEEK on the rotation of CNT shown in Figure 5.20 (d) can be discussed in terms of percent change of angle, γ with respect to its initial value. For the presented result of uncompressed initial angle, γ = 45° = 0.785392 rad, the percent change are given below in Table 5.5

Table 5.5: Comparison of change of angle (γ) without matrix and with matrix

Applied Pressure (MPa)	Strain	Change in γ (without matrix) by analysis	Change in γ (with matrix) by FEM
2	0.0515	4.66%	0.35%
24	0.0680	6.18%	0.83%
40	0.0764	6.96%	1.18%

It can be seen that the polymer matrix opposes the rotation of CNT in the direction of applied pressure. The amount of this restriction depends on the magnitude of its modulus of elasticity. PEEK is a considerably stiff material with high modulus of elasticity

(3.7~4.0 GPa). To compute overall conductivity of the composite, the rotation of CNT inside PEEK can be neglected. Thus, angle change phenomena indicated in the Figures 5.18 and 5.20 is not strong enough to change the overall electrical conductivity of the CNT-PEEK sample under compression.

5.4.3.3 Change of electrical property of an individual CNT

Cao et al. [180] experimentally measured electrical properties of single walled carbon nanotubes (SWCNTs) under stretching and their report shows that the electrical conductivity of metallic SWCNTs vary linearly with a small finite slope. In the present study, only multi walled carbon nanotubes (MWCNTs) were used which are simply composed of multiple numbers of concentric SWCNT. Therefore, it is reasonable to assume that most MWCNTs are insensitive to external strain and in the present analysis; the effect of change of intrinsic electrical conductivity due to external compression is ignored. Thus, the bulk electrical conductivity of CNT-PEEK composite film is not affected by the intrinsic conductivity change of an individual MWCNT inside the matrix.

5.4.3.4 Change of tunneling distance between CNTs

Carbon nanotubes inside the matrix can be regarded as a network of conductors. There are two primary components of electrical resistance of the network, namely the intrinsic electrical resistance of an individual CNT (R_c) and the tunneling resistance (R_t) between two adjacent CNTs. Since the first component has been ignored under external strain as discussed in the previous section, the second one i.e. tunneling resistance is thought to be the major parameter affecting the electrical properties.

For polymer nanocomposites, Yasuoka et al. [181] approximated Simmons' equation of tunneling resistance R_t by factoring out of the constant term $\frac{2}{3\pi}$ from equation (5.6) as

$$R_t = \frac{h^2 s}{a^2 e^2 \sqrt{2m\psi_0}} \exp\left(\frac{4\pi s\sqrt{2m\psi_0}}{h}\right) \tag{5.46}$$

where ψ_0 is the work function of a CNT with other constants and symbols same as given in equation (5.6). The tunneling resistance ratio after and before compression is given as

$$\frac{R_t}{R_{t_0}} = \frac{s}{s_0}\frac{a_0^2}{a^2} \exp\left(\frac{4\pi\sqrt{2m\psi_0}}{h}(s - s_0)\right) \tag{5.47}$$

where the subscript 0 represent the uncompressed state of the sample.

The new distance s between two CNTs due to uniaxial compression loading can be written from equation (5.12) as

$$\frac{s}{s_0} = 1 - \frac{\Delta z}{z_0} \tag{5.48}$$

$$s - s_0 = -s_0 \frac{\Delta z}{z_0} \tag{5.49}$$

Substitution of the above two expressions into equation (5.47),

$$\frac{R_t}{R_{t_0}} \approx \left(1 - \frac{\Delta z}{z_0}\right) \exp\left(-\frac{4\pi s_0 \Delta z}{z_0 h}\sqrt{2m\psi_0}\right) \tag{5.50}$$

In this equation, Plank's constant, h = 6.62 × 10^{-34} J.s, Mass of an electron, m = 9.11 × 10^{-31} Kg and Work function of a CNT, $\psi_0 \approx 4.8 \sim 4.95$ eV [144].

Equation (5.50) shows that under the application of compressive strain ε, tunneling resistance decreases exponentially with original distance s_0 between two CNTs. In high volume fraction composites, because of closer packing, the initial distance between two

adjacent CNTs is smaller than that in low volume fraction composites; therefore, the applied strain vs. resistance behaviour can be quite different for high volume and low volume fraction composite films. Using the procedure described in chapter 4, the initial distance between two CNTs rods can be correlated to volume fraction by assuming a power law $s_0 = K\phi^{\eta}$. Putting the value of constants K and η, s_0 for different CNT loadings and then tunnel resistance R_t for different ε values under applied compression can be calculated. The following Figure 5.21 shows relative resistance (R_t/R_{t0}) for 8 wt%, 9 wt% and 10 wt% CNT-PEEK composites calculated by using above mentioned constants, equation (5.50) and the fitting parameters obtained by Simmons' model (equations (4.6), (4.9) – (4.14)) in chapter 4. From the graph, it is seen that contact resistance decreases drastically by about 3 orders of magnitude after applying the first load of 2 MPa. For example in the case of 9 wt% CNT-PEEK composites, R_t/R_{t0} decreases from 1.0 to 1.72×10^{-3} when pressure increases from zero to 2 MPa. Subsequent application of load gradually decreases the contact resistance in an exponential pattern. At the highest load of experiment (40 MPa), R_t/R_{t0} is in the order of 10^{-5}. Among the three samples, initial distance between two CNTs is highest in 8 wt% CNT (1.33Å) and lowest in 10 wt% CNT sample (1.29Å), thereby possessing highest and lowest initial contact resistances respectively. Under the application of pressure, contact resistances decrease and the difference between new contact resistances among the samples is very marginal. Accordingly, in Figure 5.21, lowest value of R_t/R_{t0} for 8 wt% CNT and highest value of R_t/R_{t0} for 10 wt% CNT composites are observed. It also implies that concentration of carbon nanotubes has very marginal effect in the change of contact resistance of highly conductive composites under pressure. Application of compression load causes the

polymer chains to move which in turn affects the movement of CNT network and eventually CNTs get closer to each other. As a result, tunneling resistance and hence contact resistance decreases with increase in pressure. The ultimate result is an increase in electrical conductivity.

It is now understood that out of four parameters [(a) change of volume of the sample, (b) change of angle of an individual CNT, (c) change of electrical property of an individual CNT and (d) change of tunneling distance between CNTs], the effect of tunneling distance is more significant while the effect of the other three's is almost negligible.

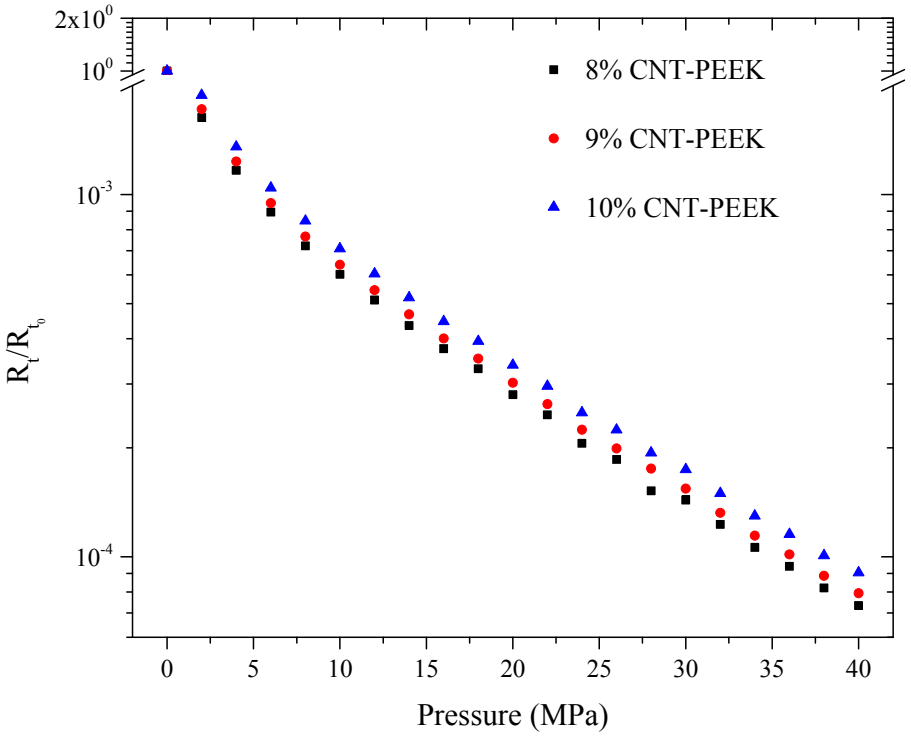

Figure 5.21: Relative contact resistance against applied pressure for 8 wt% – 10 wt% CNT-PEEK composites.

Earlier it was mentioned that two processes play an important role on the electrical conductivity at the same time when pressure is applied: One is the tunneling distance/gap among the CNT aggregates that becomes smaller due to compression accompanied by the

decrease of contact resistance and hence increase of electrical conductivity and the other is the conductive pathways which are re-established due to the orientation of the plane. These two processes would assist each other, so the electrical conductivity should be determined by the net result of these two different processes. When the pressure is completely removed, the conductive pathways are temporarily interrupted and gap between CNTs may restore to its original value and the conductivity of the samples decreases. Relaxation of CNTs also has effect in this process. However, since PEEK is considerably a stiff material, this relaxation is not very significant.

5.5 Development of pressure model

A simple semi-empirical mathematical model has been developed to correlate the experimental data of electrical resistance under the effect of compression.

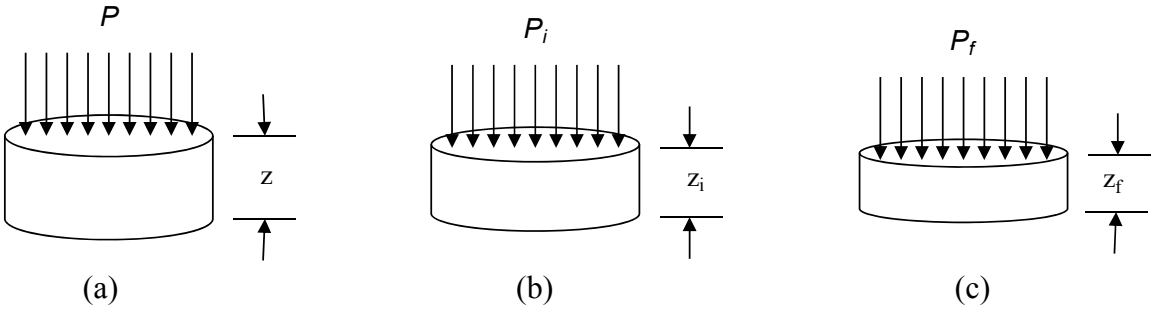

Figure 5.22: Schematic of a composite sample under applied pressure.

Let us consider a small sample of thickness z and cross sectional area A. At two different pressures P_i and P_f, the electrical resistances are given by

$$R_i = \frac{\rho_i z_i}{A} \tag{5.51}$$

$$R_f = \frac{\rho_f z_f}{A} \tag{5.52}$$

where ρ_i and ρ_f are the resistivity and z_i and z_f are the thicknesses of the sample at two pressures P_i and P_f shown in Figure 5.22.

Dividing equation (5.52) by equation (5.51)

$$\frac{\mathrm{R_f}}{\mathrm{R_i}} = \frac{\rho_f z_f}{\rho_i z_i} = \frac{\rho_f \left(z + \varepsilon_f z\right)}{\rho_i \left(z + \varepsilon_i z\right)} = \frac{\rho_f \left(1 + \varepsilon_f\right)}{\rho_i \left(1 + \varepsilon_i\right)} = \frac{\rho_f \left(1 + \frac{P_f}{E}\right)}{\rho_i \left(1 + \frac{P_i}{E}\right)} \tag{5.53}$$

Since the resistivity ρ is not strongly dependent on pressure, to simplify the analysis, for the same temperature, this material property can be assumed to be constant. After simplification,

$$R_f = R_i \frac{E + P_f}{E + P_i} \tag{5.54}$$

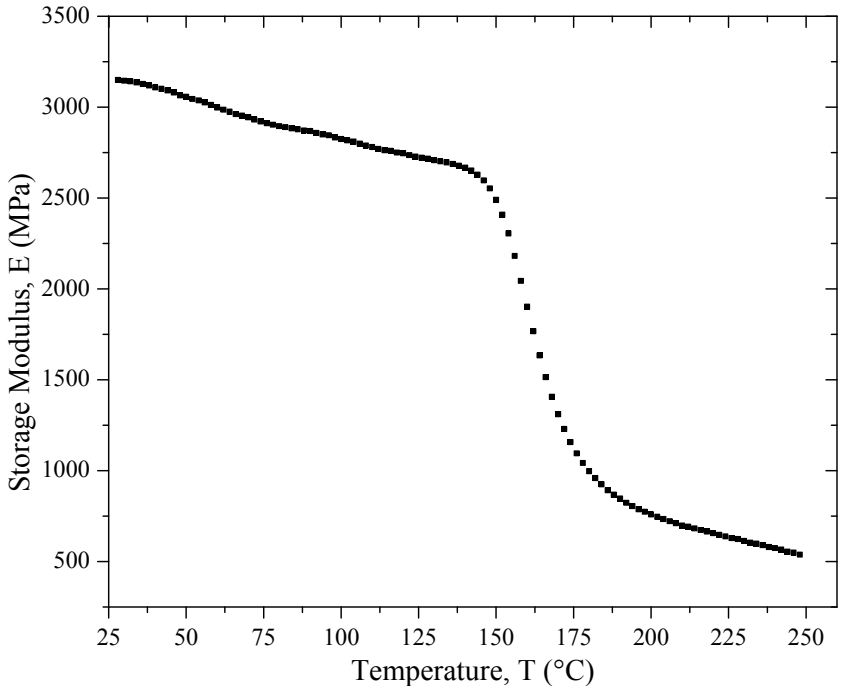

Figure 5.23: Dynamic Mechanical Analysis (DMA) of 9 wt% CNT-PEEK Composites.

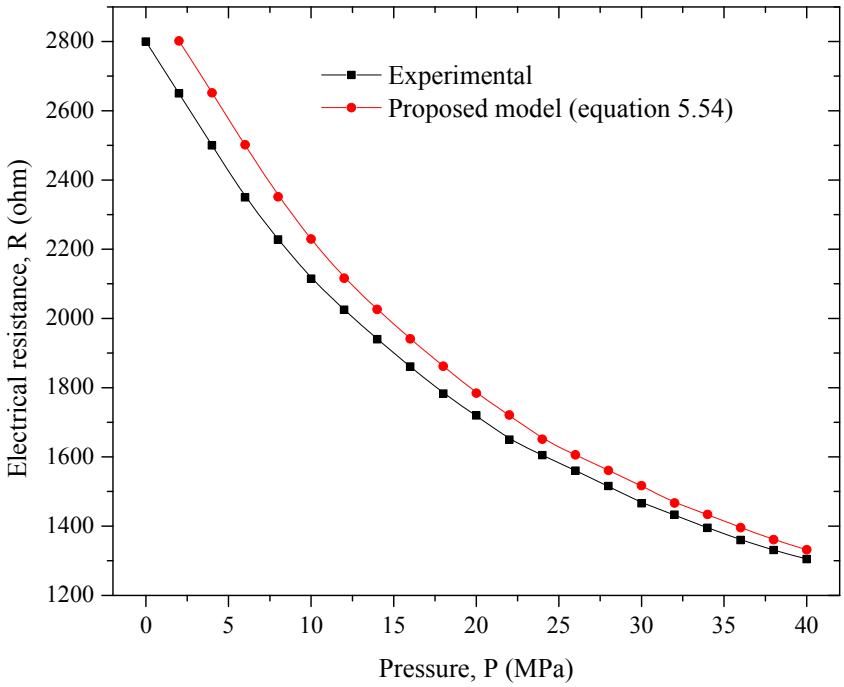

Figure 5.24: Comparison of electrical resistance of 9 wt% CNT-PEEK composites at room temperature obtained by experiment and the proposed model.

In equation (5.54), modulus of elasticity, E was taken from the results of Dynamic Mechanical Analysis (DMA) carried out from room temperature to 250°C as shown in Figure 5.23. Typical value of E at room temperature as obtained from this analysis is 3149 MPa. Electrical resistances (in ohm) at room temperature with respect to applied pressure (in MPa) for 9 wt% CNT-PEEK sample are calculated using equation (5.54) and compared with the experimental data shown in Figure 5.24. The results obtained by the simple model are in good agreement with those obtained by experiment.

5.6 Summary

1. Electrical conductivity increases with increasing pressure up to a certain level and after that the increase is very marginal.

2. Electrical conductivity increases in the case of repeated loading-unloading cycles. Electrical hysteresis and electrical set gradually decreases on successive loading-unloading cycles. Nanotube content does not have significant effect on this electrical set and electrical hysteresis.

3. Applied pressure reduces the gap between carbon nanotubes which causes the increase in electrical conductivity. Applied pressure causes an increase (redistribution) of the number of conducting paths.

4. Under application of pressure, effect of tunneling distance is significant in increasing electrical conductivity, while the effects of change of volume of the sample, change of angle of an individual CNT and change of electrical property of an individual CNT are negligible.

5. The proposed semi-empirical pressure model is verified well by the experimental data.

Chapter 6

Effect of Temperature on Electrical Conductivity of CNT-PEEK Composites

6.1 Introduction

One of the important properties of electrically conductive composites is the temperature coefficient effect which means that electrical resistivity of the composites either increases (Positive Temperature Coefficient, PTC) or decreases (Negative Temperature Coefficient, NTC) during the heating process. Apart from the conventional application in semiconducting materials for dissipation of static electricity, these conductive materials have found widespread applications including heating elements, self-regulating heaters, gas sensors, switching materials, over-current protectors [145]. In a changing temperature environment, stabilization of conductive composites is also important. Hou et al. [182] studied the stabilization performance of conductive carbon black (CB) filled conductive polymer composites. A large number of authors published their work on temperature dependence of electrical conductivity and conduction mechanism for polymer composites, rubber composites, metal matrix composites etc. In this chapter, discussion on a few representative polymeric composite systems made of thermoplastic matrices will be presented.

Zhang et al. [183] studied the temperature dependence of electrical properties of Carbon Black (CB) filled Ultra High Molecular Weight Polyethylene (UHMWPE) composites prepared by hot compaction. Using two different molecular weight UHMWPE, they reported that (i) The percolation threshold of these composites decreases with the

increase of molecular weight of UHMWPE and with the decrease of particle size of CB, (ii) PTC effect of the CB-filled lower (145 million) UHMWPE composite decreases with increase of CB size, (iii) for higher (630 million) UHMWPE, no NTC effect was observed above percolation threshold, but two PTC effects were observed; first one was near the melting temperature (T_m) of polymer and second one was at a very high temperature (210 °C). By repeating the measurement on several heating-cooling cycles, they found that second PTC effect disappeared after the first heating-cooling cycle and the resistivity at room temperature increased with the number of cycles and thus they concluded that at higher temperature, reduction of viscosity and hence increased intermixing of UHMWPE and CB particles were attributed to the second PTC.

Natsuki et al. [184] investigated the influence of CNT concentration on electrical resistivity as a function of temperature using VGCF/UPR and VGNF/UPR nanocomposites made by solvent evaporation method. They reported a sharp increase in electrical resistivity (PTC) with strong temperature dependence near the percolation limit of 1 wt% of VGNF. But with the increase of thermal cycles, electrical resistivity decreased which was attributed to the thermal stabilization of CNFs within the polymer matrix. In their study, weak temperature dependence was noticed at temperatures close to the melting temperature. PTC effects of VGNF/UPR composites showed higher stability than those of VGCF/UPR composites.

Li et al. [119] investigated the temperature dependence of electrical conductivity of pristine and oxidized MWCNT-PVDF composites and reported that transition temperature (T_t) from PTC to NTC of the oxidized MWCNT-PVDF composites shifted

to a higher temperature which was attributed to the chemical functionalization of CNTs. With the increase in temperature, they found a subsequent number of increase and decrease of dielectric constant of those composites generating a 'wavy' phenomenon. Interfacial polarization effect was considered to be the cause of such behaviour.

Nakamura and Tomimura [185] obtained PTC and NTC in their study of temperature dependence of electrical resistivity of CB-PE composites below and above percolation threshold respectively. They explained PTC with tunneling conduction model by incorporating the effect of thermal expansion of the composites into the tunneling gap and NTC by a combination of both tunneling conduction and thermally activated electrical conduction.

Hindermann-Bischoff and Ehrburger-Dolle [186] reported that electrical resistivity of CB filled HDPE increased (PTC) significantly when composites were heated to the melting temperature of the matrix. Since an expansion of polymer matrix during heating increased the gaps between CB particles, a sufficient amount of CB particles were required to ensure that the gaps between CB particles were small enough to allow electron tunneling. Lisunova et al [187] also observed same PTC effect for MWCNT-UHMWPE in the region of temperatures higher than melting point.

Logakis et al. [86] studied frequency and temperature dependence of electrical conductivity of CNT-polyamide composites for various concentrations of CNTs (for samples both below and above percolation threshold) as well as pure PA6. They reported a steeper increase of electrical conductivity above glass transition temperature (T_g) than that below glass transition temperature (T_g) regardless of nanotube content and hence

suggested that conductivity of conductive samples above T_g is governed by the motion of polymeric chains as it is in the case of non conductive samples [188]. A different explanation was given by Bin et al. [189] to describe a similar behavior obtained in their study of MWCNT-UHMWPE composites by reasoning that when heated to/above melting point, mobility of polymer molecules increases and their active movement and rearrangement enhances nanotube to nanotube contact, thereby increasing the conductivity of composites. They pointed out that thermal expansion of polymer was insignificant to disrupt the conduction between nanotubes and mobility of the polymer was controlled by CNTs.

The above review of literature shows that strong interests prevail among the researchers to explore and understand the phenomena of temperature dependence of electrical conductivity of composites. However, a close observation reveals that most of these researches on polymeric composites were done using polymers of low glass transition temperature and low modulus. For example, T_g of PE is –120°C, PVDF –35°C, PA 50°C etc. In terms of their electrical conductivity, to understand the behaviour of CNT composites using high modulus and high T_g thermoplastic polymer for high temperature application has rarely been attempted. At high temperatures, some factors like nanotube content, thin insulating film, thermal expansion and modulus of matrix, mobility/activity of electrons below or above T_g etc. make the phenomenon quite complex.

In this chapter, focus will be given on the variation of electrical conductivity of the composites for different CNT loadings with temperature for heating and cooling, conduction mechanism and how those are affected by above mentioned factors.

6.2 Experimental

6.2.1 Testing of samples

To determine the electrical conductivity at elevated temperatures, the entire electrode system was placed in a confined mica insulated aluminium band heater where the temperature could be monitored and controlled over the range 20°C – 500°C. Heat was supplied to the surfaces of the heater as well as to the sample by a programmable i-series Temperature/Process controller from Omega Engineering Inc. USA. The heater was covered with insulating material to prevent heat loss to the surroundings by convection heat transfer (Figure 6.1). Temperature was increased from room temperature (20°C) to 140°C at intervals of 5°C. Each temperature level was kept constant for 5 minutes to get stable readings of sample resistance.

To examine the combined effect of temperature and pressure on electrical conductivity, the above procedure was repeated while the samples were being compressed using an MTS testing machine. The details are described in section 5.2.4.

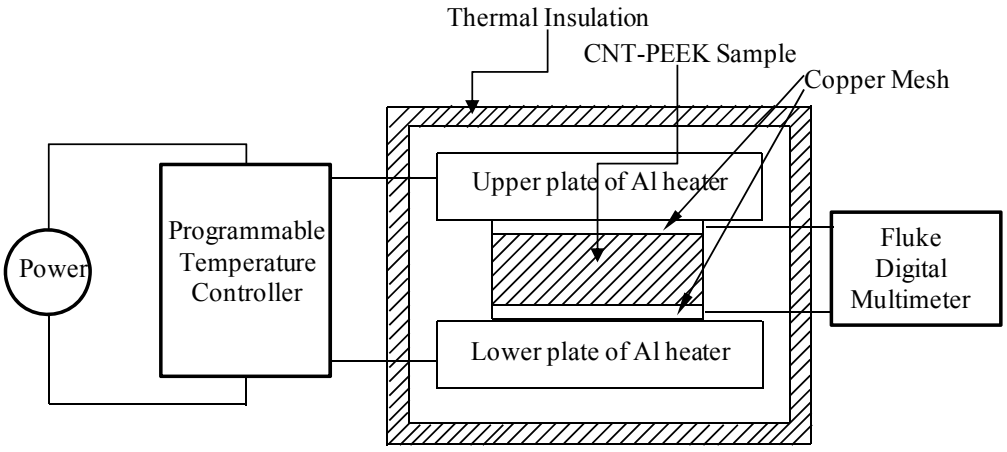

Figure 6.1: Schematic of the Experimental Set-up.

6.2.2 Investigation of the effect of Joule heating

Due to the increase of conductivity at elevated temperatures, there is a possibility of further temperature increase due to Joule heating, also known as resistive heating or Ohmic heating. Because of heating, thermal emission of electrons between two separated CNTs (when their distance of separation is small, but not equivalent to physical contact) increases, leading to an increase in conductivity. To investigate the effect of Joule heating, the sample temperature was measured using a K-type thermocouple attached directly to the sample and compared with the oven temperature. This measurement was repeated several times for different wt% of CNT-PEEK composites and reproducible results were obtained. As shown in Figure 6.2, a slope equal to 1 indicates that thermocouple temperature is same as the oven temperature which proves that Joule heating in the present case has no effect on increasing conductivity.

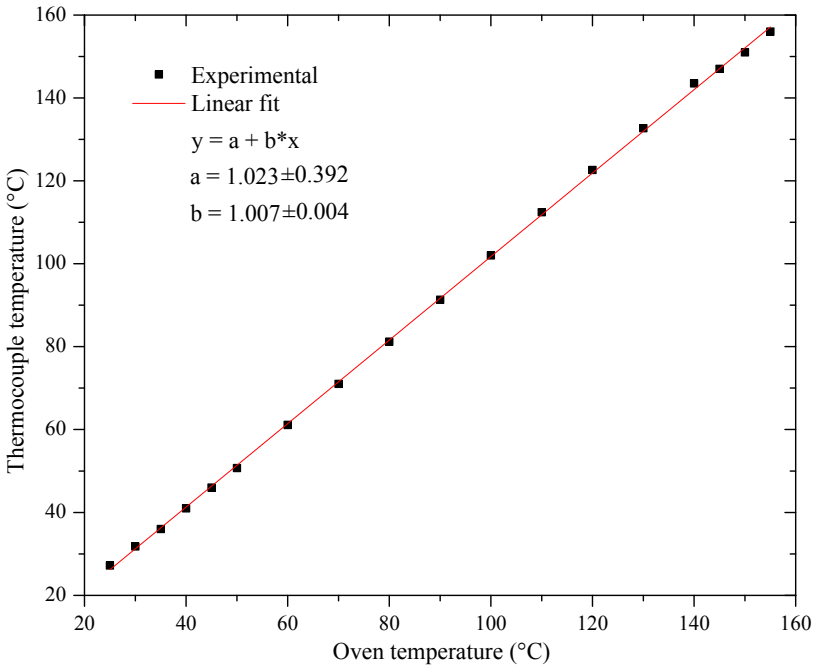

Figure 6.2: Plot of thermocouple temperature versus oven temperature.

6.2.3 Thermo Mechanical Analysis (TMA)

Thermo Mechanical Analysis (TMA) of the nanocomposite samples containing 8 wt%, 9 wt% and 10 wt% CNTs was performed with a TA instrument (TMA Q400) in penetration mode with 5mN load by ramp method. The temperature range was 20°C to 140°C with a heating rate of 3 °C/min.

6.2.4 Thermal analysis (DSC)

The crystallization and melting behaviour of pure PEEK and its composites were investigated by Differential Scanning Calorimetry (DSC) using TA instruments, DSC Q200-2211 in the temperature range of 40~380°C at a heating rate of 10°C/min. Samples varying from 9.9 to 11.5 mg were placed and sealed in open Aluminum Hermitic pans. A constant nitrogen flow of 50 ml/min was used to purge the instrument. Before starting the test, the instrument was calibrated according to the manufacturer's recommendation.

The transition temperatures were taken as the peak maximum or minimum in the calorimetric curves. For pure PEEK and CNT-PEEK composites, the degree of crystallinity was calculated using the following relation:

$$X_c = \frac{(Q_m - Q_c)}{w_m Q_X} \times 100 \tag{6.1}$$

where X_c is the degree of crystallinity expressed in percentage, Q_m and Q_c are the experimentally obtained melting and crystallization enthalpies respectively, w_m is the weight fraction of PEEK in the composites and $Q_X \approx 130$ J/g [190, 191] is the extrapolated value of enthalpy corresponding to the melting of a 100% crystalline PEEK sample.

6.3 Results and discussion

The experiments were performed for at least three samples for each of the 8 wt%, 9 wt% and 10 wt% of CNTs and their average results have been presented in this section.

6.3.1 Thermo-mechanical properties

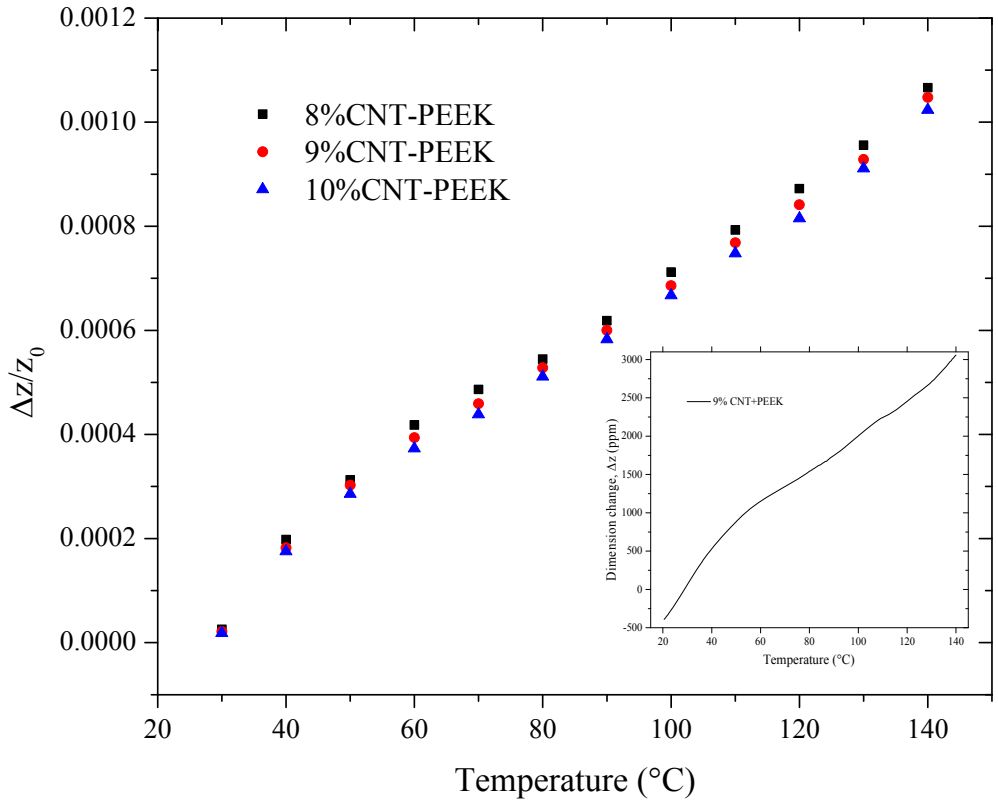

Figure 6.3: Relative change of composite sample thickness with temperature. Inset shows TMA of a representative 9 wt% CNT-PEEK sample.

Using the Thermo Mechanical Analysis (TMA), ratios of thermal expansion of the samples along the thickness direction (Δz) to their initial thickness (z_0) were calculated. As shown in Figure 6.3, the relative change of $\Delta z/z_0$ at most of the temperatures of experiment was found to be in the order of 10^{-4} and hence in calculation of electrical conductivity using equation (5.3), the thickness variation due to thermal expansion of the

samples was ignored and a constant sample thickness was assumed for all temperatures during the experiments. Discussion on these results will mainly focus on effect of temperature on electrical conductivity of CNT-PEEK composites for both heating and cooling.

6.3.2 Thermal properties

Figure 6.4 shows the DSC thermograms of pure PEEK and CNT-PEEK composites. These curves are the first heating scans of the matrix and the composites. An exothermic peak at about 160°C indicating the glass transition point (T_g) and an endothermic peak at about 340°C indicating the melting point (T_m) are clearly seen.

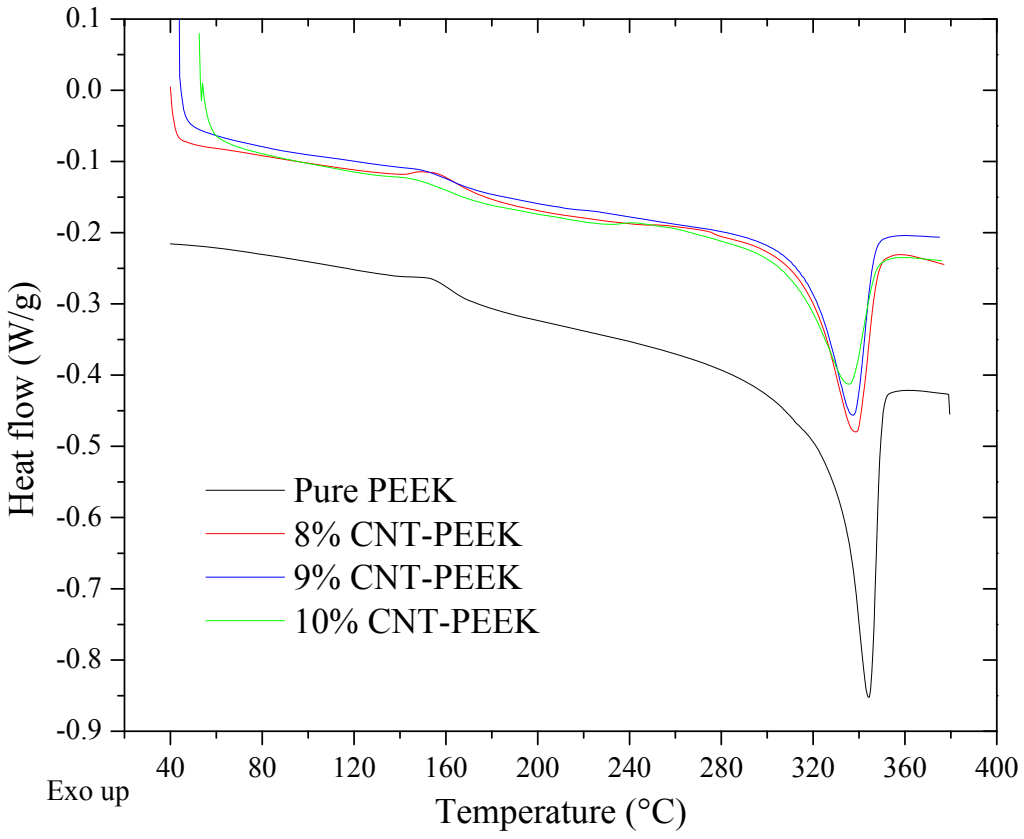

Figure 6.4: DSC thermograms of PEEK and the CNT-PEEK composites.

An exotherm was expected to appear at a temperature above the glass transition temperature (T_g), because semicrystalline polymers above T_g attain sufficient molecular mobility and as a result, they wiggle and squirm and try to move into an ordered arrangement. When polymer chains are in such crystalline arrangement, they give off heat. But in the present case, such exothermic peak does not exist due to the previous thermal history of the samples during their manufacturing process. This means that the polymer chains are already mostly ordered. At melting point (T_m), these chains come out of their ordered arrangements and begin to move around freely. The melting peak decreases by the addition of CNTs which indicates an effective association between PEEK and CNTs. The melting enthalpies (Q_m) were calculated as the normalized integral of melting peak from DSC thermograms, crystallization enthalpies (Q_c) were taken to be zero as there is no crystallization exotherm and accordingly the percent crystallinity was calculated for pure PEEK and CNT-PEEK composites using equation (6.1). The glass transition and melting temperatures, the melting enthalpies and the calculated percent crystallinity are listed below in Table 6.1.

Table 6.1: Thermal properties of PEEK and CNT-PEEK composites obtained by DSC

Sample	Glass Transition Temperature, T_g (°C)			Melting Temperature, T_m (°C)	Melting enthalpy, Q_m (J/g)	Degree of crystallinity X_c (%)
	Onset	Ave.	Offset			
Pure PEEK	144.1	146	149.1	344.5	47.71	36.7
8 wt% CNT-PEEK	154.8	162.8	174.6	338.44	34.95	29.22
9 wt% CNT-PEEK	153.2	162.3	172.4	338.35	32.85	27.77
10 wt% CNT-PEEK	149.9	151	158	335.65	28.87	24.68

The data presented in Table 6.1 shows that with an increase in CNT concentrations, the glass transition temperatures (T_g), the melting enthalpies (Q_m) and the degree of crystallinity decrease, and there is no significant change in the melting temperatures (T_m). These observations are unusual and intriguing, because CNTs usually act as nucleating agent [192, 193] which increases the rate of crystallinity by simultaneously starting nucleation at multiple points. This unusual behavior can be explained in terms of confinement effect [194] that the CNT network imposes a confinement or barrier on polymer chain diffusion which slows down the overall phase transformation process. Similar observations were also reported by Sandler et al. [195] and Diez-Pascual et al. [81] on DSC analysis of CNF-PEEK and SWCNT-PEEK composites, respectively.

6.3.3 Effect of temperature

To understand the charge transport mechanism in the nanocomposites under consideration, the temperature dependence of electrical conductivity in three different weight concentrations of CNT samples were investigated where the fluctuations of conductivity data among a number of same weight concentrations of CNT samples were minimum and repeatability of the results was satisfactory. Variations of electrical conductivity with temperature for 8 wt% – 10 wt % CNT-PEEK samples are presented in Figure 6.5. It reveals that, while the electrical conductivity increases with increase in temperature, the trend of electrical conductivity is concave downward for 8 wt% CNT-PEEK while those for 10 wt% CNT-PEEK is concave upward with the increasing temperature. This phenomenon can be attributed to the complex combination of the effect of temperature and the effect of increasing number of CNT contacts.

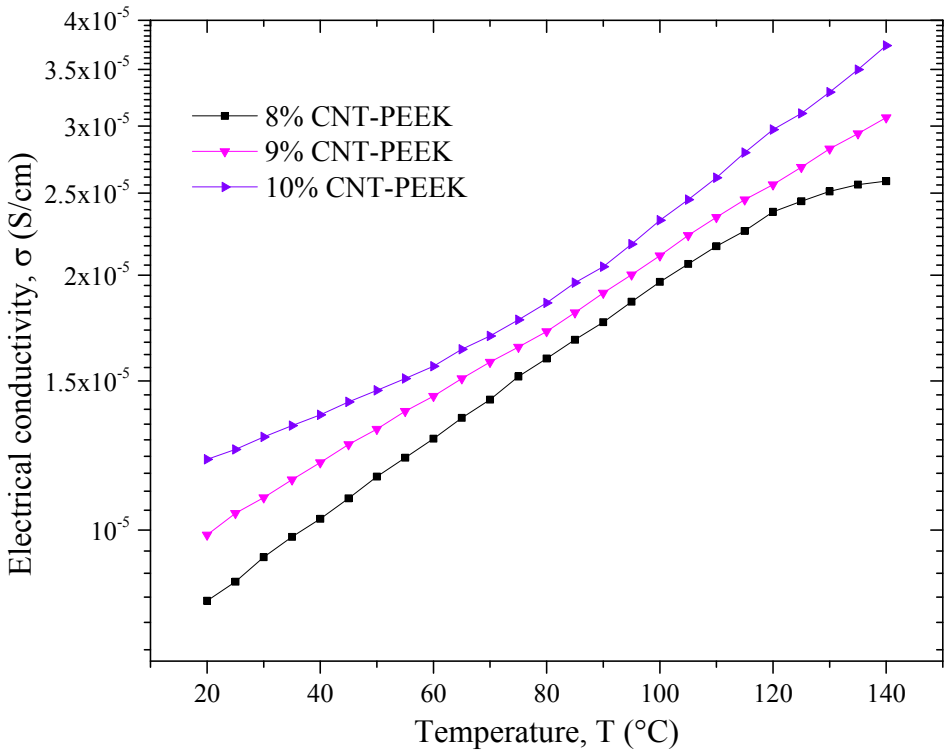

Figure 6.5: Electrical conductivity of samples of 8 wt% – 10 wt% of CNTs at different temperatures.

For samples with 8 wt% CNTs

According to the tunneling mechanism, electrons tend to jump from nanotube to nanotube across the gap made of polymeric material. With increasing temperature, this gap will increase, which makes the jumping of the electrons more difficult. However the increase of the gap depends on the stiffness of the polymeric material. Increasing the temperature tends to reduce the modulus (stiffness) of the polymer and correspondingly enlarge the tunneling gap. This enlargement of the gap reduces the effect of the increase in electronic activities due to temperature increase. The concave downward shape of the 8 wt% CNT curve can be explained by the rapid reduction in modulus of the polymer material at higher temperatures.

For samples with 10 wt% CNTs

For these samples, the amount of CNTs is high and there are significant numbers of contacts between the CNTs, and the polymeric gap is smaller (as compared to samples containing 8 wt% CNTs). When the number of electrical contacts is sufficiently large, the conduction by electronic movement is dominant as compared to the tunneling mechanism. Increasing temperature tends to increase the electronic movement, thus resulting in higher electrical conductivity. This can be used to explain the concave-upward shape of the 10 wt% CNT curve.

For samples with 9 wt% CNTs

The amount of CNTs in these samples is intermediate between those of 8 wt% and 10 wt% CNTs. The curve is straight indicating that the effects of reducing polymer stiffness (thus enlarging the gap and reducing conductivity) and increasing electronic movement in the CNTs balance out over the temperature range.

6.3.3.1 Heating-cooling curves

The experimental data of electrical conductivity for heating and cooling cycles of 8 wt% – 10 wt% CNT-PEEK composites are shown Figure 6.6. It is noted that heating and cooling curves in the $\sigma = f(T)$ plots do not follow the same path, as a result electrical hysteresis (i.e. the difference between the areas of electrical conductivity-temperature curves) has been generated. The initial and final conductivity at room temperature after the heating and cooling cycles are found to be different and this difference is termed as 'electrical set' in a similar fashion of the loading and unloading cycles described in chapter 5. As shown in Figure 6.6, the electrical set gradually decreases with increasing

wt% of CNTs. A small increase in electrical conductivity is observed during the cooling cycle. In the heating cycle, electrical conductivity increases because of increased electron activity at higher temperature. On cooling, conductive CNT fillers may re-agglomerate which can be the cause of higher conductivity, as compared to heating. The total contribution of all these processes on electrical conductivity is more than the effect of conductive network breakdown process due to differential thermal expansion of polymer network and CNT aggregates [65]. For higher concentration CNT composites, conducting CNTs are available in greater number and their average distance is much less. As a result, process of agglomeration or electron activity becomes less significant, because only a few more conducting networks will effectively be added to the large number of networks already present in the system.

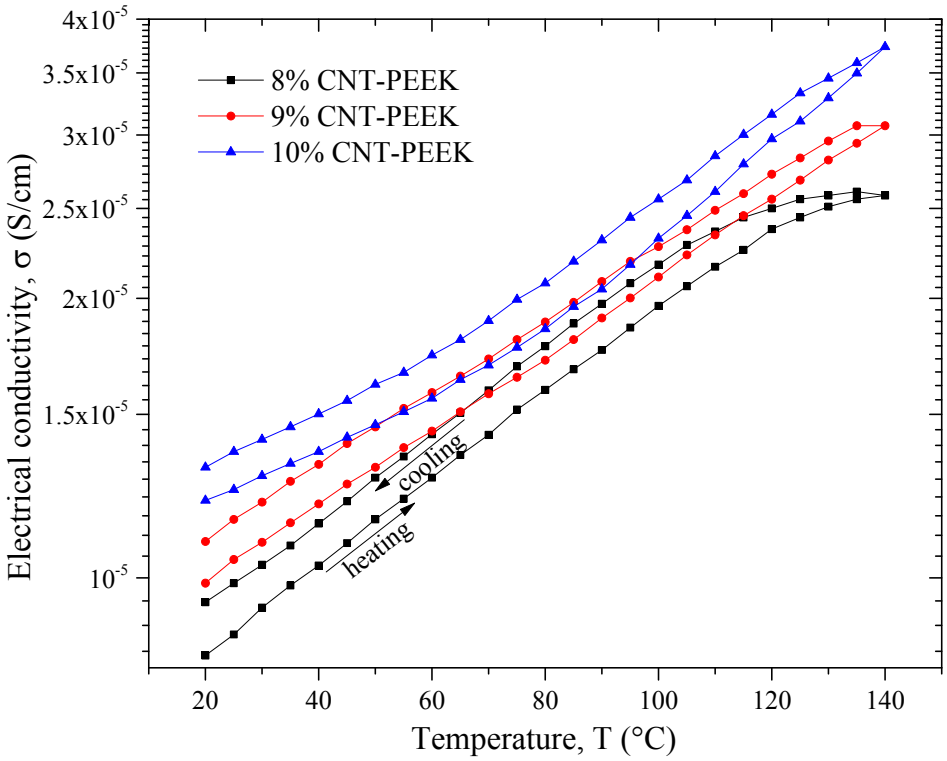

Figure 6.6: Electrical Conductivity vs. temperature during 1st heating-cooling cycle of 8 wt% – 10 wt% CNT-PEEK composites.

When polymer composites are used as thermistors for electrical heating, they are subjected to repeated thermal cycles, and it becomes necessary to understand how electrical conductivity changes with repeated thermal cycles. The changes of conductivity during repeated heating-cooling cycle for 8 wt% – 10 wt% CNT-PEEK samples are shown in Figures 6.7, 6.8 and 6.9. It is observed that the electrical set is higher in the first heating-cooling cycle than that in the second heating-cooling cycle for all CNT concentrations. It progressively decreases and becomes almost zero after the third cycle onwards. The electrical hysteresis decreases progressively for repeated heating-cooling cycles. The change in electrical conductivity with temperature during the heating-cooling cycle is not completely reversible in nature, which may be due to some irreversible changes in conducting networks, i.e. the change in conducting network occurs during the heating cycle, but not completely recoverable during the cooling [65]. The conductivity increases after each cycle of heating and cooling for which same explanation as above can be applied. In addition, conductivity also increases after repeated cycles, for example, at 140°C during the first cycle, conductivity for 9 wt% (Figure 6.8) CNT-PEEK sample is 3.07×10^{-5} S/cm while during the second and third cycle, the conductivity is 4.19×10^{-5} S/cm and 4.85×10^{-5} S/cm respectively. This increase of conductivity after repeated cycles of heating and cooling can be attributed to the redistribution of CNTs which ensures better conducting networks. The increase is also influenced by the concentration of CNTs. For 8 wt%, 9 wt% and 10 wt% CNT composites (Figures 6.7, 6.8 and 6.9) at 140°C, electrical conductivity increases during the second cycle by about 39%, 36% and 30% compared with first cycle, but during the third cycle this increment is smaller (18%, 16% and 15% respectively compared with second cycle).

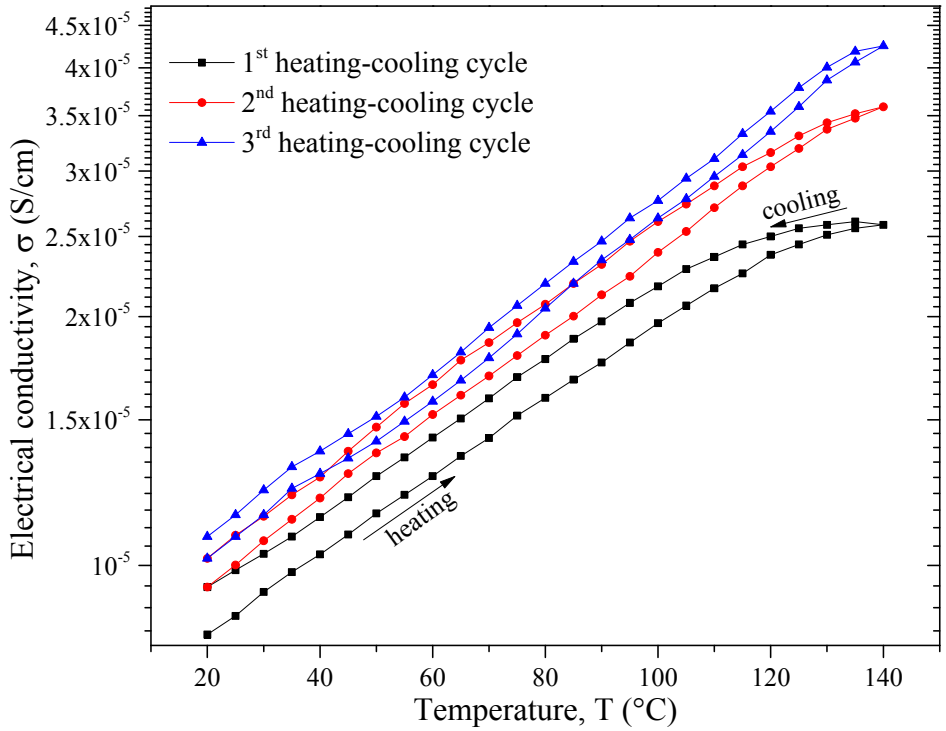

Figure 6.7: Repeated heating-cooling curves for 8 wt% CNT-PEEK composites.

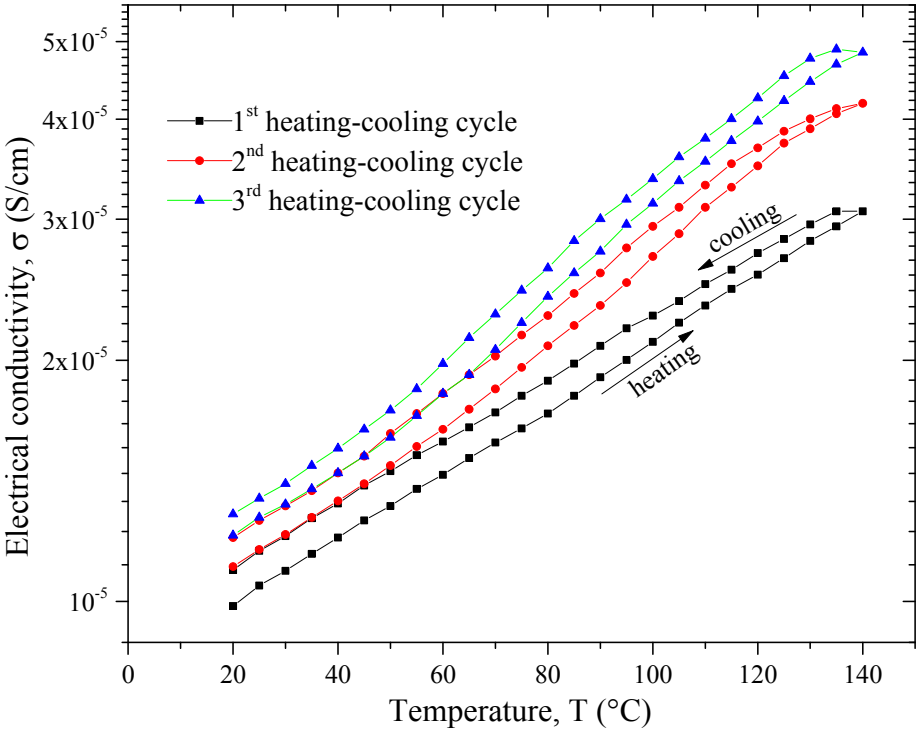

Figure 6.8: Repeated heating-cooling curves for 9 wt% CNT-PEEK composites.

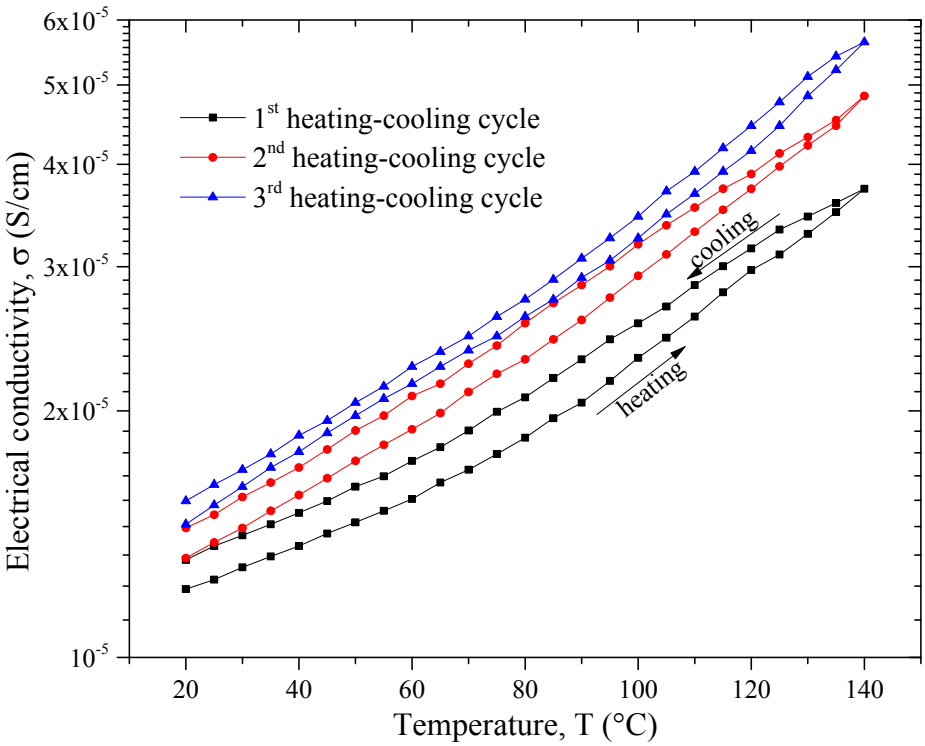

Figure 6.9: Repeated heating-cooling curves for 10 wt% CNT-PEEK composites.

Irrespective of CNT concentration, with the increase in number of heating and cooling cycles, hysteresis decreases, formation and breakdown of conducting networks become less prominent and eventually the conductivity becomes almost stable.

6.4 Charge transport mechanism

Electrical conduction through composites with a random distribution of conductive fillers is generally discussed by three main theories:

(a) Conduction path theory

Principle of conduction path theory lies in the fact that when dispersed in a non-conducting matrix, conducting fillers establish a few continuous conductive paths and through this path, electrons move from one end to the other under an applied electrical

field. This movement of electrons causes electrical conduction. Thus, the formation of a conducting network through physical contacts of conductive particles is essential. Formation of such conductive network is more probable at the critical concentration, i.e., percolation limit [196].

(b) Electron tunnelling theory

According to this theory, electrical conduction is believed to take place not only by inter-particle contact but also by electrons being able to jump (hop) across a gap or tunnel through energy barriers between conducting elements in the polymer matrix. There is a maximum value for these gaps which was estimated to be 1.7 nm in chapter 4.

(c) Electric field radiation theory

When conducting elements are separated by a gap of a few nanometres [197], it is believed that an emission current is caused to flow under a high electric field. The basic difference between this theory and the two other theories is that, conduction path theory and tunnelling theory describe the conduction as ohmic in nature, while electron field radiation theory describe a non-ohmic conduction behaviour for the system. Electric field radiation theory is believed to be valid at concentrations less than the critical limit [198].

However, the actual conduction mechanism in CNT reinforced polymer composites is quite complex in nature. The net result may be due to a combined effect of different mechanisms.

Since the present composite systems are well above the percolation limit, electrical conduction is more realistic to be explained by the conduction path theory as mentioned above in mechanism (a). But at the same time, nanotubes are possibly coated with thin

polymer film which acts as a potential barrier to inter-nanotube conduction; therefore electrical conduction is also limited by tunneling between nanotubes. Several models have been proposed to explain the electrical conductivity mechanisms in polymer composites. Fluctuation-induced tunneling (FIT), Arrhenius Conduction etc. are well pronounced among them.

6.4.1 Fluctuation Induced Tunneling (FIT)

The FIT model introduced by Sheng et al. [199] takes into account tunneling through potential barriers of varying height due to local temperature fluctuations. According to this model, electrical conduction of disordered systems is dominated by electron transfer between large conducting segments rather than by hopping between localized sites [200] and electrical conductivity below the glass transition temperature (T_g) is predicted by

$$\sigma = \sigma_0' \exp\left(-\frac{T_1}{T+T_0}\right), \qquad T < T_g \tag{6.2}$$

with $T_1 = \frac{sA_c\vartheta_0}{8\pi k_B}$ and $T_0 = \frac{2T_1}{\pi \Psi s}$ where $\Psi = \sqrt{\frac{2m\psi}{h^2}}$ and $\vartheta_0 = \frac{4\psi}{es}$, σ_0' is a pre-exponential factor, m and e are electron mass and charge, respectively, ψ is the initial potential barrier height, s is the inter-particle gap and A_c is the area of the capacitance formed by the junction. In this equation, T_1 can be regarded as the temperature below which conduction is dominated by the charge tunneling through the barrier (T_1 can be due to the energy required to move an electron across the insulating gap between the CNTs), T_0 as the temperature above which the thermally activated conduction over the barrier begins to occur.

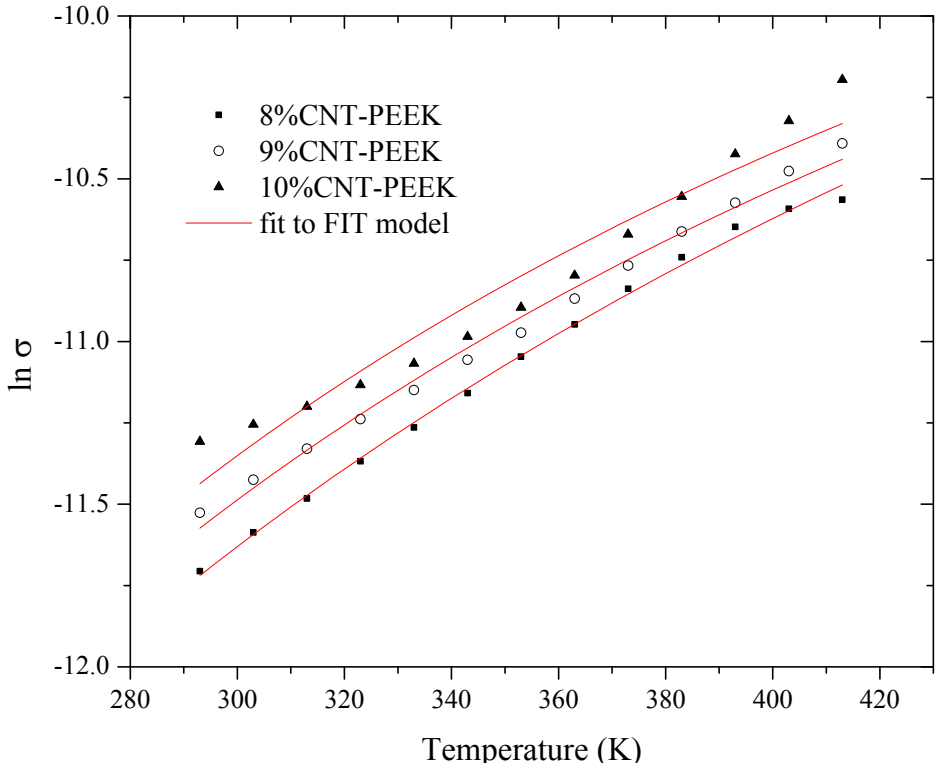

Figure 6.10: Fitting of Electrical conductivity to FIT model for 8 wt% – 10 wt% CNT-PEEK samples.

Fitting of equation (6.2) to the experimental data (solid line in Figure 6.10) gives the following values of T_1, T_0 and σ_0' listed in Table 6.2:

Table 6.2: Coefficients of determination in FIT model

Samples	T_1 (K)	T_0 (K)	σ_0' (S/cm)
8 wt% CNT-PEEK	2216.33	121.61	1.71×10^{-3}
9 wt% CNT-PEEK	1592.24	61.98	2.27×10^{-3}
10 wt% CNT-PEEK	1367.53	36.71	2.41×10^{-3}

These values are higher than the previously reported values for poly (ethylene terephthalate)/carbon black composites [126] and CNT-polyamide composites [86], but it is not surprising because these coefficients are strongly dependent of many parameters,

such as nature of the polymer, structure of conductive filler, filler content, sample processing etc.[199].

The above equation (6.2) describing FIT model can be written in the form [201]

$$\sigma = \sigma_0' \exp\left(-2\Psi_T\, s\right) \tag{6.3}$$

where $\Psi_T = \sqrt{\frac{2m\psi_T}{h^2}}$

with $\psi_T = \frac{\psi}{\left(1+\frac{16\pi\Psi k_B T}{A_c\, \vartheta_0^{\,2}}\right)^2}$ is the temperature modified barrier height.

Thus, equation (6.3) represents a tunneling process and the electrical conductivity is envisioned as a tunneling conductivity where the potential barrier height decreases with increasing temperature. At a constant temperature, equation (6.3) can be rewritten as [45]

$$\ln\sigma \propto -s \tag{6.4}$$

For a random homogeneous distribution of CNTs in insulating matrix, the composite conductivity can be described by the behavior of a single tunnel junction and the average distance (s) among the CNTs can be assumed to be proportional to $p^{-1/3}$ [202, 203]. Therefore, the conductivity data should follow the rule given by

$$\ln\sigma \propto p^{-1/3} \tag{6.5}$$

A weak indication in favour of FIT model is shown in Figure 6.11 by linear relationship between ln(σ) and $p^{-1/3}$ where p is the weight concentration of the filler, but this indication is very strong for the samples with CNT concentrations below percolation threshold (inset in Figure 6.11). The experimental results of temperature dependence of conductivity are also closely reproducible by the general conduction model.

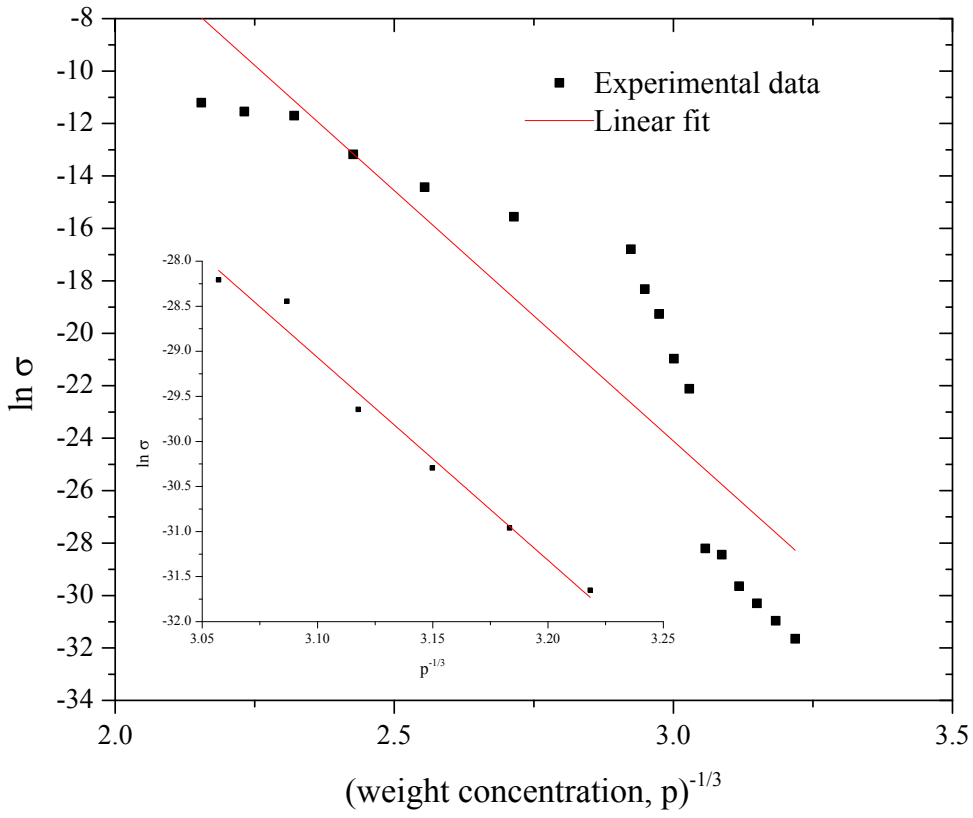

Figure 6.11: linear relationship of ln σ vs. $p^{-1/3}$

Therefore, possible limitations of the present analysis by FIT model can be emphasized based on the following two observations:

(i) Conductivity below the percolation threshold is well explained by tunneling conduction mechanism where homogeneously distributed particles are not yet in physical contact and obey the rule given by equation (6.5) [45, 121] whereas the present analysis is limited to samples far above percolation threshold.

(ii) FIT model is applicable only at sufficiently low temperatures [204] and is inappropriate above room temperatures [205] whereas, these experiments were carried out above room temperatures up to 140°C.

6.4.2 General conduction mechanism

A satisfactory result was obtained by fitting the experimental data to the general Arrhenius conduction activation model, which is commonly used to characterize the band conduction:

$$\sigma = \sigma_0' \exp\left(\frac{-E_{cond}}{k_B T}\right) \tag{6.6}$$

where σ is the electrical conductivity in S/cm, E_{cond} is the activation energy for the conductivity, k_B is the Boltzman constant, σ_0' is the pre-exponential factor and T is the temperature on the absolute scale (K).

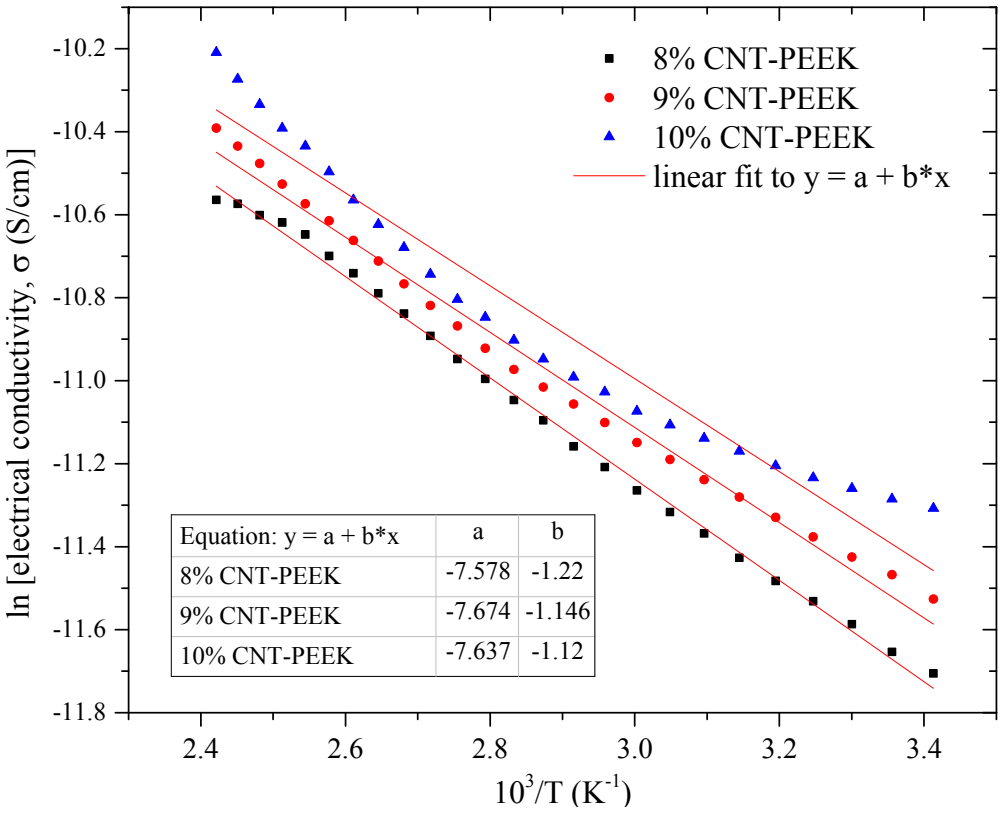

Figure 6.12: Plot of the logarithm of conductivity versus the reciprocal of temperature (1/T) for 8 wt% – 10 wt% CNT-PEEK composite samples.

The linear best fit graph of log conductivity versus 1/T (K^{-1}) shows a continuous linear curve for 8 wt% and 9 wt% CNT-PEEK composites (Figure 6.12) which indicates one activation energy for the hopping process, while σ = f(1/T) plot for 10 wt% CNT-PEEK sample has two slopes at two distinct temperature regions, one at the lower temperature range (20°C–60°C) and the other at higher temperature range (60°C–140°C) which indicates two activation energies for two different temperature regions (Figure 6.13).

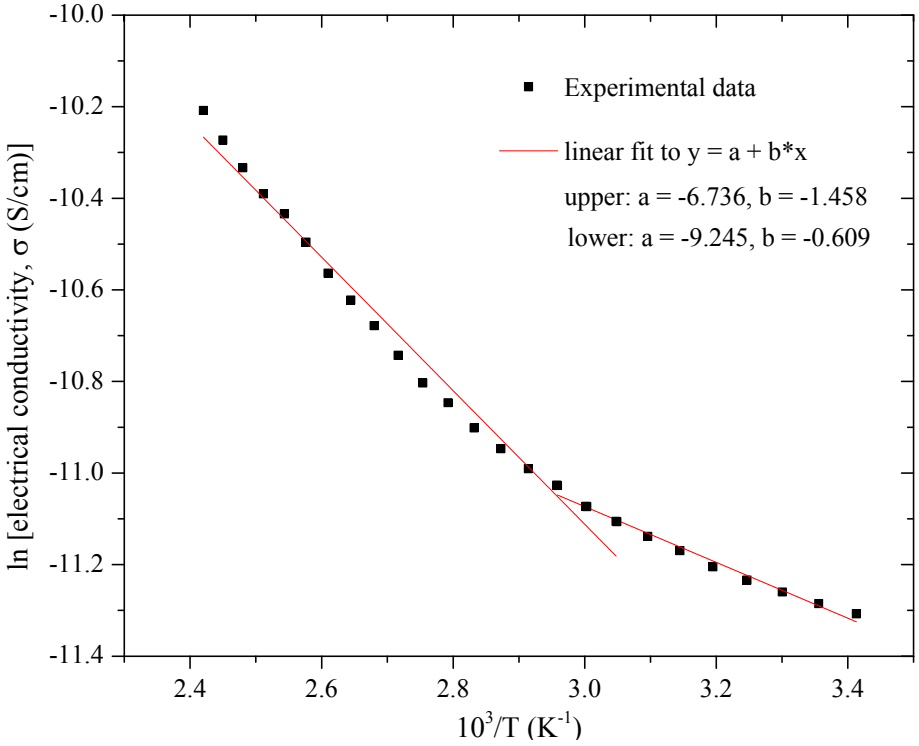

Figure 6.13: Plot of the logarithm of conductivity versus the reciprocal of temperature (1/T) for 10 wt% CNT-PEEK composite sample showing two slopes.

The pre-exponential factor σ'_0 and activation energy E_{cond} calculated by fitting the plot to equation (6.6) are presented in Table 6.3. Lower activation energy has been noticed in higher wt% of CNT composites as expected. The average value of pre exponential factor σ'_0 is slightly higher for 10 wt% CNT-PEEK than that for 9 wt% CNT-PEEK while the value is individually less in both upper and lower temperature regions.

Table 6.3: Constants obtained from curve fitted to equation (6.6)

Sample	σ'_0 (S/cm)	E_{cond} (eV)
8 wt% CNT-PEEK	5.12×10^{-4}	1.04×10^{-4}
9 wt% CNT-PEEK	4.65×10^{-4}	9.88×10^{-5}
10 wt% CNT-PEEK	4.83×10^{-4}	9.64×10^{-5}

For 10 wt% CNT-PEEK sample, it has been found that activation energy is comparatively higher at higher temperature region than that at the lower temperature region. Similar behavior has also been observed in previous investigations for carbon fiber-filled [65] and CNT-filled [206] elastomeric composites and CNT-polyamide composites [86]. No explanation was provided for this increased activation energy at higher temperature region. The conduction mechanism may be influenced by some other unknown factors in this region. More investigation can be carried out to explore this phenomenon.

From the above analysis, it is believed that above percolation threshold, the electrical charge transport is mostly dominated by metallic conduction through the conducting paths/networks formed by conducting CNTs.

In order to incorporate temperature dependence of σ above percolation limit, equation (3.3) and equation (6.6) can be combined as

$$\sigma = \sigma'_0 \left\{ \exp\left(\frac{-E_{cond}}{k_B T} \right) \right\} \left(\phi - \phi_c \right)^t \tag{6.7}$$

In equation (6.7) the value of ϕ_c and exponent t are taken to be 2.05 vol% and 2.517 determined by statistical analysis in chapter 3. The effect of thermal expansion on ϕ is taken into account by

$$\phi(T) = \frac{\phi_0}{1 + 3\frac{\Delta z}{z_0}} \tag{6.8}$$

where ϕ_0 is the volume fraction at room temperature (assumed at 30°C), Δz (T) is the difference between thickness of the sample at T and the original thickness, z_0 at 30°C. The relative change of $\Delta z/z_0$ for the temperature range of 30°C ~140°C was obtained from Thermo Mechanical Analysis (TMA).

Equation (6.7) is based on an assumption of thermally activated conduction process which requires that apparent activation energy E_{cond} and pre-exponential factor σ_0 are independent of volume fraction, ϕ in order to satisfy equation (6.6) with the universal scaling law of conductivity. The temperature dependence of $\ln[\sigma(T)/(\phi(T)-\phi_c)^t]$ for three different weight concentrations of CNTs is shown in Figure 6.14.

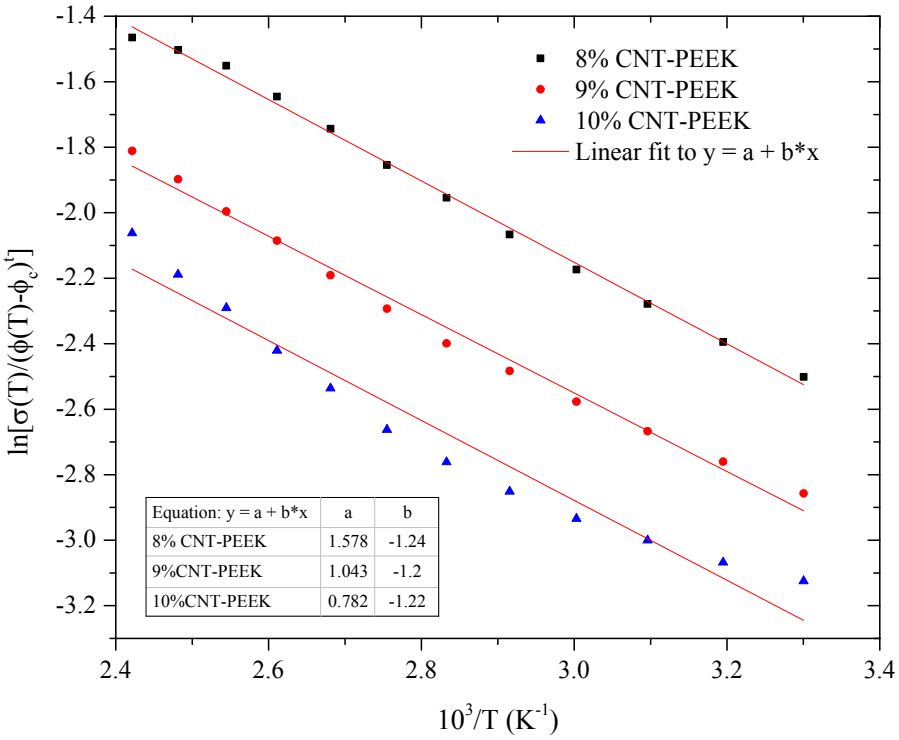

Figure 6.14: Temperature dependence of electrical conductivity of samples with $\phi > \phi_c$ in which effect of thermal expansion has been taken into account.

The value of activation energy is calculated from the slope of the linear fit of $\ln[\sigma(T)/(\phi(T)-\phi_c)^t]$ vs. reciprocal of temperature (K^{-1}). It is clear that plot of all three different concentrations of CNT samples are similar with identical slope. The average activation energy is estimated to be 1.05×10^{-5} eV which is close to the value obtained by Arrhenius conduction model [equation (6.6)]. Therefore, it can be concluded that temperature dependence of electrical conductivity above percolation limit of the present composite system can be explained by general conduction mechanism without violating universal scaling law of conductivity.

6.5 Combined effect of temperature and pressure on electrical conductivity

It is worthy to investigate the effect of temperature on electrical conductivity of the samples at different applied loads. Figures 6.15, 6.16 and 6.17 show the variation of electrical conductivity of 8 wt%, 9 wt% and 10 wt% CNT-PEEK composites respectively against temperatures of experiment up to 140°C for the compression loads from 0 to 40 MPa. Electrical conductivity increases with increasing pressure. In the case of 8 wt% and 9 wt% CNT samples, this increase is more or less same for all temperatures, but in the case of 10 wt% samples, the effect of pressure is more pronounced at lower temperatures than at higher temperatures. The curves are slightly concave downward for 8 wt% CNT and concave upward for 10 wt% CNT samples, while for 9 wt% CNT samples, these are almost straight. This behavior was previously explained in section 6.3.3.

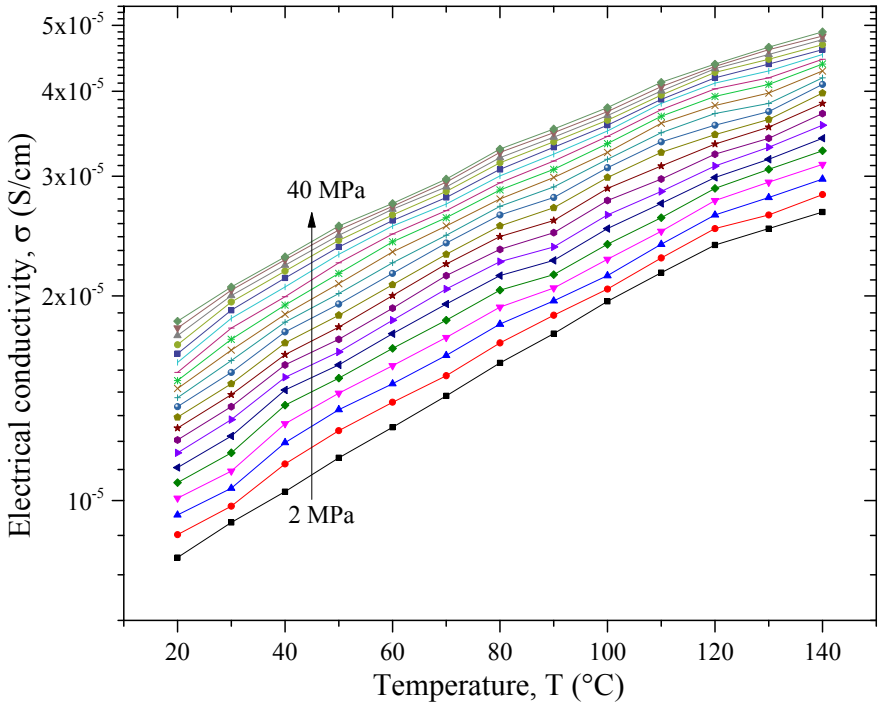

Figure 6.15: Electrical conductivity of 8 wt% CNT-PEEK composites as a function temperature for different applied pressures [2, 4, 6, 8,….40 MPa].

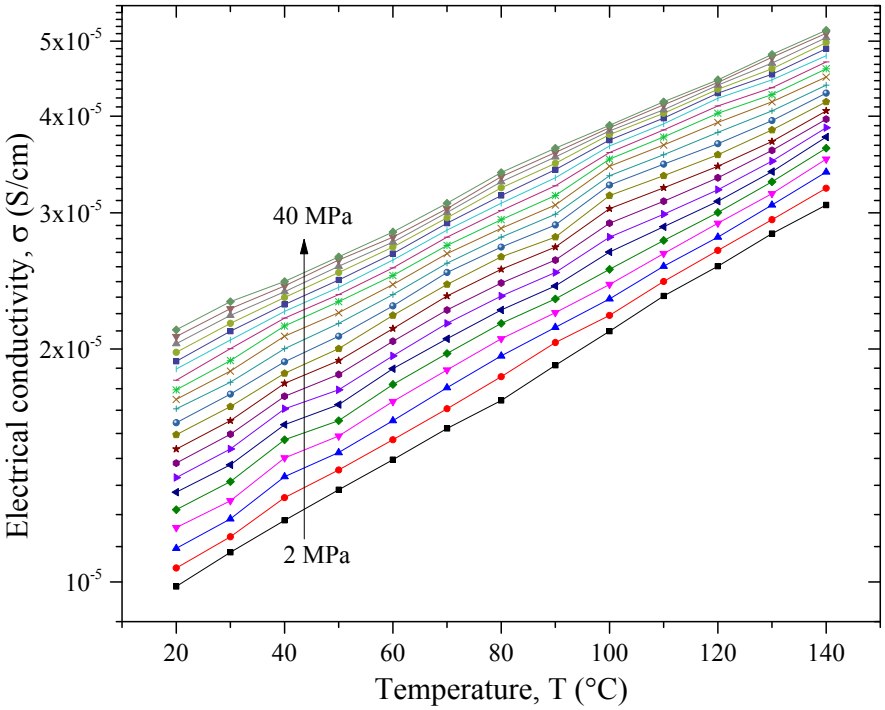

Figure 6.16: Electrical conductivity of 9 wt% CNT-PEEK composites as a function temperature for different applied pressures [2, 4, 6, 8,….40 MPa].

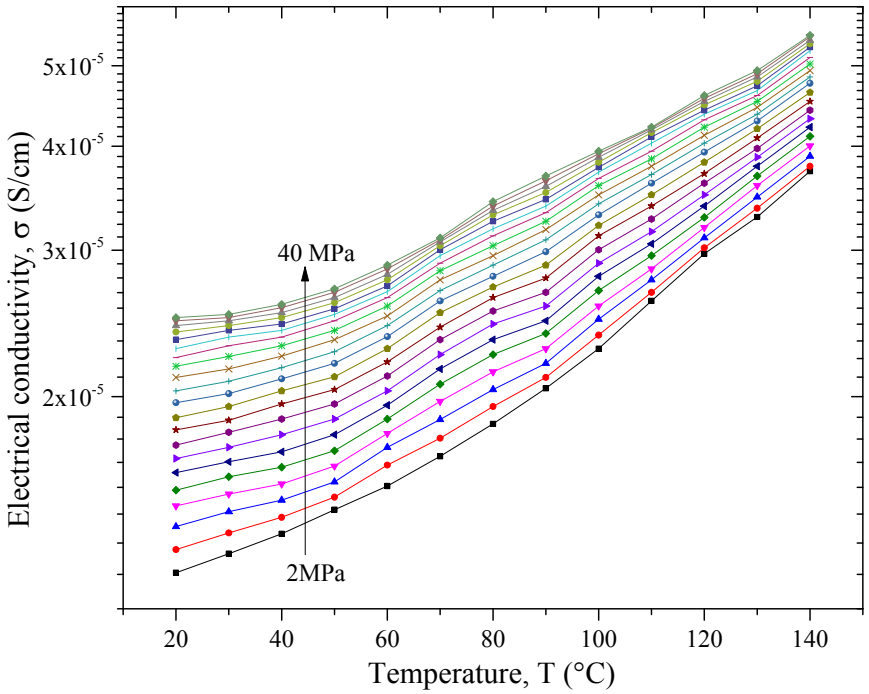

Figure 6.17: Electrical conductivity of 10 wt% CNT-PEEK composites as a function temperature for different applied pressures [2, 4, 6, 8,….40 MPa].

To visualize the effect of temperature at room temperature and at 140°C at different pressures on the change of electrical conductivity, the Figure 5.4 is reproduced as shown below (Figure 6.18). The lower set of curves presents the results for room temperature, while the upper ones for 140^{o}C. For both set of curves, it is observed that the slope of the curve gradually decreases with the increase of pressure and for 10 wt% CNT samples at 140^{o}C, this slope is almost zero at the highest applied pressure of 40 MPa. The differences in the decrease of the slopes for 8 wt%, 9 wt% and 10 wt% CNT samples are marginal. Comparison of the two sets of curves reveals that the electrical conductivity of the samples approach to its saturation level more quickly at higher temperature than at room temperature for the same applied pressure. Effect of nanotube concentration on approaching this saturation level of electrical conductivity for these highly conductive composites is not very strong.

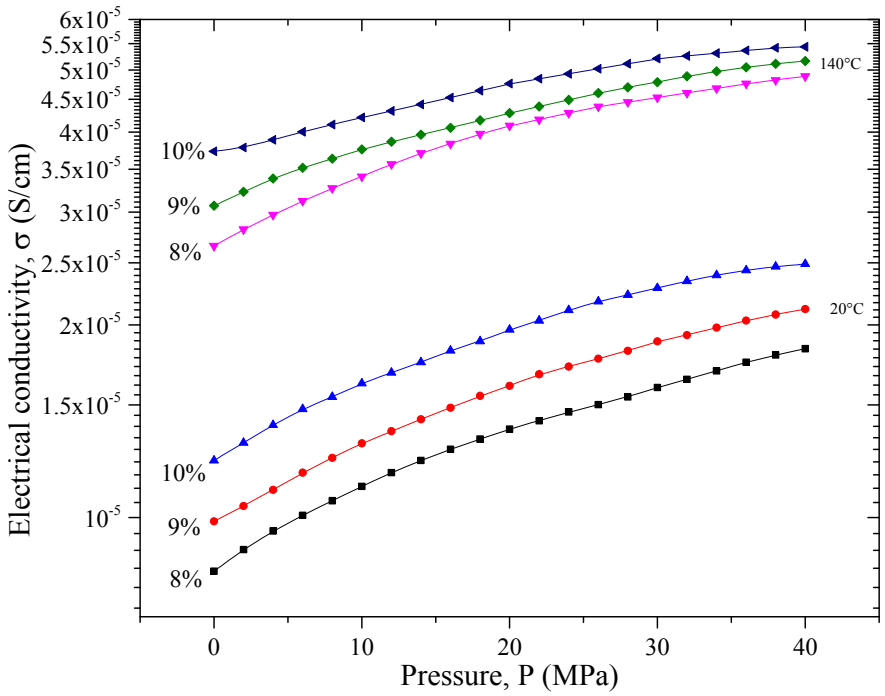

Figure 6.18: Electrical conductivity vs. Pressure at room temperature (20°C) and 140°C.

Previously it was mentioned in section 5.3.1 that the samples behave like an efficient pressure sensor up to a certain pressure beyond. Similarly from Figure 6.18, it can be said that the samples can be used as temperature sensor up to a certain temperature as there is no appreciable change in electrical conductivity above that critical temperature.

6.5.1 Explanation of the effect of temperature and pressure on electrical conductivity of CNT-polymer composites

The effect of temperature on electrical conductivity of polymer composites is quite complex. According to the hopping or tunneling mechanism of charged particles (i.e. electrons) in the system, with increasing temperature, the thin gap between two adjacent conductive CNTs increases because of uneven thermal expansion coefficient of the polymer matrix and the CNTs. An expansion of polymer matrix during heating induces

greater mobility to the CNT particles, and thus the process of electron tunneling is enhanced. Accordingly, the probability of tunneling of electrons increases which is reflected in the significant increase of conductivity with temperature. The number of existing physical contacts among the CNT and formation of further conductive networks during heating are primarily responsible for this behavior. With the gradual increase of CNT loading, the presence of large number of CNT contacts ensures a much higher probability of tunneling.

In composite materials, as mentioned earlier the temperature coefficient of resistivity is denoted as positive (PTC) when electrical resistivity of composite increases (electrical conductivity decreases) with the increase of temperature, or negative (NTC) when electrical resistivity of composite decreases (electrical conductivity increases) with the increase of temperature, or zero when electrical resistivity of composite remains constant with the change of temperature. The characteristic of each system depends on the concentration of filler and the nature of the polymers and the filler. As shown in Figures 6.5, 6.15, 6.16 and 6.17, a negative temperature coefficient of resistivity (NTC effect) applies for the case of CNT-PEEK composites, that is, electrical conductivity of the composites increases during the heating process over a temperature range from room temperature to 140°C which is below the glass transition temperature of the matrix (144°C). The effect of temperature on electrical conductivity of this CNT-PEEK composite system above the glass transition temperature will be discussed later.

The effect of temperature and pressure on the electrical resistance of CNT-polymer composites may be explained based upon two main mechanisms responsible for electrical conductivity CNT-polymer composites.

- *Conduction by electron transport (nanotube contact):* The contacts between different CNTs provide the circuit for electrons to flow. At the percolation threshold, there is just sufficient contact for the material to be conductive. Above the percolation threshold, parameters that affect the number of contacts are:
    - Amount of fillers: More CNTs provide more contacts and higher electrical conductivity. This is evident in Figure 6.18.
    - Compression: Compression squeezes the CNTs together, giving better probability for contacts (Figures 6.15, 6.16 and 6.17).
    - There is a saturation phenomenon for both the amount of fillers and the level of compression. This means that the rate of increase of electrical conductivity is more at lower concentrations of CNTs and compression and the rate reduces as the concentrations of filler or compression are increased. This is because once full electrical conductivity is established; it becomes difficult to increase it.
    - Aspect ratio of fillers: The aspect ratio of the fillers has an important influence on the electrical conductivity. Larger aspect ratio increases electrical conductivity. Ansari et al. [207] studied the electrical conductivity of PVDF reinforced with two types of fillers. They found that Functionalized Graphene sheet (FGS)-PVDF system exhibited NTC while exfoliated graphite (EG)-PVDF system exhibits PTC. The explanation given is that FGS has higher aspect ratio than EG.

- *Conduction by electron tunneling:* In addition to conduction by electron transport across contact points, conductivity in CNT-polymer system also occurs by electron tunneling across gaps between the CNTs. Conduction by electron tunneling depends on the length of the gap between the CNTs. The longer is the gap, the more difficult is the electron tunneling and the lower is the electrical conductivity. Parameters that affect the electron tunneling are:
    - The relative dominance between the number of contacts and the gaps between the CNTs. If the number of contacts is dominant then increase in temperature would increase in electron activity and this would increase the electrical conductivity. There should be a critical amount of contacts beyond which the gaps between the CNTs would become irrelevant.
    - The stiffness of the polymer material: In situations where there is a relatively small amount of fillers, the stiffness of the polymer material plays an important role. For material with higher stiffness, increasing in temperature may not produce large deformation of the gaps between CNTs, while the opposite holds true for material with lower stiffness. Work done in references [65, 186, 208-210] showed PTC. These experiments were performed above the glass transition temperature (T_g) of the polymers (T_g of Elastomer –70°C, PE –120°C, PVDF –35°C). The present investigation for CNT-PEEK composites was carried out below glass transition temperature, T_g (T_g of PEEK is 144°C) and NTC was obtained. However, Figure 6.18 shows that the NTC effect decreases with increasing temperature, due to the softening of the polymer at higher temperature.

From the above discussion, it was understood that the contribution of pressure on the electrical conductivity is always positive whether it is accompanied by temperature or not, i.e. applied pressure always increases electrical conductivity by narrowing the gaps between CNTs. It can be done either by electron transport (nanotube contact) or electron tunneling depending on the nanotube concentrations. But contribution of temperature towards the electrical conductivity can either be positive or negative or zero due to the involvement of other parameters mentioned above. Thus, combined effect of pressure and temperature on electrical conductivity is determined by their net contribution.

To further investigate those parameters involved in the effect of temperature, experiments were done by heating the samples of 8 wt%, 9 wt% and 10 wt% above glass transition temperature up to 200°C. Similar experiments were also carried out on 3 wt%, 4 wt% and 5 wt% CNT-PEEK samples. The results shown in the Figures 6.19 and 6.20 respectively are explained under the following two categories:

Category 1: When a sufficiently large number of contacts are available in the conductive network

It is presumed that PEEK composites made with 8 wt%, 9 wt% and 10 wt% CNTs are highly conductive with sufficiently large number of available nanotube contacts. From the graphs in Figure 6.19, the rate of increase of electrical conductivity with the increase of temperature gradually decreases. Thus, it can be said that electrical conductivity of those conductive samples after a certain temperature (it can be termed as saturation temperature), which is above glass transition temperature, is not much affected on further increasing temperature. Thus, the thermal expansion of the polymer matrix is not dominant enough to separate the CNTs or increase the gap between them. As a result,

electrical conductivity is fully controlled by physical contacts among CNTs. Application of compression in such case may increase the conductivity slightly until a saturation point has been reached. When the saturation point of electrical conductivity has already been reached, further increase in nanotube concentration, pressure and/or temperature do not make any significant change in the composite conductivity.

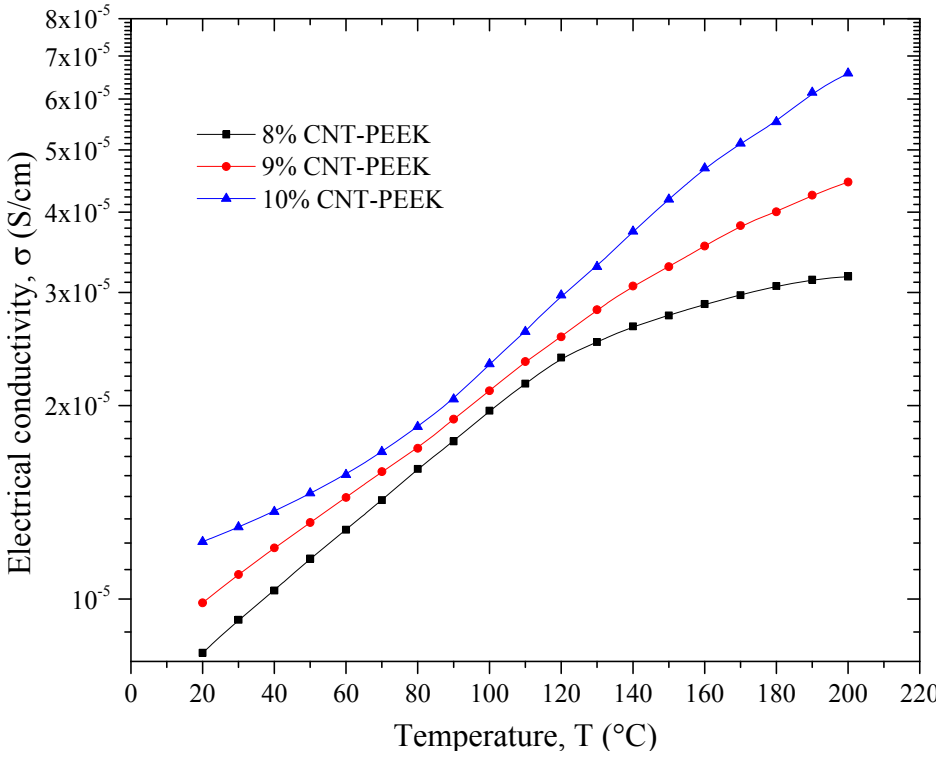

Figure 6.19: Electrical conductivity of 8 wt%, 9 wt% and 10 wt% CNT-PEEK composites from room temperature to 200°C (T_g of PEEK = 144°C).

Category 2: When a sufficiently large number of contacts are NOT available in the network

Figure 6.20 shows the electrical conductivity of 3 wt%, 4 wt% and 5 wt% CNT composites. These samples have lower number of nanotube contacts than those of 8 wt% – 10 wt% nanotubes and from previous DEA analysis (Figure 3.1), it can be assumed that they do not have sufficient nanotube contacts.

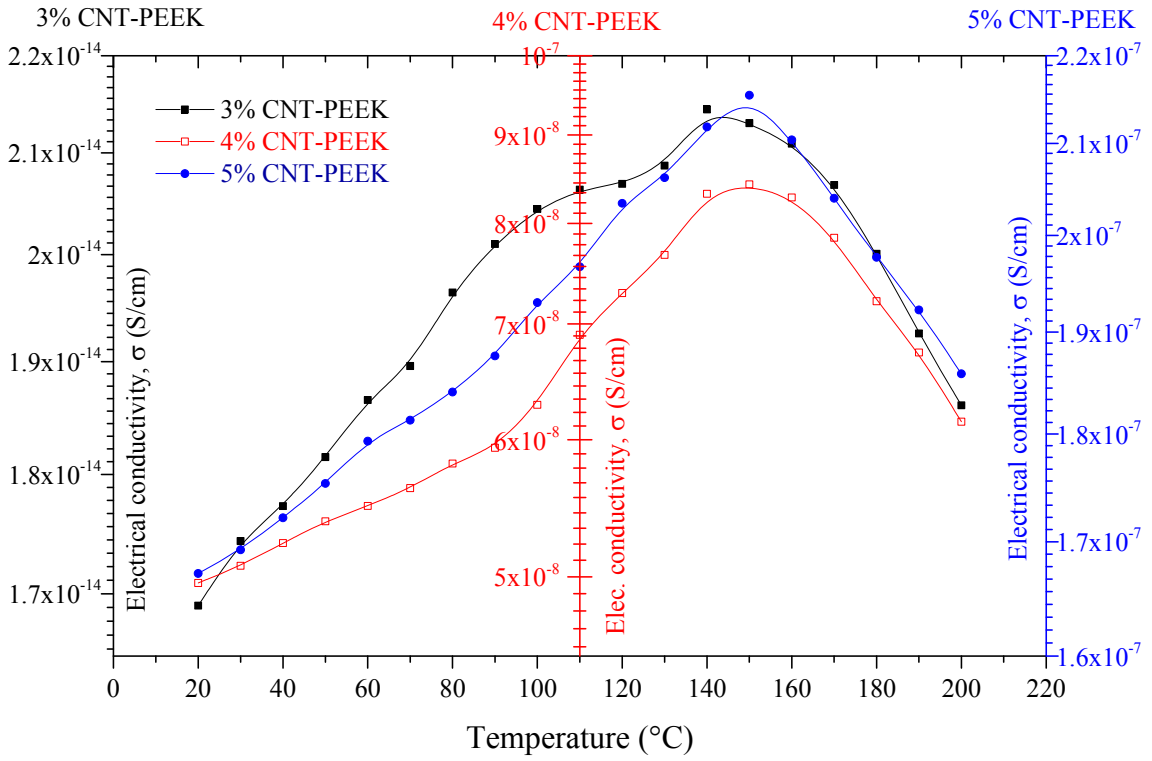

Figure 6.20: Electrical conductivity of 3 wt%, 4 wt% and 5 wt% CNT-PEEK composites from room temp to 200°C (T_g of PEEK = 144°C).

A rise in electrical conductivity (NTC) of the composites up to a certain temperature and then a decrease in conductivity (PTC) were observed for these composite samples. At the beginning due to increase in temperature, the electron activity increases, resulting in an increase in conductivity. But since the number of nanotube contacts is not sufficiently large to maintain the solid intimate contact, after certain temperature, volumetric expansion of PEEK due to heat increases the gap between nanotubes and decreases the number of conductive pathways, resulting in a decrease in conductivity. This certain temperature is not necessarily the same for all concentrations, but it is near to the glass transition temperature (T_g) as observed. This temperature depends on the number of nanotube contacts and their gaps in between. It can be termed as transition temperature

(T_t) because at this temperature, behaviour of electrical conductivity changes from NTC to PTC. This transition temperature is higher for higher nanotube concentration and vice versa. Below T_t, nanotube contacts and their electron activity plays dominant role while above T_t, thermal expansion of polymer, nanotube gap and hence electron tunneling play the dominant role in determining electrical conductivity. At temperatures higher than T_t, crystalline phase of the polymer begins to become softened and gradually it transforms from semi-crystalline phase to rubbery phase. As a result, the fluidity of the polymer matrix increases and the CNTs at such high temperatures attain energy to overcome the potential barrier and lose their contact with each other. Number of conductive paths also decreases in such situation. Application of compression enhances the increase of conductivity below T_t, but above T_t, the total conductivity is determined by their net effect as temperature and pressure are opposing each other. Further increase of nanotube concentration has also similar effect as like as pressure until the solid continuous network of nanotubes are established at such elevated temperatures so as to fall into the first category described above. Based on the observations, all those parameters together with their effects are summarized below in Table 6.4.

Table 6.4: Summary of the effect of parameters on electrical conductivity of nanocomposites

With an increase in	Parameters involved	Electrical conductivity
1. Nanotube content	nanotube gap: decreases electron activity: no effect number of conducting paths: increases	increases up to a certain level, then might decrease
2. Pressure	nanotube gap: decreases number of conducting paths: increases / redistributed	increases up to saturation level
3. Temperature • when large number of nanotube contacts are available	electron activity: increases nanotube gap: no significant change	increases up to saturation level
• when large number of nanotube contacts are NOT available	(i) below T_t: electron activity increases, nanotube gap: no significant change (ii) above T_t: electron activity increases, nanotube gap: increases number of conducting paths: decreases	increases decreases
4. Modulus of Elasticity (stiffness) of polymer	With the increase in temperature, rate of decrease of nanotube gap decreases	depends on the level of temperature and nanotube content

6.6 Application to sensor

To examine how sensitive and to what extent the conductivity response will be after being stimulated by the change of pressure and temperature, the relative conductivity can be used to characterize the effect of temperature coefficient(σ_T) and pressure co-efficient (σ_P) given by:

$$\sigma_T = \log\left(\frac{\sigma_{140^\circ C}}{\sigma_{20^\circ C}}\right) \text{ at different pressures} \tag{6.9}$$

$$\sigma_P = \log\left(\frac{\sigma_{40MPa}}{\sigma_{0MPa}}\right) \text{ at different temperatures} \tag{6.10}$$

The temperature sensitivity and pressure sensitivity for the pressure and temperature ranges used throughout the experiment are shown in Figures 6.21 and 6.22 respectively.

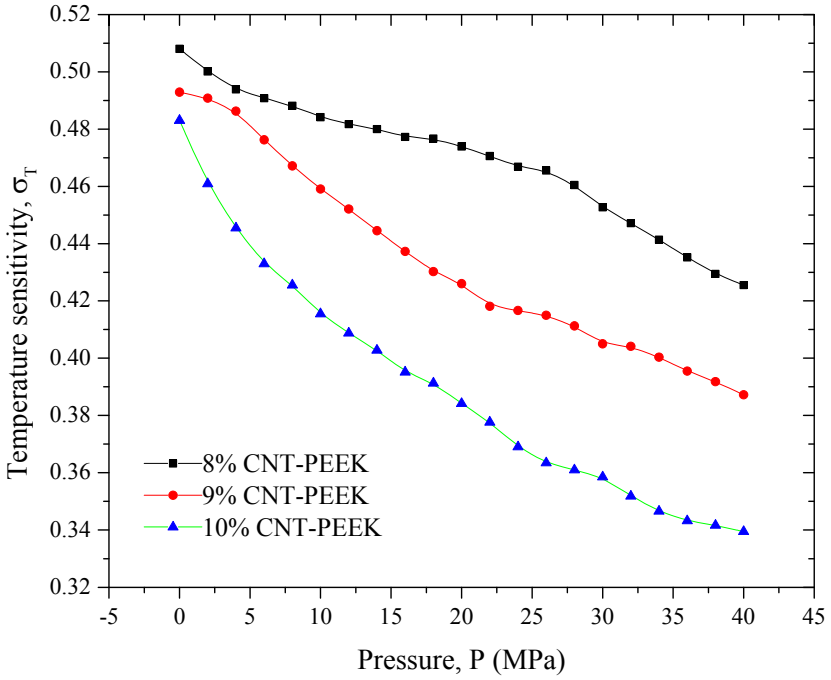

Figure 6.21: Temperature sensitivity of CNT-PEEK samples at different pressures.

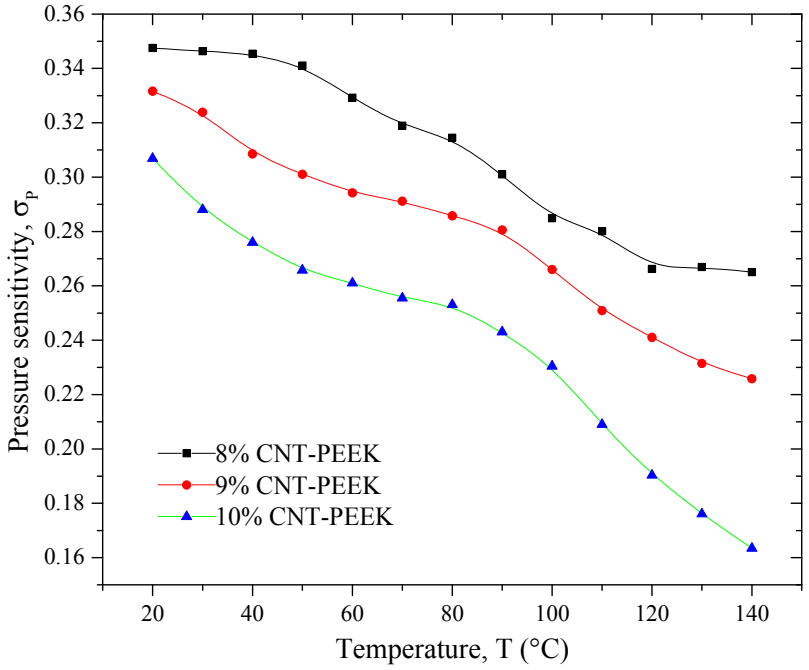

Figure 6.22: Pressure sensitivity of CNT-PEEK samples at different temperatures.

As expected the composite samples are highly sensitive at low pressure and low temperature regardless of their nanotube concentrations. Again, the samples are highly sensitive at lower nanotube concentration and less sensitive at higher nanotube concentration, but the range of sensitivity is higher for higher nanotube concentrations. Comparison of the above two graphs indicate that the CNT-PEEK samples under investigation are highly temperature sensitive than pressure sensitive.

6.7 Summary

1. Effect of Joule heating on increasing conductivity at elevated temperatures was investigated. The Joule heating was not significant in this study.

2. Thermal expansion of the samples was measured in their thickness direction by Thermo Mechanical Analysis (TMA) and its effect was ignored in the calculation of electrical conductivity under the application of heat.

3. Differential Scanning Calorimetry (DSC) shows that with the addition of extra CNTs, the glass transition temperatures (T_g), the melting enthalpies (Q_m) and the amount of crystallinity of the samples decrease, and there is no significant change in the melting temperatures (T_m). This phenomenon was explained by confinement effect.

4. Negative temperature coefficient of resistivity (NTC effect) has been observed in the case of CNT-PEEK composites, i.e. electrical conductivity of CNT-filled PEEK composite progressively increases with the increase of temperature up to the highest temperature of 140°C in these experiments.

5. Electrical set and electrical hysteresis were observed in the conductivity vs. temperature plot during heating and cooling cycle and this can be due to some irreversible change occurring in the conducting network system.

6. Fluctuation induced tunneling (FIT) model does not satisfy the experimental data of these highly conductive composites, because the samples' CNT concentration was above percolation threshold and the temperatures of experiments were far above the room temperature.

7. Lower activation energy has been found for higher concentration of CNTs and for higher temperature region in the case of 10 wt% CNT-PEEK composite.

8. With increase in temperature, electron mobility increases which causes higher electrical conductivity (electronic conduction), but at the same time, thin gap between CNTs becomes larger due to thermal expansion of PEEK which reduces the conductivity (electron tunneling). Composite's electrical conductivity is determined by the net effect of these two opposite phenomena. Dominance of electronic conduction was observed in the case of higher concentration of CNTs because of sufficiently larger number of existing CNT contacts as compared to lower concentration of CNTs. On the other hand, electron tunneling was dominant in lower CNT concentrations where, enlargement of film gap reduces the effect of the increase in electronic activities due to increase in temperature.

9. The analyzed composite samples were found to be more temperature sensitive than to be pressure sensitive.

Chapter 7

Summary, Conclusions, Contributions and Recommendations for Future Work

7.1 Summary

(1) Optimum process parameters of 100 rpm rotor speed, 380°C mixing temperature and 20 minutes of mixing time were determined.

(2) Nanocomposite samples were manufactured using PEEK and CNTs via high shear melt mixing technique.

(3) Electrical and dielectric properties of the nanocomposite samples were investigated in a wide range of frequencies (1 to 10^5) at room temperature.

(4) Percolation threshold was obtained when the concentration of CNTs increased from 3.5 wt% to 3.6 wt%. The results show that conductivity is frequency dependent below the percolation threshold and frequency independent above percolation threshold.

(5) With the increase of CNT concentration, the gap between two neighboring CNTs decreases and thus formation of conducting paths minimizes the hopping effect thus makes the sample more conductive.

(6) Contact resistance of crossing CNTs with an insulating layer in between was calculated using different theoretical equations.

(7) The highest tunneling distance in this composite system was found to be 17Å by Simmons' equation which is comparable to the previously reported one of 18 Å [39].

(8) Electrical conductivity increases with increasing pressure up to a certain level. A small increase was also observed for repeated loading unloading until stabilization.

(9) Under application of compression, carbon nanotubes come closer to each other thereby reducing tunneling distance in between and conducting paths are redistributed. These are the two main causes of increase in electrical conductivity of composites when pressure is applied.

(10) For highly conductive composites (conducting region), electrical conductivity increases significantly under application of heat until the glass transition temperature of the polymer matrix (PEEK). Above glass transition temperature, the rate of increase gradually decreases and eventually it becomes almost constant. Conduction by nanotube contact (electron transport) plays dominant role in this case.

(11) For less conductive composites (insulating and semi-conducting regions), the electrical conductivity increases up to a certain temperature followed by a decrease. Electron tunneling plays dominant role over electron transport in this case.

7.2 Conclusions

Electrical properties of polymer nanocomposites can be improved by incorporating CNTs in the polymer matrix. Uniform dispersion, formation of conductive networks and thin insulating film around the CNTs are some of the key parameters that determine the electrical properties. Fabrication, processing and electrical properties of polymer nanocomposites were studied in this dissertation.

High temperature composites using MWCNTs as fillers and advanced thermoplastic polymer PEEK as matrix were fabricated by conventional melt processing technique with co- rotating intermeshing twin screw extruder. SEM micrographs showed that aggregates of CNT were formed around the grain boundary of semi crystalline PEEK. The boundary thickness increased with increase of CNT concentrations. Electrical properties of these nanocomposites were investigated at room temperature by impedance spectroscopy. A percolation threshold between 3.5 wt% to 3.6 wt% was observed when the electrical conductivity increased by several orders of magnitude. Frequency dependence (below percolation threshold) and frequency independence (3.6 wt% to 7 wt% of CNTs up to a critical frequency) of electrical conductivity were observed. The critical frequency disappeared for the samples containing 8 wt% or more CNTs indicating a fully conducting network. The AC and DC responses of the composites were analyzed in the light of percolation theory and the results were compared with those available in the literature. The estimated electrical conductivity for close to 100% CNT composites should theoretically be comparable to the intrinsic electrical conductivity of CNTs, but a large discrepancy in the order of 10^6 was observed which is due to the formation of thin insulating film around CNTs. It gives rise to the phenomenon of tunnel effect. The detail study of this tunnel effect based on theoretical models along with the experimental results showed that the maximum possible distance between two adjacent CNTs is about 1.7 nm for the electrons to jump across the tunnel. This value is close to 1.8 nm previously reported by Li et al. [39] using Monte Carlo simulation technique.

Under application of high pressure (up to 40 MPa), the change of electrical conductivity was studied for highly conductive composites containing 8 wt% to 10 wt% CNTs. Instead

of conventional metallic coats, a new technique was developed to measure DC electrical conductivity at high pressure and temperature by introducing conductive copper mesh and its accuracy of measurement was satisfactory. This new technique opens door for future researchers to conduct experiments at high pressures and temperatures because of its simplicity and feasibility. Increase in electrical conductivity of the samples under compression was mainly due to (i) the decrease of tunneling distance and (ii) redistribution of number of conducting paths. Electrical conductivity increases up to a certain level of pressure and after that it becomes saturated with no significant change in electrical conductivity on further application of pressure. This observation was different than the results published by Wang et al. [151] for CB-HDPE system, Yongliang et al. [152] for CB-PMVS system etc. where they observed a transition from PPCR to NPCR. A simple pressure model was developed to relate electrical resistance and pressure which reproduces the experimental result within satisfactory agreement.

While the pressure has acted favorably in increasing electrical conductivity, effect of temperature was found to be complex. The electrical conductivity increased with increase in temperatures up to a certain temperature near glass transition temperature. Above that transition temperature, electrical conductivity was found to decrease for less conductive samples, but it was almost constant without any significant change in electrical conductivity for highly conductive samples (containing 8 wt% to 10 wt% CNTs). Two possible mechanisms, namely (i) conduction by electron transport dominated by CNT contacts and (ii) conduction by electron tunneling dominated by tunneling distance between CNTs were proposed to explain such contradicting behavior. Coefficient of thermal expansion and modulus of the polymer matrix are also considered contributing

factor in the change of electrical conductivity. The result presented in this study was different than that obtained by Logakis et al. [86] and Bin et al.[189]. Logakis et al. [86] found a steeper increase in conductivity above glass transition temperature (T_g) than below T_g regardless of nanotube content while Bin et al. [189] found an increase in conductivity above melting point (T_m). Their explanation was given in terms of molecular activity that active motion of polymeric chain enhances the CNT–CNT contact causing an increase in electrical conductivity. Sensitivity of the experimented samples showed that the samples were more temperature sensitive than to be pressure sensitive.

7.3 Contributions and list of publications

The major contributions of this research to the field of polymer nanocomposites are summarized as:

- This study is the first in the literature to manufacture electrically conductive CNT-PEEK composites having capability of sensing for high pressure and temperature application. This is the first report on the effect of pressure and temperature on electrical conductivity of CNT-PEEK composites.

- Available theoretical models on tunneling contact are successfully verified by the experimental results obtained in this study. Maximum possible tunneling gap between CNTs was estimated to be 1.7 nm.

- In the literature of composites science, temperature dependence of electrical conductivity is usually believed to show either PTC or NTC regardless of filler content and temperature range. Two available explanations are: (i) with the increase in temperature, polymer matrix expands more than the filler and thus

increased distance between filler particles causes a drop in electrical conductivity (PTC) and (ii) with the increase in temperature, electronic movement of the polymer molecules and filler particles increases and thus increased interaction among the molecules causes an increase in electrical conductivity (NTC).

Based on the experimental results, a comprehensive explanation with proper identification of all possible contributing factors has been given. A general procedure has been proposed to explain temperature dependence and pressure dependence of electrical conductivity of polymer nanocomposites using the following parameters:

(i) Nanotube contacts: depending on nanotube concentration, three distinct regions, namely, insulating region up to percolation threshold, semiconducting region (percolation threshold to conduction threshold) and conducting region (above conduction threshold) were identified. Higher concentration of nanotube gives more number of contacts and hence higher electrical conductivity.

(ii) Pressure: Application of pressure in all three regions of conductivity mentioned above, reduces the nanotube to nanotube distance thereby reducing the tunneling resistance and increases the number of conducting paths due to redistribution of existing conducting particles. The resultant effect is an increase in electrical conductivity (NTC effect).

(iii) Temperature: Electrical conductivity of composites in conducting region is governed by 'conduction by nanotube contact' rather than 'conduction by

tunneling' irrespective of temperature. Conductivity increases up to a saturation temperature and then it becomes stable (therefore, it always shows NTC effect).

On the other hand, electrical conductivity of composites in insulating and semi-conducting region is determined by the relative dominance of nanotube contact and tunneling. Up to a transition temperature, electrical conductivity is dominated by 'conduction by nanotube contact' (conductivity increases/NTC effect). Above this transition temperature, electrical conductivity is dominated by 'conduction by tunneling' (conductivity decreases/PTC effect).

List of Publications

Journal Publications

1. M. Mohiuddin, S.V. Hoa. "Electrical Resistance of CNT-PEEK Composites under Compression at Different Temperatures", *Nanoscale Research Letters*, 2011, 6 (1), p. 419 (5 pages).

2. M. Mohiuddin, S.V. Hoa. "Temperature Dependent Electrical Conductivity of CNT-PEEK Composites", *Composites Science and Technology*, 2011, 72 (1), pp. 21–27.

3. M. Mohiuddin, S.V. Hoa. "Effect of Pressure on Electrical Conductivity of CNT-PEEK Composites", *To be submitted.*

4. M. Mohiuddin, S.V. Hoa. "Parameters Affecting Electrical Conductivity of CNT-PEEK Composites under Compression", *To be submitted.*

5. M. Mohiuddin, S.V. Hoa. "Frequency Dependent Electric and Dielectric Properties of Carbon Nanotubes/Poly Ether Ether Ketone Composites", *To be submitted.*

6. M. Mohiuddin, S.V. Hoa. "Estimation of Contact Resistance and its Effect on Electrical Conductivity of Carbon Nanotubes/Poly Ether Ether Ketone Composites", *To be submitted.*

7. M. Mohiuddin, S.V. Hoa. "Charge Transport Phenomena in Conductive Carbon Nanotubes/Poly Ether Ether Ketone Composites", *To be submitted.*

8. M. Mohiuddin, S.V. Hoa. "A General Explanation of Pressure and Temperature Dependence of Electrical Conductivity of Polymer Nanocomposites" *Under preparation.*

Conference Posters/Papers/Proceedings

1. M. Mohiuddin and S.V. Hoa. "Electrically Conductive Carbon Nanofiber Based Thermoplastic Composites for Fusion Bonding", *SAMPE'07*, Baltimore, Maryland, USA. June 3 –7, 2007.

2. M. Mohiuddin and S.V. Hoa. "Effect of Temperature and Compression on Electrical Conductivity of CNT-PEEK Composites", *ICCM-17*, Edinburgh, UK July 27–31, 2009.

3. M. Mohiuddin and S.V. Hoa. "Effect of Compression on Electrical Conductivity of CNT-PMMA composites", *25th ASC Annual Technical Conference*, Dayton, Ohio, USA, September 20–22, 2010.

4. M. Mohiuddin and S.V. Hoa. "Electrical Resistance of CNT-PEEK Composites under Temperature and Compression", *11th Trends in Nanotechnology International Conference (TNT2010)*, Braga, Portugal, September 06–10, 2010.

5. M. Mohiuddin and S.V. Hoa. "Potential Pressure and Temperature Sensors using PEEK and CNT", *Nanotechnologies: source of innovation and competitiveness (NanoQuebec 2012)*, Montreal, Canada, March 20–21, 2012.

7.4 Recommendations for future work

In addition to the above findings of this research, the following is recommended to be done:

(1) Study of the effect of nanotube quality, purity and initial conditions on the electrical conductivity of the composites.

(2) An extensive theoretical analysis can be done by incorporating modulus of polymer material to get the contribution of the change of angle of an individual CNT towards the change of composite conductivity.

(3) The effect of temperature on electrical conductivity above glass transition temperature using other high performance thermoplastic polymers (for example, PMMA, PEKK etc.) can be studied to verify the mechanism proposed in this thesis.

(4) An equation to estimate the electrical conductivity of nanocomposites can be developed including different parameters and phenomenon, e.g. above and below glass transition temperature, above and below percolation threshold, high and low modulus polymer materials, applied pressure etc.

(5) It might be interesting to further investigate the charge transport mechanism of this composite system below percolation threshold by extending the temperature range down to liquid helium temperatures.

References

[1] S. Iijima. "Helical microtubules of graphitic carbon", *Nature,* vol. 354 (6348), pp. 56-58, 1991.

[2] E. T. Thostenson, Z. Ren and T.-W. Chou. "Advances in the science and technology of carbon nanotubes and their composites: a review", *Composites Science and Technology,* vol. 61 (13), pp. 1899-1912, 2001.

[3] R. Khare and S. Bose. "Carbon Nanotube Based Composites-A Review", *Journal of Minerals & Materials Characterization & Engineering,* vol. 4 (1), pp. 31-46, 2005.

[4] F. Hussain, M. Hojjati, M. Okamoto and R. E. Gorga. "Review article: Polymer-matrix nanocomposites, processing, manufacturing, and application: An overview", *Journal of Composite Materials,* vol. 40 (17), pp. 1511-1575, 2006.

[5] M. Moniruzzaman and K. I. Winey. "Polymer nanocomposites containing carbon nanotubes", *Macromolecules,* vol. 39 (16), pp. 5194-5205, 2006.

[6] P. M. Ajayan, O. Stephan, C. Colliex and D. Trauth. "Aligned carbon nanotube arrays formed by cutting a polymer resin-nanotube composite", *Science,* vol. 265 (5176), pp. 1212-1214, 1994.

[7] V. L. Bravo, A. N. Hrymak and J. D. Wright. "Numerical simulation of pressure and velocity profiles in kneading elements of a co-rotating twin screw extruder", *Polymer Engineering & Science,* vol. 40 (2), pp. 525-541, 2000.

[8] B.-K. Zhu, S.-H. Xie, Z.-K. Xu and Y.-Y. Xu. "Preparation and properties of the polyimide/multi-walled carbon nanotubes (MWNTs) nanocomposites", *Composites Science and Technology,* vol. 66 (3-4), pp. 548-554, 2006.

[9] S.-M. Yuen, C.-C. M. Ma, C.-Y. Chuang, K.-C. Yu, S.-Y. Wu, C.-C. Yang and M.-H. Wei. "Effect of processing method on the shielding effectiveness of electromagnetic interference of MWCNT/PMMA composites", *Composites Science and Technology,* vol. 68 (3-4), pp. 963-968, 2008.

[10] Y.-L. Huang, S.-M. Yuen, C.-C. M. Ma, C.-Y. Chuang, K.-C. Yu, C.-C. Teng, H.-W. Tien, Y.-C. Chiu, S.-Y. Wu, S.-H. Liao and F.-B. Weng. "Morphological, electrical, electromagnetic interference (EMI) shielding, and tribological properties of functionalized multi-walled carbon nanotube/poly methyl methacrylate (PMMA) composites", *Composites Science and Technology,* vol. 69 (11-12), pp. 1991-1996, 2009.

[11] S. J. Park, S. T. Lim, M. S. Cho, H. M. Kim, J. Joo and H. J. Choi. "Electrical properties of multi-walled carbon nanotube/poly(methyl methacrylate) nanocomposite", *Current Applied Physics,* vol. 5 (4), pp. 302-304, 2005.

[12] F. Du, R. C. Scogna, W. Zhou, S. Brand, J. E. Fischer and K. I. Winey. "Nanotube networks in polymer nanocomposites: Rheology and electrical conductivity", *Macromolecules,* vol. 37 (24), pp. 9048-9055, 2004.

[13] B. Sundaray, V. Subramanian, T. S. Natarajan and K. Krishnamurthy. "Electrical conductivity of a single electrospun fiber of poly(methyl methacrylate) and multiwalled carbon nanotube nanocomposite", *Applied Physics Letters,* vol. 88 (14, Nanoscale Science and Design), p. 143114 (3 pages), 2006.

[14] O. Regev, P. N. B. ElKati, J. Loos and C. E. Koning. "Preparation of conductive nanotube-polymer composites using latex technology", *Advanced Materials,* vol. 16 (3), pp. 248-251, 2004.

[15] R. Haggenmueller, H. H. Gommans, A. G. Rinzler, J. E. Fischer and K. I. Winey. "Aligned single-wall carbon nanotubes in composites by melt processing methods", *Chemical Physics Letters,* vol. 330 (3-4), pp. 219-225, 2000.

[16] Q. Zhang, S. Rastogi, D. Chen, D. Lippits and P. J. Lemstra. "Low percolation threshold in single-walled carbon nanotube/high density polyethylene composites prepared by melt processing technique", *Carbon,* vol. 44 (4), pp. 778-785, 2006.

[17] P. Potschke, M. Abdel-Goad, I. Alig, S. Dudkin and D. Lellinger. "Rheological and dielectrical characterization of melt mixed polycarbonate-multiwalled carbon nanotube composites", *Polymer,* vol. 45 (26), pp. 8863-8870, 2004.

[18] S. B. Kharchenko, J. F. Douglas, J. Obruzut, E. A. Grulke and K. B. Migler. "Flow-induced properties of nanotube-filled polymer materials", *Nature Materials,* vol. 3 (8), pp. 564-568, 2004.

[19] D. S. Bangarusampath, H. Ruckdaschel, V. Altstadt, J. K. W. Sandler, D. Garray and M. S. P. Shaffer. "Rheology and properties of melt-processed poly(ether ether ketone)/multi-wall carbon nanotube composites", *Polymer,* vol. 50 (24), pp. 5803-5811, 2009.

[20] Z. Li, G. Luo, F. Wei and Y. Huang. "Microstructure of carbon nanotubes/PET conductive composites fibers and their properties", *Composites Science and Technology,* vol. 66 (7-8), pp. 1022-1029, 2006.

[21] O. Meincke, D. Kaempfer, H. Weickmann, C. Friedrich, M. Vathauer and H. Warth. "Mechanical properties and electrical conductivity of carbon-nanotube filled polyamide-6 and its blends with acrylonitrile/butadiene/styrene", *Polymer,* vol. 45 (3), pp. 739-748, 2004.

[22] E. T. Thostenson, C. Li and T.-W. Chou. "Nanocomposites in context", *Composites Science and Technology,* vol. 65 (3-4), pp. 491-516, 2005.

[23] D. A. Walters, M. J. Casavant, X. C. Qin, C. B. Huffman, P. J. Boul, L. M. Ericson, E. H. Haroz, M. J. O'Connell, K. Smith, D. T. Colbert and R. E. Smalley. "In-plane-aligned membranes of carbon nanotubes", *Chemical Physics Letters,* vol. 338 (1), pp. 14-20, 2001.

[24] I. M. Daniel, Y. D. S. Rajapakse and E. E. Gdoutos. *Major Accomplishments in Composite Materials and Sandwich Structures*. London, UK: Springer, 2009, p. 694.

[25] D. Qian, E. C. Dickey, R. Andrews and T. Rantell. "Load transfer and deformation mechanisms in carbon nanotube-polystyrene composites", *Applied Physics Letters,* vol. 76 (20), pp. 2868-2870, 2000.

[26] S. G. Advani and E. M. Sozer. *Process Modeling in Composite Manufacturing*. Basel, Switzerland: Eastern Hemisphere distribution, 2002, p. 125.

[27] J. H. Koo. *Polymer Nanocomposites-Processing, Characterization, and applications*: McGraw Hill, NewYork, 2006, p. 72.

[28] S. R. Broadbent and J. M. Hammersley. "Percolation processes. I. Crystals and mazes", *Proceedings of Cambridge Philosophical Society,* vol. 53, pp. 629-641, 1957.

[29] D. Stauffer, Aharony, A. *Introduction to Percolation Theory*. 2nd Revised edition. UK: Taylor & Francis, 2003.

[30] M. Weber and M. R. Kamal. "Estimation of the volume resistivity of electrically conductive composites", *Polymer Composites,* vol. 18 (6), pp. 711-725, 1997.

[31] F. Lux. "Models proposed to explain the electrical conductivity of mixtures made of conductive and insulating materials", *Journal of Materials Science,* vol. 28 (2), pp. 285-301, 1993.

[32] S. Kirkpatrick. "Percolation and Conduction", *Reviews of Modern Physics,* vol. 45 (4), pp. 574-588, 1973.

[33] D. S. Bangarusampath, H. Ruckdaschel, V. Altstadt, J. K. W. Sandler, D. Garray and M. S. P. Shaffer. "Rheological and electrical percolation in melt-processed poly(ether ether ketone)/multi-wall carbon nanotube composites", *Chemical Physics Letters,* vol. 482 (1-3), pp. 105-109, 2009.

[34] M. S. P. Shaffer and A. H. Windle. "Fabrication and characterization of carbon nanotube/poly(vinyl alcohol) composites", *Advanced Materials,* vol. 11 (11), pp. 937-941, 1999.

[35] J. K. W. Sandler, J. E. Kirk, I. A. Kinloch, M. S. P. Shaffer and A. H. Windle. "Ultra-low electrical percolation threshold in carbon-nanotube-epoxy composites", *Polymer,* vol. 44 (19), pp. 5893-5899, 2003.

[36] A. Moisala, Q. Li, I. A. Kinloch and A. H. Windle. "Thermal and electrical conductivity of single- and multi-walled carbon nanotube-epoxy composites", *Composites Science and Technology,* vol. 66 (10), pp. 1285-1288, 2006.

[37] K. Yoshino, H. Kajii, H. Araki, T. Sonoda, H. Take and L. Sergey. "Electrical and optical properties of conducting polymer-fullerene and conducting polymer-carbon nanotube composites", *Proceedings of the 2nd Taiwan-Japan Cooperative Meeting of Fullerene Science and Technology,* vol. 7 (4), pp. 695-711, 1999.

[38] C. Li, E. T. Thostenson and T.-W. Chou. "Effect of nanotube waviness on the electrical conductivity of carbon nanotube-based composites", *Composites Science and Technology,* vol. 68 (6), pp. 1445-1452, 2008.

[39] C. Li, E. T. Thostenson and T.-W. Chou. "Dominant role of tunneling resistance in the electrical conductivity of carbon nanotube-based composites", *Applied Physics Letters,* vol. 91, p. 223114 (3 pages), 2007.

[40] A. Buldum and P. L. Jian. "Contact resistance between carbon nanotubes", *Physical Review B (Condensed Matter and Materials Physics),* vol. 63 (16), p. 161403 (4 pages), 2001.

[41] S. Paulson, A. Helser, M. B. Nardelli, R. M. Taylor, II, M. Falvo, R. Superfine and S. Washburn. "Tunable resistance of a carbon nanotube-graphite interface", *Science,* vol. 290 (5497), pp. 1742-1744, 2000.

[42] F. Gao, J. Qu and M. Yao. "Electronic structure and contact resistance at an open-end carbon nanotube and copper interface", *Applied Physics Letters,* vol. 96 (10), 2010.

[43] F. Wakaya, K. Katayama and K. Gamo. "Contact resistance of multiwall carbon nanotubes", *Microelectronic Engineering,* vol. 67-68, pp. 853-857, 2003.

[44] M. Foygel, R. D. Morris, D. Anez, S. French and V. L. Sobolev. "Theoretical and computational studies of carbon nanotube composites and suspensions: electrical and thermal conductivity", *Physical Review B (Condensed Matter and Materials Physics),* vol. 71 (10), p. 104201 (8 pages), 2005.

[45] B. E. Kilbride, J. N. Coleman, J. Fraysse, P. Fournet, M. Cadek, A. Drury, S. Hutzler, S. Roth and W. J. Blau. "Experimental observation of scaling laws for alternating current and direct current conductivity in polymer-carbon nanotube composite thin films", *Journal of Applied Physics,* vol. 92 (7), pp. 4024-4030, 2002.

[46] F. H. Gojny, M. H. G. Wichmann, B. Fiedler, I. A. Kinloch, W. Bauhofer, A. H. Windle and K. Schulte. "Evaluation and identification of electrical and thermal conduction mechanisms in carbon nanotube/epoxy composites", *Polymer,* vol. 47 (6), pp. 2036-2045, 2006.

[47] W. Bauhofer and J. Z. Kovacs. "A review and analysis of electrical percolation in carbon nanotube polymer composites", *Composites Science and Technology,* vol. 69 (10), pp. 1486-1498, 2009.

[48] N. Grossiord, J. Loos, L. Van Laake, M. Maugey, C. Zakri, C. E. Koning and A. John Hart. "High-conductivity polymer nanocomposites obtained by tailoring the characteristics of carbon nanotube fillers", *Advanced Functional Materials,* vol. 18 (20), pp. 3226-3234, 2008.

[49] R. Ramasubramaniam, J. Chen and H. Liu. "Homogeneous carbon nanotube/polymer composites for electrical applications", *Applied Physics Letters,* vol. 83 (14), pp. 2928-2930, 2003.

[50] E. S. Choi, J. S. Brooks, D. L. Eaton, M. Al-Haik, M. Y. Hussaini, H. Garmestani, D. Li and K. Dahmen. "Enhancement of thermal and electrical properties of carbon nanotube polymer composites by magnetic field processing", *Journal of Applied Physics,* vol. 94 (9), pp. 6034-6039, 2003.

[51] F. Du, J. E. Fischer and K. I. Winey. "Coagulation method for preparing single-walled carbon nanotube/poly(methyl methacrylate) composites and their modulus, electrical conductivity, and thermal stability", *Journal of Polymer Science, Part B: Polymer Physics,* vol. 41 (24), pp. 3333-3338, 2003.

[52] A. Behnam, J. Guo and A. Ural. "Effects of nanotube alignment and measurement direction on percolation resistivity in single-walled carbon nanotube films", *Journal of Applied Physics,* vol. 102 (4, Nanoscale Science and Design), p. 044313 (7 pages), 2007.

[53] C. Li and T.-W. Chou. "Electrical conductivities of composites with aligned carbon nanotubes", *Journal of Nanoscience and Nanotechnology,* vol. 9 (4), pp. 2518-2524, 2009.

[54] F. Du, J. E. Fischer and K. I. Winey. "Effect of nanotube alignment on percolation conductivity in carbon nanotube/polymer composites", *Physical Review B (Condensed Matter and Materials Physics),* vol. 72 (12), p. 121404 (4 pages), 2005.

[55] C. Li, E. T. Thostenson and T.-W. Chou. "Sensors and actuators based on carbon nanotubes and their composites: A review", *Composites Science and Technology,* vol. 68 (6), pp. 1227-1249, 2008.

[56] J. Z. Kovacs, R. E. Mandjarov, T. Blisnjuk, K. Prehn, M. Sussiek, J. Muller, K. Schulte and W. Bauhofer. "On the influence of nanotube properties, processing conditions and shear forces on the electrical conductivity of carbon nanotube epoxy composites", *Nanotechnology,* vol. 20 (15), p. 155703 (6 pages), 2009.

[57] N. Grossiord, P. J. J. Kivit, J. Loos, J. Meuldijk, A. V. Kyrylyuk, d. S. van and C. E. Koning. "On the influence of the processing conditions on the performance of electrically conductive carbon nanotube/polymer nanocomposites", *Polymer,* vol. 49 (12), pp. 2866-2872, 2008.

[58] A. Celzard, E. McRae, C. Deleuze, M. Dufort, G. Furdin and J. F. Mareche. "Critical concentration in percolating systems containing a high-aspect-ratio filler", *Physical Review B (Condensed Matter),* vol. 53 (10), pp. 6209-6214, 1996.

[59] J. B. Bai and A. Allaoui. "Effect of the length and the aggregate size of MWNTs on the improvement efficiency of the mechanical and electrical properties of nanocomposites - Experimental investigation", *Composites Part A: Applied Science and Manufacturing,* vol. 34 (8), pp. 689-694, 2003.

[60] C. A. Martin, J. K. W. Sandler, M. S. P. Shaffer, M. K. Schwarz, W. Bauhofer, K. Schulte and A. H. Windle. "Formation of percolating networks in multi-wall carbon-nanotube-epoxy composites", *Composites Science and Technology,* vol. 64 (15), pp. 2309-2316, 2004.

[61] M. Narkis and A. Vaxman. "Resistivity behaviour of filled electrically conductive crosslinked polyethylene.", *Journal of Applied Polymer Science,* vol. 29 (5), pp. 1639-1652, 1984.

[62] P. K. Pramanik, D. Khastgir and T. N. Saha. "Conductive nitrile rubber composite containing carbon fillers: studies on mechanical properties and electrical conductivity", *Composites,* vol. 23 (3), pp. 183-191, 1992.

[63] K. Miyasaka, K. Watanabe, E. Jojima, H. Aida, M. Sumita and K. Ishikawa. "Electrical conductivity of carbon-polymer composites as a function of carbon content", *Journal of Materials Science,* vol. 17 (6), pp. 1610-1616, 1982.

[64] A. R. Blythe. *Electrical Properties of Polymers*. Cambridge, UK: Cambridge University Press, 1979, p. 126.

[65] K. P. Sau, T. K. Chaki and D. Khastgir. "Carbon fibre filled conductive composites based on nitrile rubber (NBR), ethylene propylene diene rubber (EPDM) and their blend", *Polymer,* vol. 39 (25), pp. 6461-6471, 1998.

[66] K. P. Sau, T. K. Chaki and D. Khastgir. "Conductive rubber composites from different blends of ethylene-propylene-diene rubber and nitrile rubber", *Journal of Materials Science,* vol. 32 (21), pp. 5717-5724, 1997.

[67] A. V. Kyrylyuk and P. van der Schoot. "Continuum percolation of carbon nanotubes in polymeric and colloidal media", *Proceedings of the National Academy of Sciences of the United States of America,* vol. 105 (24), pp. 8221-8226, 2008.

[68] C. Li and T.-W. Chou. "Continuum percolation of nanocomposites with fillers of arbitrary shapes", *Applied Physics Letters,* vol. 90 (17), p. 174108 (3 pages), 2007.

[69] C. Li and C. Tsu-Wei. "Precise determination of backbone structure and conductivity of 3D percolation networks by the direct electrifying algorithm", *International Journal of Modern Physics C,* vol. 20 (3), pp. 423-33, 2009.

[70] S. I. White, B. A. DiDonna, M. Mu, T. C. Lubensky and K. I. Winey. "Simulations and electrical conductivity of percolated networks of finite rods with various degrees of axial alignment", *Physical Review B (Condensed Matter and Materials Physics),* vol. 79 (2), p. 024301 (6 pages), 2009.

[71] M. S. Fuhrer, J. Nygard, L. Shih, M. Forero, Y. Young-Gui, M. S. C. Mazzoni, J. C. Hyoung, J. Ihm, S. G. Louie, A. Zettl and P. L. McEuen. "Crossed nanotube junctions", *Science,* vol. 288 (5465), pp. 494-497, 2000.

[72] R. Holm. "The Electric Tunnel Effect across Thin Insulator Films in Contacts", *Journal of Applied Physics,* vol. 22 (5), pp. 569-572, 1951.

[73] F. Dalmas, R. Dendievel, L. Chazeau, J.-Y. Cavaille and C. Gauthier. "Carbon nanotube-filled polymer composites. Numerical simulation of electrical conductivity in three-dimensional entangled fibrous networks", *Acta Materialia,* vol. 54 (11), pp. 2923-2931, 2006.

[74] K. P. Sau, T. K. Chaki and D. Khastgir. "The change in conductivity of a rubber-carbon black composite subjected to different modes of pre-strain", *Composites Part A (Applied Science and Manufacturing),* vol. 29A (4), pp. 363-370, 1998.

[75] N. C. Das, T. K. Chaki and D. Khastgir. "Effect of processing parameters, applied pressure and temperature on the electrical resistivity of rubber-based conductive composites", *Carbon,* vol. 40 (6), pp. 807-816, 2002.

[76] F. Carmona and A. El Amarti. "Temperature and pressure dependence of the conductivity anisotropy of unidirectional short carbon fiber filled polymers", *Journal of Materials Research,* vol. 7 (1), pp. 117-123, 1992.

[77] M. L. Homer, J. R. Lim, K. Manatt, A. Kisor, A. M. Manfreda, L. Lara, A. D. Jewell, S. P. S. Yen, H. Zhou, A. V. Shevade and M. A. Ryan. "Temperature effects on polymer-carbon composite sensors: Evaluating the role of polymer molecular weight and carbon loading", in *Proceedings of IEEE Sensors*, Piscataway, NJ, USA, 2003, vol. 2(2) pp. 877-881.

[78] O. B. Searle and R. H. Pfeiffer. "Victrex® poly(ethersulfone) (PES) and Victrex® poly(etheretherketone) (PEEK)", *Polymer Engineering & Science,* vol. 25 (8), pp. 474-476, 1985.

[79] C. L. Kane, E. J. Mele, R. S. Lee, J. E. Fischer, P. Petit, H. Dai, A. Thess, R. E. Smalley, A. R. M. Verschueren, S. J. Tans and C. Dekker. "Temperature-dependent resistivity of single-wall carbon nanotubes", *Europhysics Letters,* vol. 41 (6), pp. 683-688, 1998.

[80] A. M. Diez-Pascual, M. Naffakh, M. A. Gomez, C. Marco, G. Ellis, J. M. Gonzlez-Dominguez, A. Anson, M. T. Martinez, Y. Martinez-Rubi, B. Simard and B. Ashrafi. "The influence of a compatibilizer on the thermal and dynamic mechanical properties of PEEK/carbon nanotube composites", *Nanotechnology,* vol. 20 (31), 2009.

[81] A. M. Diez-Pascual, M. Naffakh, M. A. Gomez, C. Marco, G. Ellis, M. T. Martinez, A. Anson, J. M. Gonzalez-Dominguez, Y. Martinez-Rubi and B. Simard. "Development and characterization of PEEK/carbon nanotube composites", *Carbon,* vol. 47 (13), pp. 3079-3090, 2009.

[82] L. J. Hall, V. R. Coluci, D. S. Galvao, M. E. Kozlov, M. Zhang, S. O. Dantas and R. H. Baughman. "Sign change of Poisson's ratio for carbon nanotube sheets", *Science,* vol. 320 (5875), pp. 504-507, 2008.

[83] E. Logakis, C. H. Pandis, P. Pissis, J. Pionteck and P. Potschke. "Highly conducting poly(methyl methacrylate)/carbon nanotubes composites: Investigation on their thermal, dynamic-mechanical, electrical and dielectric properties", *Composites Science and Technology,* vol. 71 (6), pp. 854-862, 2011.

[84] G. D. Liang and S. C. Tjong. "Electrical properties of low-density polyethylene/multiwalled carbon nanotube nanocomposites", *Materials Chemistry and Physics,* vol. 100 (1), pp. 132-137, 2006.

[85] C.-W. Nan. "Physics of inhomogeneous inorganic material physics", *Progress in Materials Science,* vol. 37 (1), pp. 1-116, 1993.

[86] E. Logakis, C. Pandis, V. Peoglos, P. Pissis, J. Pionteck, P. Potschke, M. Micuik and M. Omastova. "Electrical/dielectric properties and conduction mechanism in melt processed polyamide/multi-walled carbon nanotubes composites", *Polymer,* vol. 50 (21), pp. 5103-5111, 2009.

[87] C.-R. Yu, D.-M. Wu, Y. Liu, H. Qiao, Z.-Z. Yu, A. Dasari, X.-S. Du and Y.-W. Mai. "Electrical and dielectric properties of polypropylene nanocomposites based on carbon nanotubes and barium titanate nanoparticles", *Composites Science and Technology,* vol. 71, pp. 1706-1712, 2011.

[88] Z. Ounaies, C. Park, K. E. Wise, E. J. Siochi and J. S. Harrison. "Electrical properties of single wall carbon nanotube reinforced polyimide composites", *Composites Science and Technology,* vol. 63 (11), pp. 1637-1646, 2003.

[89] J. Dai, Q. Wang, W. Li, Z. Wei and G. Xu. "Properties of well aligned SWNT modified poly (methyl methacrylate) nanocomposites", *Materials Letters,* vol. 61 (1), pp. 27-29, 2007.

[90] H. Peng and X. Sun. "Highly aligned carbon nanotube/polymer composites with much improved electrical conductivities", *Chemical Physics Letters,* vol. 471 (1-3), pp. 103-105, 2009.

[91] Z. Khattari, M. Maghrabi, T. McNally and S. Abdul Jawad. "Impedance study of polymethyl methacrylate composites/multi-walled carbon nanotubes (PMMA/MWCNTs)", *Physica B: Condensed Matter,* vol. 407 (4), pp. 759-764, 2012.

[92] W. Zheng and S.-C. Wong. "Electrical conductivity and dielectric properties of PMMA/expanded graphite composites", *Composites Science and Technology,* vol. 63 (2), pp. 225-235, 2003.

[93] Y. C. Li, R. K. Y. Li and S. C. Tjong. "Frequency and Temperature Dependences of Dielectric Dispersion and Electrical Properties of Polyvinylidene Fluoride/Expanded Graphite Composites", *Journal of Nanomaterials,* p. 261748 (10 pages), 2010.

[94] E. El Shafee, M. El Gamal and M. Isa. "Electrical properties of multi walled carbon nanotubes/ poly(vinylidene fluoride/trifluoroethylene) nanocomposites", *Journal of Polymer Research,* vol. 19 (1), pp. 1-8, 2012.

[95] H.-P. Xu, H.-Q. Xie, D.-D. Yang, Y.-H. Wu and J.-R. Wang. "Novel dielectric behaviors in PVDF-based semiconductor composites", *Journal of Applied Polymer Science,* vol. 122 (5), pp. 3466-3473, 2011.

[96] J. J. George, S. Bhadra and A. K. Bhowmick. "Influence of carbon-based nanofillers on the electrical and dielectric properties of ethylene vinyl acetate nanocomposites", *Polymer Composites,* vol. 31 (2), pp. 218-225, 2010.

[97] J. Zhang, M. Mine, D. Zhu and M. Matsuo. "Electrical and dielectric behaviors and their origins in the three-dimensional polyvinyl alcohol/MWCNT composites with low percolation threshold", *Carbon,* vol. 47 (5), pp. 1311-1320, 2009.

[98] A. K. Jonscher. "The `universal' dielectric response", *Nature,* vol. 267 (5613), pp. 673-679, 1977.

[99] J. C. Dyre and T. B. Schroder. "Universality of ac conduction in disordered solids", *Reviews of Modern Physics,* vol. 72 (3), pp. 873-892, 2000.

[100] I. Alig, S. M. Dudkin, W. Jenninger and M. Marzantowicz. "Ac conductivity and dielectric permittivity of poly(ethylene glycol) during crystallization: Percolation picture", *Polymer,* vol. 47 (5), pp. 1722-1731, 2006.

[101] J. P. Clerc, G. Giraud, J. M. Laugier and J. M. Luck. "The electrical conductivity of binary disordered systems, percolation clusters, fractals and related models", *Advances in Physics,* vol. 39 (3), pp. 191-309, 1990.

[102] M. Sahimi. *Applications of percolation Theory*. Bristol, Pennsylvania: Taylor and Francis, 1991.

[103] G. T. Mohanraj, P. K. Dey, T. K. Chaki, A. Chakraborty and D. Khastgir. "Effect of temperature, pressure, and composition on DC resistivity and AC conductivity of conductive styrene-butadiene rubber-particulate metal alloy nanocomposites", *Polymer Composites,* vol. 28 (5), pp. 696-704, 2007.

[104] Y. Song, W. N. Taw, L. Sung-Ik and J. R. Gaines. "Experimental study of the three-dimensional AC conductivity and dielectric constant of a conductor-insulator composite near the percolation threshold", *Physical Review B (Condensed Matter),* vol. 33 (2), pp. 904-908, 1986.

[105] L. Wang and Z.-M. Dang. "Carbon nanotube composites with high dielectric constant at low percolation threshold", *Applied Physics Letters,* vol. 87 (4), pp. 1-3, 2005.

[106] J. Meyer. "Glass transition temperature as a guide to selection of polymers suitable for PTC materials", *Polymer Engineering and Science,* vol. 13 (6), pp. 462-468, 1973.

[107] K. Ahmad, W. Pan and S.-L. Shi. "Electrical conductivity and dielectric properties of multiwalled carbon nanotube and alumina composites", *Applied Physics Letters,* vol. 89, p. 133122 (3 pages), 2006.

[108] D. Stauffer. "Scaling theory of percolation clusters", *Physics Reports,* vol. 54 (1), pp. 1-74, 1979.

[109] I. Alig, D. Lellinger, S. M. Dudkin and P. Potschke. "Conductivity spectroscopy on melt processed polypropylene-multiwalled carbon nanotube composites: Recovery after shear and crystallization", *Polymer,* vol. 48 (4), pp. 1020-1029, 2007.

[110] J. M. Benoit, B. Corraze, S. Lefrant, W. J. Blau, P. Bernier and O. Chauvet. "Transport properties of PMMA-carbon nanotubes composites", *Synthetic Metals,* vol. 121 (1-3), pp. 1215-1216, 2001.

[111] J. Z. Kovacs, B. S. Velagala, K. Schulte and W. Bauhofer. "Two percolation thresholds in carbon nanotube epoxy composites", *Composites Science and Technology,* vol. 67 (5), pp. 922-928, 2007.

[112] I. Balberg, C. H. Anderson, S. Alexander and N. Wagner. "Excluded volume and its relation to the onset of percolation", *Physical Review B (Condensed Matter),* vol. 30 (7), pp. 3933-3943, 1984.

[113] I. Balberg, N. Binenbaum and N. Wagner. "Percolation thresholds in the three-dimensional sticks system", *Physical Review Letters,* vol. 52 (17), pp. 1465-1468, 1984.

[114] D. S. McLachlan, C. Chiteme, C. Park, K. E. Wise, S. E. Lowther, P. T. Lillehei, E. J. Siochi and J. S. Harrison. "AC and DC percolative conductivity of single wall carbon nanotube polymer composites", *Journal of Polymer Science, Part B (Polymer Physics),* vol. 43 (22), pp. 3273-3287, 2005.

[115] A. Allaoui, S. V. Hoa and M. D. Pugh. "The electronic transport properties and microstructure of carbon nanofiber/epoxy composites", *Composites Science and Technology,* vol. 68 (2), pp. 410-416, 2008.

[116] M. B. Bryning, M. F. Islam, J. M. Kikkawa and A. G. Yodh. "Very low conductivity threshold in bulk isotropic single-walled carbon nanotube-epoxy composites", *Advanced Materials,* vol. 17 (9), pp. 1186-1191, 2005.

[117] M. O. Saar and M. Manga. "Continuum percolation for randomly oriented soft-core prisms", *Physical Review E - Statistical, Nonlinear, and Soft Matter Physics,* vol. 65 (5), p. 056131 (6 pages), 2002.

[118] S. M. Hong and S. S. Hwang. "Physical properties of thin PVDF/MWNT (multi-walled carbon nanotube) composite films by melt blending", *Journal of Nanoscience and Nanotechnology,* vol. 8 (9), pp. 4860-4863, 2008.

[119] Q. Li, Q. Z. Xue, X. L. Gao and Q. B. Zheng. "Temperature dependence of the electrical properties of the carbon nanotube/polymer composites", *eXPRESS Polymer Letters,* vol. 3 (12), pp. 769-777, 2009.

[120] Y. P. Mamunya, Y. V. Muzychenko, P. Pissis, E. V. Lebedev and M. I. Shut. "Percolation phenomena in polymers containing dispersed iron", *Polymer Engineering and Science,* vol. 42 (1), pp. 90-100, 2002.

[121] T. A. Ezquerra, C. S. Cruz and F. J. Balta Calleja. "Charge transport in polyethylene-graphite composite materials", *Advanced Materials,* vol. 2 (12), pp. 597-600, 1990.

[122] I. Balberg. "Tunneling and nonuniversal conductivity in composite materials", *Physical Review Letters,* vol. 59 (12), pp. 1305-1308, 1987.

[123] P. M. Kogut and J. P. Straley. "Distribution-induced non-universality of the percolation conductivity exponents", *Journal of Physics C (Solid State Physics),* vol. 12 (11), pp. 2151-2159, 1979.

[124] E. Logakis, C. Pandis, V. Peoglos, P. Pissis, C. Stergiou, J. Pionteck, P. Potschke, M. Micuik and M. Omastova. "Structure-property relationships in polyamide 6/multi-walled carbon nanotubes nanocomposites", *Journal of Polymer Science, Part B: Polymer Physics,* vol. 47 (8), pp. 764-774, 2009.

[125] B. McCarthy, J. N. Coleman, R. Czerw, A. B. Dalton, M. I. Panhuis, A. Maiti, A. Drury, P. Bernier, J. B. Nagy, B. Lahr, H. J. Byrne, D. L. Carroll and W. J. Blau. "A microscopic and spectroscopic study of interactions between carbon nanotubes and a conjugated polymer", *Journal of Physical Chemistry B,* vol. 106 (9), pp. 2210-2216, 2002.

[126] M. T. Connor, S. Roy, T. A. Ezquerra and F. J. Balta Calleja. "Broadband ac conductivity of conductor-polymer composites", *Physical Review B (Condensed Matter),* vol. 57 (4), pp. 2286-2294, 1998.

[127] S. Barrau, P. Demont, A. Peigney, C. Laurent and C. Lacabanne. "Dc and ac conductivity of carbon nanotubes-polyepoxy composites", *Macromolecules,* vol. 36 (14), pp. 5187-5194, 2003.

[128] I. Balberg, D. Azulay, D. Toker and O. Millo. "Percolation and tunneling in composite materials", *International Journal of Modern Physics B,* vol. 18 (15), pp. 2091-2121, 2004.

[129] D. M. Bigg and D. E. Stutz. "Plastic composites for electromagnetic interference shielding applications", *Polymer Composites,* vol. 4 (1), pp. 40-46, 1983.

[130] T. Ota, M. Fukushima, Y. Ishigure, H. Unuma, M. Takahashi, Y. Hikichi and H. Suzuki. "Control of percolation curve by filler particle shape in Cu-SBR composites", *Journal of Materials Science Letters,* vol. 16 (14), pp. 1182-1183, 1997.

[131] G. R. Ruschau, S. Yoshikawa and R. E. Newnham. "Resistivities of conductive composites", *Journal of Applied Physics,* vol. 72 (3), pp. 953-959, 1992.

[132] R. Strumpler and J. Glatz-Reichenbach. "Conducting polymer composites", *Journal of Electroceramics,* vol. 3 (4), pp. 329-346, 1999.

[133] H. P. Wu, X. J. Wu, M. Y. Ge, G. Q. Zhang, Y. W. Wang and J. Z. Jiang. "Effect analysis of filler sizes on percolation threshold of isotropical conductive adhesives", *Composites Science and Technology,* vol. 67 (6), pp. 1116-1120, 2007.

[134] T. McNally, P. Potschke, P. Halley, M. Murphy, D. Martin, S. E. J. Bell, G. P. Brennan, D. Bein, P. Lemoine and J. P. Quinn. "Polyethylene multiwalled carbon nanotube composites", *Polymer,* vol. 46 (19), pp. 8222-8232, 2005.

[135] J. N. Coleman, S. Curran, A. B. Dalton, A. P. Davey, B. McCarthy, W. Blau and R. C. Barklie. "Percolation-dominated conductivity in a conjugated-polymer-carbon-nanotube composite", *Physical Review B (Condensed Matter),* vol. 58 (12), pp. 7492-7495, 1998.

[136] J. C. Grunlan, A. R. Mehrabi, M. V. Bannon and J. L. Bahr. "Water-based single-walled-nanotube-filled polymer composite with an exceptionally low percolation threshold", *Advanced Materials,* vol. 16 (2), pp. 150-153, 2004.

[137] L. S. Schadler, S. C. Giannaris and P. M. Ajayan. "Load transfer in carbon nanotube epoxy composites", *Applied Physics Letters,* vol. 73 (26), pp. 3842-3844, 1998.

[138] D. J. Yang, S. G. Wang, Q. Zhang, P. J. Sellin and G. Chen. "Thermal and electrical transport in multi-walled carbon nanotubes", *Physics Letters A,* vol. 329 (3), pp. 207-213, 2004.

[139] C. M. van Wyk. "Note on the Compressibility of Wool", *Journal of Textile Institute,* vol. 37 pp. T285-T292, 1946.

[140] X.-W. Zhang, Y. Pan, Q. Zheng and X.-S. Yi. "Time dependence of piezoresistance for the conductor-filled polymer composites", *Journal of Polymer Science, Part B: Polymer Physics,* vol. 38 (21), pp. 2739-2749, 2000.

[141] M. I. Alkhagen. "Nonlinear Elasticity of Fiber Masses", Ph.D. thesis, Chalmers University, Göteborg, Sweden, 2002.

[142] R. Holm. *Electric contacts: theory and application* vol. 4th edition. Berlin, New York: Springer-Verlag, 1967.

[143] J. G. Simmons. "Generalized Formula for the Electric Tunnel Effect between Similar Electrode Separated by a Thin Insulating Film", *Journal of Applied Physics,* vol. 34 (6), pp. 1793-1803, 1963.

[144] M. Shiraishi and M. Ata. "Work function of carbon nanotubes", *Carbon,* vol. 39 (12), pp. 1913-1917, 2001.

[145] R. Strumpler. "Polymer composite thermistors for temperature and current sensors", *Journal of Applied Physics,* vol. 80 (11), pp. 6091-6096, 1996.

[146] N. Sinha, J. Ma and J. T. W. Yeow. "Carbon nanotube-based sensors", *Journal of Nanoscience and Nanotechnology,* vol. 6 (3), pp. 573-590, 2006.

[147] L. G. Pedroni, M. Soto-Oviedo, J. M. Rosolen, M. I. Felisberti and A. F. Nogueira. "Conductivity and mechanical properties of composites based on MWCNTs and styrene-butadiene-styrene block copolymers", *Journal of Applied Polymer Science,* vol. 112 (6), pp. 3241-3248, 2009.

[148] M. Taya, W. J. Kim and K. Ono. "Piezoresistivity of a short fiber/elastomer matrix composite", *Mechanics of Materials,* vol. 28 (1), pp. 53-59, 1998.

[149] P. K. Pramanik, D. Khastagir and T. N. Saha. "Effect of extensional strain on the resistivity of electrically conductive nitrile-rubber composites filled with carbon filler", *Journal of Materials Science,* vol. 28 (13), pp. 3539-3546, 1993.

[150] K. Yoshimura, K. Nakano, T. Miyake, Y. Hishikawa, C. Kuzuya, T. Katsuno and S. Motojima. "Effect of compressive and tensile strains on the electrical resistivity of carbon microcoil/silicone-rubber composites", *Carbon,* vol. 45 (10), pp. 1997-2003, 2007.

[151] K. Wang, G. Zhang, Z. Zhao, Y. Peng, W. Di and C. Du. "Influence of unidirectional pressure on electrical conductivity of carbon black filled polyethylene", *Journal Wuhan University of Technology, Materials Science Edition,* vol. 21 (3), pp. 76-78, 2006.

[152] C. Yongliang, S. Yihu, Z. Jianfeng and Z. Qiang. "Effect of uniaxial pressure on conduction behavior of carbon black filled poly(methyl vinyl siloxane) composites", *Chinese Science Bulletin,* vol. 50 (2), pp. 101-107, 2005.

[153] G. Chen, J. Lu, W. Lu, D. Wu and C. Wu. "Time-dependence of piezo-resistive behavior for polyethylene/foliated graphite nanocomposites", *Polymer International,* vol. 54 (12), pp. 1689-1693, 2005.

[154] S. Qu and S.-C. Wong. "Piezoresistive behavior of polymer reinforced by expanded graphite", *Composites Science and Technology,* vol. 67 (2), pp. 231-237, 2007.

[155] N. Kchit and G. Bossis. "Piezoresistivity of magnetorheological elastomers", *Journal of Physics: Condensed Matter,* vol. 20 (20), p. 204136 (5 pages), 2008.

[156] Y. Wang, L. Zhang, Y. Fan, D. Jiang and L. An. "Stress-dependent piezoresistivity of tunneling-percolation systems", *Journal of Materials Science,* vol. 44 (11), pp. 2814-2819, 2009.

[157] G. T. Pham, Y.-B. Park, Z. Liang, C. Zhang and B. Wang. "Processing and modeling of conductive thermoplastic/carbon nanotube films for strain sensing", *Composites Part B: Engineering,* vol. 39 (1), pp. 209-216, 2008.

[158] M. Park, H. Kim and J. P. Youngblood. "Strain-dependent electrical resistance of multi-walled carbon nanotube/polymer composite films", *Nanotechnology,* vol. 19 (5), p. 055705 (7 pages), 2008.

[159] P. Wang, T. Ding and F. Xu. "A Novel Flexible Sensor for Compression Stress Relaxation", in *Second International Conference on Sensors: IEEE Sensors*, Toronto, Ontario, Canada, October 22 - 24, 2003, vol. 2, pp. 265-268.

[160] M. Hussain, Y.-H. Choa and K. Niihara. "Fabrication process and electrical behavior of novel pressure-sensitive composites", *Composites - Part A: Applied Science and Manufacturing,* vol. 32 (12), pp. 1689-1696, 2001.

[161] L. Flandin, Y. Brechet and J. Y. Cavaille. "Electrically conductive polymer nanocomposites as deformation sensors", *Composites Science and Technology,* vol. 61 (6), pp. 895-901, 2001.

[162] A. E. Job, F. A. Oliveira, N. Alves, J. A. Giacometti and L. H. C. Mattoso. "Conductive composites of natural rubber and carbon black for pressure sensors", *Synthetic Metals,* vol. 135-136, pp. 99-100, 2003.

[163] M. Knite, V. Teteris, A. Kiploka and J. Kaupuzs. "Polyisoprene-carbon black nanocomposites as tensile strain and pressure sensor materials", *Sensors and Actuators A: Physical,* vol. 110, pp. 142-149, 2004.

[164] W. E. Mahmoud, A. El-Lawindy, M. H. El Eraki and H. H. Hassan. "Butadiene acrylonitrile rubber loaded fast extrusion furnace black as a compressive strain and pressure sensors", *Sensors and Actuators, A: Physical,* vol. 136 (1), pp. 229-233, 2007.

[165] L. Wang, T. Ding and P. Wang. "Effects of instantaneous compression pressure on electrical resistance of carbon black filled silicone rubber composite during compressive stress relaxation", *Composites Science and Technology,* vol. 68 (15-16), pp. 3448-3450, 2008.

[166] L. Wang, T. Ding and P. Wang. "Thin flexible pressure sensor array based on carbon black/silicone rubber nanocomposite", *IEEE Sensors Journal,* vol. 9 (9), pp. 1130-1135, September 2009.

[167] P. Wang, S. Geng and T. Ding. "Effects of carboxyl radical on electrical resistance of multi-walled carbon nanotube filled silicone rubber composite under pressure", *Composites Science and Technology,* vol. 70 (10), pp. 1571-1573, 2010.

[168] P. Dharap, Z. Li, S. Nagarajaiah and E. V. Barrera. "Nanotube film based on single-wall carbon nanotubes for strain sensing", *Nanotechnology,* vol. 15 (3), pp. 379-382, 2004.

[169] J. Wu, J. Zang, B. Larade, H. Guo, X. G. Gong and F. Liu. "Computational design of carbon nanotube electromechanical pressure sensors", *Physical Review B (Condensed Matter and Materials Physics),* vol. 69 (15), p. 153406 (4 pages), 2004.

[170] T. Furukawa. "Piezoelectricity and pyroelectricity in polymers", *IEEE Transactions on Electrical Insulation,* vol. 24 (3), pp. 375-394, 1989.

[171] T. Ogasawara, T. Tsuda and N. Takeda. "Stress-strain behavior of multi-walled carbon nanotube/PEEK composites", *Composites Science and Technology,* vol. 71 (2), pp. 73-78, 2011.

[172] S.-H. Wu, I. Masaharu, T. Natsuki and Q.-Q. Ni. "Electrical conduction and percolation behavior of carbon nanotubes/UPR nanocomposites", *Journal of Reinforced Plastics and Composites,* vol. 25 (18), pp. 1957-1966, 2006.

[173] L. Wang, T. Ding and P. Wang. "Effects of conductive phase content on critical pressure of carbon black filled silicone rubber composite", *Sensors and Actuators, A: Physical,* vol. 135 (2), pp. 587-592, 2007.

[174] K. Ohe and Y. Naito. "A new resistor having an anomalously large positive temperature coefficient", *Japanese Journal of Applied Physics,* vol. 10 (1), pp. 99-108, 1971.

[175] J. G. Simmons. "Electric Tunnel Effect between Dissimilar Electrodes Separated by a Thin Insulating Film", *Journal of Applied Physics,* vol. 34 (9), pp. 2581-2590, 1963.

[176] J. G. Simmons. "Low Voltage Current-Voltage Relationship of Tunnel Junctions", *Journal of Applied Physics,* vol. 34 (1), pp. 238-239, 1963.

[177] J. G. Simmons and J. U. George. "Potential Barrier Shape Determination in Tunnel Junctions", *Journal of Applied Physics,* vol. 34 (6), pp. 1828-1830, 1963.

[178] D. S. McLachlan, M. Blaszkiewicz and R. E. Newnham. "Electrical resistivity of composites", *Journal of the American Ceramic Society,* vol. 73 (8), pp. 2187-2203, 1990.

[179] Y. J. Liu and X. L. Chen. "Evaluations of the effective material properties of carbon nanotube-based composites using a nanoscale representative volume element", *Mechanics of Materials,* vol. 35 (1-2), pp. 69-81, 2003.

[180] J. Cao, Q. Wang and H. Dai. "Electromechanical properties of metallic, quasimetallic, and semiconducting carbon nanotubes under stretching", *Physical Review Letters,* vol. 90 (15), p. 157601 (4 pages), 2003.

[181] T. Yasuoka, Y. Shimamura and A. Todoroki. "Piezoresistivity of Carbon Nanotube Composite", in *9th Japan International SAMPE Symposium*, 2005, pp. 341-344.

[182] Y. H. Hou, M. Q. Zhang and M. Z. Rong. "Performance stabilization of conductive polymer composites", *Journal of Applied Polymer Science,* vol. 89 (9), pp. 2438-2445, 2003.

[183] C. Zhang, C.-A. Ma, P. Wang and M. Sumita. "Temperature dependence of electrical resistivity for carbon black filled ultra-high molecular weight polyethylene composites prepared by hot compaction", *Carbon,* vol. 43 (12), pp. 2544-2553, 2005.

[184] T. Natsuki, Q.-Q. Ni and S.-H. Wu. "Temperature dependence of electrical resistivity in carbon nanofiber/unsaturated polyester nanocomposites", *Polymer Engineering and Science,* vol. 48 (7), pp. 1345-1350, 2008.

[185] S. Nakamura and T. Tomimura. "Temperature dependence of resistivity of carbon black-polyethylene composites below and above the percolation threshold", in *8th International Conference on Dielectric Materials, Measurements and Applications (CP473)*, Edinburgh, UK, 17-21 September, 2000, pp. 265-269.

[186] M. Hindermann-Bishoff and F. Ehrburger-Dolle. "Electrical conductivity of carbon black–polyethylene composites Experimental evidence of the change of cluster connectivity in the PTC effect", *Carbon,* vol. 39 (3), pp. 375-382, 2001.

[187] M. O. Lisunova, Y. P. Mamunya, N. I. Lebovka and A. V. Melezhyk. "Percolation behaviour of ultrahigh molecular weight polyethylene/multi-walled carbon nanotubes composites", *European Polymer Journal,* vol. 43 (3), pp. 949-958, 2007.

[188] A. Kyritsis, P. Pissis and I. Grammatikakis. "Dielectric relaxation spectroscopy in poly(hydroxyethyl acrylates)/water hydrogels", *Journal of Polymer Science, Part B (Polymer Physics),* vol. 33 (12), pp. 1737-1750, 1995.

[189] Y. Bin, M. Kitanaka, D. Zhu and M. Matsuo. "Development of highly oriented polyethylene filled with aligned carbon nanotubes by gelation/crystallization from solutions", *Macromolecules,* vol. 36 (16), pp. 6213-6219, 2003.

[190] D. J. Blundell and B. N. Osborn. "The morphology of poly(aryl-ether-ether-ketone)", *Polymer,* vol. 24 (8), pp. 953-958, 1983.

[191] L. A. Pothan, Z. Oommen and S. Thomas. "Dynamic mechanical analysis of banana fiber reinforced polyester composites", *Composites Science and Technology,* vol. 63 (2), pp. 283-293, 2003.

[192] A. R. Bhattacharyya, T. V. Sreekumar, T. Liu, S. Kumar, L. M. Ericson, R. H. Hauge and R. E. Smalley. "Crystallization and orientation studies in polypropylene/single wall carbon nanotube composite", *Polymer,* vol. 44 (8), pp. 2373-2377, 2003.

[193] G.-W. Lee, S. Jagannathan, H. G. Chae, M. L. Minus and S. Kumar. "Carbon nanotube dispersion and exfoliation in polypropylene and structure and properties of the resulting composites", *Polymer,* vol. 49 (7), pp. 1831-1840, 2008.

[194] L. Li, C. Y. Li, C. Ni, L. Rong and B. Hsiao. "Structure and crystallization behavior of Nylon 66/multi-walled carbon nanotube nanocomposites at low carbon nanotube contents", *Polymer,* vol. 48 (12), pp. 3452-3460, 2007.

[195] J. Sandler, P. Werner, M. S. P. Shaffer, V. Demchuk, V. Altstadt and A. H. Windle. "Carbon-nanofibre-reinforced poly(ether ether ketone) composites", *Composites Part A: Applied Science and Manufacturing,* vol. 33 (8), pp. 1033-1039, 2002.

[196] F. J. Balta Calleja, T. A. Ezquerra, D. R. Rueda and J. Alonso-Lopez. "Conductive polycarbonate-carbon composites", *Journal of Materials Science Letters,* vol. 3 (2), pp. 165-168, 1984.

[197] L. K. H. van Beek and B. I. C. F. van Paul. "Internal field emission in carbon black-loaded natural rubber vulcanizates", *Journal of Applied Polymer Science,* vol. 6 (24), pp. 651-655, 1962.

[198] R. M. Scarisbrick. "Electrically conducting mixtures", *Journal of Physics D (Applied Physics),* vol. 6 (17), pp. 2098-2110, 1973.

[199] P. Sheng, E. K. Sichel and J. I. Gittleman. "Fluctuation-induced tunneling conduction in carbon-polyvinylchloride composites", *Physical Review Letters,* vol. 40 (18), pp. 1197-1200, 1978.

[200] C. Barone, S. Pagano and H. C. Neitzert. "Effect of concentration on low-frequency noise of multiwall carbon nanotubes in high-density polyethylene matrix", *Applied Physics Letters,* vol. 97, p. 152107 (3 pages), 2010.

[201] E. K. Sichel. *Carbon Black-Polymer Composites: The Physics of Electrically Conducting Composites (Plastics engineering)*. New York: Dekker, 1982.

[202] H. Böttger and V. V. Bryksin. *Hopping Conduction in Solids*: Vch Pub, 1986.

[203] T. A. Ezquerra, M. Kulescza and F. J. Balta Calleja. "Electrical transport in polyethylene-graphite composite materials", *Synthetic Metals,* vol. 41 (3), pp. 915-920, 1990.

[204] P. Sheng. "Fluctuation-induced tunneling conduction in disordered materials", *Physical Review B (Condensed Matter),* vol. 21 (6), pp. 2180-2195, 1980.

[205] Z. Spitalsky, G. Tsoukleri, D. Tasis, C. Krontiras, S. N. Georga and C. Galiotis. "High volume fraction carbon nanotube-epoxy composites", *Nanotechnology,* vol. 20 (40), p. 405702 (7 pages), 2009.

[206] L. D. Perez, M. A. Zuluaga, T. Kyu, J. E. Mark and B. L. Lopez. "Preparation, characterization, and physical properties of multiwall carbon nanotube/elastomer composites", *Polymer Engineering and Science,* vol. 49, pp. 866-874, 2009.

[207] S. Ansari and E. P. Giannelis. "Functionalized graphene sheet-Poly(vinylidene fluoride) conductive nanocomposites", *Journal of Polymer Science, Part B: Polymer Physics,* vol. 47 (9), pp. 888-897, 2009.

[208] X. J. He, J. H. Du, Z. Ying and H. M. Cheng. "Positive temperature coeffcient effect in multiwalled carbon nanotube/high-density polyethylene composites", *Applied Physics Letters,* vol. 86 (6), p. 062112 (3 pages), 2005.

[209] J.-H. Lee, S. K. Kim and N. H. Kim. "Effects of the addition of multi-walled carbon nanotubes on the positive temperature coefficient characteristics of carbon-black-filled high-density polyethylene nanocomposites", *Scripta Materialia,* vol. 55 (12), pp. 1119-1122, 2006.

[210] Y. Xi, H. Ishikawa, Y. Bin and M. Matsuo. "Positive temperature coefficient effect of LMWPE-UHMWPE blends filled with short carbon fibers", *Carbon,* vol. 42 (8-9), pp. 1699-1706, 2004.